Modelling SuDS at the Street-Scale

Shuxin Ren

Supervised by:

Prof Virginia Stovin

Dr Simon De-Ville

A thesis submitted in partial fulfilment of the requirements

For the degree of Doctor of Philosophy in Civil Engineering

School of Mechanical, Aerospace and Civil Engineering

The University of Sheffield

March 2026

Declaration

I declare that no portion of the work contained in this thesis has been submitted in support of an application for another degree or qualification of this or any university or other institutes of learning. The work is my own except where indicated. All quotations have been distinguished by quotation marks and the sources acknowledged.

Acknowledgements

I would like to express my sincere gratitude to Prof Virginia Stovin, my primary supervisor, for her encouragement, guidance and support throughout every stage of this PhD. Her thoughtful advice, high academic standards and continuous encouragement have been invaluable in shaping both this research and my development as a researcher.

I am also grateful to Dr Simon De-Ville, my second supervisor, for his technical guidance and practical insights. His expertise and experience were particularly helpful in navigating the methodological and modelling challenges of this research.

My thanks also go to Dr Peng Zhangjie, a colleague in the research group, who generously shared her experience and advice during the early stages of my work, and to Dr Frederick Sonnenwald for his support with MATLAB coding and technical discussions. I would also like to thank Bruce Wickham, a fellow PhD student in the group, for the encouragement and camaraderie we shared throughout the PhD journey.

Special thanks to Shikun Lin and Michael E Evans; you will be my good memory of England, held in my heart.

I would also like to thank Hongyu Fang, a long-time friend whose experiences and perspectives beyond academia have been a constant source of inspiration. My thanks also go to Yiqi Liu, another PhD friend from a different discipline, for the many conversations and exchanges of ideas that expanded my thinking beyond my own field.

I am deeply grateful to Qiang Zhang, whose thoughtful conversations and daily support have broadened my perspectives and helped me approach both research and life with patience and soft.

Finally, I wish to thank my parents, who have always supported my education and provided an environment that allowed me to focus fully on my studies.

This PhD has also been a journey of personal growth. Through persistence, structured effort and a commitment to developing both professional expertise and broad skills, my thinking has gradually evolved. All of these people and experiences have formed the anchors of my PhD journey.

Abstract

Sustainable drainage systems (SuDS) are increasingly implemented to manage urban runoff, yet their hydrological representation across spatial scales remains challenging. Key knowledge gaps arise in three areas: the representation of unsaturated flow within engineered media, the reliability of simplified device-scale models, and the validity of aggregation strategies for heterogeneous SuDS systems at the street-scale.

The aim of this thesis was to examine how model detail, process representation, and spatial aggregation interact across scales to shape the accuracy, and applicability of SuDS simulations. To achieve this, a structured investigation was undertaken. First, the representation of unsaturated percolation within engineered media was evaluated and refined through analysis of hydraulic conductivity formulations. Second, commonly used device-scale simplifications were systematically assessed against physically explicit SWMM-LID representations to quantify their impact on runoff predictions. Third, aggregation strategies for heterogeneous SuDS deployments at the street-scale were examined using Monte Carlo simulation to evaluate the trade-offs between model efficiency and hydrological accuracy. Finally, the proposed modelling framework was demonstrated through application to a real-world urban catchment.

At the device-scale, unsaturated drainage was shown to exert strong control over detention behaviour, and a revised hydraulic conductivity formulation (*NewHCF*) was proposed. This provided more stable and structurally consistent predictions than conventional exponential or power-based approaches. Also, at the device-scale, simplified representations frequently overestimated SuDS performance and were unreliable when internal drainage dynamics governed system response. At the street-scale, typology-based aggregation (*LumpN*) preserved overall runoff dynamics (NSE generally > 0.9 and exceeding 0.95 in application), whereas full aggregation (*LumpOne*) produced severe errors in heterogeneous systems, including runoff underestimation of up to 80–90% in extreme cases.

Overall, the study demonstrates that reliable SuDS modelling requires a balance between model detail, predictive accuracy and computational complexity, with modelling strategies needing to adapt as objectives and levels of aggregation change.

Contents

List of Figures

List of Tables

List of Abbreviations

ADWP	Antecedent Dry Weather Period
BIO	Bioretention
BS	Bioswale
CN	Curve Number
CSO	Combined Sewer Overflow
ET	Evapotranspiration
FC	Field Capacity
GI	Green Infrastructure
GR	Green Roof
GRR	Greenfield Runoff Rate
HCF	Hydraulic Conductivity Function
LID	Low Impact Development
MCS	Marie Curie Substrate
MRA	Mining Remediation Authority
NSE	Nash-Sutcliffe model efficiency
PE	Peak Runoff Error
PET	Potential Evapotranspiration
PP	Permeable Pavement
PWP	Permanent Wilting Point
RDP	Rainwater Downpipe Planter
SuDS	Sustainable Drainage System
SWMM	Storm Water Management Model
SWRC	Soil Water Release Curve
WSUD	Water Sensitive Urban Design

List of Symbols

A_i	SuDS treated area in each subcatchment
b	Shapter parameter in Campbell function
d_{50}	50% pass particle size
ET	Evapotranspiration
h	Suction head
HCO	Soil hydraulic slope
$K(h)$	Unsaturated hydraulic conductivity at suction head h
$K(S_e)$	Unsaturated hydraulic conductivity at S_e
K_{Sat}	Saturated hydraulic conductivity
q_m	Simulated data
q_o	Observed data
R_t^2	Coefficient of determination
S_{act}	Actual saturation
S_e	Relative saturation
T	Total number of observed data
u	Empirical parameter in the *NewHCF* formulation
Var_{Lump}	SuDS parameter in *LumpN* and *LumpOne* methods
Var_i	SuDS parameter in *Detailed* method in each subcatchment
w	Empirical parameter in Durner model
Z	Elevation of discretised spatial step
α_1, n_1, m_1	Empirical parameters in Durner model
α_2, n_2, m_2	Empirical parameters in Durner model
ΔS	Storage volume in substrate
θ	Substrate moisture content
θ_{FC}	Moisture content at field capacity

θ_{PWP}	Moisture content at permanent wilting point
θ_r	Residual moisture content
θ_S	Saturated moisture content
ψ	Suction head (*kPa*)

1. Introduction

1.1 Background

Urban drainage systems are facing increasing pressure as a result of rapid urbanisation, climate change, and the progressive ageing of existing infrastructure. The expansion of impervious surfaces associated with urban growth has substantially altered natural hydrological processes, leading to increased runoff volumes, higher peak flows, and reduced infiltration. These changes have contributed to a growing incidence of surface water flooding, combined sewer overflows (CSOs), and the degradation of receiving water bodies in many urban areas. Climate change projections further intensify these challenges, with anticipated increases in rainfall intensity and variability placing additional strain on drainage systems that were largely designed based on historical conditions and deterministic design storm approaches.

Traditional responses to urban flooding have focused on expanding or upgrading existing drainage infrastructure. However, such approaches are increasingly recognised as economically costly, spatially constrained, and environmentally unsustainable, particularly in dense urban environments where opportunities for large-scale infrastructure expansion are limited. As a result, there has been a paradigm shift in urban water management towards more decentralised and process-oriented solutions that seek to manage stormwater runoff closer to its source.

Sustainable Drainage Systems (SuDS) have emerged as a central component of this shift. By promoting infiltration, storage, evapotranspiration (ET), and delayed release of runoff, SuDS aim to restore elements of the pre-development hydrological regime that are disrupted by urbanisation. Internationally, similar concepts are referred to as Low Impact Development (LID), Water Sensitive Urban Design (WSUD), or Green Infrastructure (GI), reflecting a shared emphasis on distributed, nature-based approaches to stormwater management. In the UK context, the growing policy emphasis on SuDS—including the proposed implementation of Schedule 3 (Department for Environment Food & Rural Affairs, 2023) of the Flood and Water Management Act—signals a transition from optional best practice to regulatory expectation, particularly for new developments and major redevelopments.

As SuDS adoption increases, so too does the need for robust tools to predict their hydrological performance. Modelling plays a crucial role in supporting SuDS design and planning, enabling engineers and decision-makers to assess runoff reduction, peak flow attenuation, and downstream impacts prior to construction. Among the modelling tools currently used in practice, the U.S. EPA Storm Water Management Model (SWMM) has become one of the most widely adopted platforms for urban drainage analysis, owing to its open-source availability. Unlike conventional drainage assets, however, SuDS performance is governed by a combination of interacting hydrological processes, including rainfall interception, infiltration, percolation, evapotranspiration, drainage, and overflow, that are strongly influenced by material properties, antecedent conditions, and device configuration. These processes are inherently dynamic and nonlinear, posing challenges for representation within operational hydrological and hydraulic models, including widely used tools such as the SWMM LID module.

The complexity of SuDS modelling becomes particularly evident when considering scale. At the device-scale, detailed representations of internal processes can provide valuable physical insight and improve predictive accuracy, and are increasingly supported within modelling tools, such as the SWMM LID module. However, such representations often require extensive parameterisation and incur significant computational cost, limiting their practicality for large networks or long-term simulations. To add complexity, at larger spatial scales, such as streets or subcatchments, SuDS are typically deployed in fragmented and heterogeneous patterns, reflecting local design choices, site constraints, opportunities, and decentralised implementation strategies. At these scales, fully resolved modelling of each individual SuDS device may be impractical, motivating the use of simplified or aggregated modelling approaches.

In engineering practice, simplifications are unavoidable. SuDS are frequently represented using reduced-order models, lumped parameterisations, or proxy representations embedded within conventional drainage network models. While these approaches improve computational efficiency and facilitate integration with legacy models, they inevitably involve assumptions about hydrological processes and spatial homogeneity. The consequences of these assumptions, for predicted runoff volumes, peak flows, and hydrograph timing, are not yet fully understood, particularly under continuous rainfall conditions and when multiple SuDS types or configurations coexist.

Several key knowledge gaps arise from this context. First, within many SuDS devices, water movement through engineered media occurs predominantly under unsaturated conditions. However, unsaturated flow is commonly represented using highly simplified formulations, and the accuracy of these approaches when applied to engineered substrates remains insufficiently evaluated. The suitability of these formulations for engineered substrates remains uncertain. Second, at the device-scale, a range of simplified modelling strategies is widely used in practice, but there exists limited systematic evaluation of how such simplifications affect hydrological predictions relative to more physically explicit representations. Third, at the street scale, the aggregation of multiple SuDS devices that are often heterogeneous in type and configuration introduces further uncertainty regarding the validity of lumped or averaged parameterisations.

Addressing these challenges requires a structured investigation into how SuDS hydrological processes are represented and simplified across spatial scales. A clearer understanding of the implications of model simplification and aggregation is essential to support reliable SuDS design, evaluation, and large-scale implementation in contemporary urban drainage systems.

1.2 Aim and Objectives

The overall aim of this research is to develop, test, and synthesise modelling frameworks for predicting the hydrological performance of SuDS across multiple spatial scales, from individual devices to street-scale implementations. Rather than proposing a new universal modelling tool, the research seeks to critically evaluate how different levels of process representation and model simplification influence predictive accuracy, robustness, and practical applicability in engineering design and planning contexts.

To address this aim, the thesis is structured around four interconnected research objectives, each targeting a key source of uncertainty in SuDS hydrological modelling:

Objective 1:

To evaluate and improve the representation of unsaturated percolation in engineered media used in device-scale SuDS devices.

This objective focuses on the hydraulic conductivity functions (HCFs) employed to describe unsaturated flow within SuDS growing media and aggregate layers. Laboratory data and existing formulations are analysed to assess the suitability of commonly used approaches derived from natural soils. A revised HCF formulation is proposed and evaluated to better capture unsaturated percolation behaviour in engineered media (Chapter 3).

Objective 2:

To quantify the hydrological accuracy of simplified device-scale SuDS modelling approaches.

This objective examines how commonly used simplifications—such as representing SuDS using generic storage, routing, or land-use conversion approaches—affect predictions of runoff retention and detention. Using detailed SWMM-LID representations as a baseline, a series of simplified modelling frameworks are developed and tested for both green roofs and bioretention systems under design storms and continuous rainfall conditions (Chapter 4).

Objective 3:

To evaluate aggregation strategies for modelling SuDS performance at the street-scale under parameter heterogeneity.

This objective investigates how multiple SuDS devices, potentially varying in type and configuration, can be aggregated within a subcatchment-scale model without unacceptable loss of hydrological accuracy. Monte Carlo simulation is employed to explore the sensitivity of aggregated model performance to parameter variability and to assess the feasibility of rapid modelling strategies for heterogeneous SuDS implementations (Chapter 5).

Objective 4:

To demonstrate the practical application of the proposed modelling framework through a real-world street-scale case study.

This objective applies the developed methods to an urban catchment, illustrating how the findings from street-scale analyses can inform engineering SuDS implementation strategies in practice (Chapter 6).

Together, these objectives establish a coherent multi-scale investigation into SuDS hydrological modelling, providing both theoretical insight into key process representations and practical guidance for engineers and planners tasked with evaluating SuDS performance under real-world constraints.

1.3 Thesis Structure and Content

This thesis comprises 7 chapters.

Chapter 1 introduces the background and motivation for the research. It outlines the increasing challenges associated with urban runoff management, the growing reliance on SuDS, and the central role of hydrological modelling in supporting SuDS design and assessment. The chapter defines the overall research aim, sets out the specific objectives, and positions the thesis within the context of current engineering practice and scientific knowledge gaps.

Chapter 2 reviews the literature that underpins the research objectives. It provides a synthesis of existing knowledge on SuDS concepts, hydrological processes, and modelling approaches across different spatial scales. Particular attention is given to unsaturated flow in engineered media, device-scale SuDS modelling, and aggregation strategies at the street-scale. The chapter identifies limitations in current modelling practice and highlights gaps that motivate the subsequent methodological investigations.

Chapter 3 focuses on unsaturated flow in engineered media used within SuDS devices. It critically examines the representation of percolation processes in widely used hydrological models and evaluates the suitability of existing hydraulic conductivity formulations derived from natural soils. Based on experimental evidence, the chapter proposes and assesses an improved hydraulic conductivity function for describing unsaturated percolation in engineered substrates.

Chapter 4 investigates simplified modelling approaches for SuDS at the device-scale. Using SWMM-LID representations as a baseline, this chapter evaluates the hydrological accuracy of commonly adopted simplifications that may be used when explicit SuDS modules are unavailable or impractical. The analysis focuses on green roofs and bioretention systems and examines the implications of simplification for runoff volume, peak flow, and hydrograph timing under both design storm and continuous simulation conditions.

Chapter 5 extends the analysis to the street-scale by examining strategies for aggregating multiple SuDS devices within subcatchment-scale models. This chapter evaluates different aggregation frameworks for both homogeneous and heterogeneous SuDS implementations and employs Monte Carlo simulation to explore the influence of parameter variability on model accuracy. The results provide insight into the feasibility and limitations of rapid modelling approaches for complex, real-world SuDS configurations.

Chapter 6 presents a real-world case study application, using the Mining Remediation Authority (MRA), Mansfield site to demonstrate the practical implementation of the proposed modelling framework. The chapter illustrates how street-scale findings can be combined to support engineers to assess the cumulative hydrological impact of SuDS retrofitting at the urban street-scale.

Chapter 7 synthesises the findings from Chapters 3 to 6 and discusses their implications for SuDS hydrological modelling and urban drainage practice. The section on practical implications explains how the SuDS modelling framework developed in this thesis can be applied in real engineering contexts. The limitations section outlines potential constraints in the research process, including overlooked conditions and the risks associated with limitation of using validation data. The chapter concludes with a discussion of future research directions, highlighting opportunities to strengthen validation of simplified modelling approaches and to extend aggregation frameworks to larger spatial scales and integrated urban water management applications.

1.4 Publications

Chapter 3:

De-Ville, S., **Ren**, **S.**, Stovin, V., 2025. Bioretention column detention test data for percolation model evaluation. *Urban Water Journal* 22, 693–705. https://doi.org/10.1080/1573062X.2025.2495874

De-Ville, S., **Ren, S.**, Stovin, V., 2025. A New Hydraulic Conductivity Function for LID Percolation Modelling in SWMM. Presented at the *Urban Drainage Modelling Conference 2025*.

(My main contribution was the conceptual development, analysis and validation of the new hydraulic conductivity function.)

Chapter 4:

Ren, S., De-Ville, S., Stovin, V., 2025. Evaluation of SuDS Device-scale Simplified Modelling Methods in SWMM. Presented at the *Urban Drainage Modelling Conference 2025*.

Ren, S., De-Ville, S., Stovin, V., 2026. Evaluation of SuDS device-scale simplified modelling methods. *Nature-Based Solutions* 9, 100319. https://doi.org/10.1016/j.nbsj.2026.100319

(I led the study design, methodology development, data analysis, visualisation, validation and manuscript writing.)

Chapter 5:

Ren, S., De-Ville, S., Stovin, V. Performance of SuDS Aggregation Methods at the Street Scale: A Monte Carlo Assessment and Case Study Application (Under review).

(I led the study design, modelling framework, data analysis, visualisation, validation and manuscript writing.)

2. Literature Review

2.1 Urban Drainage

Urban expansion fundamentally reshapes the natural hydrological cycle by altering both land cover and subsurface conditions. As cities grow, natural vegetation and permeable soil are replaced with lawns, paved surfaces, and compacted ground, reducing opportunities for infiltration, evapotranspiration (ET) and groundwater recharge (Hibbs and Sharp, 2012). At the same time, natural watercourses are often redirected or replaced by piped drainage networks, and local topography is levelled to accommodate construction and transport infrastructure (Gomes et al., 2012). These modifications simplify and harden the landscape, removing many of the physical features that previously moderated stormwater pathways. In urban redevelopment projects, the proportion of impervious surfaces often increases as the built environment intensifies (Davis et al., 2022; Hekl and Dymond, 2016).

The expansion of impervious infrastructure, such as rooftops, roads, and car parks, disrupts natural infiltration and exfiltration processes. These surfaces increase the proportion of rainfall that is rapidly converted into surface runoff. The altered water balance leads to a range of consequences: higher and more frequent flood peaks, accelerated stream channel erosion, reduced baseflow contributions, and the deterioration of downstream water bodies (Davis et al., 2022; Digman et al., 2012; Woods-Ballard et al., 2015; Zevenbergen et al., 2010). In cities served by combined sewer systems, these hydrological changes translate directly into more frequent and severe combined sewer overflow (CSO) events, whereby untreated wastewater is discharged to receiving waters during storm conditions to prevent sewer surcharge. CSOs pose significant risks to aquatic ecosystems, public health, and amenity value, and their impacts are increasingly subject to regulatory scrutiny and public concern (Perry et al., 2024).

Climate change further amplifies these pressures by altering rainfall characteristics, particularly through increases in rainfall intensity and the frequency of extreme events. Evidence suggests that even modest changes in precipitation regimes can significantly affect CSO frequency, duration, and seasonal distribution (Fortier and Mailhot, 2015). When superimposed on already urbanised catchments, these changes exacerbate the limitations of conventional drainage infrastructure, which was typically designed using deterministic design storms and historical climate assumptions. Expanding sewer capacity may provide effective hydraulic control in some contexts, but it is not always the most economically. As there is also a growing body of literature and evidence to the contrary, e.g. the Gill et al. (2021) Storm Overflows Evidence Report, where SuDS were found to be a more expensive solution to reducing CSOs compared with grey solutions (e.g. storage tanks). Its cost-effectiveness depends on the scope of assessment, including capital costs, construction disruption, long-term maintenance, management requirements and wider environmental and social benefits. When these wider benefits are included, SuDS can offer a complementary and potentially valuable alternative to conventional sewer expansion (Johnson and Geisendorf 2019; Ossa-Moreno et al., 2017). As a result, there is growing recognition that upstream, decentralised interventions are required to manage runoff at source, reduce inflows to combined sewer networks, and improve overall system resilience.

In this context, Sustainable Drainage System (SuDS) have gained increasing attention as a complementary approach to conventional drainage. By reducing runoff volumes, increasing flow concentration times, and redistributing stormwater storage across the urban landscape, SuDS have been shown to substantially mitigate CSO discharges under a wide range of rainfall conditions, often at a fraction of the cost of large end-of-pipe storage solutions (Joshi et al., 2021). Importantly, their effectiveness depends not only on individual device performance, but also on deployment strategy, spatial configuration, and interaction with existing drainage networks. These factors underscore the need for robust hydrological modelling frameworks capable of evaluating SuDS performance under both current and future climatic conditions.

2.2 Sustainable Drainage System (SuDS)

2.2.1 Concept of SuDS

Sustainable Drainage System (SuDS) are integrated networks of engineered vegetated areas and open spaces designed to effectively manage surface water runoff from developed areas, aiming to mimic natural hydrological processes. Specifically, SuDS serve as a complement to centralized conventional sewer networks to mitigate the hydrological urbanization impacts and improve resilience and robustness to extreme rainfall events in urban areas (Lisenbee et al., 2021; Liu et al., 2014). Additionally, SuDS can provide multiple environmental, ecological and social benefits (Figure 2.1) (Hamann et al., 2020). In various contexts, SuDS may be referred to using several similar terms, including Best Management Practices (BMPs) (Schueler, 1987), Green Infrastructure (GI) (Benedict and McMahon, 2012), Low Impact Development (LID) (Dietz, 2007), source control, sponge city (Xia et al., 2017), and Water Sensitive Urban Design (WSUD) (Wong, 2006).

SuDS are designed to play a central role in re-establishing natural hydrological processes within urban environments. Rather than allowing rainfall to be rapidly conveyed away, SuDS seek to retain soil moisture, maintain water balance, and safeguard natural baseflows across a wide range of rainfall conditions, from minor showers to more intense storm events. In this way, SuDS aim to replicate the key ecological functions of pre-development catchments, ensuring that runoff is managed in a manner consistent with natural systems. These objectives are addressed through a set of integrated measures, including the capture, infiltration, temporary storage, conveyance and on-site treatment of rainfall, with a preference for surface-based rather than subsurface solutions. By employing such strategies, SuDS not only moderate hydrological impacts but also contribute to the creation and improvement of green spaces within developments. In doing so, they strengthen connections with wider ecological networks and foster habitats where wildlife can thrive. For communities, the added value of SuDS extends beyond flood management, offering enhanced wellbeing, healthier living environments, and greater quality of life. Collectively, these outcomes can also yield economic advantages by improving property values and supporting local prosperity.

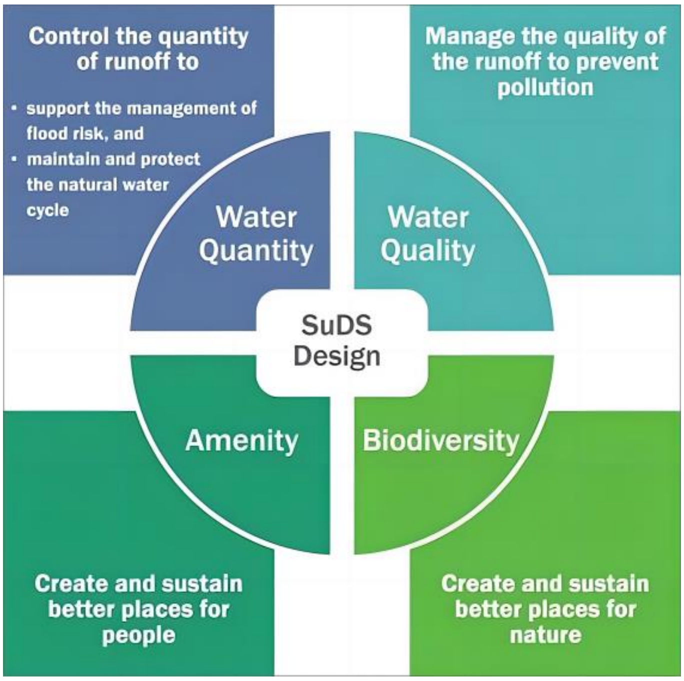

Figure 2.1. Four pillars of SuDS design (Woods-Ballard et al., 2015)

SuDS are particularly effective in mitigating surface water runoff and flooding resulting from urbanization. Uncontrolled surface water runoff from impermeable sites typically exhibits significantly higher peak rates compared to the same site in its greenfield state (Figure 2.2). The accelerated runoff from developed sites, compared to greenfield sites, leads to diminished water infiltration and interception. On sites with naturally sandy, well-drained soils, peak runoff rates could be at least an order of magnitude higher. Consequently, such uncontrolled runoff poses substantial risks to receiving watercourses by elevating flow velocities and the probability of flooding and bank erosion. The risks are further amplified when sites discharge into existing piped drainage networks, given their restricted capacities and susceptibility to flow rate fluctuations.

By reducing surface runoff, the volume of rainwater entering a combined sewer system is also decreased, resulting in several benefits. Firstly, the likelihood and severity of CSO events are reduced (Ghodsi et al., 2021; Muhandes et al., 2022; Stovin et al., 2013a), thereby lowering the risk of pollution incidents, protecting water quality, and safeguarding public health. Secondly, SuDS relieve pressure on wastewater treatment facilities by reducing hydraulic loads, which not only decreases energy and operational costs but also improves the reliability of treatment performance during storm events.

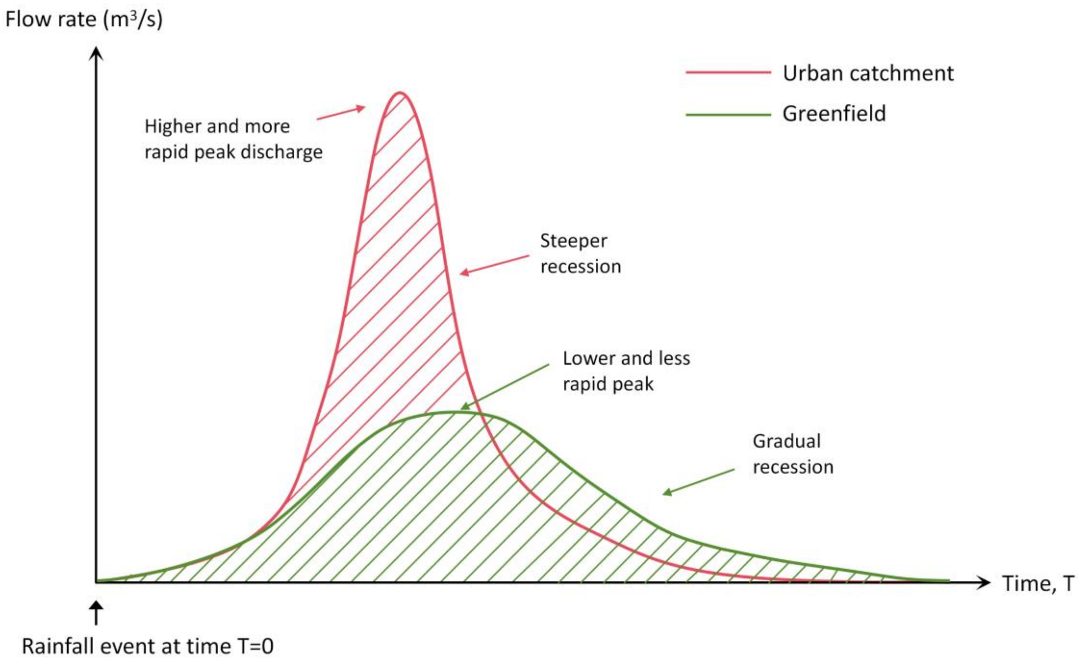

Figure 2.2. Example of a runoff hydrograph

SuDS should be conceptualised as an integrated system rather than individual components, devised to comprehensively manage, treat, and optimise the utilization of surface water from its point of origin as rainfall to its ultimate discharge into the receiving environment beyond the site boundaries. SuDS components perform up to six specific functions, contributing to the overall effectiveness and efficiency of the SuDS approach (Davis et al., 2022; Woods-Ballard et al., 2015):

1. Rainwater harvesting. These components are designed to capture rainfall for beneficial use, thereby reducing runoff volumes while providing an alternative water source that alleviates demand on potable supplies. The economic benefits of harvesting can be significant, particularly where large cisterns are used in commercial or institutional buildings. At the household scale, smaller rain barrels attached to downspouts are common approaches.

2. Pervious surfaces. Surfaces such as green roofs and permeable pavements allow rainfall to infiltrate, with subsequent removal via evaporation, transpiration, exfiltration or controlled overflow. Many systems also incorporate subsurface storage and treatment layers. Through these mechanisms, runoff quality is improved by filtering sediments and other pollutants.

3. Infiltration. Purpose-built storage features with permeable bases and sides, such as infiltration trenches and basins, facilitate the percolation of stored water into underlying soils. In addition to reducing surface runoff, they also contribute to the recharge of groundwater where conditions allow.

4. Conveyance. Vegetated channels such as swales convey stormwater to downstream controls while also attenuating flows, promoting infiltration, and filtering pollutants. These systems represent a departure from traditional pipes by slowing and treating runoff during transport.

5. Storage & attenuation. These components serve the crucial function of regulating the flow rates and, whenever feasible, volumes of runoff discharged from the site by storing water and releasing it gradually. Furthermore, many also provide water quality benefits, such as sedimentation of suspended solids, adsorption by soils, and bioremediation through plants and microbial processes, e.g. within a pond.

6. Treatment. Treatment elements remove or degrade contaminants in stormwater, often by harnessing physical, chemical, and biological processes. These components are typically embedded within other SuDS measures, enhancing pollutant removal and protecting downstream watercourses.

With the increase in SuDS applications, it is crucial to consider the cumulative effect of all SuDS devices within the catchment area, especially when coupled with the potential effects of climate change. The collective influence of multiple SuDS installations on the hydrological system warrants careful consideration and evaluation (Woods-Ballard et al., 2015).

2.2.2 Different Types of SuDS Components

SuDS encompass a wide spectrum of measures that vary in form, function, and scale, but collectively aim to manage stormwater in a more sustainable and resilient manner. These measures can be categorised according to their physical form, ranging from vegetated systems like swales and bioretention cells to structural systems such as permeable pavements and rainwater harvesting units.

The following sections therefore provide an overview of the four types of SuDS within the thesis – green roofs, bioretention systems, permeable pavements and rainfall downpipe planters. These systems were selected because they represent widely implemented SuDS categories with distinct structural configurations and dominant hydrological processes, allowing for systematic comparison of modelling approaches. The discussion then considers how these components can be strategically integrated and applied at varying spatial scales to address the challenges of urban water management. Section 2.3 provides detailed descriptions of the key hydrological processes.

2.2.2.1 Green Roofs

Green roofs (GR) are vegetated systems installed on the rooftops of buildings (Figure 2.3), typically consisting of a growing medium, drainage and filter layers, and waterproofing membranes. They function as source-control measures to manage rainfall close to the point of impact by capturing precipitation on building surfaces that would otherwise generate immediate runoff. Green roofs can be broadly categorised into extensive systems, which are lightweight and shallow, and intensive systems, which support deeper substrates and more diverse vegetation (Woods-Ballard et al., 2015).

Figure 2.3. University of Sheffield green roof performance monitoring test bed, during vegetation establishment phase

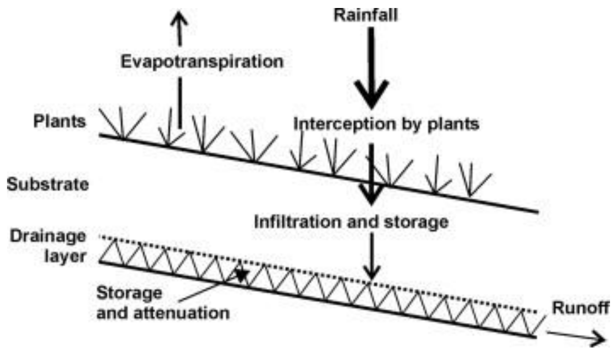

Figure 2.4. Green roof hydrological processes (Stovin et al., 2012).

Green roofs function as source-control measures that can effectively mitigate and delay stormwater runoff. When rainfall occurs, several hydrological processes take place (Figure 2.4): precipitation is first intercepted by the vegetation layer, after which water infiltrates and is retained within the substrate. Additional storage is provided in the underlying drainage layer, which acts as a temporary reservoir. Once this storage capacity is exceeded, surplus water is conveyed into the downstream drainage network. Between storm events, part of the retained water is gradually removed through evapotranspiration (ET), thereby restoring the system's capacity for subsequent rainfall (retention).

A substantial body of empirical work has established that green roofs can markedly influence the water balance of urban catchments by reducing, detaining, and delaying stormwater runoff. Retention and detention behaviour are strongly controlled by rainfall depth, antecedent moisture conditions, and substrate properties such as depth, porosity, and organic content.

Field monitoring under UK conditions showed that an extensive test bed retained on average 50% of annual rainfall, with mean peak-flow reductions of about 60% during significant storm events, although retention decreased sharply as storm depth increased (Stovin et al., 2012). In a four-year dataset from nine test beds, vegetation treatments improved rainfall retention and peak attenuation compared with unvegetated controls, and deeper or more moisture-retentive substrates enhanced performance for events below 5 mm rainfall depth (Stovin et al., 2015). Complementary laboratory experiments confirmed that detention capacity increases with substrate depth and organic content, and that a one-parameter reservoir-routing model can reliably reproduce observed delay times and runoff attenuation (Yio et al., 2013). High-resolution monitoring of vertical moisture profiles revealed that moisture responses occur almost simultaneously across substrate depths once field capacity (FC) is exceeded, and that hydraulic conductivity functions strongly influence both runoff rate and water-content distribution (Peng et al., 2019). These findings highlight the importance of substrate hydraulic characteristics in determining the onset and duration of roof runoff.

Building on these empirical insights, model development has progressively incorporated the dominant hydrological controls identified in monitoring studies. Stovin et al. (2013a) proposed a conceptual hydrological flux model (Figure 2.4) for the long-term continuous simulation, demonstrating that retention performance depends not only on physical configuration, but also on climatic controls, particularly rainfall depth and the recovery of retention capacity through evapotranspiration. Their results showed strong climate dependency, with volumetric retention ranging from 0.19 in cool-wet regions to 0.59 in warm-dry areas, and highlighted the dominance of small, frequent storms in overall performance.

Subsequent studies have extended and reinforced these findings. A similar water-balance modelling framework (Figure 2.4), additionally incorporating alternative evapotranspiration formulations and Green–Ampt infiltration, calibrated across multiple green-roof configurations, achieved high predictive accuracy (Nash–Sutcliffe efficiencies of 0.93–0.98) and identified initial substrate moisture as the most sensitive parameter influencing runoff response (Liu et al., 2021). Similarly, large-scale simulations across eight climatic zones in China confirmed substantial climate dependence, with retention rates from 28% ± 3% in humid Guangzhou to 84% ± 5% in arid Urumqi, emphasising both the influence of climate and the potential to enhance performance though configuration optimisation (Yan et al., 2022). Modelling studies further demonstrated that detention behaviour is highly event-dependent, with antecedent moisture conditions and storm characteristics exerting strong influence on runoff attenuation (Stovin et al., 2017). Together, these studies consistently indicate that climate, antecedent moisture conditions, and substrate design are key determinants of green roof hydrological performance through modelling study.

At broader spatial scales, watershed-based simulations in the Pacific Northwest showed that even when roof areas constitute only about 10% of total catchment area, widespread installation could reduce mean annual runoff by 10-15% for extensive and 20-25% for intensive systems, though reductions diminish during high-flow regimes when storage capacity becomes exhausted (Barnhart et al., 2021).

Collectively, these studies demonstrate that green roofs are most effective for small to medium rainfall events, where retention and detention mechanisms operate efficiently before substrates become exhausted. Performance is governed by substrate and vegetation configuration, hydraulic conductivity, and climatic drivers, while at city scale their cumulative impact can yield measurable reductions in runoff volumes and peak discharges. Despite inherent limits under extreme storms, the evidence confirms that well-designed green roofs function as reliable source-control measures capable of mitigating frequent urban runoff events and contributing to overall flood-risk reduction.

2.2.2.2 Bioretention

Bioretention systems (BIO), also referred to as rain gardens or biofilters, are vegetated depressions designed to collect, store, and infiltrate stormwater runoff close to its source (Figure 2.5). They are among the most versatile SuDS components, combining hydrological control with pollutant treatment within an engineered soil-plant system (Woods-Ballard et al., 2015). Typically, a bioretention cell consists of a vegetated surface layer, a filter media layer of engineered soil, an optional internal water storage zone, and an underdrain for controlled discharge. Water entering the system is temporarily stored in the surface ponding area, then filtered vertically through the media where exfiltration, evapotranspiration, subsurface storage processes and outflow controls act to reduce runoff volume and peak flow before release or infiltration to the ground.

Figure 2.5. Picture of Courthouse raingarden (De-Ville et al., 2024)

The hydrological behaviour of bioretention (Figure 2.6) is governed by infiltration, percolation, ET, temporary storage, exfiltration, and delayed drainage (i.e., underdrain flow). During a rainfall event, water initially becomes surface runoff on impervious surfaces and subsequently enters the bioretention. Within the bioretention, the rainwater infiltrates the soil's pores, until it reaches FC. If the moisture level of the soil layer (substrate) exceeds the permanent wilting point (PWP), the rainwater will eventually be released from the system through ET. The soil's retention capacity corresponds to its FC minus PWP, representing the maximum quantity of capillary suspended water that can be sustained against the force of gravity. Once the substrate moisture reaches its maximum retention storage capacity, any additional water will start to fill the pores within the drainage layer under the influence of gravity. The exfiltration rate below the drainage layer is typically slower than the infiltration rate into the substrate and drainage layer, and it depends on the characteristics of the surrounding native soil. In most bioretention systems, ponding is allowed once the substrate becomes saturated, and any excess water will overflow. Ponding may also occur prior to saturation, if infiltration is slow. Processes in GR and BIO substrate are the same.

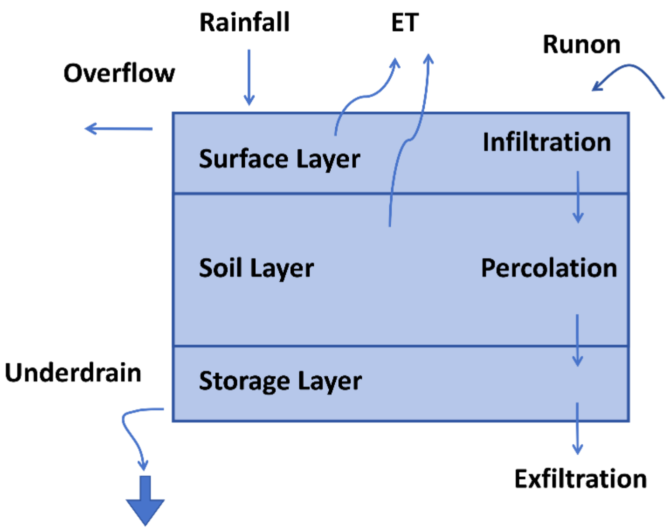

Figure 2.6. SuDS conceptual hydrological processes (Rossman, 2016a)

Field investigations consistently demonstrate that bioretention systems can substantially reduce runoff volume and peak flow. In a long-term monitoring study, Davis (2008) observed that two bioretention cells receiving parking-lot runoff in Maryland retained the entire inflow for nearly 20% of storm events, with mean peak-flow reductions of 49-58% and delays in peak timing by a factor of two or more. Chapman and Horner (2010) reported that a street side bioretention facility in Seattle lost 48-74% of inflow to infiltration and ET, confirming the combined role of media permeability and ET in real-weather conditions. Winston et al. (2016) monitored three cells constructed on clay soils and found runoff reductions of 36–59%, with peak-flow reductions up to 96% during moderate storms. The internal water storage zone thickness and exfiltration rate were identified as dominant controls on volume reduction.

These observed performance patterns are closely linked to the hydraulic behaviour of the engineered filter media. In particular, the unsaturated hydraulic conductivity of bioretention substrates is governed by complex pore-size distributions and particle interactions, which regulate how water is stored, transmitted, and released during storm events (Liu and Fassman-Beck, 2018, 2017). Variations in media composition therefore directly influence infiltration dynamics, moisture redistribution, and the timing of drainage, providing a mechanistic explanation for the strong sensitivity of runoff reduction to storage configuration and antecedent conditions observed in field studies (De-Ville et al., 2021).

Collectively, the evidence confirms that well-designed bioretention systems can achieve runoff volume reductions between 40% and 70%, peak-flow reductions exceeding 50%, and substantial delays in hydrograph response across a wide range of climates and soil conditions. Their performance depends strongly on media hydraulic properties, storage configuration, and local rainfall characteristics. Although less effective under prolonged or extreme rainfall due to limited storage capacity, bioretention cells remain one of the most effective SuDS options for controlling frequent urban storm events and restoring near-natural hydrological conditions.

2.2.2.3 Permeable pavements

Permeable pavements (PP) are load-bearing surface systems that allow rainfall to pass through a porous or jointed wearing course into a highly voided sub-base, where water is stored, exfiltrated to ground, or is slowly released via underdrains. As source-control measures within SuDS, they are commonly applied to parking areas (Figure 2.7), access roads, and pedestrian zones to mitigate surface runoff from impervious surfaces (Woods-Ballard et al., 2015).

Figure 2.7. Permeable pavements in Mansfield, UK

The hydrological processes in permeable pavements can be understood as a multi-layered system, as shown in Figure 2.8. When rainfall reaches the pavement surface, water penetrates through the permeable wearing layer, such as porous asphalt, permeable interlocking concrete blocks, or grass pavers, rather than forming surface runoff. The rate of infiltration depends on the surface porosity and joint configuration. After passing through the geotextile (bedding or joint-filling) layer, stormwater is briefly detained and filtered before percolating into the base or sub-base, where open-graded aggregates provide the main storage and attenuation capacity, reducing peak flow and prolonging discharge. Depending on design, water then either infiltrates into the subgrade in unlined systems or is conveyed laterally through an underdrain in lined systems, allowing controlled release to downstream drainage or infiltration zones. The hydrological functional layer structures of permeable pavement and bioretention systems are largely similar, with the primary distinction being the presence of an additional pavement layer in permeable pavement, typically consisting of a porous or permeable structural layer (Figure 2.6).

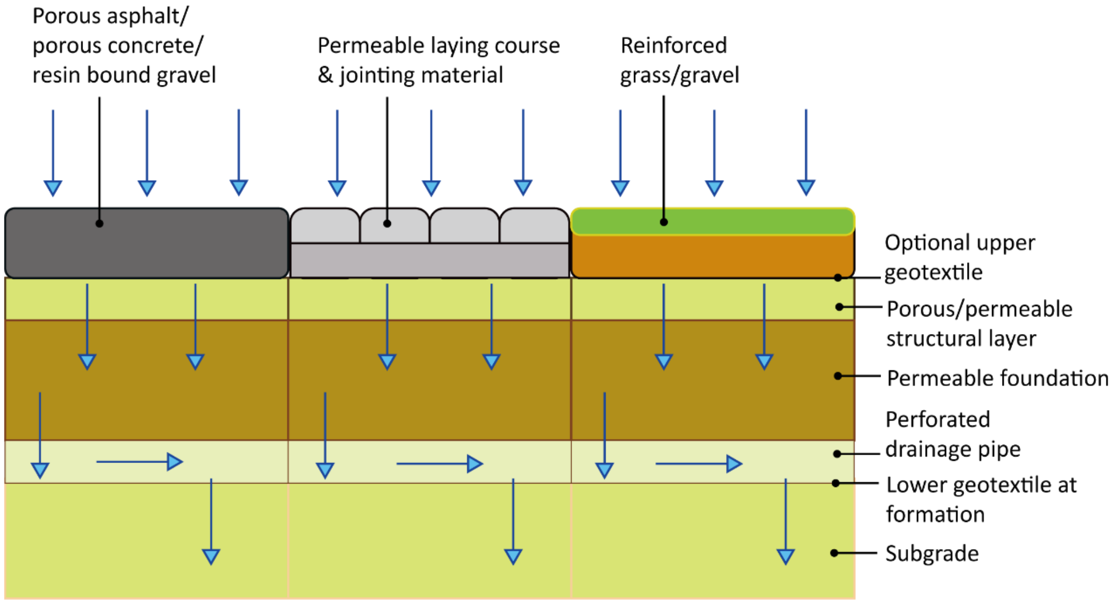

Figure 2.8. Pervious pavements components (Woods-Ballard et al., 2015)

Field observations demonstrate that permeable pavements can substantially restore natural infiltration dynamics. Ball and Rankin (2010) reported that a retrofitted urban street reduced effective imperviousness from 40% to below 5%, with runoff initiation requiring around 4 mm of rainfall or intensities above 20 mm/hr. In North Carolina, Collins et al. (2008) found all permeable pavement types reduced runoff volumes and peak flows significantly compared with asphalt, while extended storage in the base layer delayed peak timing. Even on steep or low-permeability sites, Fassman and Blackbourn (2010) observed underdrain discharges comparable to predevelopment flows and runoff coefficients of 0.3-0.7, confirming effective attenuation. Laboratory work further shows that both surface type and sub-base aggregate characteristics influence retention and lag times (Rodriguez-Hernandez et al., 2016).

Over time, infiltration capacity declines due to clogging, but long-term studies indicate performance remains satisfactory. Lucke and Beecham (2011) found more than 90% of trapped sediments accumulated within the paving and bedding layers, yet overall infiltration stayed functional after eight years. A review by Razzaghmanesh and Beecham (2018) highlighted the early decrease in surface infiltration within the first two years and the importance of appropriate cleaning regimes to sustain performance.

Model sensitivity analyses confirm that hydrologic performance is primarily controlled by storage depth, drain offset, exfiltration rate, and impervious fraction of the cell, while surface roughness, soil suction head, soil wilting point and soil conductivity slope are less influential (Madrazo-Uribeetxebarria et al., 2021). Design optimisation should therefore prioritise sub-base capacity and connectivity. Other reviewers also stress the need for integrated design linking hydraulic, structural, and maintenance aspects (Kuruppu et al., 2019)

Permeable pavements consistently reduce runoff volume, peak discharge, and effective imperviousness. Their efficiency depends on subsurface storage, exfiltration potential, and maintenance quality but can remain stable for many years. With proper design and upkeep, permeable pavements serve as one of the most reliable SuDS source-control options for restoring infiltration and mitigating urban runoff.

2.2.2.4 Rainfall Downpipe Planters

Rainfall downpipe planters (RDPs) are small-scale stormwater control devices (Figure 2.9) designed to intercept and manage runoff directly from building roofs. Roof runoff is typically conveyed through vertical drainage pipes, commonly referred to as downpipes or downspouts, which transport rainfall collected from roof surfaces to the ground drainage network.

Functionally, RDPs can be considered a compact form of source-control SuDS designed to manage roof-derived runoff close to its point of generation. RDPs typically operate as passive systems without mechanical pumping. Runoff attenuation is achieved through temporary storage, infiltration into the planter media, evapotranspiration by vegetation, and controlled drainage. Their distributed placement along building allows them to contribute to decentralised stormwater management by reducing the effective impervious area directly connected to urban drainage systems (Woods-Ballard et al., 2015).

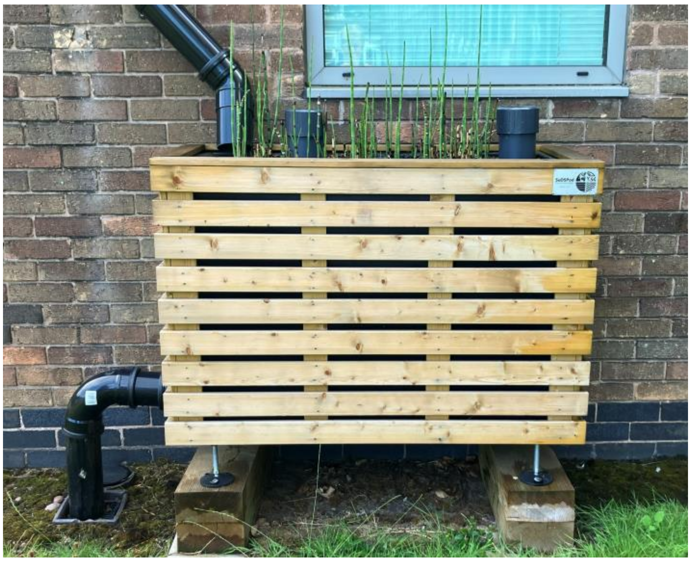

Figure 2.9. Rainfall downpipe planter in Mining Remediation Authority, Mansfield, UK (GreenBlue

Urban Ltd, 2026)

In some configurations, the conceptual hydrological behaviour of RDPs resembles that of small-scale bioretention systems (Figure 2.6). These systems therefore utilise multiple functional layers, providing limited infiltration, filtration, and detention within the soil profile to achieve source control. Other commercial RDPs operate differently, as illustrated in Figure 2.10. Although a vegetated surface layer is present, the majority of runoff storage occurs within a large internal chamber beneath the soil media. In such cases, the device can be conceptualised as a small detention tank equipped with a hydraulic flow control structure. Roof runoff entering from the downpipe is partially absorbed by the soil layer, but most of the inflow is conveyed into the main storage chamber. Outflow is then regulated through an internal flow control system, commonly an orifice or similar head-discharge mechanism, allowing water to be released gradually through the underdrain. This controlled release reduces peak discharge and increases runoff residence time, thereby providing attenuation before water re-enters the drainage network.

Empirical studies have demonstrated that rainfall downpipe planters can contribute to stormwater management by reducing runoff volumes and delaying discharge from roof drainage systems. Storage-based RDP systems, which function similarly to small detention cisterns, can provide measurable benefits for urban drainage networks. For example, Ghodsi et al. (2021) showed that cisterns could reduce combined sewer overflow (CSO) volumes by 8-18% in Buffalo, New York. Bioretention-type RDPs, rely on engineered substrate layers to provide additional hydrological regulation. Study by Nissen et al. (2026) demonstrated that flow-through bioretention planters are capable of capturing small rainfall events and delaying runoff discharge even under relatively high hydraulic loading conditions. During a 15-month monitoring campaign, 38% of rainfall events produced no measurable outflow, indicating complete runoff capture. When discharge occurred, lag times between rainfall onset and outflow ranged from 5 to 1,841 minutes, with a median delay of approximately 77.5 minutes.

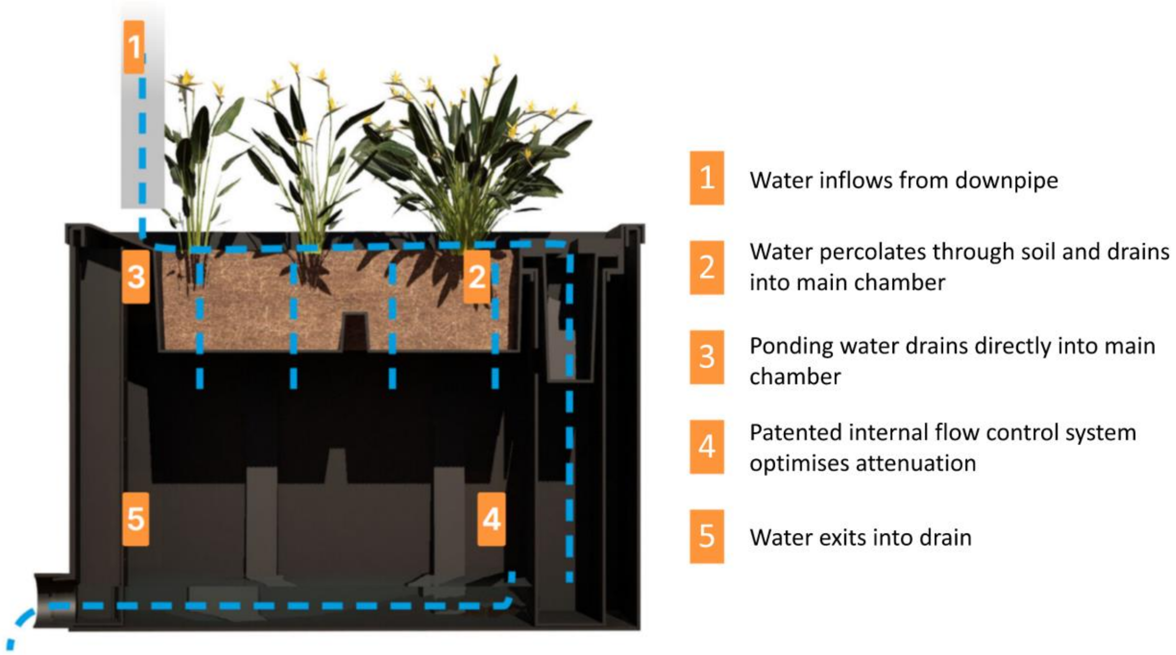

Figure 2.10. Rainfall downpipe planter example hydrological mechanism (GreenBlue Urban Ltd, 2026)

In conventional drainage systems, roof runoff is rapidly conveyed into the sewer system with little opportunity for storage, infiltration, or delay. RDPs modify this pathway by diverting roof runoff from the downpipe into a planter box located at ground level, where the water can be temporarily stored and filtered through engineered soil media before being discharged to the downstream drainage system. It should be noted that planter-based systems are also widely used as rainwater harvesting installations, where the primary objective is to capture and reuse roof runoff for non-potable water demand (de Sá Silva et al., 2022; Raimondi et al., 2023; Ward et al., 2012). This type RDP are not considered within the scope of this thesis.

2.3 SuDS Hydrological Processes

SuDS are designed to reproduce the natural hydrological cycle that is disrupted by urbanisation. Instead of rapidly conveying runoff through sealed drainage pipes, SuDS promote a series of surface and subsurface processes (as shown in Figure 2.6) that slow down, store, and infiltrate rainfall, thereby mitigating flood risk and restoring the pre-development water balance (Rossman, 2016b, 2016c, 2016a; Woods-Ballard et al., 2015). The hydrological functioning of SuDS can be broadly conceptualised as a continuum of interconnected processes — beginning with rainfall input and culminating in controlled discharge or infiltration of water to the natural environment. A water mass balance equation of the SuDS system is expressed as:

$$Inflow = ET + Infiltration + Overflow + Underdrain\ flow + \Delta S \quad \text{Equation 2.1}$$

where ΔS is the water storage volume in substrate (including ponding depth, pores in drainage layer and pores in substrate).

Rainfall and inflow. The hydrological cycle within SuDS begins with precipitation that reaches the system either directly from rainfall or as surface inflow from adjacent impermeable areas. The intensity, duration, and antecedent moisture condition strongly influence how much of this rainfall is initially intercepted by vegetation or stored in surface depressions. In vegetated systems such as green roofs and bioretention cells, part of the rainwater is intercepted by plant canopies before reaching the substrate, which slightly delays runoff generation and enhances subsequent evapotranspiration losses.

Infiltration and percolation. Once rainfall reaches the surface of the SuDS component, infiltration governs the downward movement of water through the porous surface or engineered soil medium. The infiltration rate depends on the hydraulic conductivity of the substrate or fill material, which typically decreases with depth and moisture saturation. As water infiltrates, it percolates through the unsaturated zone, replenishing storage layers or the base aggregate, where significant temporary detention occurs. This process attenuates peak flows and facilitates pollutant filtering through physical and biological mechanisms.

Exfiltration and groundwater interaction. In systems constructed without impermeable liners, infiltrated water can percolate further downward and exfiltrate into the underlying natural subgrade. This exfiltration process contributes to groundwater recharge and enhances baseflow restoration in nearby watercourses. Conversely, in lined systems or those installed above low-permeability soils, and stored water is conveyed laterally through outlets.

Underdrain and controlled outflow. The underdrain flow from SuDS occurs through designed drainage pathways such as underdrains, orifices, or weirs. These components regulate discharge rates to downstream systems, ensuring that post-development flows do not exceed pre-development conditions. Underdrains, often located at the base of SuDS systems, control both flow quantity and timing by providing a slow, delayed release of detained water. Orifice-controlled outlets achieve similar functions in detention-based SuDS such as ponds or tanks, maintaining system storage efficiency while preventing surcharge.

Overflow mechanisms. During high-intensity or prolonged rainfall, when storage and infiltration capacities are exceeded, overflow pathways provide a safeguard against flooding. These typically include bypass channels, raised outlets, or surface spillways that convey excess water away from the system while minimising erosion or structural damage. Effective overflow design is essential to maintain resilience under extreme storm events.

Evapotranspiration (ET). A distinctive feature of vegetated SuDS components is their ability to return stored water to the atmosphere through evaporation and plant transpiration. ET reduces the net volume of stored water, gradually restoring system capacity between rainfall events. The magnitude of ET losses varies seasonally and is influenced by vegetation type, substrate moisture, and local climate conditions. Over the long term, this process plays a critical role in balancing the hydrological budget of SuDS systems, restoring near-natural water pathways and mitigating UHI.

Collectively, SuDS performance can be understood of two primary functions: retention and detention, each achieved through distinct hydrological processes. Retention refers to any rainfall or inflow that does not ultimately become runoff. Depending on the SuDS type, this may occur through mechanisms such as capillary storage and subsequent ET within a vegetated substrate, infiltration into underlying soils, or permanent abstraction within a storage basin. In all cases, retained water is removed from the runoff pathway and does not contribute to downstream discharge.

Detention represents temporary storage that delays and attenuates runoff without permanently removing it from the system. This function may arise through resistance to vertical percolation in porous media, temporary surface ponding in basins, or controlled outlet that regulate discharge rates. In time-series terms, detention is expressed as a delay in runoff response and a reduction in peak flow magnitude.

Incorporating both retention and detention into stormwater modelling therefore enables a comprehensive water-balance framework while accurately representing the timing and magnitude of runoff hydrographs across different SuDS configurations.

2.4 Modelling Approaches for SuDS

SuDS performance reflects several hydrological processes (Section 2.3). Field monitoring is indispensable, but it cannot cover the breadth of climates, design configurations, operational scenarios, devices that have yet to be constructed and evaluated for planning and policy. Models therefore provide a structured means to quantify runoff generation and attenuation, test design alternatives, and explore long-term behaviour under changing boundary conditions (e.g., rainfall regimes, land use). The choice of approach hinges on the study aim, available data, computational budget, and the trade-off between physical realism and generalisability (Haghighatafshar et al., 2019a).

2.4.1 Process-Based Modelling Frameworks

Most SuDS models are fundamentally process-based, meaning that they represent physical mechanisms such as rainfall input, infiltration, percolation through the soil profile, evapotranspiration, drainage, and overflow. The governing principle behind these models is mass balance, using physically meaningful equations at varying levels of simplification (Lisenbee et al., 2021).

Process-based models can range from detailed mechanistic formulations to simplified empirical representations, but all are rooted in the same physical understanding of hydrological processes (Devia et al., 2015). Fully mechanistic models such as HYDRUS-1D (Šimůnek et al., 2006) and MIKE (DHI, 2024) explicitly solve the Richards and Saint-Venant equations to simulate variably saturated flow and surface routing (Liu and Fassman-Beck, 2017). These frameworks provide a physically rigorous representation of infiltration, percolation, and ET dynamics, making them highly suitable for research and process diagnostics. However, their complexity and intensive parameter requirements limits their use in routine engineering design.

To achieve broader application, many modelling systems employ physically based equations in simplified or aggregated forms. The Storm Water Management Model (SWMM) (Rossman, 2016b, 2016c, 2016a), for example, simulates rainfall-runoff transformation using continuity equations while representing infiltration through Green-Ampt or Horton formulations and outflow through orifice and underdrain equations. Its Low Impact Development (LID) module enables simulation of green roofs, bioretention cells, and other common SuDS devices, integrating hydrological processes within a single computational structure. Rather than resolving vertical moisture profiles or explicitly solving Richards equation, SWMM employs a depth-integrated percolation formulation in which vertical drainage through the growing media is represented as a bulk flux controlled by a single hydraulic conductivity function parameter. Percolation is modelled as an exponential decay function of volumetric moisture content above field capacity, governed by the saturated hydraulic conductivity and a single empirical coefficient (HCO), while drainage is assumed to cease entirely once moisture content falls below field capacity.

Recent developments have extended SWMM's process capabilities. The SWMM-UrbanEVA module introduced by Hörnschemeyer et al. (2021) adds explicit representation of vegetation and shading effects, substantially improving ET simulation accuracy (NSE improving from 0.47 to 0.87). Similarly, the SWMM-LITE approach (Dell et al., 2021) adapts the SWMM for municipal-scale hydrological assessments by retaining its rainfall-runoff and LID modules while omitting detailed hydraulic routing components. Subcatchments are defined based on administrative rather than strictly hydrological boundaries, and runoff is conveyed using simplified links that conserve volume without simulating attenuation within drainage networks. Despite this simplification, it achieves comparable annual runoff and infiltration predictions (±0.1%) with minimal data input. These advances show how physically grounded models can be simplified without losing essential hydrological realism. Other process-based models, such as InfoWorks ICM (Autodesk, 2025a), and MUSIC (eWater Ltd, 2005), also follow the same principles while providing different levels of spatial integration and computational efficiency.

In summary, these frameworks differ mainly in the extent of process simplification rather than in their physical foundations. All simulate infiltration and storage as functions of soil properties and moisture conditions, and all route drainage and overflow using hydraulically meaningful formulations. Whether applied at the scale of a single bioretention cell or an entire urban catchment, process-based models provide a consistent physical basis for evaluating SuDS performance.

However, several knowledge gaps remain. First, many simplified or aggregated implementations continue to rely on the core SWMM LID formulations for substrate percolation and evapotranspiration, yet the accuracy of these representations at the device-scale has not been systematically evaluated against alternative process descriptions under unsaturated conditions. Enhancements to ET and percolation modules have been proposed, but their implications for runoff prediction across different substrate configurations remain insufficiently quantified.

Second, while SWMM LID-based frameworks have been applied at subcatchment and catchment scales, the methodological implications of aggregating multiple homogeneous or heterogeneous SuDS devices within a single modelling structure have not been comprehensively tested. In practice, SWMM LID simplified model is used as baseline references in the absence of extensive monitoring data, yet the structural assumptions embedded within LID module formulations may propagate uncertainty when scaled beyond individual devices.

2.4.2 Spatial Representation of SuDS Components

While process-based formulations describe how hydrological mechanisms operate, spatial representation determines where these processes occur and how they interact across the catchment. SuDS models therefore differ in the way they handle spatial variability in rainfall, topography, land cover, and facility distribution.

Lumped models treat the catchment as a single unit with spatially averaged properties. They require minimal input and are suited for rapid screening and preliminary design. Tools such as MUSIC and simplified configurations of SWMM can operate in this mode, using aggregated parameters to estimate runoff, infiltration, and overflow. However, because they neglect spatial heterogeneity, their accuracy is limited for heterogeneous catchments or distributed SuDS layouts.

Semi-distributed models divide the catchment into multiple subcatchments or hydrological response units, each represented by a process-based water balance. Flow is routed between these units, allowing localised calibration and the explicit representation of SuDS placement. This structure has become the standard approach for urban hydrology because it balances physical realism and computational efficiency. For instance, SWMM is also a semi-distributed model, which operates by dividing a catchment into a collection of smaller subcatchment units, where hydrological processes are often represented using conceptual or semi-physical formulations.

Fully distributed models simulate water movement across gridded or finite-element domains, accounting for spatial variations in soil, slope, and land cover. Systems such as MIKE SHE represent the most detailed spatial approach, resolving both surface and subsurface flow at fine resolution. Although they provide a physically rich depiction of SuDS–catchment interactions, their data and runtime requirements are considerable.

While hydrological models are traditionally classified as Lumped, Semi-distributed, and Fully distributed, it is imperative to note that the boundaries between these categories are often fluid and overlapping in practical application, representing a spatial discretisation continuum rather than strict dichotomies (Hrachowitz and Clark, 2017; Jajarmizad et al., 2012). This fluidity is largely driven by the modular architecture of modern modelling platforms, which allows users to dynamically configure the spatial resolution. Many contemporary models can transition from a lumped setup to a configuration that closely approximates a fully distributed approach simply by increasing the number of computational units. Further complicating the classification is the inherent hybrid nature of many operational tools, such as the Storm Water Management Model (SWMM), which couple highly conceptualized curve number module for runoff generation (e.g., the SCS-CN method) with physically based hydraulic routing solutions (e.g., the Saint-Venant equations). Therefore, for a critical assessment, it is often more insightful to evaluate a model based on its core modelling philosophy—specifically, its requirements for process accuracy and data inputs—rather than fitting rigidly to its spatial terminology.

2.4.3 Emerging and Hybrid Techniques

Recent research increasingly integrates hydrological modelling with optimisation and data-driven algorithms to improve design and decision-making efficiency. The SUSTAIN framework (Lee et al., 2012) combines physically based simulation with optimisation algorithms to identify cost-effective configurations of stormwater best management practices at watershed scales. Similarly, Duarte Lopes and Barbosa Lima da Silva (2021) coupled SWMM with the NSGA-II genetic algorithm to optimise combinations of permeable pavements, bioretention cells, and green roofs under multiple rainfall return periods, generating sets of optimal trade-offs between cost and runoff reduction.

Parallel to these developments, data-driven techniques—such as neural networks, support vector machines, and random forests—are being explored to emulate process-based models or assist in parameter calibration (Elshorbagy et al., 2010; Solomatine and Ostfeld, 2008). However, as Lisenbee et al. (2021) emphasise, purely data-driven methods cannot fully replace physical models because they lack explicit representation of infiltration and evapotranspiration mechanisms. The most promising direction therefore lies in hybrid modelling, where physical equations define the structure of the system and data-driven components assist with calibration, optimisation, or prediction.

2.4.4 Concluding Remarks

All contemporary SuDS models are rooted in the same physical understanding of how water moves through urban systems. Whether formulated as detailed numerical solvers or simplified representations, they share a commitment to conserving mass and representing key processes such as infiltration, evapotranspiration, drainage, and overflow. Simplifications primarily serve practical needs, reducing data and computational demands without abandoning the physical principles that underpin hydrological credibility.

2.5 Unsaturated Flow in Engineered Media (feeds Ch.3)

Stormwater engineers increasingly rely on hydrological-hydraulic modelling tools to simulate SuDS performance across a range of rainfall conditions, from frequent small events to major storms. SWMM has become the most widely adopted open-source tool, featuring in nearly 40% of recent SuDS-related studies (Nazarpour et al., 2023). Its accessibility, integration with drainage network modelling, and inclusion of LID modules have made it a default choice for both research and design practice. However, the simplifications embedded within SWMM's process representations, particularly for percolation in unsaturated conditions, remain a key limitation for simulating engineered SuDS media.

In most SuDS systems, water movement through substrate or aggregate layers occurs primarily under unsaturated conditions, with only brief saturation phases during intense rainfall or near drain interfaces. Consequently, percolation within these systems is dominated by capillary and matric potential gradients rather than by gravitational flow alone. Accurately representing this unsaturated regime is crucial for predicting infiltration, retention, and delayed drainage behaviour.

Engineered media differ markedly from natural soils due to their controlled composition, artificial layering, and modified pore-size distributions, all of which alter the relationship between hydraulic conductivity and volumetric water content. These differences challenge the direct application of conventional soil-based hydraulic formulations in SuDS modelling.

Typical bioretention media comprise roughly 30-50% sand, 20-30% soil, and 20-40% organic matter by volume (De-Ville et al., 2021; Dietz and Clausen, 2005). The UK's SuDS Manual (Woods-Ballard et al., 2015) further recommends that such media achieve a porosity greater than 30%, particle-size distribution with d ⩾ 6 mm = 45%, and a saturated hydraulic conductivity between 100 and 300 mm/hr. Liu and Fassman-Beck (2018) provided detailed laboratory findings to define hydraulic conductivity functions across 14 distinct engineered media. Their work highlights a key consideration: the media commonly employed in green roofs and bioretention cells exhibits hydraulic behaviour different from that of conventional soil. These engineered mixtures are designed to balance rapid infiltration with sufficient retention for treatment processes and moisture supply to plants. However, their non-uniform pore structure—often bimodal or highly aggregated—means that flow rarely conforms to the assumptions underpinning standard unsaturated hydraulic models.

To describe transient unsaturated flow with physical rigour, physically based models such as HYDRUS-1D numerically solve the Richards equation (Equation 2.2) via finite element methods (Šimůnek et al., 2016).

To solve the Richards equation, the Soil Water Release Curve (SWRC) and the Hydraulic Conductivity Function (HCF) are needed. The van Genuchten model (Van Genuchten, 1980) for SWRC is presented in Equation 2.3. The Durner equation (Equation 2.4) (Durner, 1994) has been shown to provide a good representation of the SWRC for green roof substrates, and the Durner-Mualem equation (Equation 2.5, Equation 2.6 & Equation 2.7) was used to estimate unsaturated hydraulic conductivity as a function of the suction head (Peng et al., 2020).

$$\frac{\partial\theta}{\partial t} = \frac{\partial}{\partial Z}\left[K(h)\left(\frac{\partial h}{\partial Z} - 1\right)\right] \qquad \text{Equation 2.2}$$

$$K(S_e) = K_{Sat}S_e^{0.5}\left[1 - \left(1 - S_e^{\frac{1}{m}}\right)^{m}\right]^2 \qquad \text{Equation 2.3}$$

$$S_e = \frac{\theta - \theta_r}{\theta_S - \theta_r} = w[1 + (\alpha_1 h)^{n_1}]^{-m_1} + (1 - w)[1 + (\alpha_2 h)^{n_2}]^{-m_2} \qquad \text{Equation 2.4}$$

$$S_{e_1} = [1 + (\alpha_1 h)^{n_1}]^{-m_1} \qquad \text{Equation 2.5}$$

$$S_{e_2} = [1 + (\alpha_2 h)^{n_2}]^{-m_2} \qquad \text{Equation 2.6}$$

$$K(S_e) = K_{Sat}(wS_{e_1} + (1 - w)S_{e_2})^{0.5} \times \frac{\left(w\alpha_1\left\{1-\left(1-S_{e_1}^{\frac{1}{m_1}}\right)^{m_1}\right\} + (1-w)\alpha_2\left[1-\left(1-S_{e_2}^{\frac{1}{m_2}}\right)^{m_2}\right]\right)^2}{(w\alpha_1 + (1-w)\alpha_2)^2}$$

Equation 2.7

where θ (v/v) is moisture content, $K(h)$ is hydraulic conductivity (mm/min) at suction head h (mm) and Z (mm) is the elevation of the point relative to the reference level; S_e = relative saturation; θ_r (v/v) = residual moisture content; $w, \alpha_1, n_1, m_1, \alpha_2, n_2, m_2$= empirical parameters.

While physically based models capture moisture redistribution and capillary effects accurately (Liu and Fassman-Beck, 2018, 2017), they demand extensive parameterisation and are computationally intensive. The Richards formulation is highly sensitive to the SWRC and the HCF inputs, such that relatively small uncertainties in parameter specification can propagate into substantial errors in simulated percolation behaviour. There is no straightforward procedure for systematically calibrating this high-dimensional parameter set using limited detention test data. Consequently, they are rarely integrated into catchment-scale drainage modelling frameworks.

Campbell's HCF is a simple method for predicting unsaturated soil hydraulic conductivity from moisture retention data using a single shape parameter (Campbell, 1974).

$$K(\theta) = K_{Sat} * \left(\frac{\theta}{\theta_S}\right)^{3+2b} \quad \text{Equation 2.8}$$

where $K(\theta)$ is the percolation rate (mm/min), K_{Sat} is saturated hydraulic conductivity, θ_S is the soil porosity, θ is the soil moisture content, b is a shape parameter.

SWMM LID adopts a simplified, depth-integrated formulation that approximates percolation as an exponential function of moisture content to represent percolation. Percolation (Equation 2.9, which is referred to as the 'Kslope' HCF) is represented by the following empirical equation:

$$K(t) = \begin{cases} K_{sat} \times e^{(-HCO\,(\theta_S - \theta(t)))} & ,\theta > \theta_{FC} \\ 0 & ,\theta \le \theta_{FC} \end{cases} \quad \text{Equation 2.9}$$

where $K(t)$ is the percolation rate at time t , K_{sat} is the saturated hydraulic conductivity, HCO is a constant, θ_S is saturated moisture content (media porosity), θ_{FC} is volumetric moisture content at field capacity, and $\theta(t)$ is volumetric moisture content at time t.

The HCO term controls the rate at which conductivity declines as media dries. In the SWMM Manual (Rossman, 2016a), HCO is estimated via the Saxton and Rawls (2006) transfer function derived from natural soil databases:

$$HCO = 0.48 \times (\%Sand) + 0.85 \times (\%Clay) \quad \text{Equation 2.10}$$

However, several studies have shown that such soil-based relationships do not reliably represent the behaviour of engineered SuDS media. Liu and Fassman-Beck (2018) analysed 14 media with different compositions and found that their hydraulic conductivity-moisture content relationships deviated significantly from classical formulations, owing to complex intra- and inter-aggregate pore interaction.

Peng et al. (2020) reached similar conclusions for green roof substrates, using controlled detention tests and in situ moisture monitoring to highlight the mismatch between observed outflow dynamics and model predictions. These findings indicate that identifying appropriate HCO values based solely on soil texture may lead to unrealistic percolation simulations.

While previous researchers (Liu and Fassman-Beck, 2018; Peng et al., 2020) emphasised that natural-soil HCFs, such as the Van-Genuchten Mualem or Durner Mualem formulations, often fail to represent engineered media accurately, no direct comparison has been made with SWMM's exponential Kslope function. Peng et al. (2020) proposed a three-segment HCF curve (Figure 2.11 green dash line), showing steeper gradients near field capacity, implying that a single-slope exponential approximation (as in Equation 2.9) cannot capture the observed transition from capillary to gravitational flow regimes.

Liu and Fassman-Beck (2017) and De-Ville and Stovin (2022) suggested that Equation 2.9's oversimplification might explain the unrealistic outflow responses observed under low flow rate simulations. As illustrated in Figure 2.12, the SWMM model imposes a minimum drainage rate (in this specific case: 0.0502 l/5 min) corresponding to the hydraulic conductivity at field capacity. Below this threshold, no flow occurs, leading to an abrupt drop from measurable discharge to zero. The modelled runoff profile therefore exhibits sharp onsets and cut-offs, in contrast with the smooth, continuous outflow behaviour recorded during lysimeter tests. This "on–off" behaviour arises because, with the selected HCO value, the hydraulic conductivity at θ = field capacity is substantially overestimated, creating an artificial threshold between active drainage and complete cessation of flow.

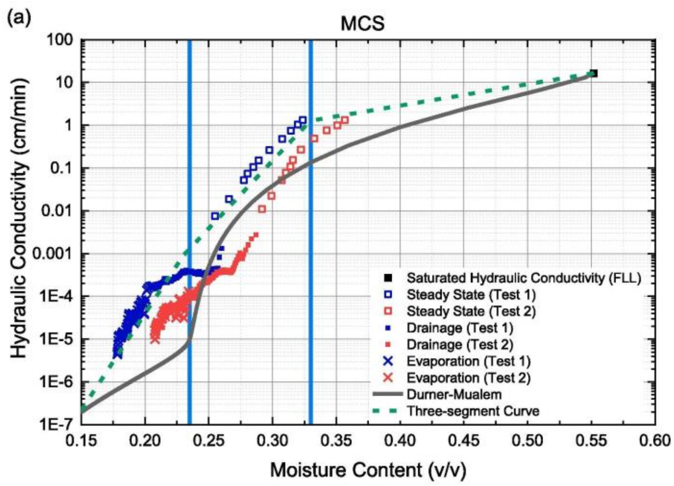

Figure 2.11. Measured unsaturated hydraulic conductivity, estimated (Durner Mualem model) and fitted (three-segment curve) HCFs for the MCS (Marie Curie substrate) (Peng et al., 2020).

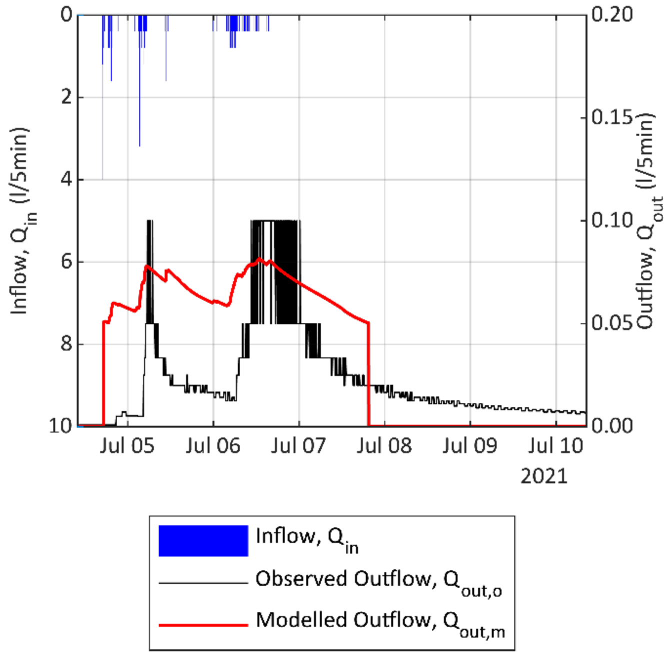

Figure 2.12. Inflow and Outflow for test Lysimeter from July 4th to 11th (De-Ville and Stovin, 2022).

In summary, existing studies show that the simplified percolation formulation used in SWMM cannot adequately capture the gradual transitions and nonlinear behaviour of unsaturated flow in engineered SuDS media. To address this gap, Chapter 3 examines and refines the representation of various substrate detention modelling approaches. The aim is to improve its physical realism and continuity under unsaturated conditions, providing a more accurate, yet computationally efficient approach for simulating SuDS percolation processes.

2.6 Simplified Device-scale Modelling of SuDS (feeds Ch.4)

Building upon the Section 2.5 examination of unsaturated flow in engineered SuDS media, it is evident that internal hydraulic mechanisms such as percolation, evapotranspiration, and drainage dynamics exert strong controls on the overall runoff behaviour of SuDS devices. Section 2.5 demonstrated that while process-based models (e.g., HYDRUS, SWMM) can represent these mechanisms with varying degrees of detail, their computational demands and parameterisation requirements often limit their applicability beyond laboratory or certain scales. Consequently, there is a growing need to translate these insights into simplified, yet hydrologically representative, models that can be applied at the device-scale where individual SuDS units are evaluated as functional components within broader drainage systems.

In contemporary drainage modelling practice, SuDS devices such as green roofs can be represented with reasonable accuracy using the SWMM LID module when considered individually. However, at the subcatchment or street scale, a single modelling unit within platforms such as InfoDrainage (Autodesk, 2025b) or SWMM may implicitly contain tens or even hundreds of SuDS installations, each with potentially distinct configurations. Explicitly representing every device (even using the simplified process) can become computationally prohibitive when applied to large urban networks comprising thousands of subcatchments.

This scaling challenge motivates two complementary modelling strategies. The first is device-scale simplification, in which individual SuDS units are represented using reduced-order process descriptions that approximate their hydrological response without explicitly modelling all internal layers and processes. The second is spatial aggregation, whereby multiple SuDS devices are combined into a smaller number of representative modelling units at the subcatchment or street scale. Both approaches involve deliberate trade-offs between physical realism and computational efficiency, and both raise a fundamental question: how much process detail must be retained for simplified models to retain the ability to predict key hydrological responses.

In this context, device-scale modelling serves as an intermediate step between detailed process representation and catchment-scale integration. It aims to preserve the essential retention and detention functions identified in detailed models, while reducing complexity to enable practical design and scenario testing. The challenge lies in determining how much physical realism must be retained for the model to remain predictive of key hydrological responses, such as runoff volume, peak flow, and drainage duration, under both event-based and continuous simulation conditions.

A range of stormwater models have been used to predict SuDS performance in these scenarios. The most commonly used models are SWMM (Rossman, 2016b, 2016c, 2016a), MUSIC (eWater Ltd, 2005), InfoWorks ICM (Autodesk, 2025a) and MIKE (DHI, 2024). The SWMM LID module is probably the best known and most widely used model for representing the runoff responses associated with vegetated SuDS devices. It is freely available, and openly documented (Rossman, 2016a). The model is essentially a one-dimensional physically based hydrological model, which incorporates all the key processes expected to influence the amount (i.e. retention losses) and timing (i.e. detention processes) of runoff from a SuDS device.

Although the SWMM LID module is widely utilised, there have been relatively few robust validation studies. In the context of green roofs, Peng and Stovin (2017) compared the model outputs to monitored runoff responses from a green roof test bed. They recommended several potential model refinements, including the representation of moisture stress effects on actual ET rates and refinements to the representation of the underlying drainage layer/board. Green roof models proposed by Stovin et al. (2013b) and Locatelli et al. (2014) both included the effect of substrate moisture content on actual ET rates, and were shown to replicate observed green roof runoff accurately. More recently, Hörnschemeyer et al. (2021) developed SWMM-UrbanEVA specifically to address the limitations to ET modelling within SWMM.

In the context of bioretention cells, Lisenbee et al. (2021) provide a comprehensive review of column, pilot, field and model-to-model comparisons that have been used to evaluate SWMM, noting that there are relatively few site-scale studies to date. They compared the performance of the SWMM LID module with field data from the Ursuline College bioretention cell located near Cleveland, Ohio, USA, alongside an alternative model, DRAINMOD-Urban. SWMM produced good, predicted volumes and outflow hydrographs even when uncalibrated, but DRAINMOD-Urban represented the measured drainage hydrograph shape better than SWMM. Lisenbee et al. (2021) noted that the simplified (bulk) representation of percolation through the variably-saturated substrate in SWMM contributes to the observed differences.

While physically based approaches can provide more mechanistic accuracy, they are often computationally expensive and unsuitable for network scale integration. This has encouraged the development of simplified device-scale models, designed to represent SuDS hydrology using reduced process sets or aggregated parameters. For large-scale SuDS retrofit schemes, such as the Mansfield Sustainable Flood Resilience Programme (De-Ville et al., 2024), accurately embedding new/proposed SuDS measures into the existing drainage model is critical. Most legacy networks in the UK—and in many other regions—were not modelled in SWMM, and a full model rebuild or transfer is rarely feasible. In these cases, using simplified SuDS representations may provide a practical alternative.

Historically, researchers did not have access to explicit SuDS modelling tools, which led to the development of alternative approaches to SuDS simulation. Stovin et al. (2013a) evaluated the potential to retrofit SuDS to address combined sewer discharges within the Thames Tideway catchment in London using InfoWorks CS. SuDS were represented by adjusting percentages associated with various area types (pervious, impervious and connected area) contributing to the model nodes and/or the adjustment of initial loss depth and storage/attenuation depth (Table 2.1). Two other simpler, but more extreme, simulation methods were also trialled: removing the modified area directly from the simulation to represent the “disconnection”; or a change of the retrofitted area from impervious area to pervious area. No validation of these approximations was undertaken.

The 25-mm initial losses scenario noted in Table 2.1 was designed to represent SuDS options that provide substantial levels of retention. Rainfall retention in vegetated SuDS results from a combination of initial and continuous losses. The initial losses correspond to evapotranspiration occurring in the antecedent dry period, which removes moisture retained in the substrate.

Continuous losses correspond to exfiltration from the device. Once the retention capacity is surpassed, SuDS will ultimately discharge into receiving systems. In practice, the actual retention depth available at the start of a rainfall event will depend on the duration of the antecedent dry weather period (ADWP), the specific weather conditions during the ADWP and the configuration of the SuDS device. Any simulation approach intended for continuous simulation needs to reproduce these processes. In contrast, for simulations focusing on an isolated design storm, care needs to be taken to determine an appropriate value for the initial losses. Stovin et al. (2012) suggested that the median retention associated with green roof test beds in 'significant' rainfall events was 6.5 mm, i.e. considerably lower than 25 mm.

Similarly, Lashford et al. (2020) noted that commercial tools often emulate SuDS using hydraulic elements (e.g., tanks or ponds) or by converting impervious surfaces to pervious types. Although computationally convenient, these methods neglect the dynamic infiltration, percolation, and drainage interactions that define SuDS behaviour, and may yield inaccurate peak flow and timing predictions.

Recent studies have therefore proposed a range of static, lumped approaches for SuDS design and screening, typically based on fixed runoff-volume reductions, constant infiltration coefficients, or event-based flow equations (Batalini De Macedo et al., 2022; Haghighatafshar et al., 2019b; Lashford et al., 2020; Metcalfe et al., 2018). These models conceptualise the device as a storage box, effectively reproducing total water balance but disregarding the temporal variability of infiltration and drainage. While such simplifications can satisfy regulatory or long-term volume criteria, they risk underestimating peak discharge or overestimating retention during design storms—limitations that can compromise hydraulic performance representation at the catchment scale.

Table 2.1. Land use types, retrofit SuDS options and assumptions used in catchment modelling (Stovin et al., 2013a)

Impermeable land use	SuDS retrofit options (in preference order)	Impermeable area removed	Impermeable area transferred to permeable	Initial losses (25 mm)	Storage/ attenuation
Building roofs	Disconnect to garden soakaways	✓			
	Disconnect to lawns		✓		
	Oversized water butts			✓	
	Green/blue roofs		✓	✓	
Nonroad hard standing	Permeable surface			✓	✓
	Disconnect to adjacent permeable		✓		
	Offsite – local detention				✓

Other man-made surfaces	Disconnect to adjacent permeable	✓		
Roads	Permeable surface		✓	✓
	Disconnect to adjacent permeable/Street Edge Alternatives streets	✓		
	Pocket street infiltration		✓	
	Offsite – detention with swale conveyance			✓

Against this backdrop, simplified SuDS modelling at the device-scale occupies a crucial research space between process fidelity and practical applicability. The challenge lies in identifying the level of simplification that retains key hydrological behaviour—particularly infiltration, exfiltration, and controlled drainage—while enabling computational efficiency and integration into broader urban models. Consequently, Chapter 4 focuses on evaluating the hydrological consequences of simplification by comparing multiple reduced-complexity modelling approaches for green roofs and bioretention systems, with the unmodified SWMM LID module serving as the baseline reference.

2.7 Aggregation and Street-scale Modelling of SuDS (feeds Ch.5)

Building upon the device-scale investigations presented in the previous section, which examined the hydrological processes associated with individual SuDS components, this section focuses on the street scale (street-scale as shown in Figure 2.13b), the level at which multiple SuDS units interact within an interconnected urban drainage context. At this intermediate level, SuDS are typically deployed in fragmented spatial patterns across street blocks, often combining several component types to achieve cumulative runoff reduction. Evaluating their aggregated hydraulic and hydrological performance thus requires modelling approaches that can reconcile spatial complexity with computational practicality.

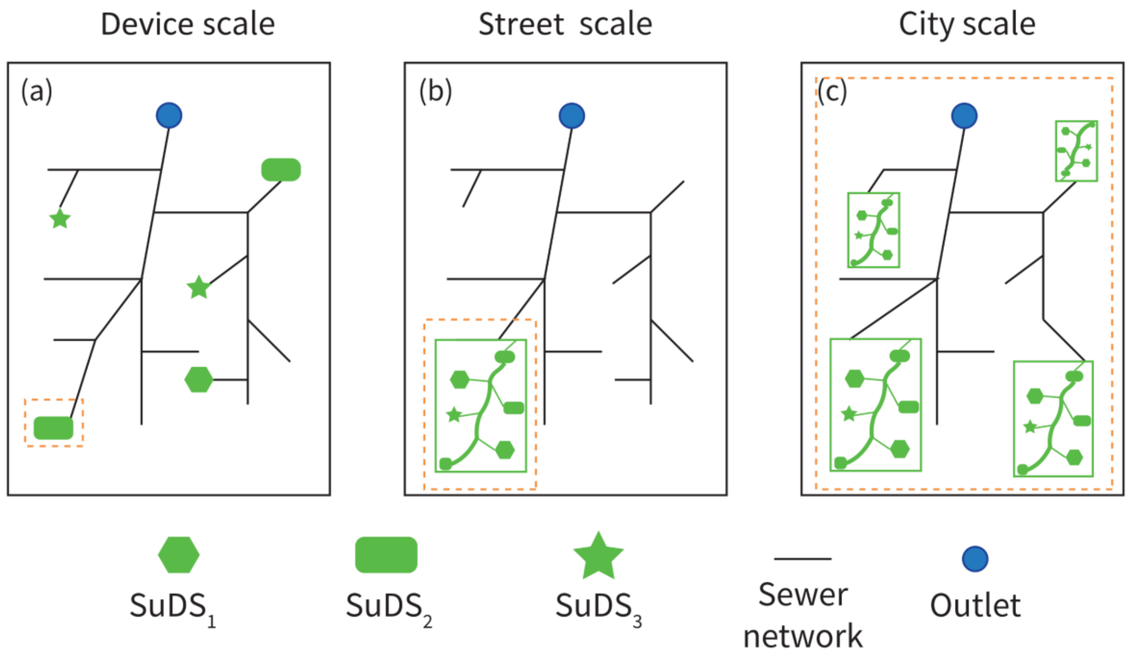

Figure 2.13. Different levels of implementation for SuDS, (a) Device scale, (b) Street scale, and (c) City scale (catchment scale)

The versatility of SuDS is evident through the wide range of components available, enabling their implementation in diverse locations. Designers have the flexibility to select from various SuDS components and customize the overall composition of a SuDS scheme to suit the specific characteristics of the local context. As a result, SuDS tend to be deployed in fragmented patterns when retrofitted across street blocks or subcatchments. At this street scale, assessing their cumulative retention and detention effects becomes essential, necessitating the use of stormwater modelling tools to predict their hydraulic and hydrological performance. While hydrological/hydraulic tools (e.g., SWMM) have been successfully employed to simulate individual SuDS components, such detailed applications are often computationally costly and time consuming, which motivates the use of aggregated modelling approaches at the street scale, even though these require simplifications that may compromise accuracy.

In practice, some projects focus on a single SuDS type. For example, Portland's downspout disconnection initiative was designed primarily to mitigate Combined Sewer Overflows (CSOs), progressively removing roof runoff from the sewer system (Environmental Services City of Portland, 2019). In Melbourne, rain gardens were selectively deployed across urban zones, though each installation exhibited variation in design parameters depending on its local context (Melbourne Water, 2022). In such scenarios, simplified aggregation approaches may be suitable for modelling the cumulative hydrological effect of homogeneous SuDS types.

However, urban SuDS implementation is characterized by heterogeneity. Multiple SuDS types—such as detention basins, permeable pavements, rain gardens, and bioswales—are co-located at the street scale, either to maximise functional performance or due to decentralised decision making across properties (Haghighatafshar et al., 2018; Severn Trent Water, 2016). A notable large-scale initiative example is the Mansfield Sustainable Flood Resilience Scheme in the UK, which represents the country's largest SuDS retrofitting programme (Severn Trent Water, 2016). The project incorporates 340 interventions, including detention basins, permeable pavements, rain gardens, and bioswales, providing a total storage capacity of 30,350 m^3. This diversity poses a critical challenge for rapid and reliable simulation of aggregated SuDS performance, especially when both the number and configuration of devices vary significantly.

The SWMM modelling framework provides two primary strategies for integrating SuDS units within catchments. In the first (Figure 2.14 A, B, C), one or more SuDS controls are embedded within an existing subcatchment, receiving a predefined fraction of the runoff from the impervious portion of that subcatchment. This approach is particularly suited for large-scale or city-wide studies, where SuDS are heterogeneously distributed across numerous subcatchments. In the second strategy (Figure 2.14 D), a subcatchment is entirely dedicated to a single SuDS unit (or a homogeneous set of replicate units). In this case, the inflow to the SuDS includes both direct rainfall and any upstream runoff conveyed to the SuDS-designated subcatchment. This configuration is adopted in detailed studies focused on individual SuDS performance or treatment trains. Although these methods offer flexibility, both rely on assumptions of spatial uniformity and consistent runoff partitioning, which may not fully represent real-world variability in design, media properties, or hydraulic configurations.

Recent studies have adopted the catchment area portion deployment framework (i.e. the first one (A, B, C) mentioned in the previous paragraph) provided by SWMM or PCSWMM to simulate SuDS implementation. For instance, Le Floch et al. (2022) modelled SuDS controls such as green roofs and permeable pavements by defining fixed, uniform SuDS units, assigning identical configurations and treatment areas to all installations of the same type across subcatchments. Similarly, Tansar et al. (2022) applied a simplified approach by allocating fixed percentages of subcatchment areas (e.g. 20–100%) to represent SuDS deployment across a larger drainage network in PCSWMM. Other studies have followed similar practices, representing a given SuDS type using a uniform parameter set at the street scale (Ercolani et al., 2018; Versini et al., 2015).

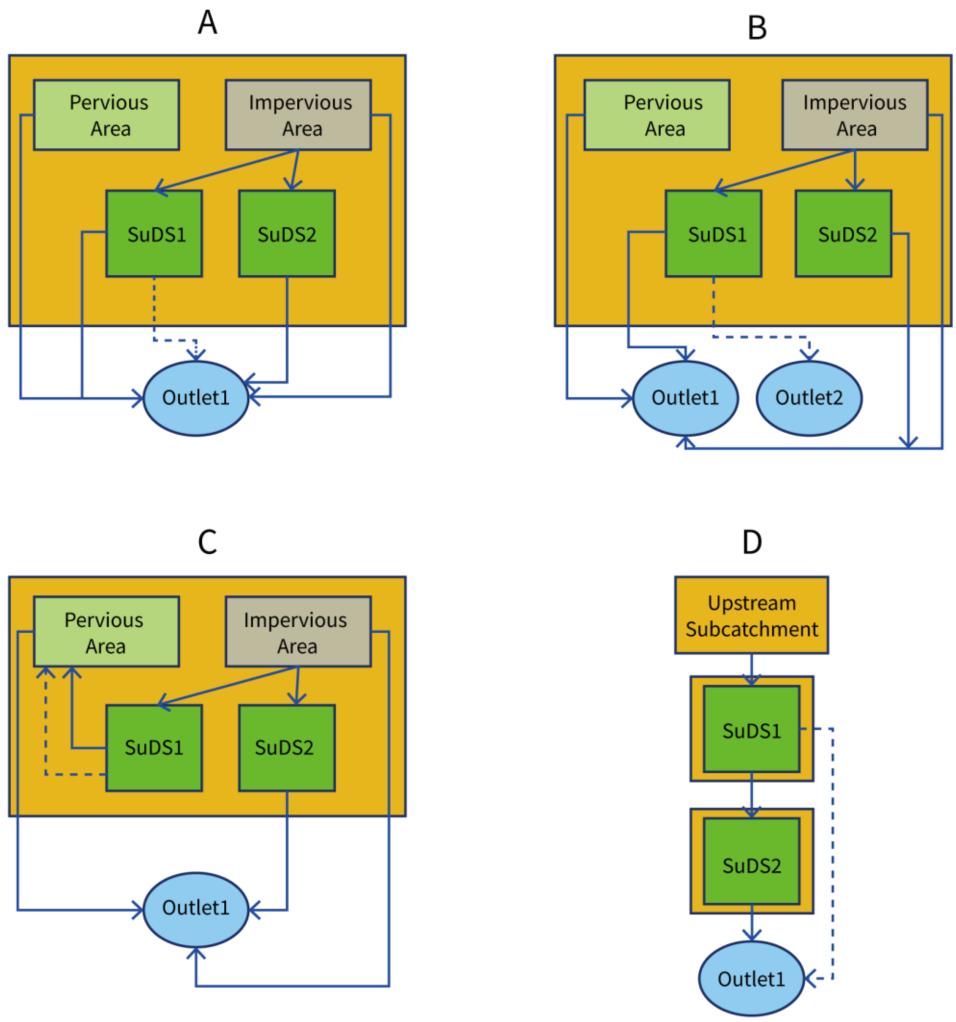

Figure 2.14. Different options for placing LID controls. A, B and C respectively illustrate how SuDS can be designed to direct runoff to different destinations. (Rossman, 2016a)

However, such simplifications overlook the fact that even within a single SuDS type, design configurations (e.g., media depth, infiltration rate, orifice sizing) may vary substantially in practice. This variation affects SuDS performance and underscores the importance of carefully selecting parameter estimation strategies. For bioretention systems, the review of sensitivity analyses has shown that soil hydraulic properties, exfiltration to native soils, and underdrain configuration exert strong control over infiltration, percolation, and outflow dynamics (Lisenbee et al., 2021). Similarly, for permeable pavements, parameters such as berm height, impervious surface fraction, soil thickness, storage seepage rate, and drain offset have been identified as dominant controls on runoff generation (Madrazo-Uribeetxebarria et al., 2021). These findings demonstrate that assuming uniform parameter sets may obscure key performance drivers and introduce structural uncertainty when scaling SuDS deployment across a drainage network.

Two fundamental challenges therefore arise. First, when a single type of SuDS is implemented using multiple configurations, it remains unclear whether these variants can be meaningfully aggregated without compromising hydrological accuracy. Second, when different types of SuDS are co-located within a catchment, the assumption that they can be treated as a single composite unit neglects their distinct runoff retention, detention, infiltration behaviours and outflow control mechanisms. While early aggregation studies, such as Elliott et al. (2009) using MUSIC and Roldin et al. (2012) using MIKE URBAN, reported only minor discrepancies between aggregated and detailed simulations, these analyses focused primarily on homogeneous infiltration systems rather than mixed-type, multi-mechanism configurations.

Taken together, the existing body of work on SuDS aggregation reveals a consistent methodological pattern. Most studies simplify spatial deployment by assuming parameter uniformity within each SuDS type, fixed runoff partitioning across subcatchments, or homogeneous infiltration-dominated systems. While such assumptions enable computational operation at large scales, they implicitly assume that device-level heterogeneity and typological diversity do not significantly alter aggregated hydrological response. However, few studies have systematically examined how structural aggregation interacts with parameter variability across mixed SuDS configurations, nor have they evaluated the extent to which simplification errors propagate from the device-scale to the street or catchment scale. As a result, the reliability limits of commonly adopted aggregation strategies remain insufficiently quantified, particularly under conditions where multiple SuDS types with distinct retention and detention mechanisms coexist.

Addressing these gaps requires a systematic evaluation of SuDS aggregation strategies that vary in typological composition and parameter uniformity. Such approaches are vital for enabling rapid, scalable simulation in urban drainage design and resilience planning, especially where detailed calibration of individual units is infeasible. Consequently, Chapter 5 investigates how different aggregation strategies—ranging from within-type lumping to cross-type compositing—affect modelled runoff volume, peak flow, and discharge timing at the street-scale. By integrating Monte Carlo-based sensitivity analyses, this study seeks to identify optimal simplification levels that balance hydrological realism and computational efficiency.

2.8 Summary and Research Gaps

The Literature Review chapter has reviewed the conceptual foundations, functional diversity, hydrological processes, and modelling approaches associated with SuDS, tracing their development from conceptual design principles to detailed process-based analyses and multi-scale modelling frameworks. Collectively, the reviewed literature reveals that while the philosophy of SuDS is well established, knowledge gaps remain concerning the quantitative simulation of their hydrological behaviour across scales. As SuDS become increasingly integrated into complex urban environments, the challenge is no longer simply to demonstrate their effectiveness, but to represent their hydrological functions consistently and efficiently within modelling frameworks that span from material-scale mechanisms to network-scale planning.

The literature points to three interrelated challenges that underpin the analytical structure of this research.

First, at the device-scale, the accurate representation of unsaturated flow within engineered media in SWMM remains a fundamental yet underdeveloped area. Although SuDS are designed to mimic natural infiltration and percolation, SWMM LID rely on empirical hydraulic conductivity functions derived from natural soils, overlooking the unique pore structures and moisture dynamics of engineered media. These simplifications hinder the realistic simulation of gradual drainage, non-linear retention, and moisture redistribution processes—highlighting the need for refined hydraulic formulations and parameterisation strategies.

Second, also at the device-scale, simplified hydrological representations introduce a trade-off between physical realism and computational efficiency. Physically based tools such as SWMM LID provide detailed insights into infiltration, evapotranspiration, and drainage. Conversely, simplified modelling approaches such as removing SuDS treated area, using basic hydrological elements to emulate retention and detention, are adopted due to their computational tractability but embed structural assumptions that may distort hydrological responses. The key challenge lies in systematically determining how progressive simplification of core hydrological processes within the SWMM LID framework influences model behaviour and predictive reliability at the device-scale.

Third, at the street or mesoscale, the aggregation of multiple SuDS components introduces further complexity arising from spatial heterogeneity and typological diversity. In real-world retrofit and new development programmes, numerous SuDS types—each with distinct retention, detention, and infiltration characteristics—may coexist within shared subcatchments. To maintain computational feasibility, modellers may adopt lumped or aggregated approaches that assume spatial homogeneity and uniform runoff partitioning. However, such assumptions can obscure localised hydrological variability and underestimate the cumulative effects of mixed-type systems. Existing aggregation studies remain limited in scope, often focusing on single SuDS types rather than heterogeneous configurations representative of actual urban implementations.

Together, these three challenges define a coherent research gap that links the microscale understanding of unsaturated processes, the device-scale evaluation of simplified modelling approaches, and the street-scale assessment of aggregation strategies.

Accordingly, this thesis adopts a multi-scale, model-comparative approach, organised around four interconnected studies:

1. Chapter 3 examines unsaturated flow in engineered media, evaluating the hydraulic conductivity functions employed in existing models and proposing refined representations for percolation within SuDS.
2. Chapter 4 assesses simplified device-scale modelling approaches for vegetated SuDS (green roofs and bioretention), quantifying how simplifications in process representation influence hydrological accuracy and response dynamics.
3. Chapter 5 extends this investigation to the street scale, developing and testing aggregation strategies for multi-type SuDS configurations to identify optimal simplification levels for urban drainage integration.
4. Chapter 6 evaluates alternative aggregation strategies through a real-world case study of the Mining Remediation Authority (MRA) SuDS retrofit scheme in Mansfield, demonstrating how street-scale SuDS representations can be integrated into a drainage network model.

Collectively, these studies aim to advance the methodological basis for SuDS modelling by bridging the gap between process realism and engineering applicability. The integrated findings across scales are expected to inform both model development and design practice, contributing to more robust, scalable, and physically grounded simulation frameworks for sustainable urban drainage management.

3. Unsaturated Percolation Modelling in Engineered Media within SWMM LID Framework

3.1 Introduction

Detention occurs when water percolates through large media pore spaces that are unable to retain moisture but nonetheless impose resistance to vertical flow. During a storm event, this process results in a time delay of runoff and a reduction in peak discharge, commonly described as peak attenuation. These detention effects are central to the hydrological functioning of SuDS substrates under unsaturated conditions (substate moisture content below saturation).

Previous experimental studies have provided detailed characterisations of percolation through engineered SuDS substrates, revealing limitations in the way detention processes are represented by commonly used hydraulic conductivity functions (HCFs). Liu and Fassman-Beck (2018) presented extensive laboratory datasets describing the hydraulic conductivity functions of 14 engineered substrates with differing compositions, demonstrating that materials typically used in green roofs and bioretention systems exhibit hydraulic behaviour that differs markedly from that of natural soils. Similar conclusions were reached by Peng et al. (2020), who examined four green roof growing media and employed controlled detention tests to characterise their outflow responses.

While these studies established that HCFs derived from natural soils (such as the Van-Genuchten Mualem or Durner Mualem HCFs) are generally unsuitable for engineered growing media, they did not explicitly compare such formulations with the simplified exponential HCF employed in the SWMM LID module. Peng et al. (2020) proposed a conceptual “three-segment” representation of HCF behaviour (see Chapter 2, Figure 2.11), in which the gradient on a semi-logarithmic scale increases as volumetric moisture content approaches field capacity. This observed behaviour suggests that characterising unsaturated hydraulic conductivity using a single slope parameter, as practiced in SWMM (Equation 2.9), may be insufficient to capture the drainage dynamics of engineered substrates.

Consistent with this interpretation, Liu and Fassman-Beck (2017) and De-Ville and Stovin (2022) hypothesised that deficiencies in the default SWMM LID HCF could contribute to the unrealistic “on-off” outflow responses observed in simulations of unsaturated flow (see Chapter 2, Figure 2.12). These findings collectively point to modelling limitations associated with simplified percolation representations in operational SuDS models.

Building on the broader discussion of unsaturated flow processes in engineered media presented in Chapter 2, this chapter addresses a specific and operational modelling challenge. Concerns have been raised in previous studies regarding the limitations of the default exponential HCF implemented in SWMM. At the device-scale, the accurate representation of unsaturated flow within engineered SuDS media is poorly resolved in widely used urban drainage models (e.g., SWMM). Although SuDS are designed to emulate natural percolation processes, existing model formulations typically rely on empirical hydraulic conductivity functions derived from natural soils. Such formulations inadequately reflect the moisture retention characteristics and drainage behaviour of engineered media. The primary aim of this chapter is to assess the accuracy of different substrate percolation modelling formulations under unsaturated conditions. This chapter also investigates whether an alternative hydraulic conductivity formulation can improve the representation of substrate percolation behaviour within the SWMM LID framework, without introducing additional input requirements for model users.

The aim is achieved via the following objectives:

1. To implement and test three different hydraulic conductivity functions (HCFs) in SWMM LID framework for SuDS (green roof) substrate layers, including:
    - Kslope HCF (termed "*Kslope*").
    - Campbell HCF (termed "*Campbell*").
    - A new HCF (termed "*NewHCF*").
2. To calibrate model parameters for each percolation representation using observed data.
3. To evaluate the performance of the bulk unified percolation model (i.e. SWMM LID module).

3.2 Materials and Methods

3.2.1 Substrate Characteristics

Test data from a representative green roof substrate (Marie Curie Substrate, MCS) was sourced from Peng et al. (2020). The characteristics of MCS were previously determined by Peng et al. (2020) using FLL (Forschungsgesellschaft Landschaftsentwicklung Landschaftsbau) methods for particle size distribution (PSD), median particle diameter (d_{50}), bulk density, porosity and water permeability (saturated hydraulic conductivity) (FLL, 2018). These properties provide the physical basis for the parameterisation of the percolation models evaluated in this chapter.

Table 3.1 presents the detailed physical characteristics of the MCS substrate. Peng et al. (2020) reported a field capacity of 0.275 m^3/m^3, representing the volumetric water content retained by a fully saturated substrate after a two-hour free drainage period.

Table 3.1. Physical characteristics of the Marie Curie Substrate (MCS)

Properties	Unit	MCS	Notes
FLL Physical Characteristics		mean	
Particle size < 0.063 mm (clay)	%	0.00	
d_{50}	mm	3.97	
Bulk density	g/cm^3	1.04	(FLL, 2018; Peng et al., 2020)
Porosity	%	55.15	
Permeability (*Ksat*)	mm/min	166.40	
Other			
Field capacity	m^3/m^3	0.275	From detention test (Peng et al., 2020)
Wilting point	m^3/m^3	0.070	From SWRC, $\psi = 1500\ kPa$ (Peng et al., 2020)
% sand	%	23	From PSD, 0.063 < d < 2.0 mm

3.2.2 MCS Substrate Measured HCF

Figure 3.1 presents the HCF measurement data for MCS. The dataset comprises two independent sets of measurements (Tests 1 and 2), obtained from two samples of the same substrate material. All measurements were conducted on a laboratory test column with a media depth of 540 mm and a diameter of 300 mm (Peng et al., 2020).

The HCF data were derived using a combination of steady-state and transient experimental techniques, corresponding to three situations (steady-state: 1. steady-state; transient: 2. drainage, 3. evaporation). The steady-state method was employed to assess the hydraulic conductivity under conditions where moisture content remains constant over time and depth, with water flow driven solely by gravity. In this state, the hydraulic conductivity is equal to the outflow rate. In contrast, the transient method involved measuring the unsaturated hydraulic conductivity using transient measurements of low moisture content and suction head. This method applies to the drainage and evaporation situations. This technique was employed under conditions of no inflow after all the steady-state measurements were finished. The hydraulic conductivity was calculated based on Darcy's Law using measured moisture content and total head from two adjacent points (Peng et al., 2020).

The steady-state HCF measurements are used to evaluate the newly proposed hydraulic conductivity formulation introduced in this chapter, since these data correspond to conditions in which substrate moisture content is at or above field capacity and percolation contributes directly to runoff generation.

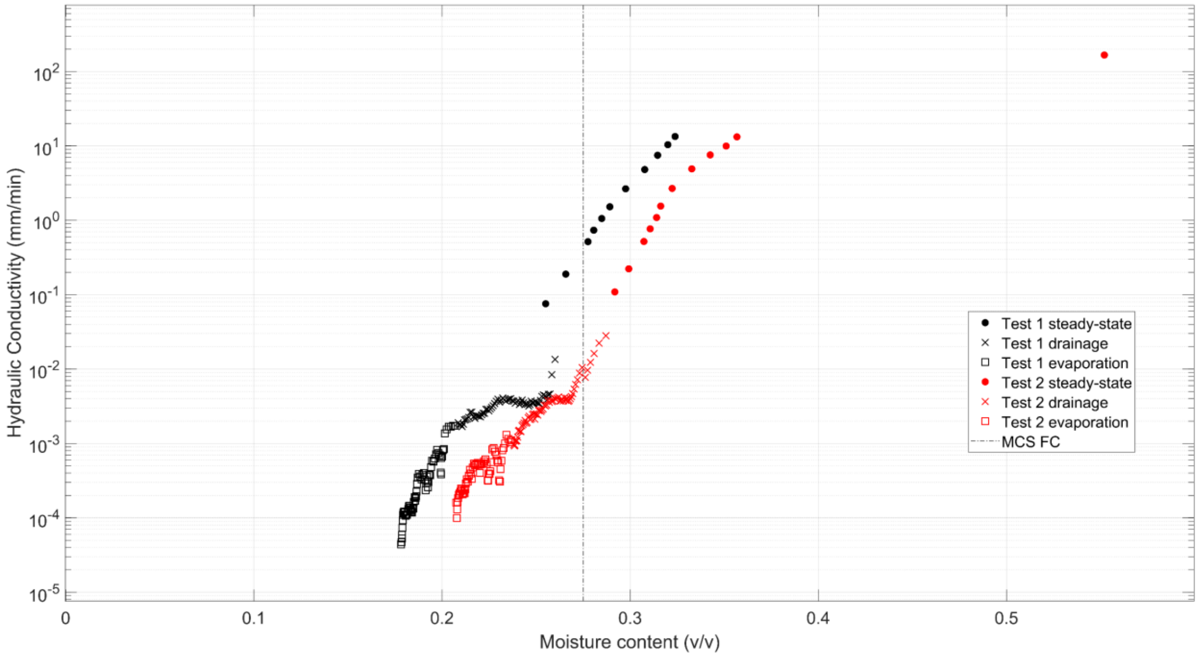

Figure 3.1. Measured unsaturated hydraulic conductivity for two samples of MCS (Peng et al., 2020).

3.2.3 Detention Test Datasets

Peng et al. (2020) conducted a series of laboratory detention tests on 200 mm deep MCS columns to evaluate substrate detention performance under different rainfall intensities and temporal rainfall profiles. During the experiments, soil moisture dynamics were monitored using moisture probes installed at the upper and lower depths of the substrate layer. Prior to each test, the substrate was placed into the test column without compaction to ensure consistent initial conditions.

The substrate was initially saturated with 1.2 mm/min rainfall for 2 hours, followed by a 2-hour drainage period to ensure it was at field capacity. This preconditioning ensured a consistent initial moisture state across all detention tests.

Four design storm scenarios were subsequently applied. For Design Storms 1, 2, and 3, the rainfall intensities were based on 1, 10 and 30-year return period one-hour events for Sheffield. However, storm durations were reduced to 30 minutes, as the runoff response during the rising and recession phases of the rainfall events was of primary interest. The applied design storms are summarised as follows:

- Design Storm 1: 0.1 mm/min constant rainfall for 30 min (one-hour 1 in 1 year Sheffield, UK, rainfall intensity (NERC, 1999))
- Design Storm 2: 0.37 mm/min constant rainfall for 30 min (one-hour 1 in 10 year Sheffield, UK, rainfall intensity (NERC, 1999))

- Design Storm 3: 0.51 mm/min constant rainfall for 30 min (one-hour 1 in 30 year Sheffield, UK, rainfall intensity (NERC, 1999))
- Design Storm 4: 9.2 mm of total rainfall distributed over five 6-minute time-steps (UK 75% summer profile)

The detention test dataset for a 200 mm depth substrate with Design Storm 3 was selected to calibrate model parameters for different percolation formulations. The remaining design storms (Design Storm 1, 2, and 4) were then used to independently evaluate and validate the performance of the detention modelling approaches.

3.2.4 Percolation Modelling

This study tested three distinct HCFs. The SWMM LID module was implemented in MATLAB (R2023a), because SWMM doesn't permit the use of alternative HCF models. The laboratory green roof test bed was modelled as a subcatchment fully occupied by a green roof, with a soil thickness of 200 mm. All simulations were conducted using 1-minute time steps. ET was excluded from all modelling approaches to ensure consistency with the experimental conditions and to isolate percolation processes. All simulations were initialised at field capacity to exclude retention effects. No specific vegetation or other friction coefficients were set for the surface layer. It should be noted that, as green roof substrates typically have very high permeabilities, surface runoff is not expected to occur. It is assumed that there is no specific restriction on outflow in the drainage layer. This assumption ensures that percolation from the substrate layer is converted directly to system outflow within each simulation time step.

For clarity and continuity, some equations presented here are repeated from Chapter 2.

3.2.4.1 SWMM LID model with Kslope HCF

As shown in Figure 2.6, in the SWMM LID model a green roof is represented using three horizontal layers: a surface layer, a substrate layer, and a drainage layer. The rainfall event causes the surface layer to receive direct rainfall that can infiltrate into the substrate. The substrate receives the infiltration from the surface layer and loses water through percolation. The drainage layer receives percolation flux, and the rainwater eventually exits the system as runoff.

The SWMM LID model applies the Green-Ampt method to simulate the infiltration of surface water into the upper soil layer. Percolation from the substrate into the drainage layer is modelled using Darcy's Law for steady-state flows (Rossman, 2016a), with the hydraulic conductivity expressed as a function of soil moisture (Equation 3.1). The SWMM model takes a lumped single-layer approach to modelling percolation in which outflow is determined based on the depth-averaged soil moisture content via an exponential HCF. The hydraulic conductivity slope coefficient (HCO) is calculated form the soil composition using Equation 3.2. Fluxes within and between layers are constrained by the available pore space and storage capacity of each layer. Specifically, percolation from the substrate layer is limited by the amount of drainable water and the available storage in the drainage layer, while runoff from the drainage layer is constrained by its inflow and storage volume.

$$K(t) = \begin{cases} K_{sat} \times e^{(-HCO\,(\theta_S - \theta(t)))} & ,\theta > \theta_{FC} \\ 0 & ,\theta \leq \theta_{FC} \end{cases} \qquad \text{Equation 3.1}$$

$$HCO = 0.48 \times (\%Sand) + 0.85 \times (\%Clay) \qquad \text{Equation 3.2}$$

where $K(t)$ is the percolation rate at time t , K_{sat} is the saturated hydraulic conductivity, HCO is a constant, θ_S is media porosity, θ_{FC} is volumetric moisture content at field capacity, and $\theta(t)$ is volumetric moisture content at time t.

3.2.4.2 SWMM LID model with Campbell HCF

An alternative power-law representation of the hydraulic conductivity function, proposed by Campbell (1974) and expressed in Equation 3.3, was also implemented within the SWMM LID framework. In this formulation, unsaturated hydraulic conductivity is described as a function of soil moisture using a single shape parameter b.

$$K(\theta) = K_{Sat} * \left(\frac{\theta}{\theta_S}\right)^{3+2b} \qquad \text{Equation 3.3}$$

$$b = \frac{\ln(1500) - \ln(33)}{\ln(\theta_{FC}) - \ln(\theta_{PWP})} \qquad \text{Equation 3.4}$$

where $K(\theta)$ is the percolation rate, K_{Sat} is saturated hydraulic conductivity, θ_S is the soil porosity, θ is the soil moisture content, b is the gradient of the SWRC between field capacity and permanent wilting point, θ_{FC} is volumetric moisture content at field capacity, θ_{PWP} is volumetric moisture content at wilting point.

It should be noted that, in the formulation used here to derive the parameter b, suction head values of 1500 kPa and 33 kPa are adopted to represent the wilting point and field capacity, respectively, based on the soil water retention curve (SWRC). The SWRC describes the substrate’s ability to hold water as a function of the suction head. However, the definition of suction head at field capacity varies across the literature (FLL, 2018; Israelsen and West, 1922; Rowell, 2014). This variability introduces additional uncertainty into the estimation of parameter b, which should be recognised when interpreting the results.

3.2.4.3 SWMM LID model with New HCF

An alternative HCF (termed '*NewHCF*') was developed in this study and implemented within the SWMM LID framework. Inspired by the power form of the *Campbell* and Durner-Mualem HCFs (Peng et al., 2020), the formulation focuses on representing hydraulic conductivity over the moisture range between field capacity and porosity, which is the range most relevant to substrate detention processes in SWMM-based simulations. Within this framework, accurately capturing the decline of hydraulic conductivity as soil moisture approaches field capacity is critical, such that conductivity smoothly tends towards zero at this threshold. This constraint enables a more realistic representation of unsaturated detention behaviour while remaining compatible with the simplified structure of the SWMM LID module.

The formulation adopts a normalised moisture-based structure. The percolation flux is defined as:

$$K(t) = \begin{cases} K(S_{act}) = K_{Sat} S_{act}{}^{u} & ,\theta > \theta_{FC} \\ 0 & ,\theta \leq \theta_{FC} \end{cases} \qquad \text{Equation 3.5}$$

$$S_{act} = \frac{\theta - \theta_{FC}}{\theta_S - \theta_{FC}} \qquad \text{Equation 3.6}$$

where S_{act} = actual saturation; θ is the moisture in this time step; θ_{FC} is soil field capacity; θ_S is saturated water content; u in the *NewHCF* function is assigned a value of 2.5, based on the bioretention media study of De-Ville et al. (2025a), and is treated here as the 'uncalibrated' value.

3.2.5 Model Parameters

Table 3.2 summarises the parameter values adopted for the three HCFs applied to the green roof system. Key physical characteristics of the substrate layer, including porosity, field capacity, and suction head were derived directly from the Peng et al. (2020) laboratory measurements. Although suction head is an important parameter for infiltration processes, it does not play a controlling role in the detention focused simulations conducted in this chapter and was therefore not treated as a calibration parameter.

The surface and drainage layers were assigned nominal thicknesses within the model configuration. However, due to the selected parameterisation, specifically the absence of surface flow resistance and the unrestricted drainage layer storage and outflow capacity, these layers did not impose hydraulic limitations during simulations. Consequently, percolation through the substrate was effectively converted directly into system outflow (runoff), ensuring that the modelling results reflect substrate percolation behaviour without additional boundary constraints.

Table 3.2. Initial parameter values for the three HCFs

Layer/ Configuration	Parameters	Unit	*Kslope* Value	*Campbell* Value	*NewHCF* Value	Notes
Surface Layer	Berm Height	mm	100	100	100	Customised no effect
	Vegetation Volume Fraction	-	0	0	0	
	Surface Roughness	-	0	0	0	
	Surface Slope	%	0	0	0	
Substrate Layer	Thickness	mm	200	200	200	(Peng et al., 2020)
	Porosity	-	0.552	0.552	0.552	
	Field Capacity	-	0.275	0.275	0.275	
	Wilting Point	-	0.070	0.070	0.070	
	K_{Sat}	mm/min	166.4	166.4	166.4	
	Suction Head	mm	109.1	109.1	109.1	
HCF	*HCO*	-	11.04			Equation 3.2, Equation 3.4, 2.5 is from De-Ville et al. (2025a)
	b	-		2.44		
	u	-			2.50	
Drainage Layer	Thickness	mm	300	300	300	Customised no effect
	Void Fraction	-	1	1	1	
	Roughness	-	0	0	0	

3.2.6 HCFs Comparison

Figure 3.2 presents a comparison of the HCFs plotted on a semi-logarithmic scale. The corresponding initial parameter values for each HCF are summarised in Table 3.2.

The comparison highlights limitations in both the exponential *Kslope* HCF and the power-law *Campbell* HCF. In particular, these formulations tend to overestimate hydraulic conductivity, and hence percolation rates, when soil moisture content approaches field capacity. This behaviour contributes to unrealistically rapid drainage under unsaturated conditions. Within a bulk representation such as the SWMM LID framework, percolation is conceptually assumed to cease as soil moisture approaches field capacity, with hydraulic conductivity tending towards zero at this threshold. Neither the *Kslope* nor the *Campbell* formulation inherently enforces this boundary condition, resulting in conductivity values exceeding the measured Test 2 HCF data points by approximately two to three orders of magnitude near field capacity.

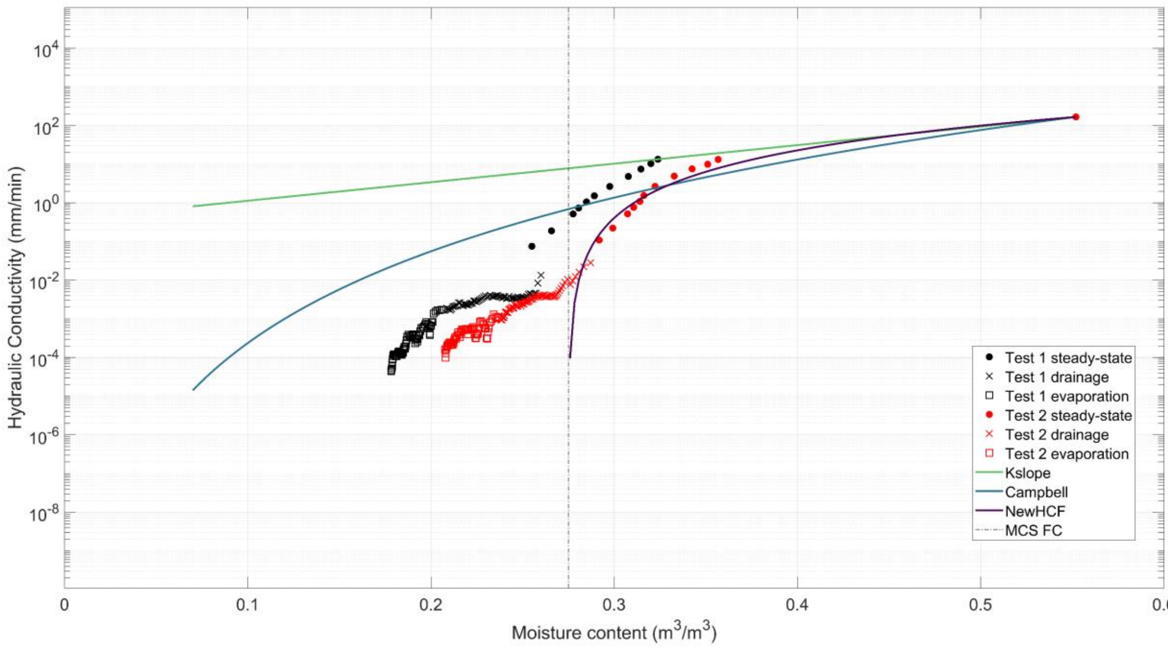

Figure 3.2. Measured unsaturated hydraulic conductivity, and HCFs (1. Kslope; 2. Campbell; 3. NewHCF) for the MCS.

3.2.7 Model Calibration

Measured runoff data obtained from the MCS detention tests (Peng et al. 2020, Section 3.2.3) were used to calibrate the three HCFs. Specifically, the hydraulic conductivity slope coefficient (*HCO*) in the Kslope model, the *b* in the *Campbell* formulation, and the *u* in the *NewHCF* were treated as calibration parameters.

Calibration was performed using the runoff response to Design Storm 3. The parameter values were adjusted to maximise the coefficient of determination between the simulated and measured runoff time series. Optimisation was conducted manually using a trial-and-error procedure in MATLAB, whereby parameter values were iteratively refined until no further improvement was achieved.

It is important to emphasise that calibration was undertaken against the measured runoff data, not directly against the laboratory-measured HCF data. The term “calibrated HCF” therefore refers to hydraulic conductivity functions whose parameter values were adjusted to reproduce observed percolation behaviour, rather than to functions fitted directly to steady-state conductivity measurements.

3.2.8 Model Evaluation

Sonnenwald et al. (2014) demonstrated that R_t^2 (Young et al., 1980) provided a robust and generically applicable indicator of model performance for temporally-varying data. Therefore, R_t^2 was used to evaluate the goodness-of-fit of the simulated runoff. A value of R_t^2 equal to 1 indicates the model can reproduce the measured outflow response perfectly.

$$R_t^2 = 1 - \frac{\sum_{i=1}^{T}\left(q_o(i) - q_m(i)\right)^2}{\sum_{i=1}^{T}\left(q_o(i)\right)^2} \qquad \text{Equation 3.7}$$

where q_o is the observed outflow, q_m is the simulated outflow; T is the total number of observed data.

3.3 Results and Analysis

3.3.1 Model Evaluation

Figure 3.3 presents the measured and modelled soil moisture and runoff profiles for the 200 mm MCS substrate under Design Storm 3, as produced by the three HCFs. The *NewHCF* approach exhibits the highest level of agreement between simulated runoff profiles and observations (R_t^2 = 0.94).

Both *Kslope* and *Campbell* HCF approaches exhibit limited ability to reproduce the observed detention behaviour. In the simulation, rainfall infiltrates into the substrate but is released almost instantaneously, resulting in a nearly constant soil moisture profile over time. Correspondingly, the simulated runoff closely mirrors the rainfall input, indicating that little or no detention is represented by these two approaches under low-intensity conditions.

The *NewHCF* approach demonstrated good consistency between simulated and measured outflow dynamics. The corresponding soil moisture simulations resemble the observed average moisture variations within the substrate. However, during the initial stage following rainfall onset, the observed soil moisture exhibits a short delay before increasing, whereas the model predicts an immediate rise. This is because the model treats the substrate as having a homogeneous moisture content profile, which does not fully reflect conditions in reality.

A similar behaviour is evident in the runoff simulations: outflow initiation occurs earlier than observed, and the recession following peak flow is also premature. In addition, although the simulated peak runoff exceeds the observed peak, the corresponding soil moisture does not fully reach the observed average peak value. During the high-flow phase, this approach reproduces a similar peak magnitude to that observed in the experimental data; however, it fails to capture the gradual recession behaviour, instead producing a rapid post-peak decline. Nevertheless, it is noteworthy that the *NewHCF* model captures the subsequent recession behaviour reasonably well, successfully reproducing the slowly declining “tail” of the observed runoff profile.

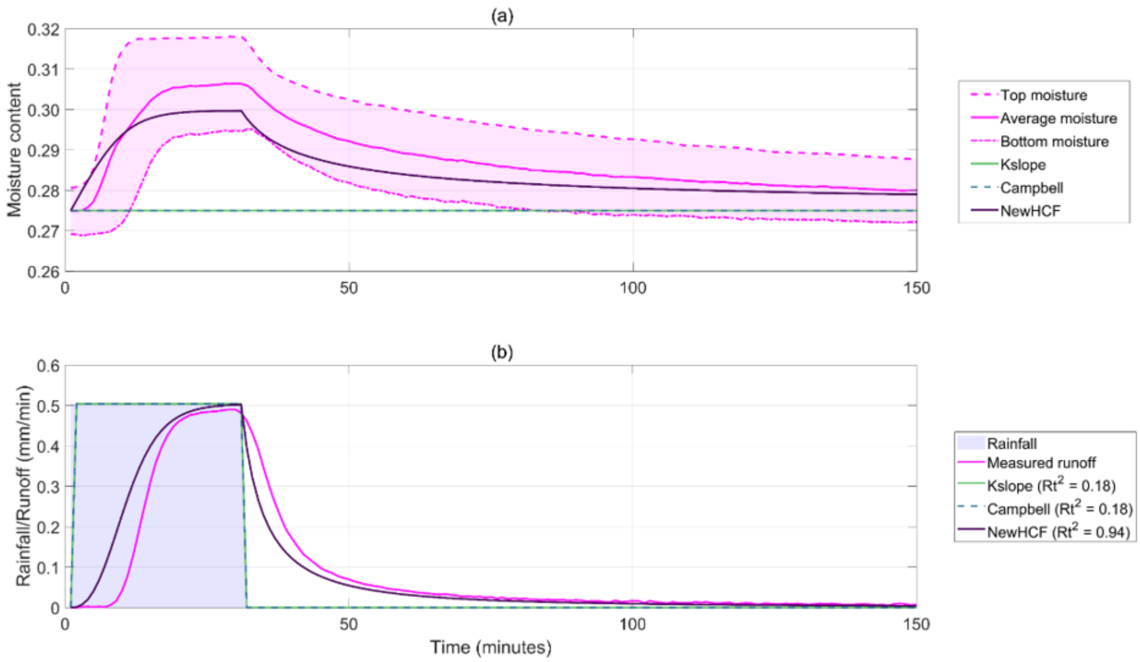

Figure 3.3. (a) Soil moisture content & (b) Rainfall-Runoff profiles from measured data and three HCFs (before calibration) using Design Storm 3.

3.3.2 Model Calibration

Figure 3.4 presents the measured HCF data from two laboratory tests and three HCFs after calibration, plotted on a semi-logarithmic scale. The calibrated parameter values are summarised in Table 3.3. Among the three alternative HCF formulations, the calibrated HCF profiles derived from the *NewHCF* model closely overlap and show good agreement with the Test 2 laboratory measurements (steady-state). The *NewHCF* profile ensures that conductivity approaches zero as soil moisture decreases towards field capacity. The *NewHCF* formulation, benefiting from its power-law formulation and definition between porosity and FC, achieves a good representation while reducing the dimensionality of calibration and preserving the explicit moisture–percolation linkage required by the SWMM LID framework. The calibrated value of 2.85 is not that dissimilar to 2.5 and this function appears to have low sensitivity to the specific power used in the *NewHCF*.

The *Kslope* HCF, expressed as an exponential function, appears as a straight line on the semi-logarithmic plot and provides a slightly improved fit compared with that presented in Figure 3.2. Although the saturated hydraulic conductivity is preserved, the HCF fails to capture the nonlinear relationship between conductivity and moisture content near field capacity, which explains the characteristic “on–off” percolation behaviour observed in Chapter 2, Figure 2.12. The *Campbell* HCF, while more physically plausible due to its power-law structure, is constrained by being defined across the full moisture content range from saturation to wilting point and is therefore unable to adequately reproduce the measured HCF data, even after calibration.

Table 3.3. Value of parameters for HCFs within SWMM LID module after Calibration (all other values of Table 3.2 remain the same)

		Kslope	***Campbell***	***NewHCF***	**Notes**
Layer/ Configuration	**Parameters**	**Value**	**Value**	**Value**	
	HCO	24.86			
HCF	*b*		3.66		Calibrated
	u			2.85	

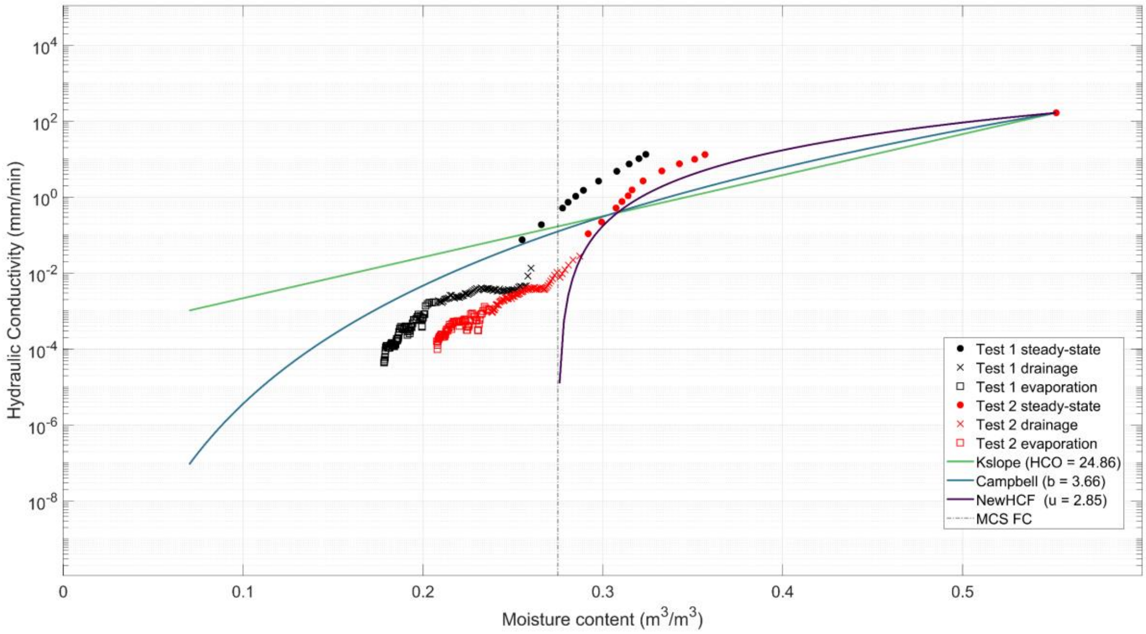

Figure 3.4. Measured unsaturated hydraulic conductivity, and calibrated HCFs (1. Kslope; 2. Campbell; 3. NewHCF) for the MCS.

Figure 3.5 presents the measured and modelled soil moisture and runoff profiles for the 200 mm MCS substrate under Design Storm 3, following calibration. Based on R_t^2 values, the *NewHCF* exhibits the highest level of agreement between simulated runoff profiles and observations.

After calibration, the *NewHCF* demonstrates good consistency between simulated and measured outflow dynamics. The corresponding soil moisture simulations closely follow the observed average moisture variations within the substrate (Figure 3.5a), indicating that the overall soil water release behaviour is well represented.

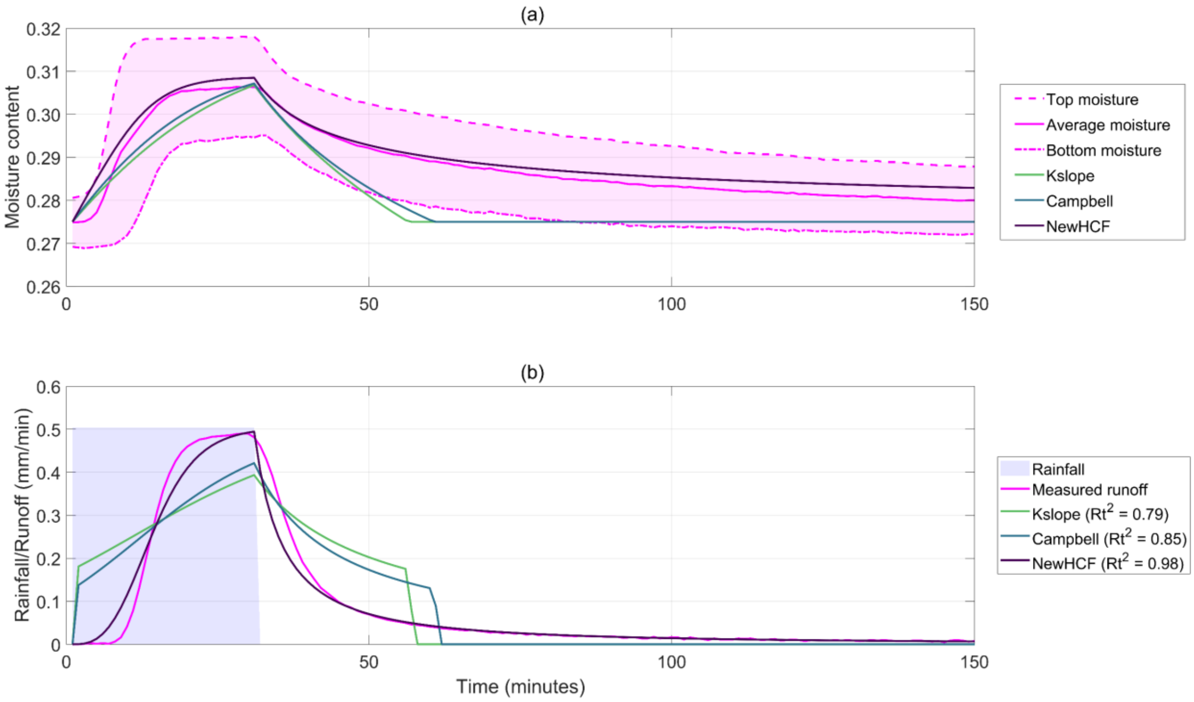

Figure 3.5. (a) Soil moisture change & (b) Rainfall-Runoff profiles from Measured data and three HCFs using Design Storm 3.

Nevertheless, some discrepancies remain. At the onset of rainfall, the observed soil moisture exhibits a short delay before increasing, while the model predicts an immediate response. A comparable pattern is observed in the runoff simulations, where outflow initiates earlier than observed and the recession limb begins prematurely. Although peak magnitudes are similar to the experimental data, the *NewHCF* formulation produces a more abrupt post-peak decline, failing to reproduce the gradual recession behaviour. All these phenomena are due to the assumption of homogenous moisture content in the SWMM LID framework.

Within the SWMM LID framework, the *Kslope* approach simulation behaved similarly to that observed by De-Ville and Stovin (2022). Specifically, abrupt changes in outflow occurred at the start and end of the rainfall event, and the simulated peak flow is substantially lower than the observed peak. The *Campbell* HCF produces a similar runoff response. This behaviour is expected from the HCFs in Figure 3.4, in which hydraulic conductivity at FC has a large non-zero value that is four to five times higher than the measured runoff (i.e. conductivity). This runoff behaviour is notably improved when the *NewHCF* formulation is applied, with a smoother and more sustained peak flow being maintained throughout the high-flow period. Although calibration yields acceptable performance according to the R_t^2 index for both *Kslope* and *Campbell* HCFs, their ability to reproduce key features of the runoff profile, particularly the behaviour associated with the rising and falling limbs, remains limited. By comparison, these deficiencies are substantially reduced when the *NewHCF* formulation is applied, with a smoother and more sustained peak flow being maintained during the high-flow period.

3.3.3 Model Validation

Figure 3.6, Figure 3.7 and Figure 3.8 present the simulated soil moisture and runoff responses produced by the three HCFs under Design Storms 1, 2 and 4, respectively, using the parameter sets calibrated against Design Storm 3.

Under the low-intensity Design Storm 1 scenario, both the *Kslope* and *Campbell* HCFs exhibit limited ability to reproduce the observed detention behaviour. As seen for Design Storm 3, rainfall infiltrates into the substrate but is released almost instantaneously, resulting in a nearly constant soil moisture profile over time. Correspondingly, the simulated runoff closely mirrors the rainfall input, indicating that little or no detention is represented by these two HCFs under low-intensity conditions.

Across all three validation scenarios, the relative performance of the HCF formulations remains broadly consistent with that observed under Design Storm 3, as also reflected by the corresponding R_t^2 values. The *NewHCF* continues to provide the best agreement with the measured runoff dynamics. In Design Storms 2 and 4, the *Kslope* and *Campbell* HCFs fail to reproduce the observed runoff patterns, with peak flows generally underestimated and recession behaviour inadequately represented. These deficiencies highlight the limited capacity of the two formulations to capture moisture-dependent percolation behaviour across varying rainfall intensities.

Overall, the validation results confirm that the relative strengths and weaknesses identified during the calibration storm are robust across different rainfall conditions. In particular, the *NewHCF* formulation demonstrates consistently good performance across all design storms, supporting its suitability as a concise yet effective representation of unsaturated percolation behaviour within the SWMM LID framework.

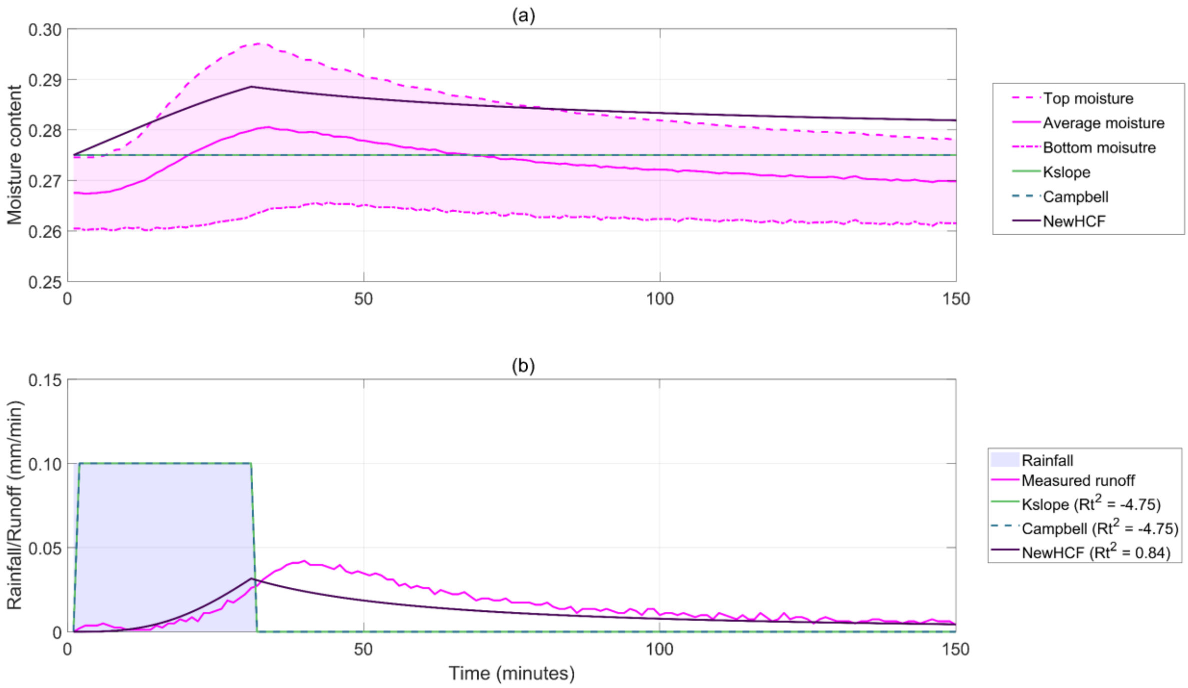

Figure 3.6. (a) Soil moisture change & (b) Rainfall-Runoff profiles from Measured data and three HCFs using Design Storm 1.

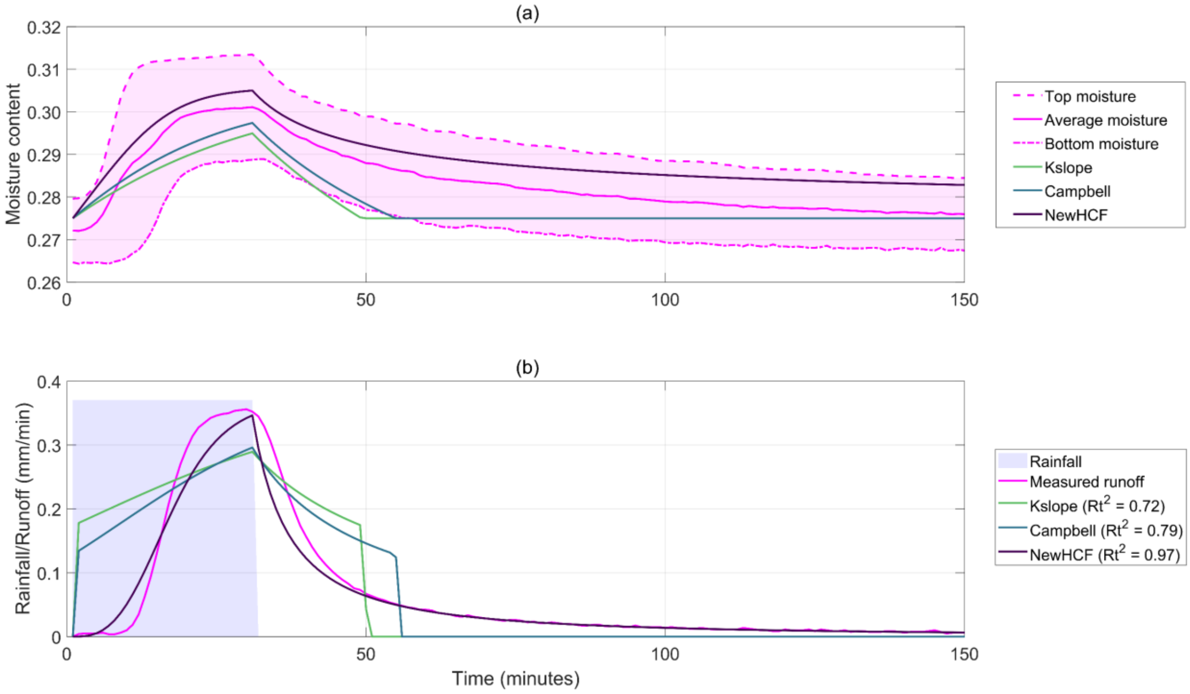

Figure 3.7. (a) Soil moisture change & (b) Rainfall-Runoff profiles from Measured data and three HCFs using Design Storm 2.

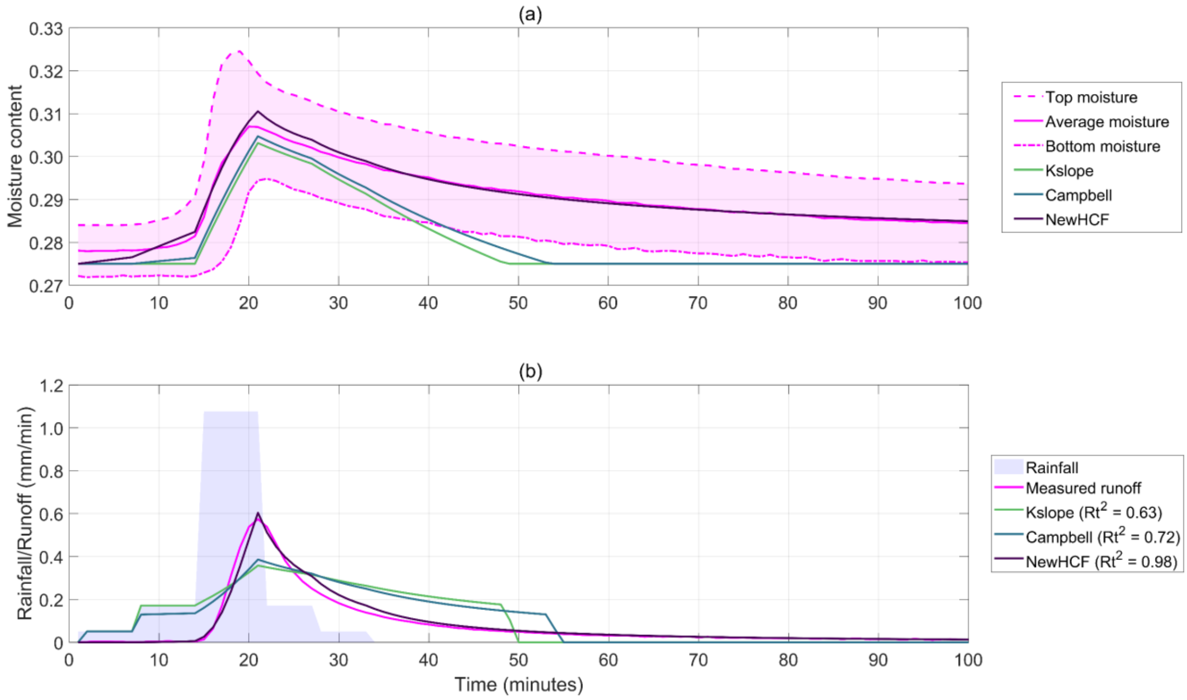

Figure 3.8. (a) Soil moisture change & (b) Rainfall-Runoff profiles from Measured data and three HCFs using Design Storm 4.

3.4 Discussion

The advantage of the *NewHCF* therefore lies in its structural compatibility with SWMM's percolation logic. This enables a concise representation of unsaturated detention behaviour that is easy to calibrate. Importantly, the proposed function reproduces the general shape of the measured HCF data and is consistent with the hydraulic behaviour reported for a range of engineered growing media in previous experimental studie (Liu and Fassman-Beck, 2018). To further examine its applicability beyond green roof substrates, Figure 3.9 compares the *NewHCF* formulation with independent infiltration column measurements obtained from a 540 mm deep bioretention growing media (De-Ville et al., 2025a). The comparison demonstrates that the *NewHCF* captures the nonlinear increase in hydraulic conductivity with volumetric water content observed in the experimental data, indicating that its functional form remains appropriate for bioretention media as well as green roof substrates.

The *NewHCF* formulation is particularly robust in this modelling context because it is explicitly constrained by both the field capacity and the saturated water content (or porosity) of the growing media. These parameters are readily obtainable from standard laboratory characterisation tests and, crucially, correspond to the physical bounds of percolation defined within the SWMM framework. Specifically, the function approaches zero hydraulic conductivity at field capacity and saturated hydraulic conductivity at full saturation, with the fitted exponent u controlling only the curvature between these two points. As a result, model estimates exhibit limited sensitivity to u, since the boundary conditions are physically fixed. Practically, the percolation becomes zero at field capacity, as the value would be so small as to be beyond any engineering precision. In contrast, the exponential *Kslope* HCF and *Campbell* HCF formulation yield larger hydraulic conductivity values than measured data at field capacity, which is inconsistent with the SWMM assumption that percolation ceases at this threshold. This inconsistency can lead to unrealistic "on–off" outflow behaviour, as previously reported by De-Ville and Stovin (2022) and Liu and Fassman-Beck (2017).

Despite these improvements, limitations remain inherent in the bulk percolation modelling approach implemented in SWMM LID. By treating the substrate as a single, vertically lumped control volume, the model assumes uniform moisture content and does not explicitly resolve vertical hydraulic gradients or internal moisture redistribution. Consequently, the detailed evolution of moisture profiles with depth cannot be captured. In the present study, measured soil moisture data were available from both upper and lower sensors within a 200 mm deep substrate. These limitations become more pronounced for deeper substrates, such as those commonly used in bioretention systems, where vertical heterogeneity and internal drainage pathways play an increasingly important role (De-Ville et al., 2025b).

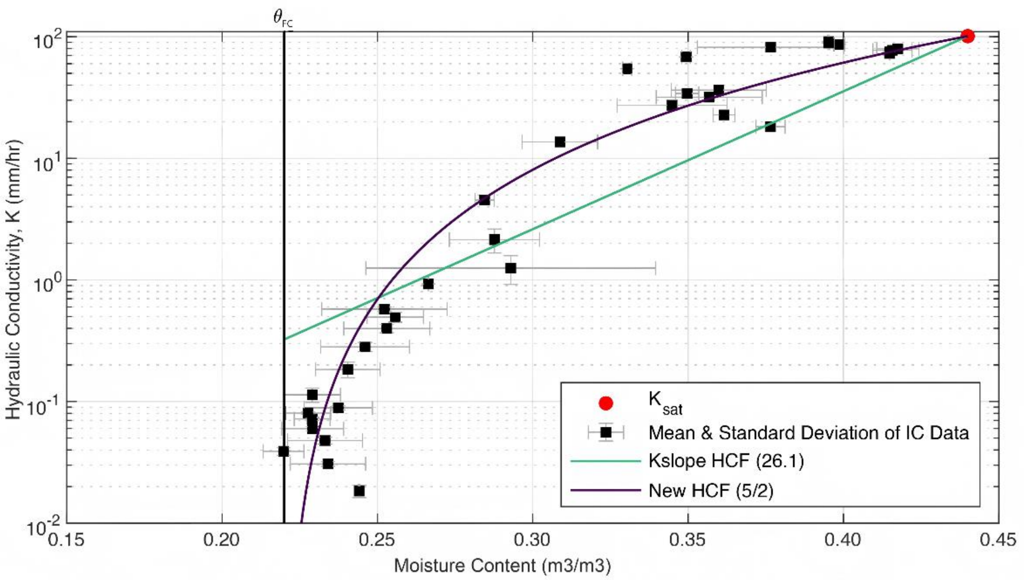

Figure 3.9. HCF data and model fits for bioretention growing media (De-Ville et al., 2025a)

Nevertheless, for many stormwater management applications, the bulk representation adopted in SWMM remains acceptable, as it is able to reproduce the key performance characteristics of interest, including peak flow attenuation and overall outflow dynamics under high inflow conditions (De-Ville et al., 2025a, 2025b; Lisenbee et al., 2021; Peng and Stovin, 2017). This is particularly relevant for practical modelling contexts where the primary objective is to compare design scenarios, estimate overall runoff reduction, or assess peak flow attenuation, rather than to reproduce detailed internal moisture redistribution within the substrate. In such applications, the existing SWMM HCF approaches remain useful because they are already implemented within the standard software framework, require relatively limited input data, and provide a transparent and computationally efficient basis for practitioner-led modelling. The *NewHCF* therefore offers a promising improvement in process representation, but its wider adoption would require further testing across additional media types, climates, event conditions and design configurations.

3.5 Conclusions

This chapter examined alternative HCFs within engineered green roof substrates, with a particular focus on how different hydraulic conductivity functions influence detention behaviour within the SWMM LID framework. The results demonstrate that model performance is strongly controlled by the functional form used to describe unsaturated hydraulic conductivity, especially near field capacity.

Among the tested approaches, the *NewHCF* formulation consistently achieved the best agreement with observed runoff dynamics following calibration. The *NewHCF* formulation provided comparable predictive performance without increasing model complexity or parameter requirements. Its principal advantage lies in its structural compatibility with the SWMM LID framework (bulk model), as percolation is expressed directly as a function of soil moisture and explicitly constrained by field capacity and saturation. This formulation yields stable behaviour across multiple design storms and avoids inconsistencies inherent in the exponential HCF representation, such as non-zero hydraulic conductivity at field capacity and abrupt "on–off" runoff responses.

The *Kslope* and *Campbell* approaches were less successful in reproducing observed detention behaviour, particularly under low- and moderate-intensity rainfall conditions. Both formulations tended to underestimate peak flows and failed to capture the gradual release of stored water, reflecting limitations in their ability to represent moisture-dependent drainage in engineered substrates.

Overall, the findings confirm that, although SWMM LID adopts a simplified, vertically lumped representation of substrate hydrological processes, it remains a suitable platform for investigating detention behaviour and the effects of model simplification. The existing SWMM HCF approaches therefore remain appropriate for practitioner applications. Their continued use is justified by their simplicity, accessibility, low data requirements and integration within an established modelling platform. The *NewHCF* should therefore be regarded as an exploratory formulation that demonstrates how improved representation of HCF shape can enhance model performance, rather than as a direct replacement for the default SWMM implementation. This conclusion provides a methodological foundation for the subsequent chapters, which continue to employ the standard SWMM LID framework to examine simplification and aggregation effects at larger spatial scales.

4. Evaluation of SuDS Device-scale Simplified Modelling Methods

4.1 Introduction

While Chapter 3 focused on the detailed evaluation of unsaturated percolation processes and their influence on runoff generation, the present chapter shifts attention to how the hydrological processes could be embedded and simplified in SWMM.

As discussed in Chapters 2 and 3, SWMM LID has been widely applied as a modelling framework for green roofs, bioretention systems, and other SuDS types, and has frequently been evaluated against monitored runoff observations. These studies have demonstrated its general capability to reproduce runoff dynamics while also identifying limitations associated with evapotranspiration representation and simplified percolation formulations, particularly in engineered media contexts. Detailed discussion of these applications and limitations is provided in the preceding chapters and is not repeated here.

Although limitations in the standard SWMM LID formulation are acknowledged, the unmodified SWMM model is retained as the reference framework throughout this chapter. Its widespread adoption, transparent structure, and inclusion of the principal hydrological processes identified as influential in Chapter 3 make it an appropriate baseline for examining simplification effects.

When SuDS are represented at larger spatial scales, particularly within existing urban drainage network models, simplified approaches have been adopted. In previous studies, SuDS were incorporated by adjusting the proportions of contributing area types—such as pervious, impervious, or directly connected surfaces—associated with model nodes. In some cases, treated areas were effectively disconnected from the drainage network to approximate runoff reduction. Other screening or sizing approaches have relied on fixed runoff-volume reductions, constant infiltration rates, or event-based runoff coefficients rather than explicit process-based representations (Batalini De Macedo et al., 2022; Haghighatafshar et al., 2019b; Lashford et al., 2020; Metcalfe et al., 2018; Stovin et al., 2013a). While these methods offer practical advantages in large-scale applications, they inherently abstract or omit the time-varying hydrological mechanisms that govern SuDS performance at the device-scale.

The aim of this chapter is to systematically examine how progressive simplification of key hydrological processes within the SWMM LID framework affects model behaviour at the device-scale based on standard (non-LID specific) hydraulic model components, as an intermedia to step of the whole thesis. The focus is on understanding the implications of simplification for the accuracy and usefulness of model outputs under conditions representative of applied drainage modelling practice.

To achieve this aim, the chapter pursues the following specific objectives:

1. To establish four alternative modelling approaches for representing individual SuDS devices without LID module, i.e. using generic hydrological/hydraulic controls in SWMM.
2. To evaluate the accuracy of outflow predictions from these simplified models in terms of runoff volume and hydrograph characteristics, using both design storm simulations and continuous rainfall time series.
3. To assess the sensitivity of model performance to variations in key controlling parameters, with particular emphasis on saturated hydraulic conductivity, outlet control configuration, and exfiltration rates for bioretention systems.

The objectives are to provide a controlled basis for evaluating how simplifications influence predicted SuDS behaviour.

Within the overall structure of this thesis, Chapter 4 serves as a methodological bridge between the process-focused analysis presented in Chapter 3 and the subsequent investigation of SuDS aggregation and subcatchment-scale representation. By clarifying the hydrological consequences of simplified device-scale modelling, this chapter underpins the aggregation strategies and modelling trade-offs explored in later chapters.

4.2 Methods and Data

4.2.1 Hydrological Model Setup

Hydrological modelling was performed using the Storm Water Management Model (SWMM 5.2), developed by the USEPA (Rossman, 2016b, 2016c, 2016a). The SWMM model simulates the rainfall/runoff process using the Green-Ampt equation for infiltration and the dynamic wave formula for runoff routing. Full details of each SuDS unit layer in the SWMM LID model are provided in the SWMM Manual (Rossman, 2016a).

Two SuDS types, a Green Roof (GR) and a Bioretention (BIO) were considered. Extensive GR are generally considered to have a relatively weak detention function (Stovin et al., 2017), as their primary function is retention through ET losses prior to the rainfall event. BIO offer much more significant detention (Haghighatafshar et al., 2019b; Lisenbee et al., 2021), due to their deeper substrates and lower hydraulic conductivities, which facilitate temporary storage. These SuDS devices encompass a range of hydrological processes and functionalities, making them suitable candidates for a comprehensive evaluation of the simplified modelling approaches. A non-SuDS scenario was also established as an experimental control.

All model formulations utilised a 10 × 10 m (0.01 ha) 100% impermeable subcatchment (Appendix A1.1). This subcatchment was connected to a junction and subsequent outfall by a conduit that was over-sized so as to cause no impediment to flow. The green roof was modelled as occupying 100% of the subcatchment. The bioretention system was modelled as occupying 20% of the subcatchment area, receiving incident rainfall on its own area and surface runoff generated from the other 80% of impervious area. This type of set-up is representative of bioretention applications in the real world with a loading ratio of 5:1.

4.2.2 SuDS Device-scale Modelling Methods

Five device-scale SuDS modelling methods were trialled. The SWMM *LID* model outputs were considered to provide baseline predictions, against which the four simplified models could be compared. Detailed model settings and parameterisation for the LID model are presented in Appendix A1.1. The four simplified models were also constructed in SWMM, utilising generic hydrological/hydraulic controls expected to also be available within the broader range of drainage network modelling tools. The four simplified models (termed *Disconnect, TransferP, Daily Loss* and *Continuous (Cont.) Loss*) represent a progression from the most basic to the most complete.

The *Disconnect* model removes impermeable areas treated by SuDS. Runoff from this subcatchment will always be zero. Detailed settings are provided in Appendix A1.2.

The *TransferP* model alters SuDS treated areas to permeable areas by adjusting the percentage of permeable area in the subcatchment. The *TransferP* model applies the exfiltration rate (7.2 mm/hr) characteristic of a clay loam. Detailed settings are provided in Appendix A1.3.

The *Disconnect* and *TransferP* models reproduce the two most drastic SuDS representations adopted in Stovin et al. (2013a).

The final two modelling frameworks – *Daily Loss* and *Cont. Loss* – employ standard hydraulic model components to represent the key hydrological processes associated with rainfall/inflow retention (resulting from infiltration and evapotranspiration) and runoff detention (due to internal percolation and/or downstream flow controls). In the context of this chapter, these two modelling frameworks are referred to as ‘simplified’ models because they can be implemented without the use of a dedicated SuDS/LID module, and because certain important hydrological processes, such as surface infiltration and percolation through the growing media, are not represented directly. The key difference between these two approaches is that the *Daily Loss* model incorporates a fixed depth of initial losses which is restored once per day, while the *Cont. Loss* model allows the initial losses to increase dynamically in proportion to the length of the antecedent dry weather period.

These two approaches require significantly higher levels of parameterisation and device level knowledge compared with the *Disconnect* and *TransferP* models. They approach the dedicated LID module in complexity and are only being considered here as substitutes for the LID module when it might not be available.

Figure 4.1 illustrates the *LID*, *Daily Loss* and *Cont. Loss* modelling frameworks.

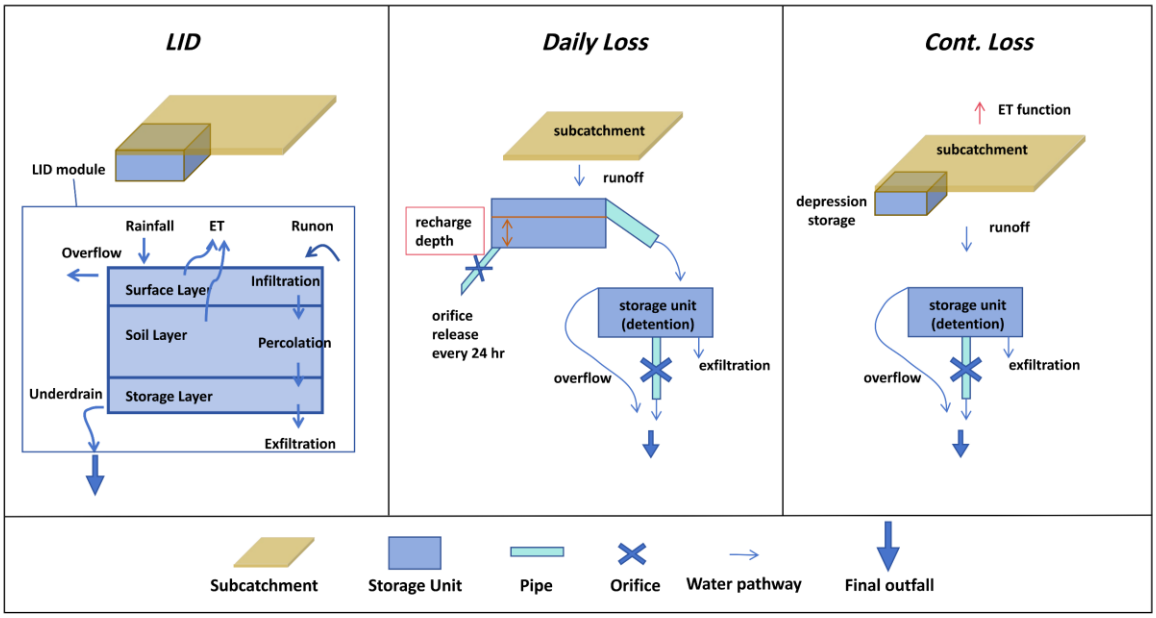

Figure 4.1. LID, Daily Loss and Cont. Loss Modelling Frameworks

The *Daily Loss* model combines the initial losses and storage options adopted by Stovin et al. (2013a). To model the replenishment of initial losses, the recharge tank (sized in plan to match the SuDS device) is designed to empty every 24 hours. The user-specified recharge depth (Figure 4.1) is assumed to represent SuDS options that provide retention as a result of ET during the antecedent dry weather period (ADWP). Once the recharge tank reaches its full recharge depth, any additional inflow during the 24-hour period is directly discharged into a 'detention' storage unit fitted with an orifice control. This orifice control is used to represent the detention effects of either percolation through the substrate or downstream flow control. In the 'detention' storage unit, the exfiltration rate can be set to represent a seepage loss to the natural soil. The detention storage depth is zero in the GR model and there is no exfiltration. The choice of a suitable recharge depth and detention settings are discussed in Section 4.2.5. Detailed settings and parameterisation are provided in Appendix A1.4.

In the *Daily Loss* model, the 24-hour emptying mechanism of the recharge tank is implemented through an orifice in SWMM, configured to empty the tank within a single time step (from 23:55 to 00:00). It should also be noted that, in this approach, the maximum possible retention is determined by the recharge depth; additional capacity does not develop during prolonged dry spells.

The *Cont. Loss* model represents an evolution of the *Daily Loss* approach, in which initial losses are represented by depression storage (sized in plan to match the SuDS device) within the subcatchment. This modification enables the initial losses to be dynamically updated through ET losses, offering a more realistic depiction of the SuDS substrate's retention capacity recovery. The depth of depression storage reflects the maximum volume of retention within the SuDS substrate. The non-SuDS area of the *Cont. Loss* model subcatchment is modelled as having 0 mm of depression storage. Due to limitations in 'within subcatchment' flow routing in SWMM, the runoff from the impervious area cannot be directed to the SuDS area and is instead routed to the modelled detention storage. Consequently, a portion of the stormwater bypasses the depression storage and is not utilized for retention; this has the effect of simulating runoff earlier than the aforementioned model formulations. The detention storage component is consistent with the *Daily Loss* model. Detailed settings and parameterisation are provided in Appendix A1.5.

In both the *Daily Loss* and *Cont. Loss* models, the storage unit (detention) is used to represent the detention effects due to either a physical flow control/orifice or percolation through a deep substrate (soil) layer. The percolation characteristics of the SuDS substrate limit the outflow rate to its saturated hydraulic conductivity. For the storage unit and orifice-controlled outflow in the *Daily Loss* and *Cont. Loss* models, the maximum outflow rate was set to reflect the lower value of the saturated hydraulic conductivity (K_{Sat}) or the underdrain flow control. Under-drain flow governed by the orifice equation varies with the square root of the water head, representing a power-law response. Percolation through the soil layer is computed with Darcy's Law, which produces an exponential rise in conductivity as saturation is approached. Consequently, the way discharge varies with soil moisture content differs between these two functions (Figure 4.2). The end points were chosen to correspond with the LID model setting, specifically zero flow under dry conditions and K_{Sat} at full saturation. However, the intermediate values are clearly fundamentally different. This may limit the simplified models' ability to reproduce dynamic outflow responses in situations where flow detention due to percolation within the substrate dominates. If necessary, a closer match to the expected hydraulic conductivity behaviour could be obtained through the use of a custom Q/h relationship.

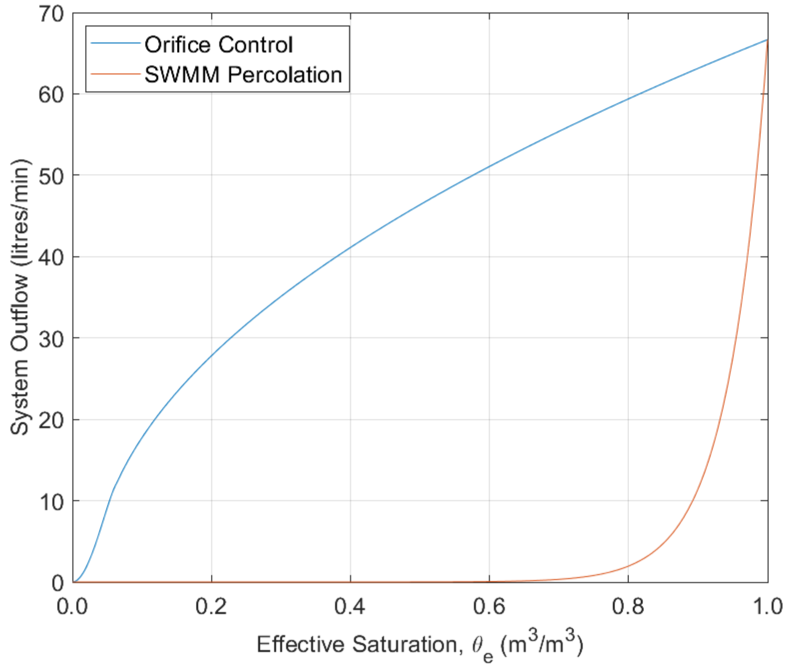

Figure 4.2. Schematic diagram of Q-h Orifice & Percolation function curve

4.2.3 Meteorological Data Inputs

SuDS hydrological modelling tools are required to quantify expected responses to both routine and extreme rainfall events, depending on whether the focus is on water quality or flood risk mitigation respectively. The comparative performance of the five modelling approaches was therefore evaluated against two design storms (10- and 30-year return periods) and a one-year continuous time-series rainfall input.

The 10yr and 30yr design storms, are storm profiles with 24.0 and 31.8 mm of total rainfall respectively, distributed over 59 minutes according to the UK 75% winter profile (NERC, 1999). These intensities are equivalent to the intensities associated with one-hour 1 in 10 and 30 years Sheffield (UK) FEH 22 rainfall (UK Centre for Ecology & Hydrology, 2024). The design storms were simulated at 1-min intervals.

The continuous simulations used the observed rainfall at 5-min intervals from an experimental site in Sheffield (UK) during 2007 (Stovin, 2024). The 2007 rainfall record was selected as it is a continuous, high-resolution dataset. The total rainfall depth (875.6 mm) is approximately 10% above the 1971-2000 mean recorded at the nearest Met Office rain gauge. Although the series is limited to a single year, it includes a number of storm events ranging from frequent, low-return-period, showers to a

99.6 mm event with an approximate 16-year return period. This captures both typical conditions and the extreme rainfall associated with the summer 2007 floods. This variety of hydrological conditions provides a rigorous testing ground for evaluating how well simplified SuDS models reproduce dynamic retention and detention behaviour across contrasting antecedent moisture states and storm magnitudes.

The annual time-series simulation was used to compare both cumulative runoff metrics and performance during selected large events. Table 4.1 highlights 8 significant rainfall events from the 2007 continuous rainfall series (Stovin et al., 2012). The minimum rainfall depth of these 'significant' events is 12.6 mm, and all events experienced peak rainfall intensities of at least 12 mm/h and a duration of at least 2 hours.

Table 4.1. Rainfall characteristics for the 'significant' rainfall events (Return period > 1 year)

Event start	Rain duration (hh:mm)	Rainfall depth (mm)	ADWP (hh:mm)	Mean intensity (mm/h)	Peak 5-min Intensity (mm/h)
18/01/2007 01:11	24:20	27	10:25	1.11	21.6
20/01/2007 19:47	24:20	38.6	9:00	1.59	14.4
13/05/2007 12:34	21:30	29.8	16:05	1.39	12.0
12/06/2007 05:38	2:05	12.8	199:15	6.24	28.8
13/06/2007 15:39	42:30	99.6	32:00	2.34	21.6
15/06/2007 17:54	9:20	16.2	7:45	1.74	12.0
24/06/2007 22:12	22:40	58	6:00	2.56	28.8
26/07/2007 06:56	13:30	12.6	13:25	0.93	33.6

The monthly potential evapotranspiration (PET) rates were calculated based on the monthly average temperature and the hours between sunrise and sunset using the Thornthwaite equations (Stovin et al., 2013b), Table 4.2. In the SWMM simulations, the ET function was only considered in the continuous rainfall series, and when there was no rainfall.

Table 4.2. Monthly PET (mm/day) in Sheffield (2007)

January	February	March	April	May	June
0.47	0.60	1.13	1.87	3.00	3.95
July	**August**	**September**	**October**	**November**	**December**
4.49	3.91	2.73	1.57	0.79	0.45

4.2.4 SuDS Configurations

Individual SuDS devices can vary considerably in their configuration. This is particularly true for bioretention cells, which may incorporate: (i) substrate with higher or lower percolation rates; (ii) the presence or absence of an outflow control; and (iii) subsoil conditions that do or do not permit exfiltration. Several different BIO configuration scenarios were therefore introduced. Variations in (extensive) green roof configuration are generally less significant; hence a single representative green roof was considered to be sufficient for the fair comparison of the simplified modelling approaches.

The following scenarios allow for a comprehensive analysis of bioretention model suitability:

- BIO1: BIO with low K_{sat} (200 mm/hr). A conductivity of 200 mm/hr approximates a low value of saturated hydraulic conductivity measured for engineered bioretention media (De-Ville et al., 2025a; Liu and Fassman-Beck, 2018; Rossman, 2016a).
- BIO2: BIO with high K_{sat} (600 mm/hr). A conductivity of 600 mm/hr represents a higher value within the range recommended for typical engineered media in recent studies (De-Ville et al., 2025a; Liu and Fassman-Beck, 2018; Rossman, 2016a).
- BIO3: BIO with low K_{sat} (200 mm/hr) + orifice (d = 10 mm). The 10 mm outlet diameter matches typical under-drain specifications in the Mansfield Sustainable Flood Resilience SuDS retrofitting programme (De-Ville et al., 2024).
- BIO4: BIO with low K_{sat} (200 mm/hr) + seepage (7.2 mm/hr). A seepage rate of 7.2 mm/hr is consistent with local soil conditions in Sheffield and has been used in other bioretention research (Berretta et al., 2018; National Cooperative Soil Survey, 2006).

Table 4.3 lists the primary parameter values for GR and BIO configurations in the *LID* model. The extensive green roof parameters were referenced from literature (Peng and Stovin, 2017) and the SWMM manual (Rossman, 2016a). The parameters for BIO were referenced from literature (Berretta et al., 2018; De-Ville et al., 2021) and the SWMM manual (Rossman, 2016a). Appendix A1 presents detailed information of SuDS parameters in various models and scenarios.

Table 4.3. SuDS devices primary parameters for the LID module

Parameter	Unit	Green Roof	Bioretention*				Notes
		GR	BIO1	BIO2	BIO3	BIO4	
Surface							
Berm Height	mm	0	100				GR parameters from Peng and Stovin (2017)
Vegetation Volume Fraction	m^3/m^3	0	0				
Surface Roughness (n)	-	0.15	0				BIO parameters from De-Ville et al. (2021)
Surface Slope	%	2.60	0				
Substrate							
Thickness	mm	100	700				GR parameters from Rossman (2016a)
Porosity	v/v	0.5	0.44				
Field Capacity	v/v	0.3	0.15				
Wilting Point	v/v	0.1	0.12				BIO parameters from (Berretta et al. (2018); De-Ville et al. (2021)
Conductivity	mm/hr	1000	200	600			
Conductivity Slope		40	40				
Suction Head	mm	50	50				
Drainage/Storage							
Thickness	mm	50	300				From National Cooperative Soil Survey (2006); Rossman (2016a)
Void Fraction	-	0.5	-				
Void Ratio	-	-	0.8				
Roughness (n)	-	0.03	-				
Seepage Rate	mm/hr	-	0			7.2	
Clogging Factor	-	-	0				
Drain							
Flow Coefficient	mm/hr	-	1000		1.25		1000 represent no orifice control. 1.25 represents a 10 mm orifice.
Flow Exponent	-	-	0.5				
Offset	mm	-	0				Other parameters from Rossman, (2016a)
Open Level	mm	-	-				
Closed level	mm	-	-				

*Only parameter values that differ from BIO1 values are presented for BIO2, BIO3 and BIO4

4.2.5 Initial Moisture Content

Continuous simulation in response to an annual time-series rainfall tests the models' abilities to reproduce the interevent draining and drying processes. Hence, the moisture content at the start of each rainfall event is determined internally as part of the simulation. In contrast, when simulating individual design storms, the initial moisture content needs to be set by the user, and a different initial condition may lead to different conclusions being reached in the comparison of the simplified modelling approaches. The design-storm based model comparisons therefore included a range of different, plausible, initial moisture content levels.

Three initial moisture conditions were trialled for the 1 in 10 & 30-year design storm simulation (detailed explanation in Appendix A2):

- PWP (permanent wilting point) condition: After a sufficiently long ADWP, the SuDS substrate reaches a maximum water moisture deficit, i.e., substrate moisture at PWP. This represents the most optimistic design assumption.
- FC (field capacity) condition: In this condition, the total moisture content equals FC, which is achieved when the moisture content remains uniform throughout the depth, with excess water movement driven only by gravity (Rossman, 2016a).
- Median condition: The Median moisture content at the onset of a rainfall event was determined based on SuDS performance simulations using the 2007 continuous rainfall series and the SWMM LID module. Rainfall events were identified as being separated by a minimum ADWP of 24 hours for both GR and BIO SuDS types. The Median initial moisture condition values were found to be 0.18 m^3/m^3 (GR) and 0.23 m^3/m^3 (BIO). A detailed explanation of this approach is provided in Appendix A2.

In the GR and BIO *Daily Loss* models, the available recharge depth was set equal to 2.08 mm, corresponding to the average PET value over 12 months in the 2007 meteorological dataset.

One limitation of the SWMM LID module is that the initial moisture content in the storage/drainage layer inherits the same initial moisture content as the substrate layer. Drainage of this water triggers unrealistic runoff profiles at the start of a simulation in the *LID* model. Trial simulations showed that this artificial initial drainage response had dissipated after approximately 20 minutes, after which the *LID* outflow hydrograph was no longer affected by the initial storage layer condition. Therefore, a 20-minute settling period was applied in the design storm simulations.

4.2.6 Simulation Scenarios

Simulations were designed to evaluate the four simplified modelling approaches against the SWMM LID model across scenarios that reflect the range of conditions under which simplified SuDS models might realistically be applied. The scenario set addresses three distinct considerations: the impact of model simplification relative to SuDS type; the greater physical variability inherent in bioretention systems; and the role of initial moisture content in design storm simulations.

The SWMM LID model and all four simplified modelling methods were applied to both GR and BIO1 scenarios across all rainfall inputs. The full range of BIO configurations (BIO1−4) was evaluated under the 30-year design storm and the continuous rainfall; the 10-year design storm was limited to BIO1 and GR. For the 30-year design storm simulations, three initial moisture conditions (PWP, FC, and Median) were tested for the *LID*, *Daily Loss*, and *Cont. Loss* models, whilst the *Disconnect* and

TransferP models—being insensitive to initial moisture state—were evaluated under PWP conditions only.

4.2.7 Model Evaluation

The Nash-Sutcliffe model efficiency (NSE) index was employed to objectively estimate how well the runoff profiles were predicted by the different hydraulic conductivity functions compared with the observed runoff. NSE ranges between −∞ and 1.0, with NSE = 1.0 being the optimal value. Values between 0.0 and 1.0 are generally viewed as acceptable levels of performance, whereas values ≤ 0.0 indicate unacceptable performance (Nash and Sutcliffe, 1970). NSE is one of the most widely applied performance metrics in hydrological modelling because it provides an integrated assessment of agreement between observed and simulated hydrographs and facilitates comparison between alternative model structures and parameterisations (Sonnenwald et al., 2013; Huang et al., 2017). Although NSE is more sensitive to errors during high-flow periods and may not fully reflect discrepancies in hydrograph timing or recession behaviour, it remains appropriate for the present study because the primary objective is to compare the overall predictive performance of alternative hydraulic conductivity formulations. Where relevant, additional discussion of differences in hydrograph shape, including the representation of rising and falling limbs, is provided alongside the NSE evaluation.

$$NSE = 1 - \left[\frac{\sum_1^N (Q_p - Q_m)^2}{\sum_1^N (Q_m - Q_{Am})^2}\right] \qquad \text{Equation 4.1}$$

where N= number of samples; Q_m= observed runoff (baseline); Q_p= modelled runoff; and Q_{Am}= mean observed runoff.

For both design storm simulations and for the analysis of the significant events from the annual time series, the time period over which the NSE was calculated was rainfall duration plus 24 hours, corresponding to the individual rainfall event definition in the Methods Section.

The peak runoff error (PE) index was employed to estimate how well the peak runoff magnitudes were predicted by the simplified SuDS modelling methods compared to SWMM LID module.

$$Peak\ Runoff\ Error\ (\%) = 100 \times \frac{Measured\ Value - True\ Value}{True\ Value} \qquad \text{Equation 4.2}$$

where $Measured\ Value$ = simplified modelled peak runoff; $True\ Value$ = control peak runoff ("*LID*" modelling method).

4.3 Results and Analysis

4.3.1 Design Storm Simulations

Figure 4.3 illustrates the modelled runoff profiles and runoff volume (in 24 hours) for GR and BIO1 in response to a 1 in 30-year design storm with an initial moisture condition of PWP. The modelled runoff profiles for GR and BIO1 in response to 1 in 10-year design storm simulation are provided in Appendix Figure A7.

The *Disconnect* method led to a complete absence of outflow. Although it achieved the highest NSE values compared to the other methods, they still indicate a poor relationship between the two approaches. This approach is clearly not realistic in terms of outflow volumes, rates, or timings.

The *TransferP* model converts SuDS-treated areas (100% of the subcatchment for both GR and BIO1) to permeable areas, allowing a portion of the stormwater to infiltrate directly into the natural soil. Once the stormwater inflow exceeds the soil conductivity, and the default depression storage is full, outflow (surface overland flow) occurs.

Both *Disconnect* and *TransferP* basically ignore the physical characteristics of SuDS, leading to identical and unrealistic profiles for GR and BIO1.

Therefore, the *Disconnect* and *TransferP* modelling approaches are not considered further within the comparisons.

In the design storm simulations, any ET losses (or mechanisms designed to mimic ET losses) were set to 0 mm, as is common practice. For the *Daily Loss* model, this manifests as the recharge tank not restoring its capacity during the simulation, and for *LID* and *Cont. Loss* model results in no ongoing losses via ET. Hence, without these ET losses, the *Daily Loss* and *Cont. Loss* models had very similar model formulations and the resultant runoff profiles were very similar for both SuDS types.

The *Daily Loss* and *Cont. Loss* models produced premature outflows and significantly overestimated peak flows in both the GR (PE > 400%) and BIO1 (PE > 2000%) scenarios compared with the SWMM LID module output (*LID*). The peak flows obtained from the simulations of these two models were almost four times higher than the *LID* model result. Both simplified modelling approaches rely on depth based approximations of the SuDS retention and detention processes, with an orifice control to restrict outflow rates. The calculated NSE values revealed a significant discrepancy between these two models and the *LID* model. Particularly in the BIO1 scenario, the large negative NSE values (Figure 4.3c) indicate that these two simplified models cannot accurately predict the outflow detention behaviour. The *LID* maintained a small outflow over the 24-hour period, whereas the two simplified methods ceased to have an outflow after about 200 minutes. As noted earlier (Figure 4.2), these two models' outflow control functions do not accurately reproduce the LID module's hydraulic conductivity response. Similar results were observed in the 1 in 10-year design storm simulation (Appendix Figure A7).

The timing of outflow initiation differed between the *Daily Loss* and *Cont. Loss* models in the BIO1 scenario, with the *Cont. Loss* model producing outflow earlier. This discrepancy arises because, as illustrated in Figure 4.1, runoff bypasses the SuDS area and is routed directly to detention storage, resulting in earlier runoff timing compared to other models.

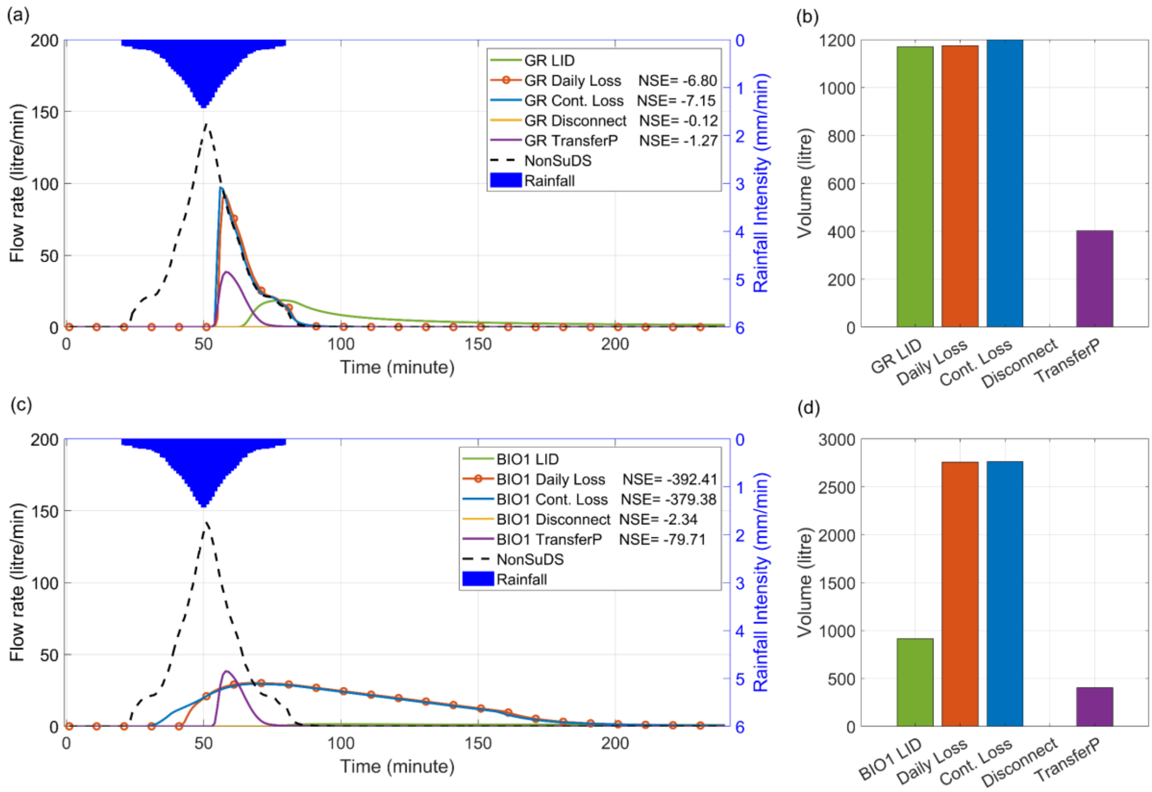

Figure 4.3. (a). GR & (c). BIO1 runoff profiles; (b). GR & (d). BIO1 runoff volumes in 24 hours, using different modelling methods for the 1 in 30-year design storm with initial moisture content set to PWP

With respect to the models' sensitivity to initial moisture content, Figure 4.4 and Figure 4.5 show the modelled runoff profiles for GR and BIO1 systems respectively using the *LID, Daily Loss* and *Cont. Loss* models under various initial moisture content conditions. Notably, when the initial soil moisture was set to FC or Median conditions, the *LID* model exhibited high runoff at the beginning of the simulation. This occurred because, in the SWMM LID module, the initial moisture is set for both the substrate and the drainage layer (Figure 1 and Section 4.2.5). In contrast, the *Daily Loss* and *Cont. Loss* models did not exhibit the unreasonable flow values in the initial phase.

For both the GR and BIO1 systems, initial moisture above PWP raised total discharge and peak flow in all models. The increase was much greater in *Daily Loss* and *Cont. Loss* because their outflow profiles rely on a fixed maximum rate and ignore soil-moisture condition. Wetter starts did raise the NSE values of these two models (computed after excluding the first 10 minutes of artefactual flow), but the hydrographs still do not capture the runoff dynamics shown in the *LID* baseline.

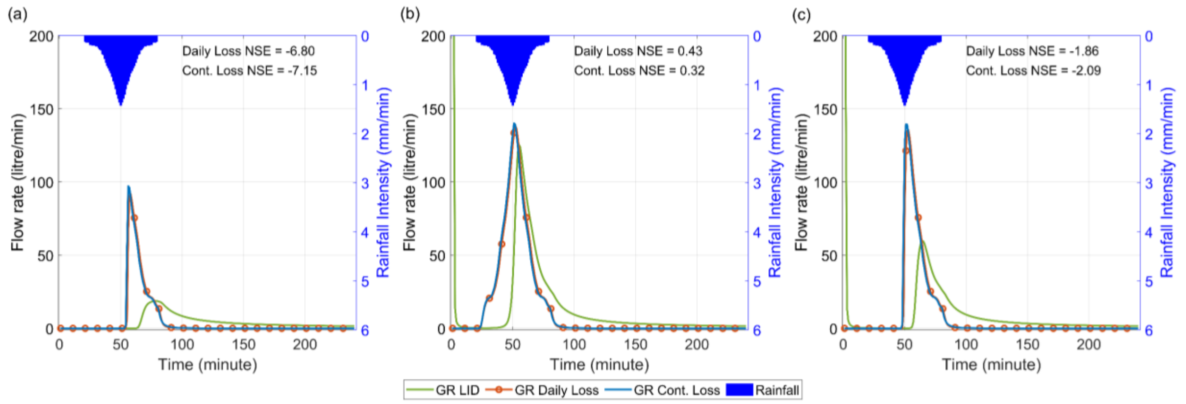

*Figure 4.4. GR runoff profiles using different modelling methods in response to the 1 in 30-year design storm with initial moisture content set at (a) PWP, (b) FC, (c) Median initial condition *NSE values were calculated starting at 10 minutes, ignoring the initial unreasonable flow.*

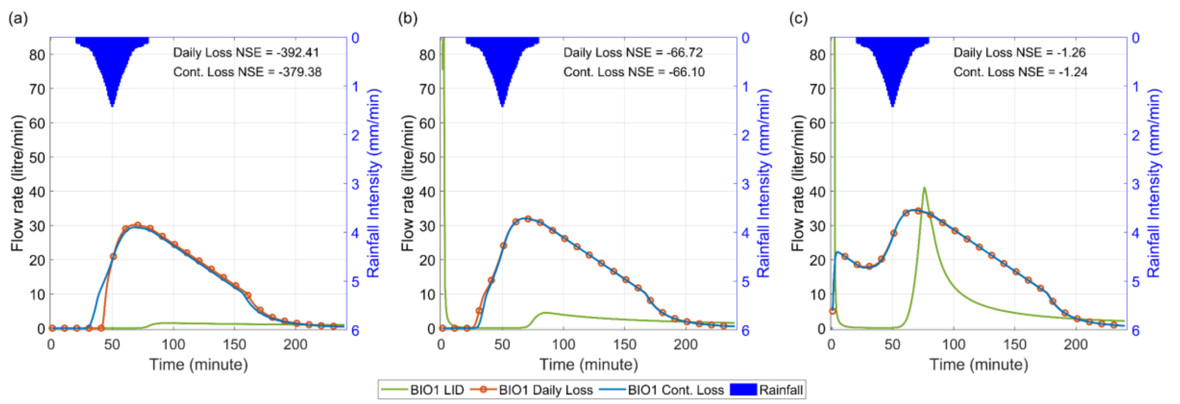

*Figure 4.5. BIO1 runoff profiles using different modelling methods in response to the 1 in 30-year design storm with initial moisture content set at: (a) PWP, (b) FC, (c) Median initial condition *NSE values were calculated starting at 10 minutes, ignoring the initial unreasonable flow.*

Considering the four different BIO configurations, Figure 4.6 compares the outflow profiles associated with modified K_{sat}, orifice control and exfiltration rate, respectively, using an initial moisture content of PWP. It may be seen that:

- Higher K_{sat} (BIO2, Figure 4.6a). A larger hydraulic conductivity accelerates percolation, so every model produces a sharper, higher peak and drains sooner.
- Orifice control (BIO3, d = 10 mm, Figure 4.6b). The orifice controls the discharge rate, flattening the peak and lengthening the tail in all models. However, detention is underestimated by the

simplified models in all cases, as a result of the orifice control overestimating runoff from partially-saturated substrate media (Figure 4.2)

- With exfiltration (BIO4, Figure 4.6c). With an exfiltration limit of 7.2 mm/hr the *LID* model let all water into the native soil and generated no surface outflow. When using an initial moisture condition of PWP, the maximum achieved moisture content within the substrate layer of BIO4 was 0.346 m^3/m^3 which has a corresponding unsaturated hydraulic conductivity of 4.66 mm/hr. Hence, the percolation rate through the substrate was lower than the maximum permissible exfiltration. The *Daily Loss* and *Cont. Loss* models showed outflow profiles (BIO4) that were lower than the original values in BIO1, with shorter drain down durations due to higher total drainage volumes per timestep.

Across scenarios, the *Daily Loss* and *Cont. Loss* models respond as expected to the physical variations, but continue to over-estimate peak flow relative to the LID model because they ignore the moisture-content-dependent responses. In all cases the peak outflow rate associated with the simplified models exceeded the *LID* peak by a factor of at least 100%. This analysis does not provide strong support for the use of any of the simplified approaches in the context of design storm modelling.

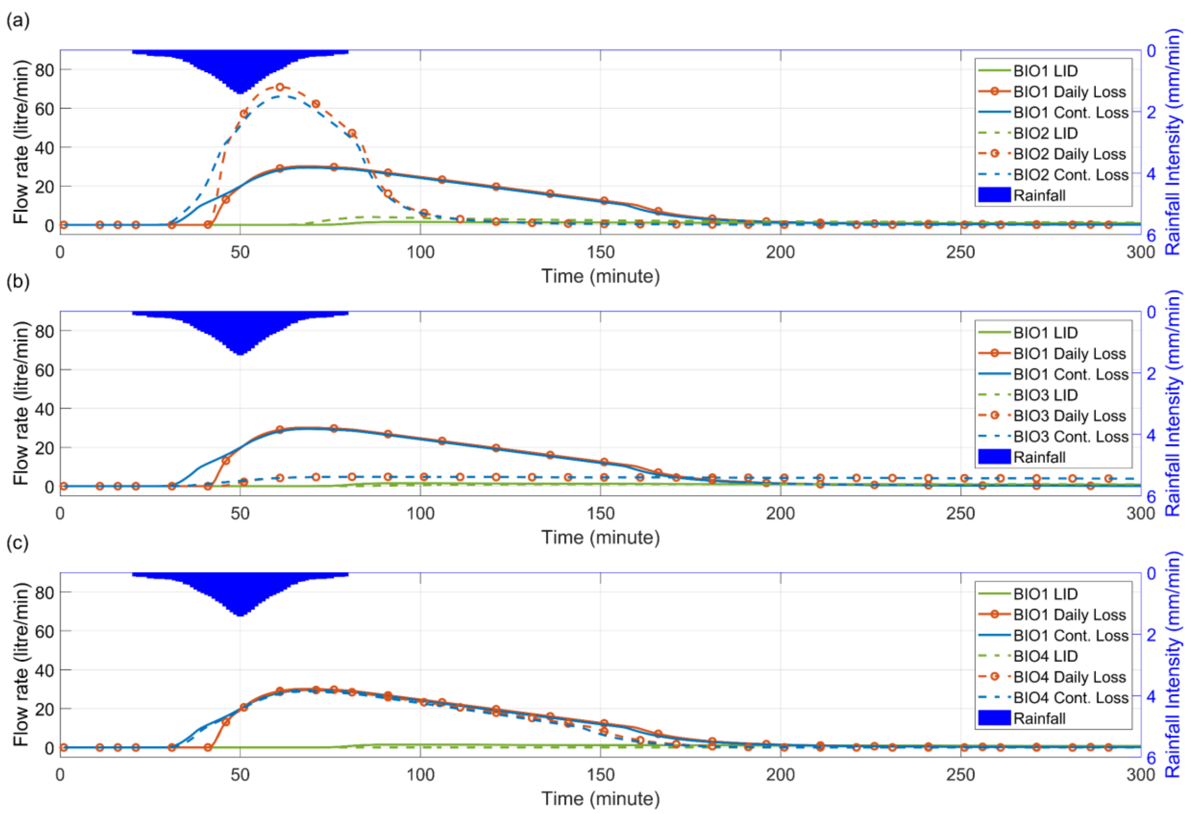

Figure 4.6. BIO outflow profiles in (a) BIO2, (b) BIO3, (c) BIO4 in 1 in 30-year design storm with initial moisture content set at PWP

4.3.2 Continuous Simulation

Figure 4.7 presents the volumetric (i.e. retention) response of the GR and BIO1 models to the annual rainfall time series.

For the GR SuDS type, the total flow volume from the *Cont. Loss* method was very similar to that of the *LID* model, while the *Daily Loss* method significantly overestimated the outflow. As shown in the cumulative flow graph, the *LID* and *Cont. Loss* methods showed no increase in flow between June and November, whereas the *Daily Loss* method continued to show an increase with rainfall. In the *LID* and *Cont. Loss* methods, more rainfall was lost through ET, whereas the *Daily Loss* method underestimated ET loss. The *LID* and *Cont. Loss* methods allow losses to accumulate over longer dry periods (up to a value of $substrate\ thickness \times (FC - PWP)$), whereas this is not possible within the *Daily Loss* framework.

For the BIO SuDS type, the trend in cumulative flow profiles reveals that while the *Daily Loss*, *Cont. Loss*, and *LID* models varied similarly with rainfall, the two simplified methods consistently produced higher outflows volumes compared with the *LID* model.

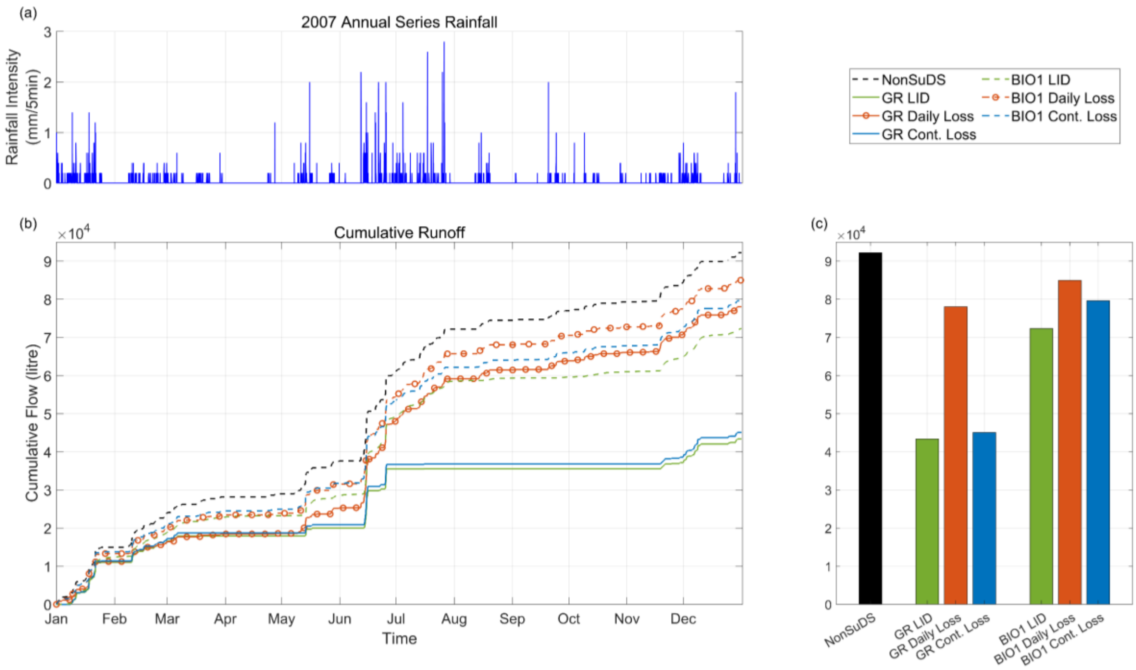

Figure 4.7. (a): Annual rainfall recorded in Sheffield in 2007 at a 5-minute timestep. (b): Cumulative flow volumes for SuDS device-scale modelling methods in response to the annual rainfall for GR and BIO1. (c): Comparison of total volumes for several SuDS device-scale modelling methods.

Figure 4.8 shows the retention performance during 8 significant events (Table 4.1) from the 2007 rainfall series. Since the GR occupies the entire subcatchment area, and both the *Cont. Loss* and *LID* models used the same ET loss mechanism, their retention performances were consistent. For GR, the match is exact, whereas in BIO1, the *Cont. Loss* model introduced some errors compared to the *LID* module. This is due to some surface runoff from the subcatchment bypassing the depression storage and escaping ET loss. The *Daily Loss* model led to more random retention performance for both GR and BIO1. This is because there is no link between the volume of water released by the recharge mechanism and the amount of rainfall during a single event.

Figure 4.9 shows the peak runoff values for eight significant events from the 2007 rainfall time series simulation. Ignoring any GR detention caused the *Daily Loss* and *Cont. Loss* methods to significantly overestimate the peak flow. In most rainfall events, the *Cont. Loss* model exhibited higher peak flows than the *Daily Loss* model. In the BIO1 scenario, these two simplified models overestimated the peak flow rates in most cases, indicating that the detention function modelled by these two simplified methods is inaccurate. The difference is greater in events with smaller rainfall amounts.

Overall, while the simplified approaches show qualitatively reasonable responses to rainfall events, limitations to the ways in which retention and detention are represented generally lead to notable quantitative errors in the temporal runoff profiles.

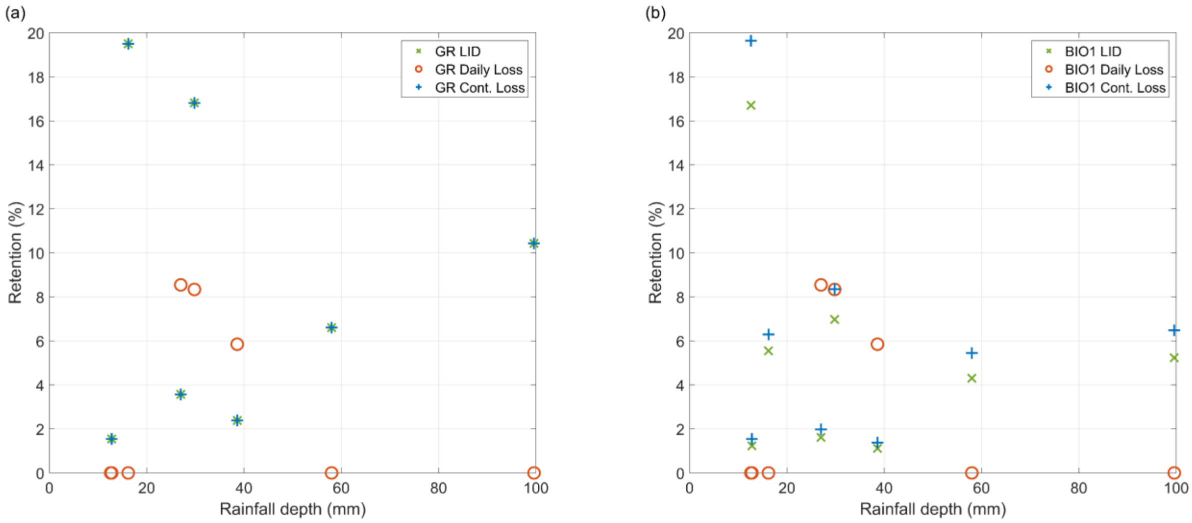

Figure 4.8. Scatter plots for selected key rainfall/runoff parameters in significant events from the 2007 rainfall time-series (a) GR and (b) BIO1

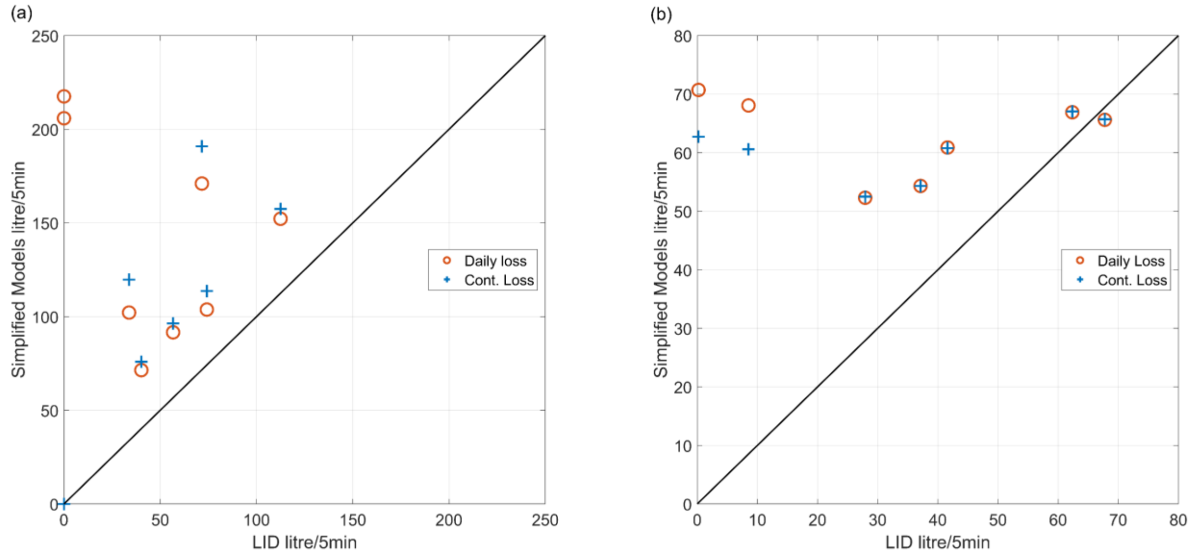

Figure 4.9. Scatter plots for peak runoff rate in significant rainfall events from the 2007 rainfall time-series (a) GR and (b) BIO1

The significant rainfall event of June 13th 2007 was selected to explore the differences in outflow profiles between models (Figure 4.10).

In the GR scenario, the *Cont. Loss* model result was closest to the *LID* method with NSE = 0.21. Despite this similarity, the outflow profile showed more fluctuations and was less smooth than the *LID* profile. This indicates that, despite the weak detention effect of GR, the percolation function in the *LID* method dynamically controls the outflow rate based on soil moisture, resulting in a smoother outflow profile. The *Daily Loss* model produced results similar to the *Cont. Loss* method after 21:00 on June 13. Before this time, the *Daily Loss* method generated runoff whenever there was rainfall, due to the recharge depth tank not being empty at the beginning of the event. It is encouraging to note that the runoff peaks were estimated well by both approaches.

In the BIO1 simulation, the *Daily Loss* model result was similar to the *Cont. Loss* model, but differed from the *LID* simulation. At approximately 21:00 on June 13, the two simplified approaches failed to retain moisture: outflow began immediately with rainfall, producing a minor peak of about 50 L/5min, while the *LID* model released only a negligible discharge. The *Daily Loss* and *Cont. Loss* models underestimated the peak runoff by roughly 20% compared to the *LID* approach. In these two models, the water volume stored in the tank cannot accurately represent the moisture content within the BIO substrate. The use of a single orifice control fails to replicate the outflow dynamic.

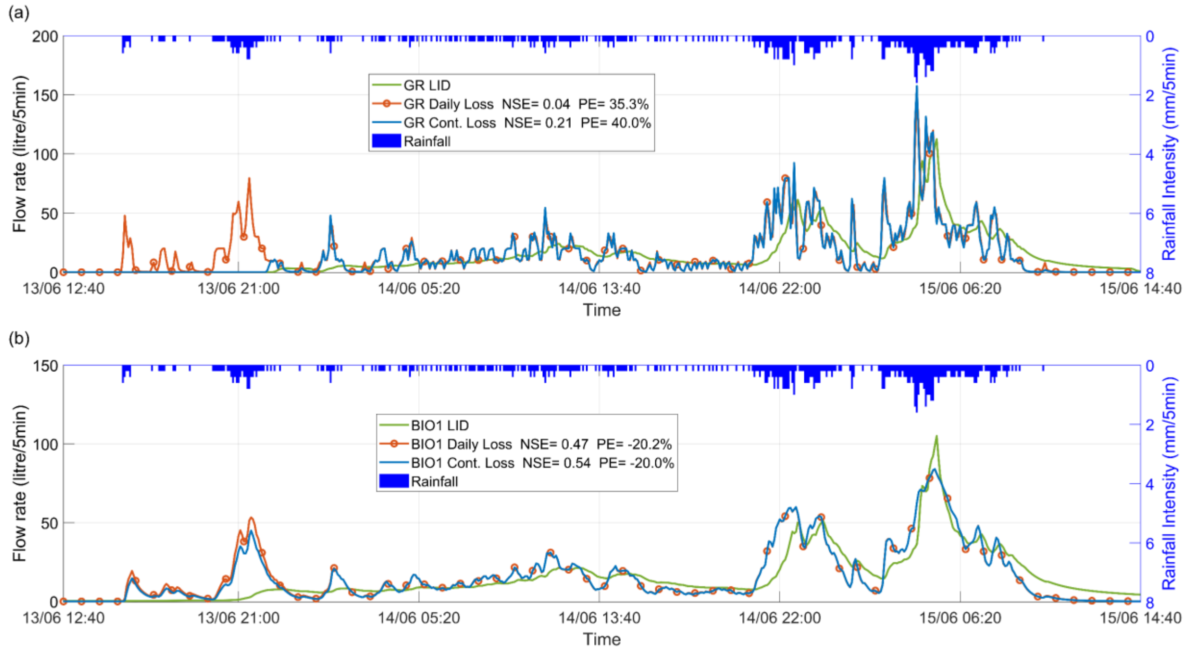

Figure 4.10. Modelled runoff profiles of (a) GR and (b) BIO1 for event June 13th 2007

Figure 4.11 shows the modelled runoff profiles for the different BIO scenarios for the June 13th , 2007 event (Table 4.1).

- Higher K_{sat} (BIO2, Figure 4.11a). Raising hydraulic conductivity accelerates percolation; however, in the *LID* model, the dominant factor is moisture within the substrate rather than K_{sat}. As a result, changes in K_{sat} have negligible impact on the *LID* simulation outputs (compare to BIO1). In contrast, the peaks of the *Daily Loss* and *Cont. Loss* models were more elevated (PE = 13.3%). This suggests that the closeness of fit between these two simplified models and the SWMM LID model is sensitive to changes in K_{sat}. The key factor here is that the outflow is ultimately controlled by the final orifice in both the *Daily Loss* and *Cont. Loss* models, meaning that the parameters of this orifice have a significant impact on the model's performance.
- Orifice control (BIO3, d = 10 mm, Figure 4.11b). With a 10 mm outlet the two simplified models reach NSE $\approx$ 0.84/0.88 against LID. Because all three model approaches are throttled by the same fixed orifice, other differences in model structure prior to this control are largely inconsequential.
- With exfiltration (BIO4, Figure 4.11c). A higher exfiltration rate changed NSE slightly, chiefly because all models led to long periods with zero outflow. The worse NSE reflects volume reduction, not a worse hydrograph profile.

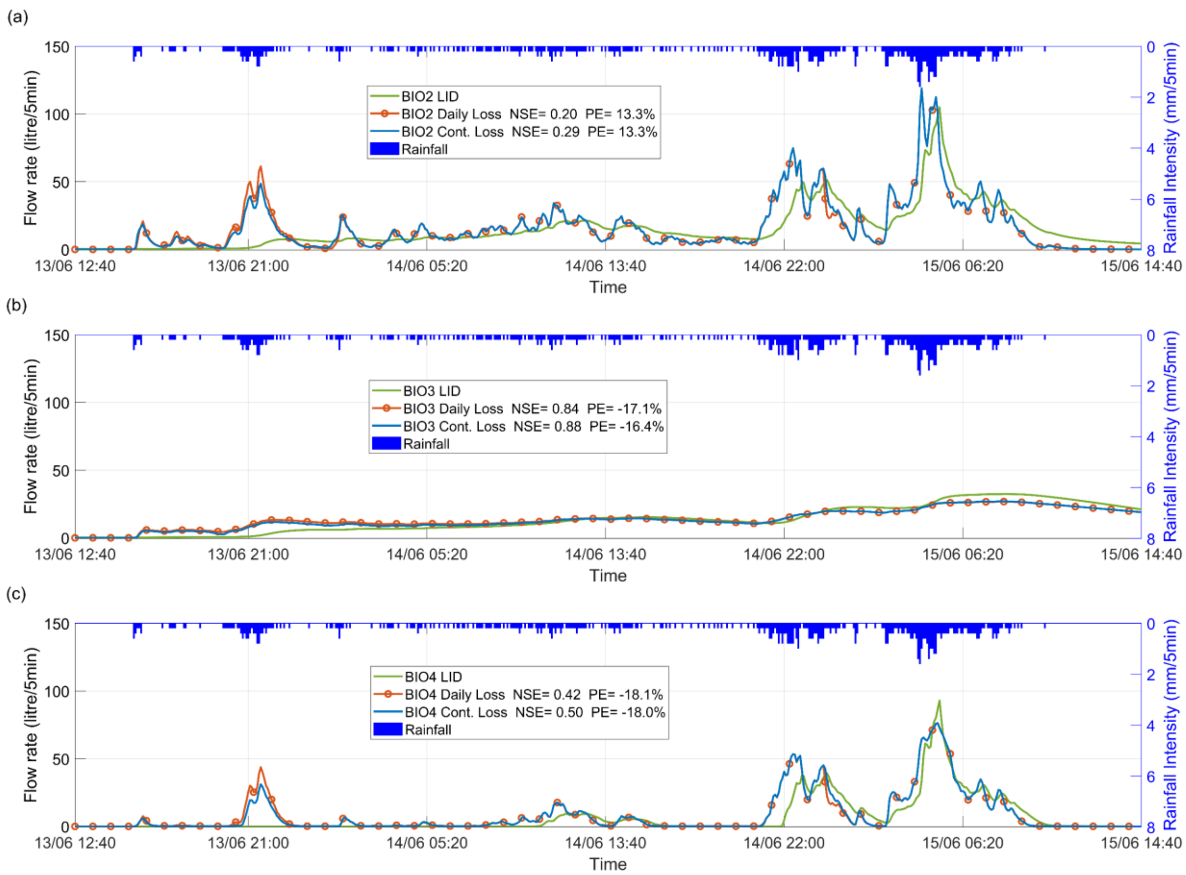

Figure 4.11. Modelled runoff profiles for a) BIO2, b) BIO3 & c) BIO4 for event June 13th, 2007

According to the cumulative outflow graphs (Appendix Figures A8, A9 & A10), both the *Daily loss* and *Cont. loss* models overestimated the total runoff volume across all three scenarios (BIO2, 3 & 4). However, hydrograph comparisons for the selected large rainfall event indicate that both simplified models still capture the approximate peak magnitude and the general temporal pattern of the outflow.

4.4 Discussion

The results of this study have highlighted that each of the simplified modelling approaches has limitations when simulating runoff processes in response to both design storms and continuous simulation. The simplest methods of *Disconnect* and *TransferP* clearly fail to reproduce the rainfall runoff response behaviour of vegetated SuDS systems except for scenarios in which no runoff would be expected to occur, such as in response to very small rainfalls (fully retained) or highly over-designed systems. Figure A7(b) shows that the BIO1 *LID* model response is matched well by both *Disconnect* and *TransferP* because only very low runoff occurs.

It should be noted that the four bioretention cell variants in this exercise were not sized to meet specific design goals; rather a constant plan area was assigned to all four. The introduction of higher percolation rates (BIO2) and exfiltration/seepage (BIO4) would potentially lead to reductions in the plan area required to meet the same design specification, whereas the introduction of an orifice control (BIO3) would potentially require an increase in the plan area to facilitate greater detention storage. Indeed, Figure 4.6(c) confirms that BIO4 generated no runoff for the 30-year design storm. In this scenario, the *Disconnect* method (not shown for clarity) generated an identical (zero runoff) result. These two models may, therefore, be useful for indicating best-case scenarios, but cannot be used to support the sizing of SuDS devices or to understand their performance in response to continuous time-series rainfall inputs.

By increasing model complexity, the *Daily Loss* and *Cont. Loss* methods provide better indications of likely runoff profiles compared with *Disconnect* and *TransferP*, but neither approach captures the complex hydrological and hydraulic processes as comprehensively as the full *LID* model. The simplified representation of ET losses in the *Daily Loss* method, and their inability to accumulate over long periods with no rainfall, severely limits the method's retention performance accuracy in the continuous simulation compared with the *Cont. Loss* or *LID* model approaches. The simplified adjustments to subcatchment perviousness and depression storage of the *Cont. Loss* method induce some retention performance error as, in small rainfall events, the initial losses may not be fully utilised. This minor error reflects the way in which the *Cont. Loss* model was implemented here; an alternative set-up, still only utilising generic hydrological and hydraulic components, could be implemented to address this.

However, these limitations in retention performance representation are small compared with the differences seen in detention performance between both the *Daily Loss* and *Cont. Loss* model formulations when compared with the LID module. These differences are present because the *Daily Loss* and *Cont. Loss* methods do not dynamically alter outflow from the systems in response to soil moisture in the same way as the unsaturated hydraulic conductivity function (percolation) of the substrate layer in the *LID* model. While the use of a generic orifice control does permit variation in percolation outflow rates as a function of the substrate moisture content between zero at PWP and K_{sat} at saturation, the shape of the function does not mirror that of the unsaturated hydraulic conductivity function applied in the SWMM LID module (Figure 4.2). At low moisture contents, the simplified models will significantly overestimate outflow. While it may be feasible to implement a 'custom' Q/h relationship within some drainage network modelling tools, this additional step was not taken here to retain a focus on 'simplified' modelling using generic hydrological and hydraulic controls. A 'custom' Q/h relationship would require significant parameterisation, which is not consistent with the use of simplified approaches.

When a final system outflow control is added, and unsaturated conductivity is no longer the restrictor of flow through the SuDS, the representation of detention performance in the *Daily Loss* and *Cont. Loss* models becomes near identical to that of the *LID* model. In practice, many bioretention cells do incorporate downstream orifice controls, implying that the *Daily Loss* and *Cont. Loss* simplified modelling approaches introduced here may be used by practitioners with confidence to model their hydrological responses, in the absence of access to the full *LID* module.

While the findings here are somewhat intuitive, the errors associated with using simplified models to represent typical SuDS devices have been quantified here for the first time, in the context of both design storms and continuous rainfall time series inputs. This new data should support practitioners to determine if/when simplified approaches may or may not be appropriate. Our recommendation is that simplified formulations are best reserved for preliminary scoping or rapid "what-if" analyses, although the *Daily Loss* and *Cont. Loss* models are robust when the SuDS devices include downstream orifice controls. In all other cases, if reliable design estimates are required, resources should be devoted to using the full SWMM-LID model (or similar).

Boucher and Howe (2025) recently highlighted the role that such simplified modelling tools may play in the context of the Mansfield Flood Resilience retrofit SuDS Programme, particularly at the planning and initial catchment flood risk assessment stage. They stated that their 'simplification focused on key hydraulic parameters that influence flood and pollution risk at the catchment scale. SuDS features were abstracted to represent inflow, attenuation rates, infiltration losses, and outflow. Each feature was modelled as 1D elements, comprising a contributing area subcatchment, a suitably sized storage node, and connecting links and weirs to simulate its hydraulic behaviour.' They also reflected that there is currently a gap in terms of practical guidance within the UK water industry on the level of representation required when including retrofitted SuDS within drainage infrastructure network models.

In the context of large-scale models incorporating multiple SuDS (and conventional drainage elements), run-time can be potentially controlled by spatially aggregating units with similar device configurations, a strategy that retains key hydrological processes while improving efficiency. Future research should focus on developing guidance around the risks and uncertainties associated with SuDS aggregation at the street or subcatchment scale.

For practitioners working with drainage network modelling tools that don't currently incorporate explicit SuDS/LID modelling, an alternative option may be to simulate individual or aggregated devices using SWMM and use the externally-generated runoff hydrograph as an input into the existing network model.

4.5 Conclusions

This study compared the predicted runoff responses of the SWMM LID module (*LID* model) with four simplified model formulations. These formulations varied in complexity, ranging from simple approaches such as subcatchment disconnection (*Disconnect* model) and transfer to pervious areas (*TransferP* model) to more detailed representations of detention processes through flow controls. Retention processes were modelled either with fixed daily losses (*Daily Loss* model) or continuous losses using dynamic evapotranspiration estimates (*Cont. Los*s model).

The study reveals that all simplified model formulations have inherent limitations in accurately simulating hydrological dynamics at the device-scale. Methods that involve complete disconnection (*Disconnect*) or transferring catchment areas to pervious surfaces (*TransferP*) do not effectively capture these dynamics, and overestimate SuDS hydraulic performance. In contrast, approaches utilizing initial losses and storage, particularly those accounting for continuous losses based on evapotranspiration (*Cont. Loss*), yield more realistic responses compared to those using a daily fixed recharge depth (*Daily Loss*) in continuous rainfall simulation. In continuous simulations, outflow simulations from *Daily Loss* and *Cont. Loss* were able to approximately capture peak flows and changes in hydrologic dynamics during rainfall events with high rainfall amounts. In particular, in a SuDS device with orifice control, the *Daily Loss* and *Cont. Loss* models perform reasonably well. However, neither model performed acceptably in scenarios where detention effects were dominated by substrate percolation.

Within the overall structure of this thesis, this chapter establishes a device-scale understanding of how SuDS behaviour is represented under different levels of model simplification. The analysis clarifies which aspects of SuDS hydrological response are most sensitive to simplification, and which can be approximated without substantial loss of predictive reliability. This device-scale perspective provides a necessary foundation for the subsequent investigation of SuDS representation at larger spatial scales.

5. Evaluation of SuDS Street-scale Aggregation Modelling Methods - Monte Carlo Simulation

5.1 Introduction

Following the evaluation presented in Chapter 4, it can be reasonably concluded that physically based representation, such as the SWMM LID module, is required to obtain reliable simulations of SuDS hydrological performance at the device-scale. Once the modelling scale shifts to the subcatchment or street scale, the question is no longer whether such tools should be used, but how they should be implemented within larger spatial units.

Two principal implementation strategies are commonly adopted in modelling tools (e.g. SWMM). The first embeds one or more LID controls within an existing subcatchment, allocating to them a predefined proportion of runoff generated from the impervious area. This configuration is typically applied in city-wide simulations where SuDS units are distributed across multiple subcatchments. The second strategy assigns an entire subcatchment to a single LID unit, or to a homogeneous set of identical units. Under this arrangement, the LID receives direct rainfall as well as any upstream inflow routed to that designated subcatchment. This approach is often employed in detailed performance assessments or treatment-train analyses.

This implies that, within a given spatial unit, SuDS installations may be arranged using different configuration strategies, particularly when both the number and type of devices are uncertain. Existing studies have treated installations of a given SuDS type as homogeneous entities, assigning identical configurations and parameter sets across subcatchments. For example, Le Floch et al. (2022) and Tansar et al. (2022) represented green roofs and permeable pavements using fixed, uniform LID units within larger drainage models. Similar assumptions have been adopted in other street-scale studies (Ercolani et al., 2018; Versini et al., 2015). Although some studies have examined SuDS aggregation approaches, these investigations have largely focused on homogeneous infiltration systems rather than mixed-type configurations involving multiple hydrological mechanisms (Elliott et al., 2009; Roldin et al., 2012). (Refer to Chapter 2 Section 2.7 for details).

The motivation for this chapter is to evaluate the hydrological accuracy of modelling SuDS performance under different aggregation strategies at the street or mesoscale. In addition, this chapter aims to provide methodological insights into the feasibility of rapid SuDS modelling, particularly when multiple SuDS types or configurations are implemented in practice, thereby enhancing flexibility in engineering applications.

The specific objectives of this chapter are as follows:

1. To develop modelling frameworks for aggregating SuDS both within the same type (e.g., multiple bioretention units with varying configurations) and across different types (e.g., green roofs, bioretention cells).
2. To define a set of representative SuDS types and associated configuration parameter ranges, and to conduct Monte Carlo simulations to examine the aggregated model accuracy under continuous rainfall conditions at the street scale.
3. To analyse the sensitivity of model performance to key factors across different modelling strategies.

5.2 Methods

5.2.1 SuDS Modelling Approach

An in-house 1D model was implemented in MATLAB (R2023a), based on the widely used and validated SWMM LID conceptual model framework (Rossman, 2016a), which enables the simulation of the hydrological and hydraulic dynamic of SuDS. The MATLAB implementation was adopted to provide greater flexibility in systematically adjusting SuDS design parameters and configuring synthetic catchment layouts, enabling rapid generation of multiple model configurations and facilitates Monte Carlo experimentation. This model is henceforth referred to as '*LIDMAT*'. It enables internal hydrological and hydraulic simulation for both single SuDS units and aggregated systems, providing a unified single structure for testing different aggregation and parameter estimation strategies.

Figure 5.1 illustrates the *LIDMAT* modelling framework. It fully replicates SWMM's infiltration (Green Ampt) and percolation functions within the soil layer. The final outflow control can be user-defined, either as infiltration or managed through other mechanisms such as an orifice. By adjusting parameters and functional layers, it can represent different devices such as green roofs, bioretention, and permeable pavements.

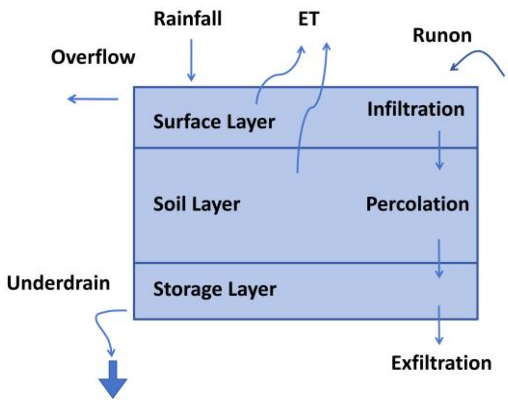

Figure 5.1. LIDMAT model framework

5.2.2 SuDS Aggregation Strategies

The *Detailed* method was established as the baseline scenario, in which each SuDS unit is explicitly assigned to a single subcatchment with user-defined spatial coverage and configuration. This high-resolution setup provides the most hydrologically accurate simulation of the catchment and serves as a reference for evaluating the performance of aggregated strategies.

Two different SuDS aggregation strategies, *LumpN* and *LumpOne,* were considered. In *LumpN*, N different types of SuDS are modelled separately, whereas in *LumpOne*, all SuDS are aggregated into one single device. Figure 5.2 presents the conceptual frameworks for these strategies.

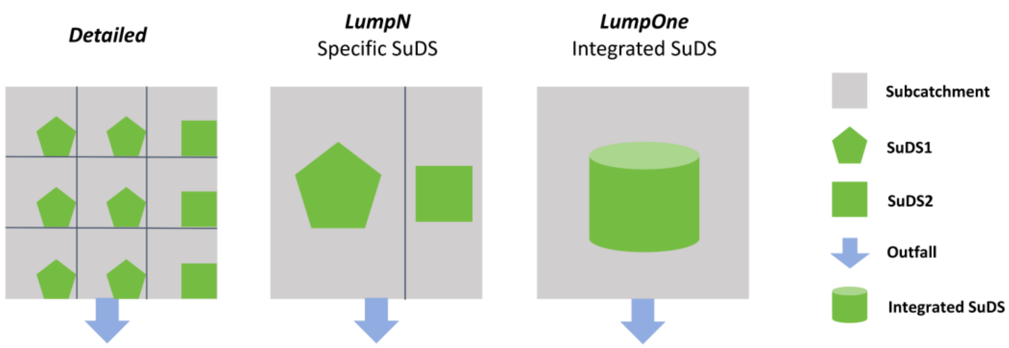

Figure 5.2. SuDS detailed representation (Detailed); SuDS aggregation strategies (LumpN, LumpOne).

In the *Detailed* method, each SuDS unit is assigned to an entire subcatchment or a specified proportion of it, managing all stormwater within that subcatchment. The input consists of direct rainfall and surface runoff from contributing areas within the catchment.

The *LumpN* method aggregates multiple small, non-homogeneous subcatchments into a larger catchment, grouping SuDS by type. For instance, all catchments served by green roofs are consolidated into a single, larger unit receiving the combined inflows from individual subcatchments.

This approach can also accommodate further subdivisions based on specific design attributes, such as distinguishing between lined and unlined BIO configurations.

The *LumpOne* method builds on the *LumpN* approach by aggregating all subcatchments and SuDS into a single composite SuDS system. Instead of maintaining separate SuDS categories, all SuDS types are integrated into a unified system. This aggregated SuDS retains the surface, soil and storage functional layers shown in Figure 5.1. Parameters are adjusted according to the presence or absence of specific SuDS components, with missing layers assigned a value of zero.

In terms of drainage system aggregation, individual subcatchments in the *Detailed* method each have designated nodes, whereas in *LumpN* and *LumpOne*, subcatchments are merged into a single unit with a shared drainage node. This aggregation involves only the summation of catchment areas, without accounting for potential differences in surface runoff concentration times or horizontal flow routing.

5.2.3 Simulation Scenarios Setup

To objectively compare the impacts of applying either *LumpN* or *LumpOne* aggregation strategies, it is clear that multiple different catchment configurations need to be considered. To represent the variability in SuDS physical configuration parameters, a Monte Carlo simulation approach was adopted. Monte Carlo simulation is widely used to quantify parameter uncertainty and its impact on model outputs. This approach is commonly used in hydrological modelling to assess uncertainty (Mooney, 1997; Zhang et al., 2022). This probabilistic framework allows for systematic assessment of parameter uncertainty and model sensitivity under a wide range of catchment conditions.

Five hundred different synthetic catchments were generated. Each synthetic catchment had 5000 m^2 area, representing a typical street-scale domain and assumed to be completely served by SuDS. The choice of 500 Monte Carlo iterations and a 5000 m^2 catchment area reflected a balance between capturing a wide range of synthetic SuDS configurations and maintaining feasible computational demand, particularly in relation to RAM requirements. Each Monte Carlo iteration represents a distinct synthetic catchment configuration with varied numbers, types, and characteristics of SuDS facilities.

As in Chapter 4, two SuDS types, Green Roofs (GR) and Bioretention (BIO) were selected for SuDS intervention scenario simulation. These SuDS devices encompass a range of hydrological processes and functionalities, making them suitable candidates for a comprehensive evaluation of the SuDS aggregation strategies. GR units were configured such that the physical area was always equal to the runoff treatment area. In contrast, each BIO unit was designed to manage a contributing drainage area larger than its plan area. The allocation process ensured that the combined treatment area of all SuDS units matched the catchment area, thus achieving complete runoff coverage. The outflow from all SuDS units was eventually combined into a single outflow from the synthetic catchment.

The simulation was conducted using a fixed temporal resolution of 5 minutes. At this timescale, the concentration time of surface runoff in the horizontal direction within the catchment is considered negligible. Therefore, the modelling approaches adopted in this research primarily focus on representing vertical hydrological processes – such as rainfall infiltration, soil moisture dynamics, percolation, storage, and outflow control – within individual SuDS units. Horizontal flow routing across SuDS elements or through the catchment was not explicitly modelled. As this study primarily focuses on SuDS model aggregation, pipe diameters were set sufficiently large to ensure that they did not restrict outflow.

Subcatchment Distribution

Figure 5.3 illustrates the allocation of subcatchment areas within an example catchment (No.71), highlighting the distinction between the physical and treatment areas of BIO units. This case is revisited in the 'Results and Analysis' section for further discussion. The red area on the left represents GR, where each rectangle corresponds to a single unit, and width indicates treatment area. On the right, green rectangles represent BIO units, with darker shading denoting the physical area proportion. The x-axis confirms a total SuDS treatment area of 5000 m^2.

(a). GR BIO Info

	GR	BIO
Count	12	2
Treatment Area	4449	551
Physical Area	4449	37

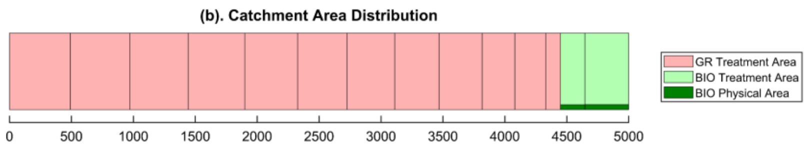

Figure 5.3. Catchment area distribution example (No. 71). (a) Table of SuDS subcatchment information; (b) Schematic diagram of catchment area distribution.

The random allocation process assigns all subcatchments (i = 1 ~ n) within a synthetic 5000 m^2 catchment to either green roofs (GR) or bioretention cells (BIO) using an area-driven algorithm with equal probability (50% chance) during each simulation iteration.

At each iteration, the algorithm randomly selects a SuDS type (GR or BIO) and assigns it a treatment area from a uniform distribution with range 50 to 500 m^2. This range, informed by real-world data from the Mansfield Sustainable Flood Resilience project (Severn Trent Water, 2016), is considered representative of typical areas treated by SuDS, such as rooftops or small car parks. This typically results in between 10 and 20 subcatchments per synthetic catchment. To ensure full allocation while satisfying minimum (50 m^2) and maximum (500 m^2) subcatchment size constraints, the following rules are applied (*A_rem* is the remaining unassigned area at the end of iteration):

1. If *A_rem* < 50 m^2: to avoid creating unrealistically small units, the algorithm checks whether the remaining area is exactly zero. If not, the remaining area is added to the smallest previously allocated subcatchment.
2. If *A_rem* > 500 m^2: the allocation loop continues, drawing and assigning a new subcatchment area.
3. If 50 < *A_rem* < 500 m^2: this remaining area is directly assigned as the final subcatchment.

Through this procedure, the total catchment area is systematically distributed between GR and BIO (Figure 5.3). A total of 500 synthetic catchments was generated.

SuDS Parameter Selection

For each GR and BIO unit, key physical parameters were independently sampled from uniform distributions within predefined bounds (Table 5.1). The parameters are those required by the SWMM LID module. The parameter ranges were informed by literature and best practice. Note that Field Capacity and Wilting Point were set as fractions of porosity to ensure media properties are internally consistent. In the case of GR, the width was also specified, which defines the under-drain flow path distance through the slope to the roof outlet. For individual GR units, the width was set at 10 m. When aggregated in different modelling frameworks, the widths of individual GR units were added together.

All GR and BIO units had independently assigned parameter values. For BIO units, the orifice diameter was estimated using a rearranged orifice flow equation to reflect a target maximum allowable flow (i.e., Greenfield runoff rate (GRR) – 3 L/s/ha) (Department for Environment, Food & Rural Affairs, 2025). A minimum practical orifice diameter of 10 mm was imposed for engineering design constraints.

The parameter settings for GR are relatively straightforward, with key parameters randomly selected from predefined ranges using uniform sampling.

In contrast, the parameterisation of BIO units requires additional considerations due to the influence of the contributing area. Two key design principles were followed: (1) BIO facilities were sized such that no overflow occurs in response to a 30-year design storm, and (2) the peak outflow from each unit remained below the Greenfield runoff rate, following the guidelines outlined in Department for Environment, Food & Rural Affairs (2025).

Seven physical parameters of BIO were sampled randomly from within the specified ranges. For the seepage rate (i.e. exfiltration to native soil), both lined and unlined configurations were considered, each with a 50% probability. If the unit was unlined, the seepage rate was randomly assigned within the range of 3.6 to 36 mm/hr (Woods-Ballard et al., 2015), reflecting commonly observed field values (Table 5.1).

For determining the BIO device plan area, an iterative process was employed. Starting from a minimum permissible value (loading ratio = 20), the plan area of each BIO unit was incrementally increased (in 1 m^2 steps) until the unit (with initial soil moisture = FC) could fully treat the runoff from its assigned subcatchment under the 30-year design storm (31 mm, 1-hour, symmetric hyetograph with a central peak) without overflow. This ensured that all BIO units in the simulation meet regulatory design criteria. The resulting loading ratio was between 6 and 20.

Table 5.1. SuDS device parameters ranges

Layer	Parameter	Unit	GR	BIO	Notes
Surface	Berm Height (surfHead)	mm	0	50–150	(De-Ville et al., 2021; Peng and Stovin, 2017; Rossman, 2016a)
Substrate	Thickness (soilThk)	mm	50–150	300–1200	(Berretta et al., 2018; De-Ville et al., 2021; Peng and Stovin, 2017; Rossman, 2016a)
	Porosity	m^3/m^3	0.45–0.6	0.4–0.6	
	Field Capacity (FC)	m^3/m^3	0.315–0.42 (70% Porosity)	0.16–0.24 (40% Porosity)	
	Wilting Point (PWP)	m^3/m^3	0.09–0.12 (20% Porosity)	0.08–0.12 (20% Porosity)	
	Conductivity (K_{sat})	mm/hr	1000–3500	50–300	
	Conductivity Slope	-	40	40	
	Suction Head	mm	50	50	
Drainage /Storage	Thickness (storThk)	mm	10–100	50–500	(De-Ville et al., 2021; National Cooperative Soil Survey, 2006; Peng and Stovin, 2017; Rossman, 2016a)
	Void Ratio (void/total)	-	0.4	0.4	
	Roughness (n)	-	0.03	-	
	Seepage Rate (Exfil)	mm/hr	-	3.6–36	
Outflow control	Orifice diameter	m	-	variable to achieve an outflow rate of 3 L/s/ha	(Department for Environment, Food & Rural Affairs, 2025)

Aggregation Strategy Scenarios

For each simulated catchment, the SuDS configuration was represented via three modelling strategies:

1. ***Detailed***: Each GR and BIO was simulated individually using the *LIDMAT* model. The total outflow was the sum of all individual units' simulated outflows.
2. ***LumpN (N=2)***: All GR units were aggregated into a single equivalent GR, and all BIO units into a single equivalent BIO. Parameter values were treatment-area-weighted averaged.
3. ***LumpOne***: All SuDS units were combined into one, with parameters weighted by their treatment area.

All scenarios were simulated using the same *LIDMAT* model, with identical meteorological data input. This structure enables comparison between the fully detailed model and aggregated approaches in terms of hydrological prediction performance and sensitivity to parameter uncertainty.

In the subsequent discussion, BIO were further classified according to whether they were *lined* or *unlined*, that is depending on the presence or absence of exfiltration (seepage) processes. This refinement is introduced as an improvement to the *LumpN* approach, resulting in another scenario: ***LumpN*** **(*N=3*).**

Aggregate Parameter Estimation Method

SuDS physical parameters were determined using a weighted average based on the areas of the corresponding subcatchments in the *Detailed* method:

$$Var_{Lump} = \frac{Var_1 \times A_1 + Var_2 \times A_2 + \cdots + Var_i \times A_i}{A_1 + A_2 + \cdots + A_i} \qquad \text{Equation 5.1}$$

where Var_{Lump} = SuDS parameter in *LumpN* and *LumpOne* methods; Var_i = SuDS parameter in *Detailed* method in each subcatchment; A_i = SuDS treated area in each subcatchment.

When combining SuDS areas, the final physical area is determined by directly summing the individual SuDS areas. For orifice-controlled outflows in BIO, the final orifice size of each BIO unit was calculated based on the Greenfield Runoff Rate, corresponding catchment area and BIO depth. To derive the aggregated BIO orifice diameter, the maximum outflow of each individual BIO was summed, and the aggregated diameter was then back-calculated using maximum total outflow and the weighted average BIO height. In cases where GRs do not employ an orifice control, outflow from the drainage layer was treated as free discharge. Within the model, this was represented by introducing a sufficiently large orifice along the side of the storage layer (a full side opening at 10 mm height), ensuring that the outlet imposed negligible hydraulic restriction. For aggregated GR configurations, the total outflow was represented by merging the corresponding outlet areas.

5.2.4 Meteorological Data Inputs

SuDS hydrological modelling tools must assess system responses to both routine and extreme rainfall events. Long-term simulations utilised 5-minute rainfall data observed at an experimental site in Sheffield (UK) during 2007 (Stovin, 2024). Table 4.1 highlights 'significant' events from the 2007 long-term rainfall series (Stovin et al., 2012). Six events were used in this chapter: 18/01; 20/01; 13/05; 13/06; 24/06; 26/07.

The monthly potential evapotranspiration (PET) rates were calculated based on the monthly average temperature and the daylight hours using the Thornthwaite equations (Stovin et al., 2013b), as shown in Table 4.2, Chapter 4. Moreover, the absolute accuracy of PET estimation is not critical in this study, as the same ET calculation method is consistently applied across all synthetic catchments, ensuring a like-for-like comparison between models. In all simulations, evapotranspiration was activated only during time steps without rainfall.

5.2.5 Parameter Normalization

A large number of SuDS physical parameters were generated for multiple facilities within each simulated catchment. To facilitate consistent comparison across different simulations and enable effective visualisation, all parameters were normalised using the minimum and maximum values of each parameter in Table 5.1. This approach ensured that the scale of each parameter remained consistent across all cases, ensuring comparability between different simulations.

By applying min-max normalisation, all parameter values were rescaled to a [0, 1] range, allowing for straightforward cross-parameter comparisons. This not only improved the interpretability of aggregated results but also made it possible to evaluate how different aggregation strategies influence model performance. Figure 5.4 presents the normalised distributions of parameters within the same example simulation synthetic catchment as Figure 5.3. The red and green boxes indicate the parameter distributions for GR and BIO, respectively, while the blue boxes represent the combined parameter distributions of all SuDS. Each circular marker within a box corresponds to the estimated parameter value (i.e. the weight average) of the aggregated GR, BIO (*LumpN*) and combined SuDS (*LumpOne*) unit.

In Figure 5.4 example, for synthetic catchment No.77, the 12 individual green roofs were randomly assigned K_{sat} values ranging between 1014 and 3417 mm/hr. From Table 5.1, the sample range for this parameter for GR was 1000-3500 mm/hr. The two BIO subcatchments had K_{sat} values of 167 and 245, sampled from a (lower) range of 50-300 mm/hr. The full range of all possible K_{sat} values is 50-3500 mm/hr. Therefore, the normalised values for the two BIO subcatchments are 0.03397 and

0.0566, with an area-weighted mean value of 0.0485. The area-weighted mean value for the 12 green roofs is 0.6118. When all 14 subcatchments are combined (COM), the area-weighted mean is 0.5497. In this case it can be seen that the combined value, used in the *LumpOne* aggregation strategy, is biased towards the GR characteristics, given the dominance of GR in this specific synthetic catchment.

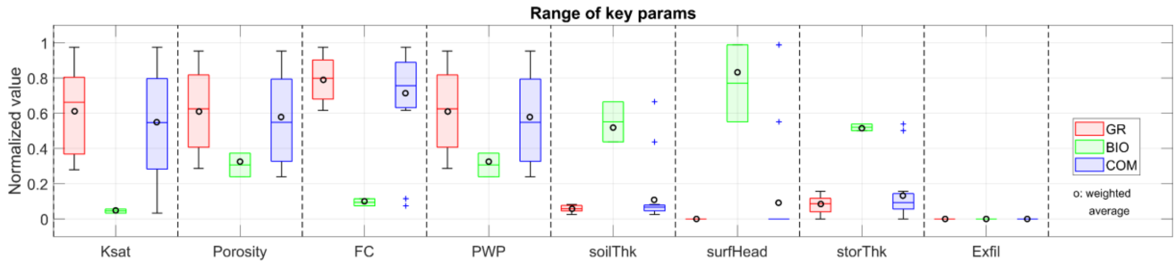

Figure 5.4. Ranges of key parameters in the example simulation synthetic catchment (No.71).

5.2.6 Model Evaluation Metrics

The effectiveness of SuDS aggregation methods was evaluated through a set of hydrological performance metrics, which quantify the deviation of aggregated-model simulations from the baseline reference. In this study, the *Detailed* configuration served as the baseline scenario, representing fully disaggregated modelling of all SuDS units. All other aggregation strategies (*LumpN* and *LumpOne*) were assessed by comparing their simulation outputs to the *Detailed* model results.

Because the purpose of this chapter is to evaluate aggregation methods from a model-development perspective, rather than to assess performance for a single operational objective, no single metric was considered sufficient. SuDS models may be used for different purposes, including local flood mitigation, runoff volume reduction, overflow assessment, or wider catchment-scale planning. Each of these purposes emphasises different aspects of model behaviour. For example, local flood assessment is strongly influenced by peak flow prediction, whereas catchment-scale flow management and CSO-related applications require greater attention to runoff volume, overflow generation and the full hydrograph response. The evaluation framework therefore considers multiple aspects of model performance, including hydrograph shape, peak response, annual runoff volume and overflow volume.

Four metrics were employed for model evaluation, reflecting both event-based and long-term hydrological accuracy:

1. **Nash-Sutcliffe Efficiency (NSE)** – Evaluates the degree to which the aggregated simulation reproduces the baseline runoff (catchment outflow) profile, especially the peak runoff.

2. **Peak Runoff Error (%)** – Measures the relative difference in peak flow between the aggregated simulation and the baseline for the specific rainfall event.
3. **Annual Runoff Volume Error (%)** – Represents the deviation in total runoff volume over the entire simulation year between the aggregated model and the baseline.
4. **Annual Overflow Volume Error (%)** – This metric compares the cumulative overflow volumes over the year.

The Nash-Sutcliffe model efficiency (NSE) index (Equation 4.1) was employed to objectively estimate how well the runoff profiles were predicted by the SuDS aggregation modelling methods compared with the *Detailed* method.

The error equation was used to calculate the difference between the peak outflow of the SuDS aggregation modelling methods and the *Detailed*:

$$Error\ (\%) = 100 \times \frac{Simulated\ Value - True\ Value}{True\ Value} \qquad \text{Equation 5.2}$$

Each of the 500 Monte Carlo simulated synthetic catchments produced distinct catchment configurations, including a randomised number and combination of GR and BIO units with independently sampled parameter sets. For each synthetic catchment, two SuDS aggregation scenarios were simulated, each compared to the *Detailed* baseline.

5.3 Results and Analysis

5.3.1 Representative Synthetic Catchments

To clearly assess the differences in model performance and to investigate the hydrological processes underlying these discrepancies, this section discusses two representative synthetic catchments selected based on NSE metrics. Specifically, these correspond to the synthetic catchments in which the difference in NSE values of annual runoff profiles between the *LumpN (N=2)* and *LumpOne* strategies simulations is minimal and maximal, respectively.

5.3.1.1 Most similar NSE case of *LumpN (N=2)* and *LumpOne*

Figure 5.5 presents simulated runoff profiles for six significant rainfall events for a representative synthetic catchment in which both *LumpN (N=2)* and *LumpOne* performed well, with a close NSE value between *LumpN (N=2)* and *LumpOne* (i.e. the largest NSE case of *LumpOne*). This is synthetic catchment No.77.

In the selected simulation, the runoff profiles for *LumpN (N=2)* were generally very close to those of the *Detailed* method, accurately reproducing the detention effect of SuDS on outflow control, particularly in the runoff recession tails. In some instances, *LumpN (N=2)* slightly overestimated peak runoff compared to the baseline (Figure 5.5c). In contrast, *LumpOne* failed to reproduce the runoff recession tails, reflecting that the only one value for each of input parameter fails to capture the variability seen in the individual devices. *LumpOne* also consistently underestimated the peak runoff relative to the *Detailed* baseline, underscoring its weakness in capturing the dynamic outflow behaviour of the SuDS facilities.

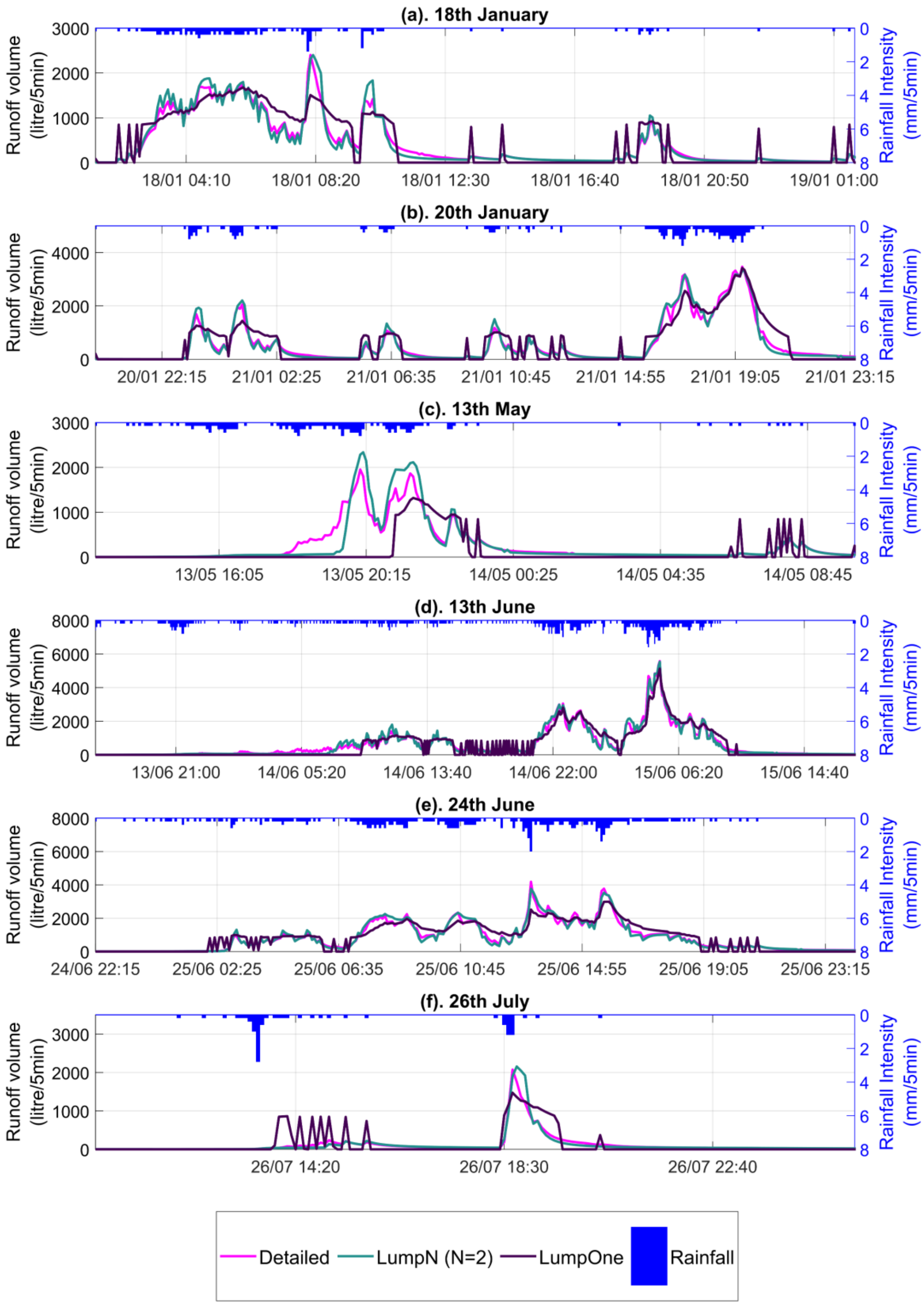

Figure 5.5. Six selected significant rainfall events runoff profiles

Parameter and Catchment Configuration

To clearly illustrate the parameter characteristics and performance of the selected simulation synthetic catchment, Figure 5.6 provides a detailed characterization of the synthetic catchment shown in Figure 5.5 (i.e. No.77). Figure 5.6a (identical to Figure 5.4) shows the distributions of key physical parameters for GR and BIO devices, as well as their combined representation (COM). Circles indicate aggregated parameter values derived from weighted means. In addition to the weighted average, arithmetic mean and median aggregation schemes were also explored in preliminary analyses. However, these approaches are not presented in detail here, as the variation in prediction accuracy resulting from their use was negligible compared with the main observations regarding parameter heterogeneity.

In the GR and BIO boxplots, the markers correspond to the parameters aggregated for *LumpN (N=2)* methods; in the COM boxplot, they represent the aggregation for *LumpOne*. By comparing normalised parameters with the aggregated values, one can assess whether the aggregation process introduces substantial error. In this case, all aggregated parameter value markers for *LumpN* method fall within the key parameters' IQR, suggesting minimal deviation from the normalised distribution. The *LumpOne* method exhibits anomalous data points for field capacity, substrate and surface layer thickness according to MATLAB boxplot rules. These arise from the large differences between parameter ranges of 12 GR and 2 BIO facilities. This highlights that SuDS types can span substantially different parameter domains, which complicates full aggregation.

Figure 5.6b (the same as Figure 5.3b) visualises the configuration of GR and BIO units in the selected catchment. Figure 5.6c (the same as Figure 5.3a) provides numerical summaries of the number of GR and BIO units, along with their total treatment and physical areas.

Runoff Profile, Metrics and Water Balance Analysis

Figure 5.6d shows the modelled runoff profiles simulated by *LumpN (N=2)* and *LumpOne* for the 13th June event. *LumpN (N=2)* reproduced an accurate representation of the hydrological dynamics of the runoff profile. *LumpOne* methods failed to effectively simulate the SuDS detention function, as they do not accurately reproduce the runoff tails (e.g., from 06:20 to 14:40 on June 15th). In the early stages of the events, both *LumpN (N=2)* and *LumpOne* showed no response (e.g., around 05:20 on 14th June), failing to capture the immediate outflow triggered by rainfall. This delay arises because, in the *Detailed* method, SuDS units initiate discharge at different times; when some units have begun to release water, other may not yet be active. Such temporal variability is lost under aggregation, where the heterogeneity of individual unit responses is smoothed out.

Figure 5.6e provides the corresponding evaluation metrics and Figure 5.6f presents the annual water balance. *LumpOne* showed a significant overflow error. While overflow typically originates from BIO facilities, aggregating GR and BIO units in the *LumpOne* models increased the effective K_{sat} (more than an order of magnitude), allowing water to pass through too quickly and preventing overflow from occurring. As a result, *LumpOne* completely failed to reproduce overflow. In this specific case, the two BIO areas are lined systems, meaning they have no exfiltration rate. Consequently, the "Exfil" term is zero across all models.

Similarly, *LumpN (N=2)* slightly underestimated the overflow volume. When different types of BIO units are aggregated, the excess water from units that would normally overflow is distributed into aggregated BIO unit with more storage space, reducing the overall overflow volume.

5.3.1.2 Greatest difference NSE case of *LumpN (N=2)* and *LumpOne*

Figure 5.7 (i.e. No.317) shows a case where *LumpN (N=2)* and *LumpOne* had the largest NSE value discrepancy (i.e. the smallest NSE case of *LumpOne*), representing a typical synthetic catchment where the *LumpOne* method performs poorly. Unlike the previous example, this case involves BIO units with exfiltration capacity, representing an unlined system. *LumpN* accurately reproduced the hydrological dynamics of the *Detailed* baseline (Figure 5.7d). In contrast, *LumpOne* significantly underestimated total outflow while overestimating both exfiltration and evapotranspiration (ET) losses (Figure 5.7f). The poor performance of the *LumpOne* methods is primarily due to the incorrect estimation of exfiltration volume (Figure 5.7a). In this case, exfiltration from BIO units accounts for roughly 38% of the total water volume in the *Detailed* case. However, in the *LumpOne* method the aggregation removes the distinction between GR and BIO, and the resulting composite unit represents a mixture of both. The effects of aggregation would be 'equivalent' to GRs with exfiltration, leading *LumpOne* to predict that approximately 50% of the total water volume exits the system via exfiltration.

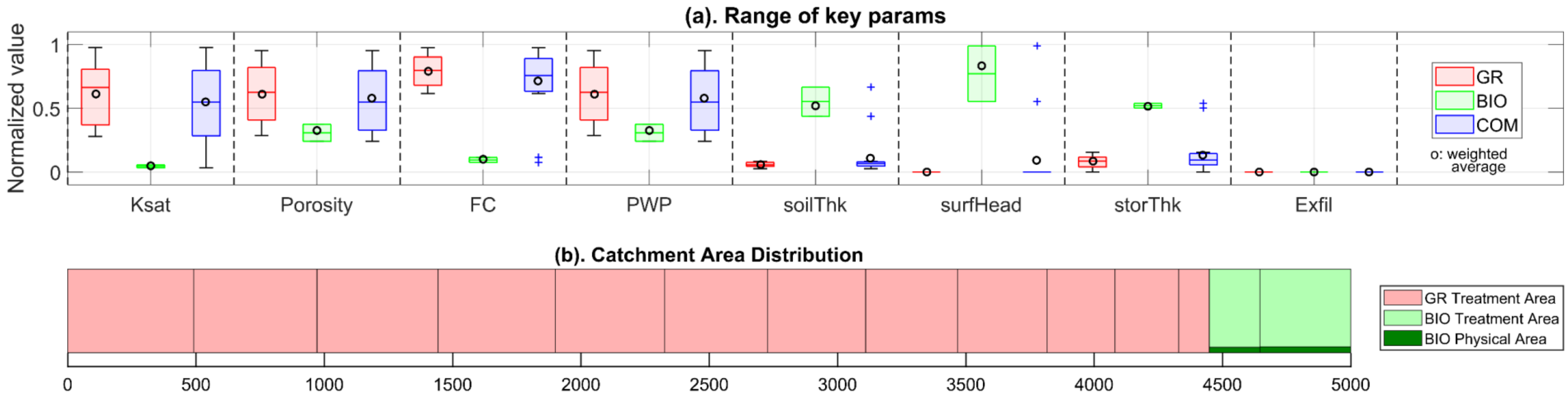

(c). GR BIO Info

	GR	BIO
Count	12	2
Treatment Area	4449	551
Physical Area	4449	37

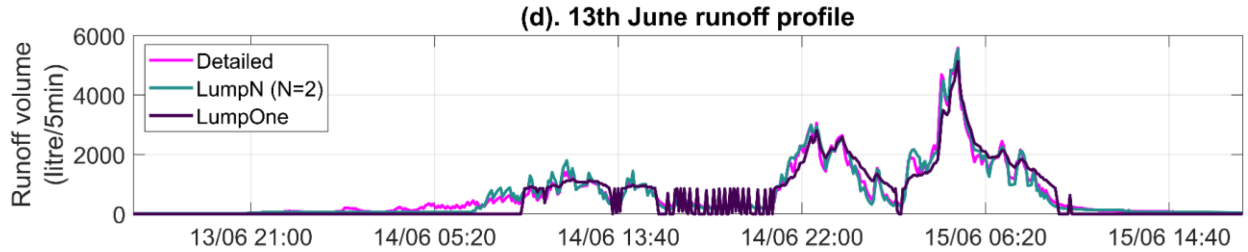

(e). Metrics

	LumpN (N=2)	LumpOne
NSE value[a]	0.976	0.901
Peak runoff error[a] (%)	-0.695	-8.060
Total runoff error[b] (%)	-0.171	-12.160
Overflow error[b] (%)	-11.579	-100.000

[a]13th June Rainfall event; [b] Whole year

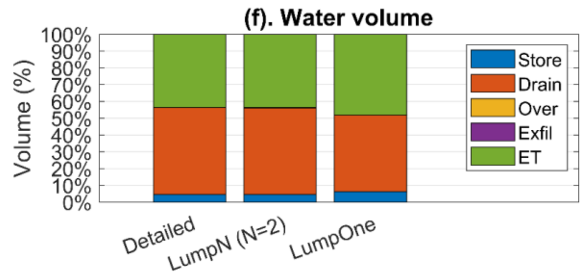

Figure 5.6. The similar case (No.77) to LumpN (N=2) and LumpOne performance. (a). Range of key parameters; (b). Catchment area distribution schematic diagram; (c). GR and BIO area information table; (d). Runoff profiles in 13th June event; (e). Performance metrics table; (f) Water volume distribution in whole year simulation.

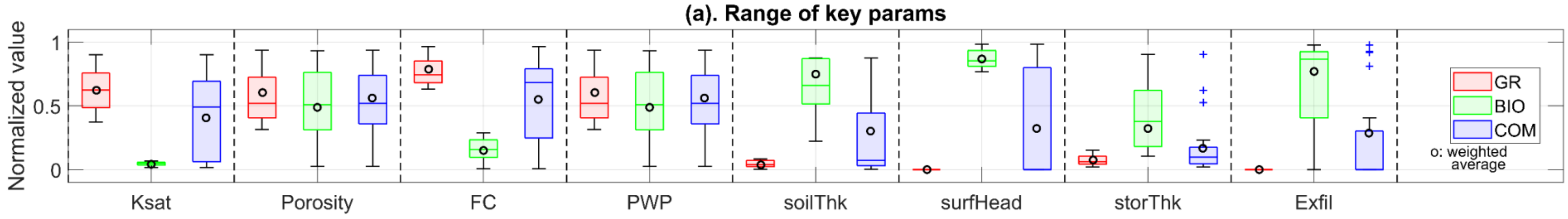

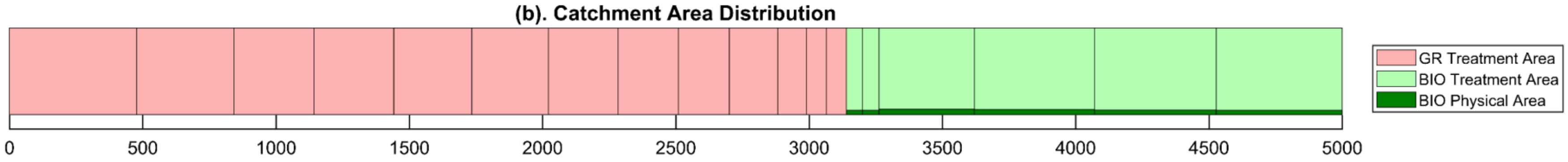

(c). GR BIO Info

	GR	BIO
Count	13	6
Treatment Area	3140	1860
Physical Area	3140	104

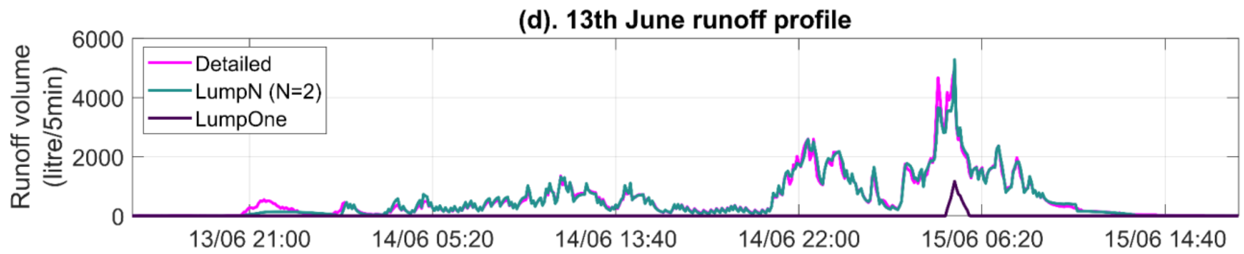

(e). Metrics

	LumpN (N=2)	LumpOne
NSE value[a]	0.972	-0.476
Peak runoff error[a] (%)	6.077	-76.538
Total runoff error[b] (%)	-3.613	-99.569
Overflow error[b] (%)	-73.588	-100.000

[a]13th June Rainfall event; [b] Whole year

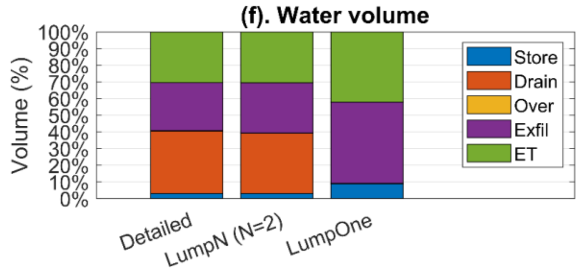

Figure 5.7. The greatest difference case (No.317) to LumpN (N=2) and LumpOne performance. (a). Range of key parameters; (b). Catchment area distribution schematic diagram; (c). GR and BIO area information table; (d). Runoff profiles in 13th June event; (e). Performance metrics table; (f) Water volume distribution in whole year simulation.

5.3.1.3 SuDS hydrological Analysis

Figure 5.8 further explains the overflow error by separating the outflow profiles of the GR and BIO facilities based on the synthetic catchment from Figure 5.7. The *LumpN* GR performance closely matches the *Detailed* GRs baseline. The *LumpN* BIO profile shows a flat period (from 22:00 on June 14th to 14:40 on June 15th), caused by orifice-controlled outflow based on the GRR. The peaks during this period are caused by overflow. Thus, overflow errors were primarily dependent on the specific BIO conditions in each synthetic catchment. Although individual BIO units were designed to comply with the GRR, the minimum orifice diameter of 10 mm (a practical engineering constraint) occasionally resulted in outflows exceeding the GRR. Under aggregation, the orifice size was derived directly from the maximum outflows of the individual BIO units, resulting in a relatively larger orifice. This led to systematic underestimation of overflow.

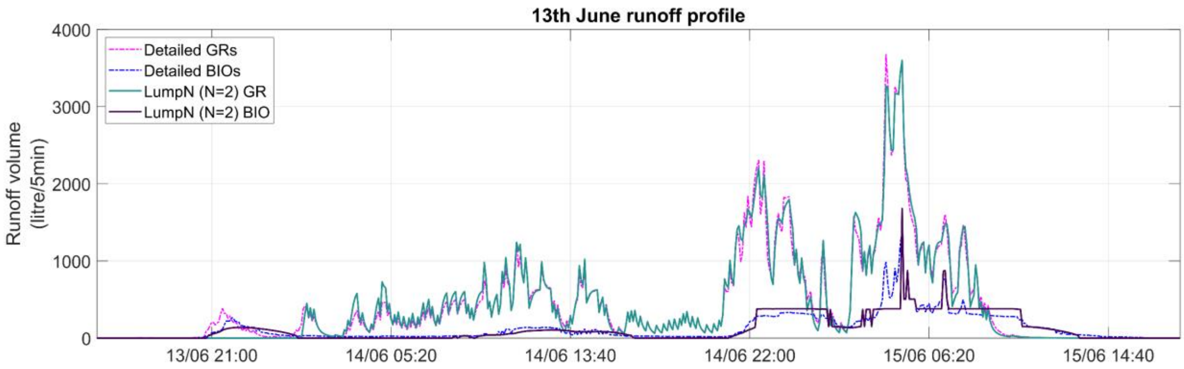

Figure 5.8. GR & BIO runoff profiles in greatest difference case in 13th June event.

Figure 5.9 provides a detailed breakdown of the orifice outflow and overflow hydrographs for six individual BIO units in the selected synthetic catchment. The sum of orifice discharge and overflow represents the total outflow from each BIO. The figure clearly illustrates substantial variability among the BIOs, including differences in the timing of flow initiation and cessation, as well as the occurrence of overflow. For example, BIO 5, which had no exfiltration, exhibited the earliest onset of outflow. In contrast, BIO 2, with the largest plan area and a loading ratio of 20, generated the highest total outflow volume. Overall, these differences highlight the heterogeneity of individual unit behaviour. In comparison, the aggregated BIO profile in *LumpN (N=2)* in (Figure 5.8) smooths out such variability, thereby contributing to errors introduced during the aggregation process.

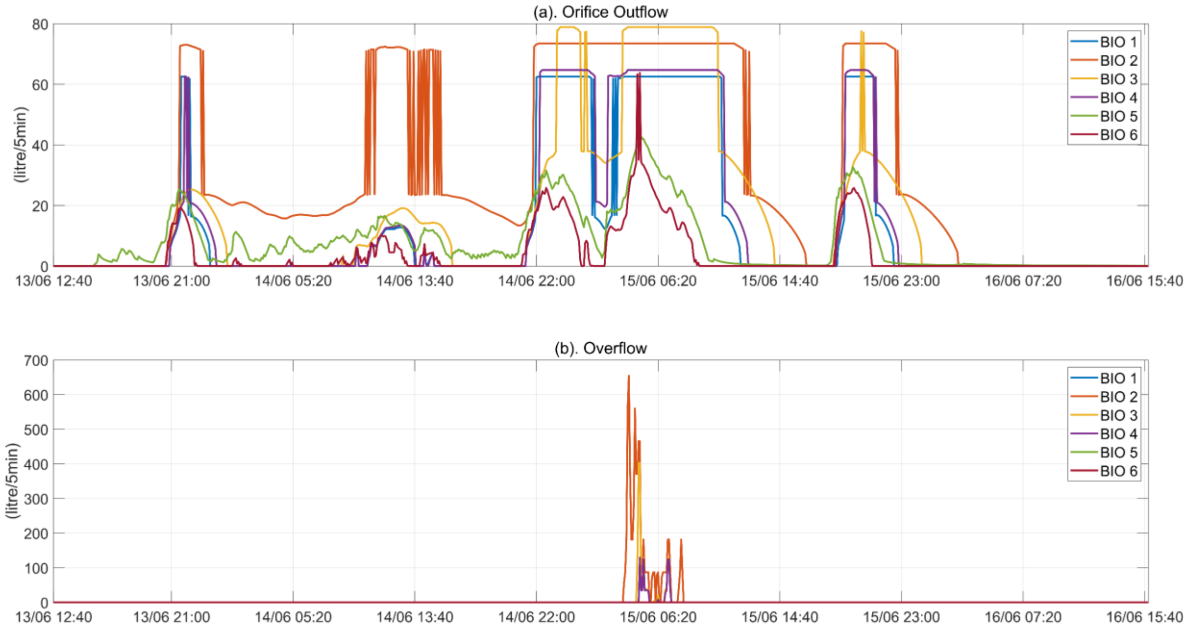

Figure 5.9. BIOs runoff and overflow profiles in greatest difference case in 13th June event. (a). BIOs orifice underdrain flow profiles; (b). BIOs overflow profiles.

Concluding Remarks

In summary, the selected cases clearly demonstrate that *LumpN (N=2)* delivered robust and accurate results across different synthetic catchments. In contrast, *LumpOne* exhibited higher variability and consistently underperformed. These findings underscore the importance of model structure: accurately capturing the hydrological behaviour of diverse SuDS elements is essential, and simplistic aggregation parameter estimation strategies cannot reliably substitute for structural representation.

5.3.2 Performance across Monte Carlo Simulations

Figure 5.10 presents the distribution of NSE values, outflow volume error and overflow volume error for the two SuDS aggregation methods across 500 Monte Carlo simulations using annual continuous rainfall. The *Detailed* model served as the baseline, and the NSE values assess the predictive performance of each method in replicating its runoff profile. In contrast, the outflow and overflow errors provide a volumetric evaluation of model accuracy.

NSE Performance Analysis: The NSE results demonstrated that the *LumpN (N=2)* strategy significantly outperformed the *LumpOne* strategy, with consistently higher NSE value and narrower interquartile range (IQR). *LumpN (N=2)* strategy achieved a median NSE of 0.959 (IQR: 0.946-0.968), whereas *LumpOne* strategy displayed greater variability and significantly lower accuracy, with a median NSE value of 0.346 (IQR: 0.25-0.462).

Outflow Volume Error: Both *LumpN (N=2)* and *LumpOne* strategies underestimated the outflow volume, with median errors of approximately -27% and -91%, respectively. These underestimations were due to an over estimation of exfiltration after the aggregation which consequently reduces the simulated outflow. In *LumpOne* strategy extreme cases, nearly all underdrain flow volume was replaced by exfiltration. More specific details can be found in Section 5.3.1 for representative simulation cases.

Overflow Volume Error: The *LumpN (N=2)* strategy demonstrated considerable uncertainty in simulating overflow, with median error of -70% (IQR: -80% to -52%). This underestimation arises because the aggregation of multiple BIOs into a single equivalent BIO suppresses the occurrence of localised overflow events that are present in the *Detailed* model. In contrast, *LumpOne* strategy consistently yielded a −100% overflow error. In *LumpOne* strategy, all GR and BIO units were aggregated into a single composite device, excessively amplifying the effective exfiltration volume and eliminating realistic control over orifice sizing, thereby preventing any overflow from occurring.

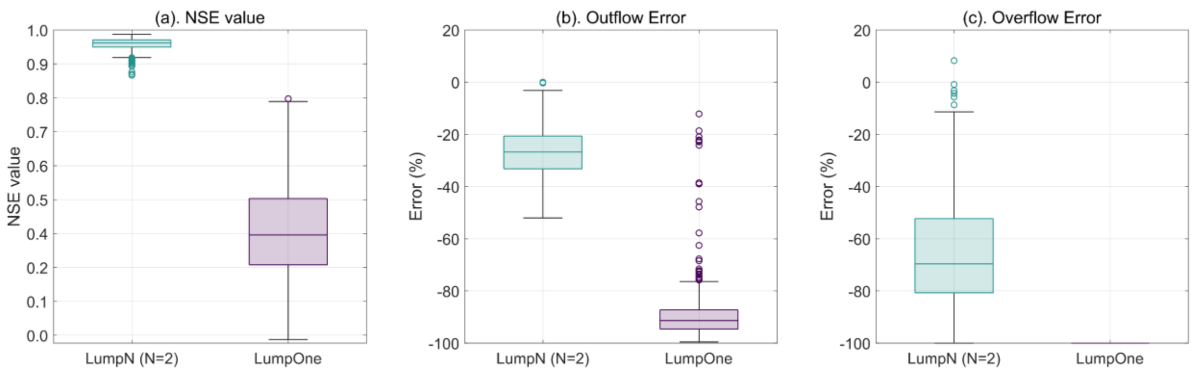

Figure 5.10. Aggregation Approach Annual Performance: (a) NSE value of annual runoff profiles, (b) outflow volume error, (c) overflow volume error.

Peak Runoff Error

Figure 5.11 displays the peak runoff error for *LumpN (N=2)* and *LumpOne* strategies across 500 synthetic catchments for each of the six rainfall events. *LumpOne* strategy resulted in poor matches to the peak runoff in *Detailed* scenario, with large error magnitudes and underestimation of peak runoff in nearly all simulations. Although *LumpN (N=2)* strategy performed considerably better, the boxplots exhibit non-negligible IQR, reflecting uncertainty in event-specific predictions.

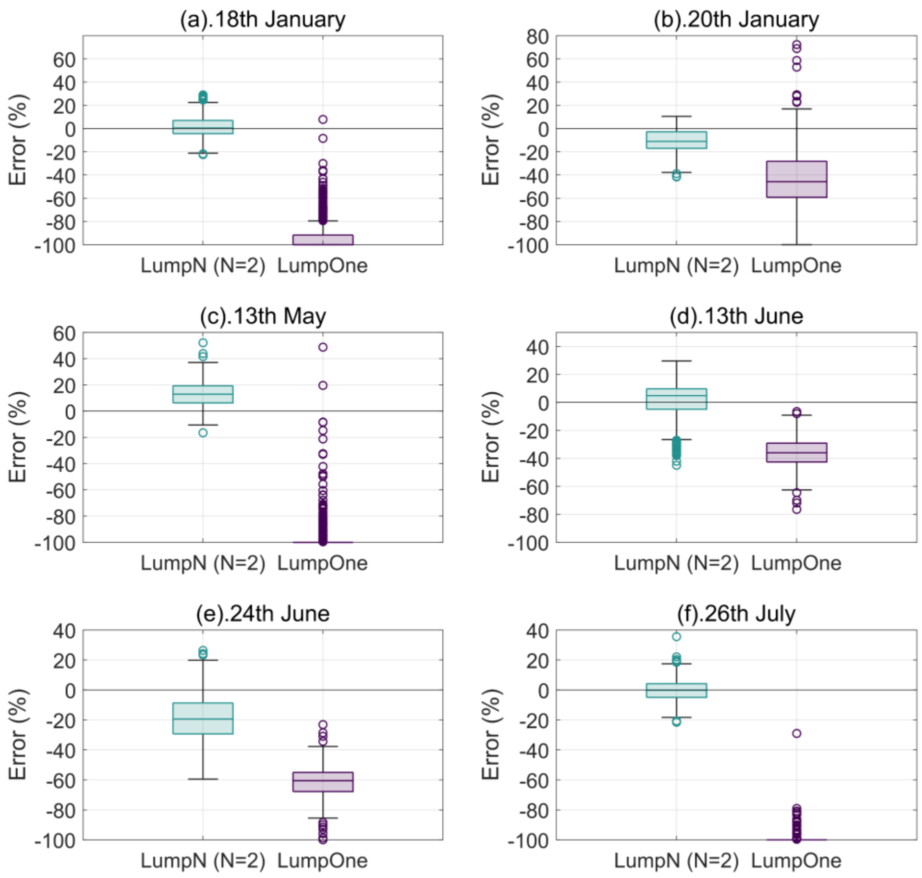

Figure 5.11. Boxplot distribution of peak runoff error in selected significant rainfall events

Concluding Remarks

LumpN (N=2) strategy represents a clear improvement over *LumpOne* strategy, despite both approaches exhibiting a significant underestimation of outflow volume and overflow volume. *LumpN (N=2)* strategy achieved strong performance in terms of NSE for the whole year runoff profile and significant rainfall event peak runoff metrics. These findings suggest that full aggregation (*LumpOne*) fails to preserve the key hydrological processes necessary for accurate simulation, and that simple parameter averaging is an insufficient approach to account for the variability of individual SuDS.

5.3.3 Influence of SuDS Configuration and Parameters

To identify which variables shape the performance of the aggregation methods, this section examines model outcomes under varying parameter settings. Figure 5.12 explores how the treatment area distribution between GR and BIO facilities affects model performance. The x-axis represents the treatment area percentage. Each subplot displays one of the four evaluation metrics.

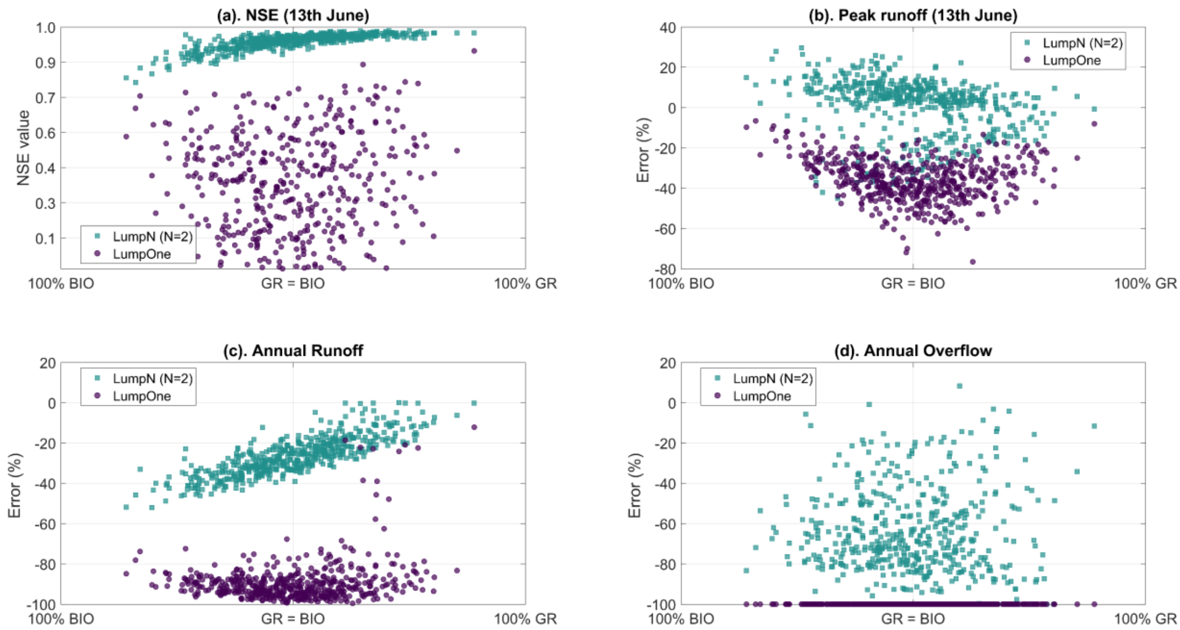

Figure 5.12. Effect of the relative treatment area of GR and BIO on various metrics

For *LumpN (N=2)*, model performance remains stable across varying GR-BIO proportions. However, subtle trends were observed:

- NSE values increased slightly when GR dominated the treatment area. This is consistent with previous findings regarding the influence of BIO exfiltration rates.
- Peak runoff exhibited a wider error range when BIO facilities predominated, whereas the error diminished as the GR share increased. Under BIO-dominated conditions, both overestimation and underestimation of peak runoff occurred, as BIO units exert stronger control over outflow. Lower K_{sat} values combined with orifice control at the outlet amplified aggregation-related errors.
- Annual runoff volume error approached zero as the GR proportion increased, whereas a higher BIO proportion led to runoff volume underestimation, again attributed to BIO exfiltration.
- Annual overflow volume error showed no clear trend; however, the majority of values indicated underestimation. Since no synthetic catchments with 100% GR coverage were included, overflow always occurred when BIOs were present. The extent of overflow was determined by the combined influence of BIO parameters, making it difficult to identify a simple trend based solely on the relative GR-BIO treatment area.

The *LumpOne* strategy aggregated predictions showed a different trend. Peak runoff error, improved when either GR or BIO facilities dominated the treatment area, compared to synthetic catchments where their areas were balanced. The other metrics did not show a clear relationship with the GR-

BIO proportion. This suggests that the *LumpOne* aggregation is more prone to error under heterogeneous SuDS configurations and performs better when applied to a more homogeneous set of facilities. Overall, the results further support the conclusion that the *LumpN* aggregation method is more robust across a range of spatial distributions.

Figure 5.13 presents each metric as a function of the mean K_{sat} value (average across GR plus BIO) for each simulation. While a wide range of K_{sat} values was tested, no strong or consistent trend was observed between K_{sat} and model error in any aggregation method. This suggests that mean saturated hydraulic conductivity alone is not a dominant factor in explaining variations in aggregation error and supports the need to consider combined parameter interactions in model simplification strategies. Similar patterns were found for other averaged physical parameters, including soil porosity; FC; PWP; soil thickness and storage thickness, none of which individually explained model performance variability.

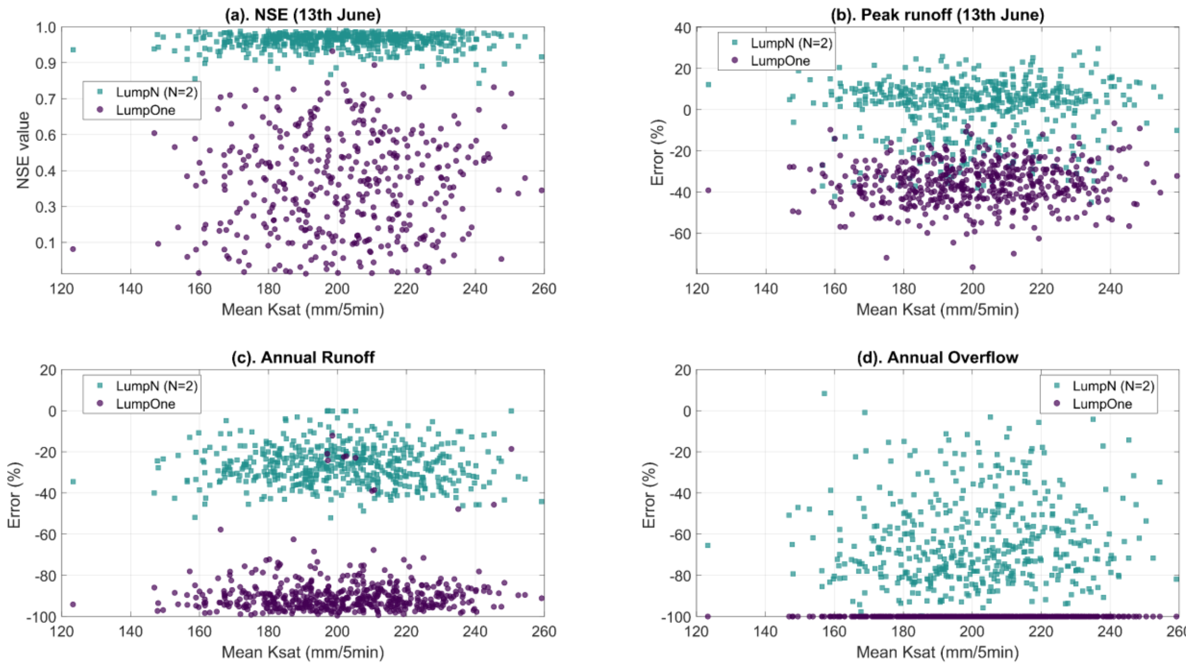

Figure 5.13. Effect of mean K_{sat} on various metrics

Figure 5.14 focuses on the influence of the mean exfiltration rate—relevant only to BIO facilities—on the four metrics. For *LumpOne,* NSE, peak runoff error, and annual runoff volume error deteriorated as exfiltration rate increased, confirming that BIO exfiltration directly affected water redistribution within the catchment. In the detailed representation, certain SuDS units do not permit exfiltration; water percolating through the substrate subsequently exits via the drainage layer and contributes to runoff. However, under the *LumpOne* aggregation, all SuDS units are combined into a single equivalent facility with a non-zero aggregated exfiltration parameter. As a result, water reaching the drainage layer is partially lost to the natural soil through exfiltration rather than directly being conveyed downstream as runoff. This aggregation therefore modifies the intended flow pathways of SuDS units that originally had zero exfiltration, leading to inconsistencies in simulated water routing and contributing to the observed performance deterioration.

For the *LumpN (N=2)*, model performance (in terms of NSE and annual runoff volume error) was slightly better when exfiltration values were either extremely low or extremely high. When exfiltration rates are very low, there is minimal water loss to the natural soil, thus reducing error. At very high rates, exfiltration constituted a large share of the water balance, diminishing the relative contribution of runoff and reducing error. The trend for peak runoff error in Figure 5.14b is similar to that in Figure 5.12b, suggesting that the primary variable influencing this error is the number of BIO units, rather than the exfiltration parameter alone. The overflow error results in Figure 5.14d were highly scattered. As the exfiltration rate increased, the degree of overflow underestimation became more pronounced. This pattern reflects the misallocation of water pathways arising from erroneous estimation of exfiltration.

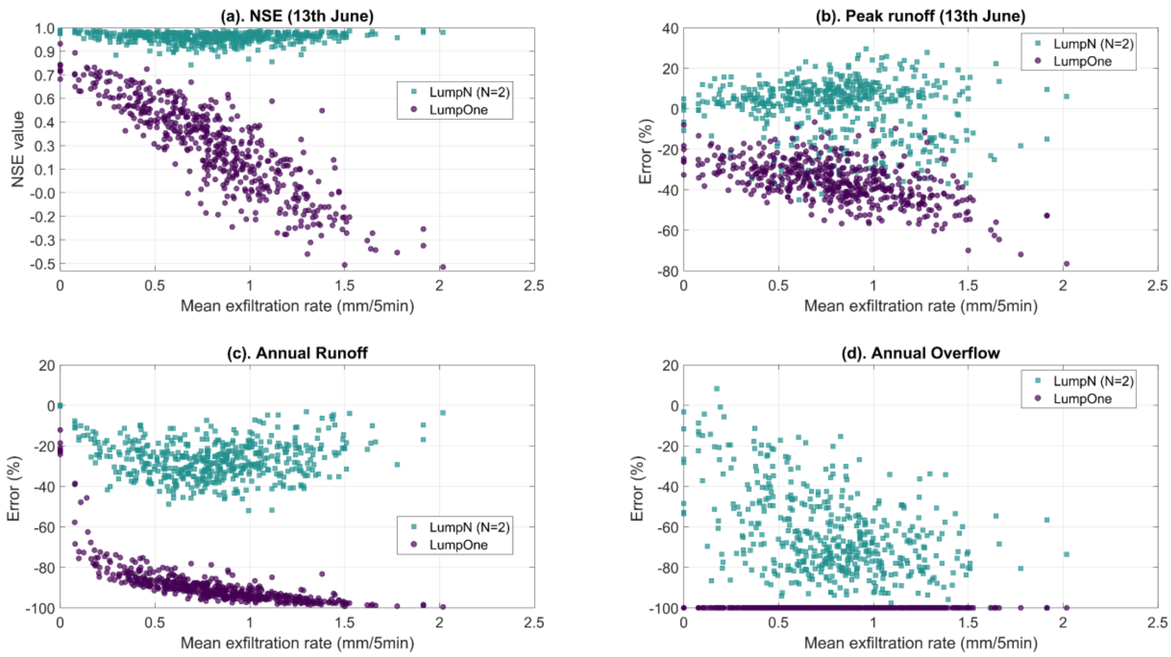

Figure 5.14. Effect of mean exfiltration rate on various metrics

Concluding Remarks

Changes in the relative distribution of GR and BIO facilities affected model performance, particularly for the *LumpOne* aggregation strategy, which showed greater sensitivity to heterogeneous SuDS compositions. The parameter tests further showed that averaged physical parameters, including mean K_{sat} and other substrate properties, did not exhibit strong correlations with model error when considered individually. This suggests that aggregation uncertainty cannot be explained by single parameter values alone, but instead emerges from the combined interaction of hydrological processes within aggregated systems.

Exfiltration associated with BIO facilities had the clearest influence on model behaviour, particularly under the *LumpOne* aggregation, where the aggregation process altered the intended flow pathways of SuDS units. These findings highlight the importance of preserving key hydrological process distinctions when simplifying or aggregating SuDS representations.

5.3.4 *LumpN (N=3)* Strategy Performance

Building on the previous section, grouping by different SuDS types with *LumpN (N=2)* strategy generally works well. As BIO units can be either lined or unlined, this led to a more detailed strategies: *LumpN (N=3)*, which separately aggregate GR, lined BIO, and unlined BIO units.

Figure 5.15 adds the *LumpN (N=3)* strategy results to the analysis from Figure 5.12. The graph clearly shows that accurately simulating different BIO types significantly improves NSE values and reduces annual runoff volume error compared to *LumpN (N=2)* strategy. For the specific 13th June event, *LumpN (N=3)* strategy did not show a significant change in peak runoff prediction but slightly reduced the error range. The scatter distribution of annual overflow volume error also showed modest improved, with the data points shifting upward overall, although the majority remained below 0%.

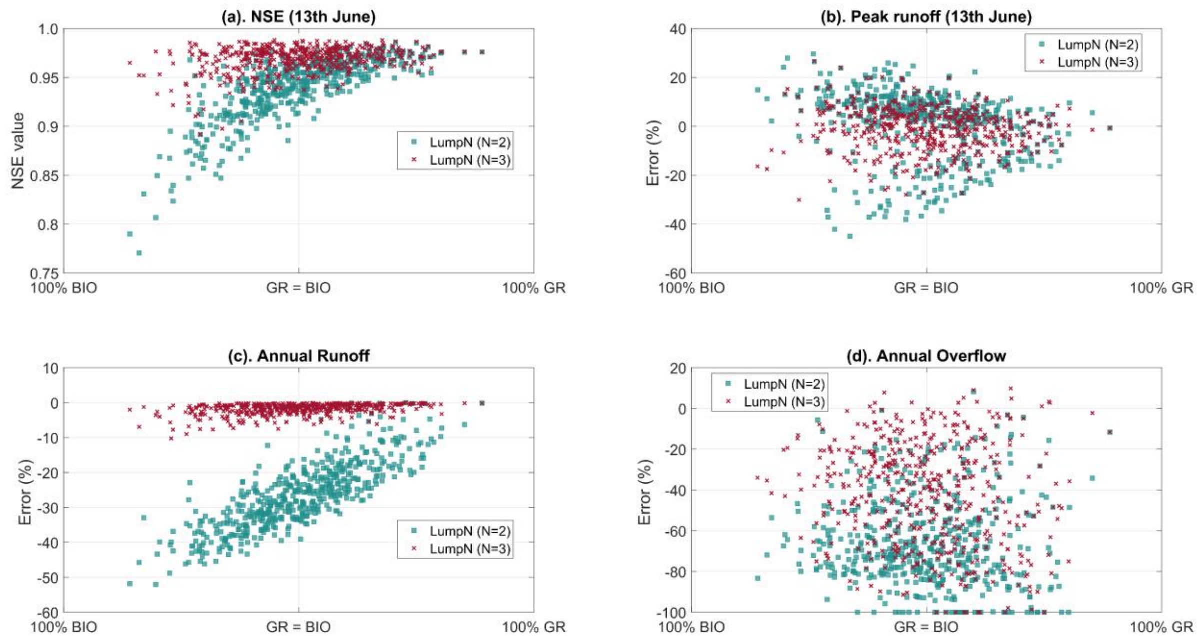

Figure 5.15. Effect of the relative contributions of GR and BIO on various metrics with BIOCLAS methods.

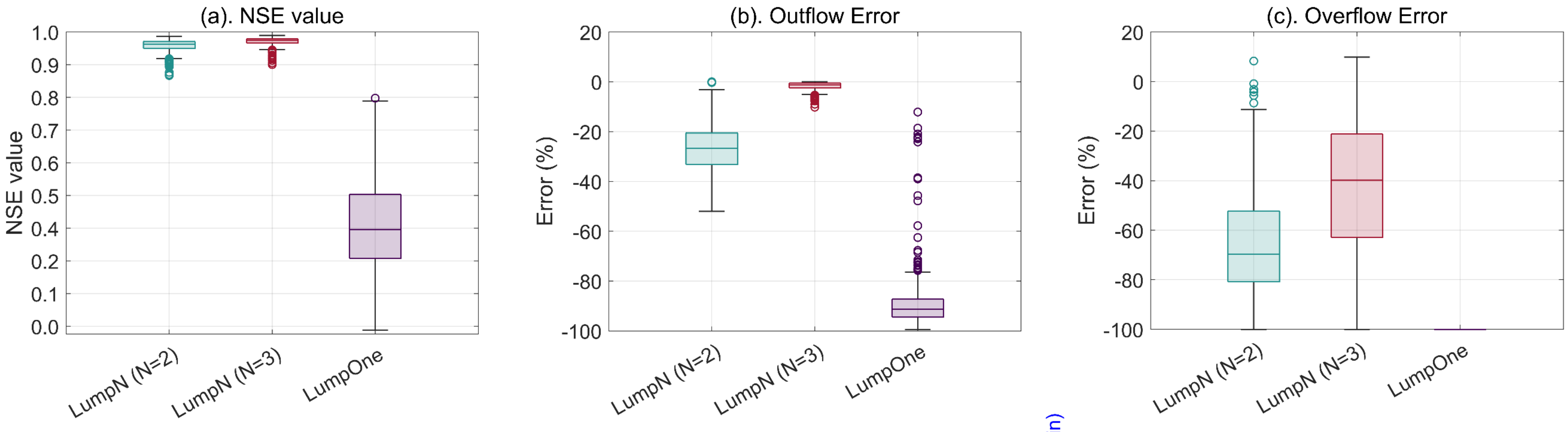

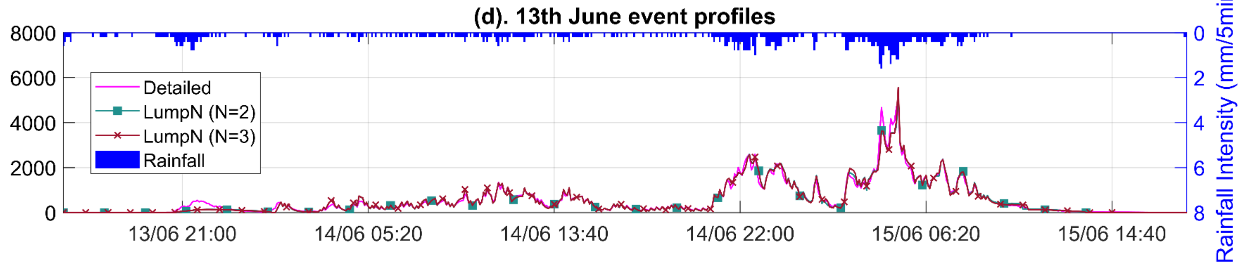

(e). Metrics

	LumpN (N=2)	LumpN(N=3)
NSE value[a]	0.972	0.971
Peak runoff error[a] (%)	6.077	11.680
Total runoff error[b] (%)	-3.613	-1.770
Overflow error[b] (%)	-73.588	-64.126

[a]13th June Rainfall event; [b] Whole year

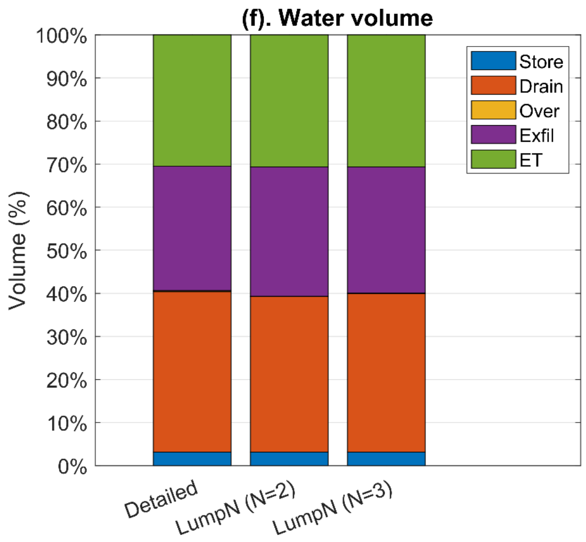

Figure 5.16. LumpN (N=2), LumpN (N=3) and LumpOne performance comparison.

Figure 5.16 a−c presents boxplots for the whole year's runoff profile NSE, outflow volume error, and overflow volume error. Figure 5.16 d−f shows the runoff profiles, evaluation metrics, and water balance for the same case study as Figure 5.7. Although in the selected synthetic catchment the 13th June event showed a slightly larger peak runoff error under *LumpN (N=3). LumpN (N=3)* strategy clearly outperformed *LumpOne* and *LumpN (N=2)* strategies, in the three metrics in boxplots. As shown in Figure 5.16f, this improvement arose because the overall water balance simulated by *LumpN (N=3)* closely matched that of the *Detailed* baseline, very subtly different to *LumpN (N=2)*.

To avoid the influence of sample specificity, Figure 5.17 shows the distribution of peak runoff errors for *LumpN (N=2) and LumpN (N=3)* strategies across approximately 172 rainfall events, identified from the full annual rainfall sequence with a minimum antecedent dry period (ADWP) of six hours. The histograms represent the probability density of peak runoff errors from 500 different synthetic catchments for each rainfall event. Compared with *LumpN (N=2)*, the *LumpN (N=3)* configuration exhibits a substantially more concentrated error distribution around zero. In the case of *LumpN (N=2),* a pronounced accumulation of errors at -100% is evident, indicating small rainfall events for which no outflow was produced and peak discharge was entirely underestimated. In contrast, *LumpN (N=3)* strategy markedly reduces the frequency of such extreme failures and demonstrates a narrower spread of erros. Approximately 85% of rainfall events achieved peak runoff errors within the range of –20% to +20%.

Overall, classifying and aggregating SuDS based on their outflow mechanisms yields the most accurate simulation results. In *LumpN (N=3)* strategy*,* the internal hydrological dynamics of these systems can be effectively captured by the aggregation.

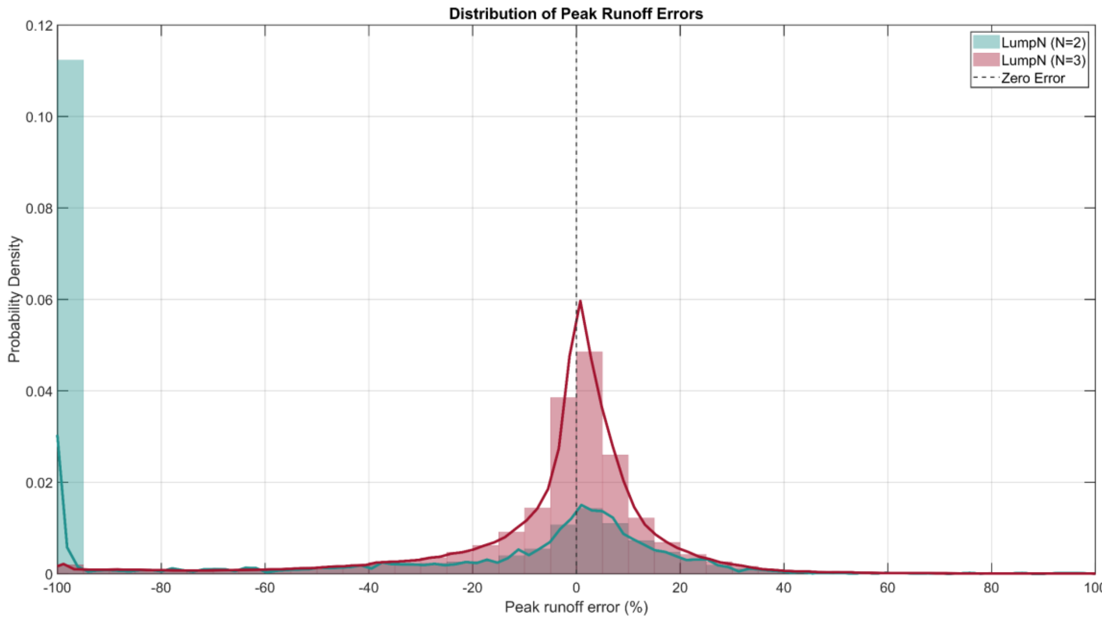

Figure 5.17. Boxplot of peak runoff error in all rainfall events of LumpN (N=2) and LumpN (N=3)

5.4 Discussion

This study evaluated the hydrological performance of different SuDS aggregation methods under a Monte Carlo framework using 500 stochastically generated catchment configurations composed of GR and BIO. The results offer several insights into how aggregation strategy and parameter identification influence simulation accuracy.

The *LumpN (N=2)* aggregation strategy consistently outperformed the *LumpOne* method across all evaluation metrics, especially in reproducing runoff dynamics and annual water balances. NSE values were above 0.9 in most synthetic catchments. These findings suggest that grouping SuDS devices by type, even when aggregated into single units, can preserve essential hydrological behaviour if parameter estimation is handled carefully.

In contrast, the *LumpOne* strategy exhibited substantial deviations, particularly in synthetic catchments with high SuDS heterogeneity. Notably, the *LumpOne* approach frequently underestimated runoff and overestimated exfiltration and evapotranspiration, leading to total runoff errors as high as -86%–95%. These inaccuracies stem largely from structural inconsistencies: when GR and BIO are merged into one composite device, the resulting unit inherits characteristics (e.g., storage thickness and exfiltration) that may not apply to all (or indeed any) of the original SuDS devices. This highlights the risk of physical over-simplification in full aggregation schemes.

Notably, the *LumpN* approach allows further differentiation within SuDS types - for example, BIO can be subdivided into infiltrating and non-infiltrating subtypes (*LumpN (N=3)*) to reflect distinct hydrological behaviours. Controlling water outflow mechanisms within the SuDS system proved decisive in improving model accuracy. Consequently, at the street scale, SuDS classification should not be based solely on typology, but also on functional characteristics related to outflows.

While the SuDS parameters, particularly those affecting percolation, can influence detention tails and peak runoff, the overall impact of parameter estimation was less pronounced than that of structural aggregation. Model performance in aggregated representations was found to depend more strongly on whether individual SuDS units shared comparable hydrological process structures than on the accuracy of individual parameter estimates.

Parameter sensitivity analysis revealed that model error was not strongly correlated with most individual variables (e.g., mean K_{sat}). Instead, error was closely associated with the combined configuration and number of aggregated SuDS units. When the aggregated devices differed markedly in hydrological function, for example in the presence or absence of processes such as exfiltration, aggregation accuracy declined relative to cases in which devices exhibited similar hydrological process representations. These results indicate that, in SuDS aggregation, structural consistency across devices plays a more decisive role in predictive accuracy than refinements in parameter estimation alone.

These findings suggest that for applications involving multiple SuDS types, maintaining typological separation in aggregation (e.g., using the *LumpN* strategy) offers a good balance between model simplification and hydrological performance. While full aggregation into a single device may be attractive for reducing model complexity, it risks substantial loss of accuracy, particularly in predicting overflow and exfiltration volumes.

Practical guidance for engineers:

- Group SuDS by type: Aggregate only units with similar structures and hydrological functions (e.g., lined BIOs, green roofs).
- Recalculated controls: When combining multiple units, adjust key controls (e.g., orifice sizing, flow path length) to reflect the aggregated scale.
- Avoid full aggregation: Do not combine all SuDS types into a single unit, as this oversimplification can severely distort overflow and exfiltration predictions.
- Balance accuracy and efficiency: Typology-based aggregation (e.g., *LumpN*) provides a workable compromise between computational efficiency and hydrological realism, suitable for design assessment and scenario testing.

Limitations and Future Work

This study focused on vertical hydrological processes using a 5-minute timestep and did not account for horizontal interactions such as overland flow routing or connectivity between SuDS units. Additionally, only GR and BIO were considered, and parameters were sampled from predefined ranges rather than empirical measurements. Future work should extend the framework to other SuDS types (e.g., permeable pavements), and incorporate spatial layout factors.

5.5 Conclusions

This study evaluated the hydrological prediction accuracy of different SuDS aggregation methods at the street scale. The modelling approach, *LIDMAT*—based on the SWMM LID conceptual framework—was used alongside three aggregation strategies: *Detailed*, *LumpN*, and *LumpOne*.

The results demonstrate that the *LumpN* aggregation strategies (*LumpN (N=2) and LumpN (N=3)*), which aggregate SuDS by type, can achieve comparable accuracy to fully detailed models. This indicates that type-specific aggregation, even when simplifying device-level variability, preserves the essential hydrological characteristics of the devices. In contrast, the *LumpOne* strategy, which combines all SuDS into a single composite unit, led to significant errors in runoff and overflow predictions. These errors were particularly pronounced in scenarios with a large number of BIO units or imbalanced GR–BIO distributions.

In summary, *LumpN* aggregation provides a robust and computationally efficient approach to SuDS modelling at the street scale, and further refinement through detailed classification (*LumpN (N>2))* demonstrates the value of functional classification based on system configuration. In contrast, full aggregation (*LumpOne*) should be applied with caution, particularly when the system includes structurally and hydraulically diverse SuDS types. These findings provide practical guidance for urban planners and hydrological modellers seeking to balance accuracy and efficiency in large-scale SuDS performance assessments.

6. SuDS Aggregation Case Study Application

6.1 Introduction

This case study evaluates the hydrological accuracy of modelling SuDS performance under different aggregation strategies at the street scale (Chapter 5), using SWMM. In retrofit contexts where multiple SuDS types and configurations coexist, practitioners need screening-level tools that are both computationally efficient and robust enough to support layout decisions and quick rainfall-runoff simulation. However, model behaviour can depend strongly on how the catchment is discretised and how devices are aggregated. Previous studies have shown that the level of subcatchment spatial discretisation influences both parameter estimation and predictive uncertainty, with finer delineations generally providing more reliable parameter sets and reduced output uncertainty compared to coarser representations (Sun et al., 2014). Conversely, device aggregation can substantially reduce data and runtime costs, although peak flows are sensitive if aggregation unduly narrows travel-time distributions (Elliott et al., 2009).

The case study tests whether SuDS aggregation strategies are "fit for purpose" at the street scale and quantifies the trade-offs relative to fully detailed representations. The case study aims to determine how SuDS layout and model aggregation influence rainfall–runoff predictions at the street scale, and to assess the feasibility of rapid SuDS modelling for screening and preliminary design.

The specific objectives of this case study are as follows:

1. Develop a SWMM model of the study area and quantify land-cover areas relevant to runoff generation.
2. Specify retrofit SuDS types (bioswale/bioretention, permeable pavement, planters) and parameters.
3. Evaluate model performance under a design storm and a continuous one-year record.
4. Compare scenario outputs across subcatchment spatial discretisation and SuDS aggregation strategies and discuss implications for engineering applicability.

6.2 Methods and Data

6.2.1 Study Area

This case study assesses a site within the Mining Remediation Authority (MRA), Mansfield, UK, represented in SWMM using the catchment footprint and SuDS retrofit layouts digitised from project mapping (Severn Trent Water, 2025). The spatial context and retrofit locations are shown in Figure 6.1; pre-retrofit land-use composition (areas and percentages) is summarised in Table 6.1.

The catchment covers 17,500 m^2 and is dominated by hard surfaces. Land use is grouped into three classes: green space (lawn), pavement, and roof. Green space constitutes the pervious portion of the site ($\approx$ 21.12%), while pavement and roofs together form the impervious area ($\approx$ 78.88%).

The retrofit design applies three SuDS types: bioswale (BS), permeable pavement (PP), and rainwater downpipe planter (RDP). Their indicative locations are shown in Figure 6.1 (c); design parameters and dimensions are provided in Section 2.2.

Given that the local drainage operates as a combined sewer, the legacy underground network and asset inventory were not fully reproduced. Instead, the block is modelled as a hydraulically closed unit discharging to a single outlet (outfall) at its downstream boundary in the south-west corner of the site. The pipe network isolates the hydrological effects of layout and aggregation choices in the SuDS scenarios while keeping model complexity appropriate for screening-level comparison.

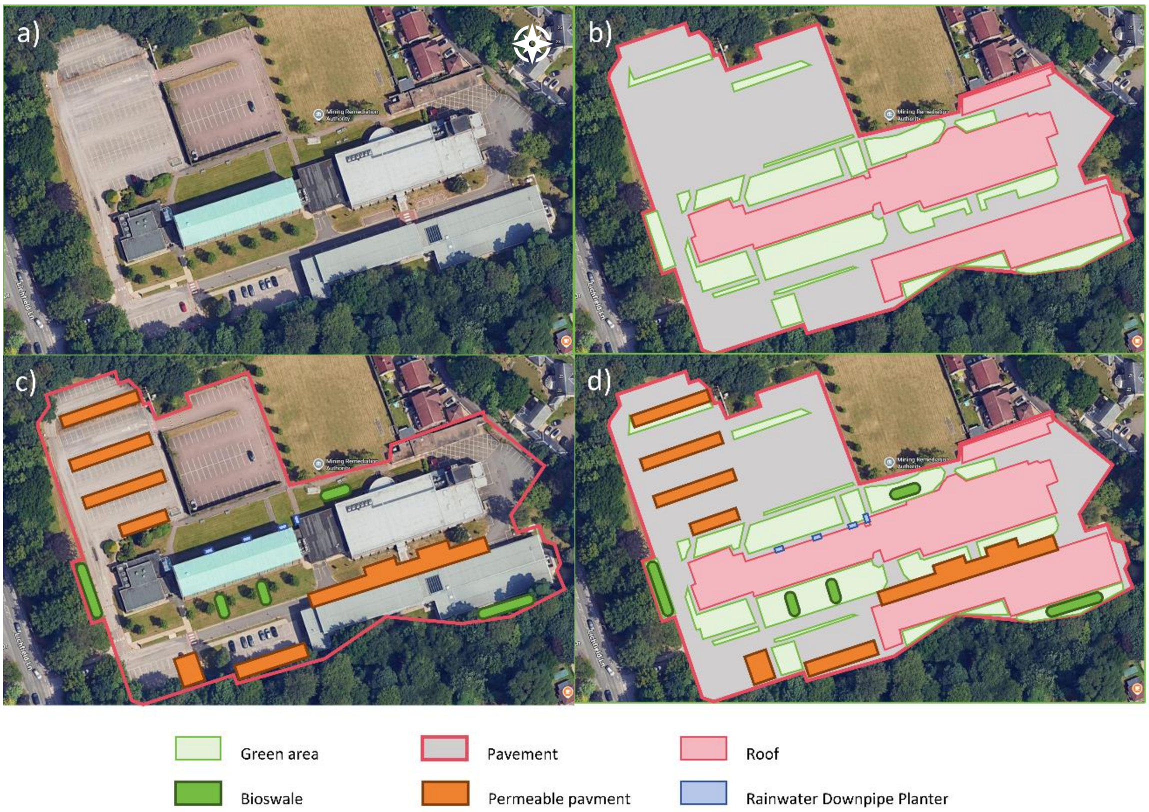

Figure 6.1. Mining Remediation Authority, Mansfield, UK. (a) screenshot of MRA (Google Maps, 2025); (b) schematic of MRA land use; (c) MRA SuDS retrofit (only SuDS); (d) MRA SuDS retrofit land use map.

Table 6.1. Summary of surface characteristics in MRA

Land use types	Total area (m^2)	Note	Percentage
Green area	3696.2	Pervious	21.12%
Pavement	9239.0	Impervious	78.88%
Roof	4564.8	Impervious	

6.2.2 SuDS Configurations

Figure 6.2 maps the names and locations of all SuDS units within the MRA study area. Table 6.2 represents each unit's footprint and its contributing area. Contributing area to footprint ratios (or loading ratios) are high for planters (≈80-170) and bioswales (≈20-30) and modest for permeable pavements (≈ 2-5).

Parameterisation followed two principles. First, key material properties (e.g., media porosity, thickness) were taken from the engineering design where available. Second, remaining parameters were assigned reasonable values from the literature and previous applications. The full parameter set is summarised in Table 6.3. In SWMM, bioswales were represented using the *Bioretention Cell* LID type, and permeable pavements using the *Permeable Pavement* LID type.

Rainwater downpipe planters (RDP005, RDP006, RDP007, RDP012) required special treatment (Severn Trent Water, 2025). RDP006 (Meristem RDP (Meristem Design Ltd, 2026)) and RDP007 (SuDSPlanter RDP (Sudsplanter Ltd, 2025)) were modelled as bioretention cells (i.e., equivalent to the bioswale configuration). In contrast, RDP005 (Freeflush RDP (Freeflush Ltd, 2026)) and RDP012 (GBU SuDSPod RDP (GreenBlue Urban Ltd, 2026)) were represented as tanks with an orifice outlet; discharge was controlled through a prescribed head-discharge relationship (Figure 6.3).

Exfiltration (seepage) settings reflect local constraints. All bioswales allow exfiltration where feasible; BS006 and BS009 were lined (no exfiltration) due to proximity to building foundations and the attendant risk of sub-surface ingress. All permeable pavement units were assumed unlined with exfiltration enabled. Although some built permeable pavements may be partially lined in practice, a uniform exfiltration assumption was adopted to reduce model complexity.

For devices with orifice control, physical diameters from the design (e.g., 10 mm, 15 mm) were converted to SWMM LID flow coefficient values using standard orifice hydraulics to ensure consistent outlet behaviour across scenarios.

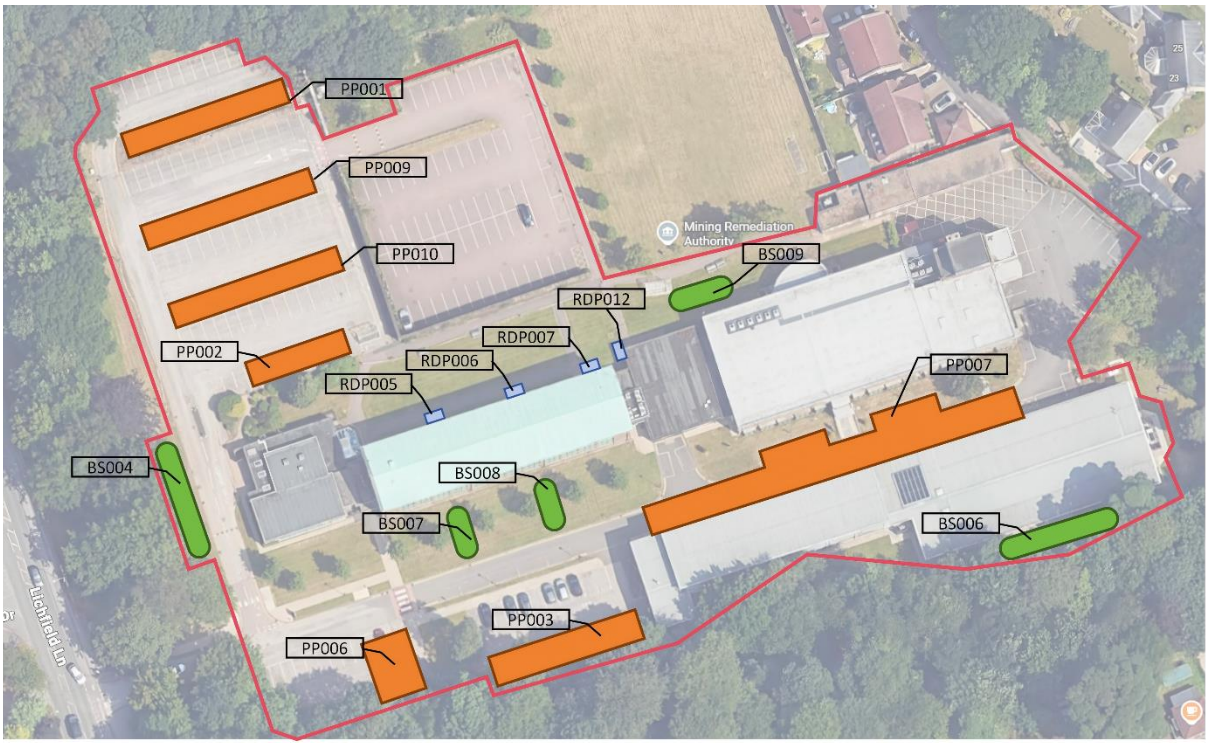

Figure 6.2. MRA SuDS map (Google Map, 2025)

Table 6.2. SuDS area information (BS = bioswale, PP = permeable pavement, and RDP = rainwater downpipe planter)

SuDS ID	SuDS footprint (m^2)	Contributing area (m^2)	Ratio
BS004	23.789	599.277	25.191
BS006	24.651	557.517	22.616
BS007	9.997	255.657	25.572
BS008	7.801	228.017	29.228
BS009	29.007	638.698	22.019
PP001	178.116	522.57	2.934
PP002	106.701	504.179	4.725
PP003	168.133	659.258	3.921
PP006	142.052	602.507	4.241
PP007	531.714	2546.660	4.754
PP009	180.997	620.626	3.429
PP010	180.497	614.76	3.406
RDP005	0.48	82.647	172.181
RDP006	1.08	82.557	76.442
RDP007	0.72	81.897	113.746
RDP012	0.729	78.954	108.305

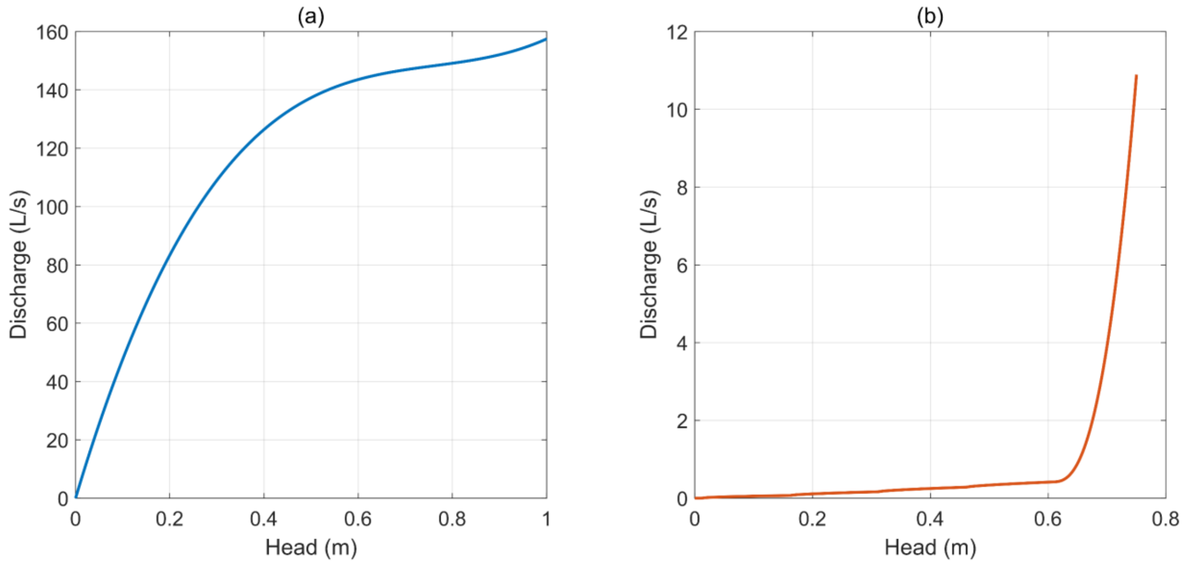

Figure 6.3. (a) RDP005 head-discharge relationship; (b) RDP012 head-discharge relationship.

Table 6.3. SuDS device parameters

Layer	Parameter	Unit	BS004	BS006	BS007	BS008	BS009	RDP006	RDP007	Notes
Surface	Berm Height (surfHead)	mm	300	300	300	300	350	0	0	
	Vegetation fraction	m^3/m^3	0	0	0	0	0	0	0	Severn Trent Water (2025)
	Surface roughness (Manning)	-	0.1	0.1	0.1	0.1	0.1	0.1	0.1	
	Surface slope	%	0.5	0.5	0.5	0.5	0.5	0.5	0.5	
Substrate	Thickness (soilThk)	mm	525	525	525	525	525	610	450	Severn Trent Water (2025)
	Porosity	m^3/m^3	0.35	0.35	0.35	0.35	0.35	0.4	0.35	Severn Trent Water (2025)
	Field Capacity (FC)	m^3/m^3	0.14	0.14	0.14	0.14	0.14	0.16	0.14	50% Porosity
	Wilting Point (PWP)	m^3/m^3	0.07	0.07	0.07	0.07	0.07	0.08	0.07	20% Porosity
	Conductivity (K_{sat})	mm/hr	400	400	400	400	400	400	400	Severn Trent Water (2025)
	Conductivity Slope	-	30	30	30	30	30	30	30	Rossman (2016a)
	Suction Head	mm	50	50	50	50	50	50	50	Rossman (2016a)
Storage	Thickness (storThk)	mm	250	250	250	250	250	150	300	Severn Trent Water (2025)
	Void Ratio (void/total)	m^3/m^3	0.38	0.38	0.38	0.38	0.38	0.94	0.96	Severn Trent Water (2025)
	Seepage Rate (Exfil)	mm/hr	7.2	0	7.2	7.2	0	0	0	National Cooperative Soil Survey (2006)
	Clogging factor	-	0	0	0	0	0	0	0	
Drain	Flow coefficient	-	1.082	1.044	2.575	3.300	0.887	25.743	20.852	Based on orifice diameter
	Flow exponent	-	0.5	0.5	0.5	0.5	0.5	0.5	0.5	Rossman (2016a)
	Offset	mm	0	0	0	0	0	0	0	
	Open level	-	0	0	0	0	0	0	0	
	Closed level	-	0	0	0	0	0	0	0	

Table 6.3 (continued). SuDS device parameters

Layer	Parameter	Unit	PP001	PP002	PP003	PP006	PP007	PP009	PP010	Notes
Surface	Berm Height (surfHead)	mm	0	0	0	0	0	0	0	Severn Trent Water (2025)
	Vegetation fraction	m^3/m^3	0	0	0	0	0	0	0	
	Surface roughness (Manning)	-	0	0	0	0	0	0	0	
	Surface slope	%	0	0	0	0	0	0	0	
Pavement	Thickness	mm	80	80	80	80	80	80	80	Severn Trent Water (2025)
	Void Ratio	m^3/m^3	0.15	0.15	0.15	0.15	0.15	0.15	0.15	
	Impervious surface fraction	-	0	0	0	0	0	0	0	
	Permeability	mm/hr	1000	1000	1000	1000	1000	1000	1000	
	Clogging factor	-	0	0	0	0	0	0	0	
	Regeneration interval	days	0	0	0	0	0	0	0	
	Regeneration fraction	-	0	0	0	0	0	0	0	
Substrate	Thickness (soilThk)	mm	50	50	50	50	50	50	50	Severn Trent Water (2025)
	Porosity	m^3/m^3	0.25	0.25	0.25	0.25	0.25	0.25	0.25	Severn Trent Water (2025)
	Field Capacity (FC)	m^3/m^3	0.1	0.1	0.1	0.1	0.1	0.1	0.1	50% Porosity
	Wilting Point (PWP)	m^3/m^3	0.05	0.05	0.05	0.05	0.05	0.05	0.05	20% Porosity
	Conductivity (K_{sat})	mm/hr	1000	1000	1000	1000	1000	1000	1000	Severn Trent Water (2025)
	Conductivity Slope	-	30	30	30	30	30	30	30	Rossman (2016a)
	Suction Head	mm	50	50	50	50	50	50	50	Rossman (2016a)
Storage	Thickness (storThk)	mm	275	500	525	450	525	275	350	Severn Trent Water (2025)
	Void Ratio (void/total)	m^3/m^3	0.3	0.3	0.3	0.3	0.3	0.3	0.3	Severn Trent Water (2025)
	Seepage Rate (Exfil)	mm/hr	7.2	7.2	7.2	7.2	7.2	7.2	7.2	National Cooperative Soil Survey (2006)
	Clogging factor	-	0	0	0	0	0	0	0	
Drain	Flow coefficient	-	0	0	0.153	0.181	0.108	0	0.143	Based on orifice diameter
	Flow exponent	-	0.5	0.5	0.5	0.5	0.5	0.5	0.5	Rossman (2016a)
	Offset	mm	0	0	0	0	0	0	0	
	Open level	-	0	0	0	0	0	0	0	
	Closed level	-	0	0	0	0	0	0	0	

6.2.3 Hydrological Model Catchment Setup

Hydrological modelling was performed using the Storm Water Management Model (SWMM 5.2), developed by the USEPA (Rossman, 2016b, 2016c, 2016a). Groundwater processes were not represented because they are not expected to materially affect the study outcomes.

In catchment scale hydrological modelling, the evaluation of SuDS aggregation strategies cannot be entirely decoupled from the manner in which the catchment itself is discretised. Subcatchment delineation governs the spatial resolution at which rainfall-runoff processes are represented. As a result, any modification to SuDS representation, particularly the aggregation of multiple devices into equivalent units, inevitably interacts with the underlying subcatchment aggregation level.

By examining multiple spatial discretisation levels, this study distinguishes changes in model response attributable to SuDS aggregation from those arising solely from catchment representation. This approach allows the assessment of whether simplified SuDS configurations remain robust across different levels of subcatchment area aggregation, thereby enhancing the transferability and practical relevance of the modelling framework for preliminary design and planning applications.

Figure 6.4 illustrates three subcatchment spatial discretisation levels for the MRA study area:

- *Fully Distributed* (71 subcatchments). All subcatchments were delineated into hydrologically homogeneous units (consistent soil and land use), with explicit flow pathways between subcatchments. Each SuDS device and its contributing area were modelled as a separate subcatchment to preserve rainfall-runoff fidelity.
- *Semi-lumped* (7 subcatchments). Units were merged guided by the pipe/node layout inferred from the *Fully Distributed* case. All subcatchments were less than 5,000 m^2, ensuring that the final catchment runoff is not influenced by times of concentration in pipe flow with a 5-min computation timestep. Heterogeneous surface covers were permitted within a subcatchment; pervious and impervious overland flow is routed to the subcatchment's drainage point. Derived geometric parameters (e.g., width) were computed as area-weighted averages of the detailed surfaces.
- *Lumped* (1 subcatchment). The entire MRA area was represented as a single subcatchment with surface runoff routed to the outlet; both impervious and pervious components drain to the terminal outfall.

In terms of conduits and boundary conditions, pipe diameters in the abstracted network were selected to be consistent with the legacy system.

Under the *Fully Distributed* representation, local catchment characteristics and inter-subcatchment flow transfers are explicitly resolved. In contrast, when the catchment is aggregated into a single lumped unit (*Lumped*), these local heterogeneities and internal flow pathways are inevitably homogenised. Specifically, overland flow between subcatchments may no longer be represented explicitly, as the lumped catchment is instead characterised by aggregated fractions of pervious and impervious area. Consequently, variations in slope, spatial difference in perviousness, and local routing effects, such as transfers of runoff from impervious to pervious surfaces, are implicitly averaged out rather than dynamically simulated.

Although representing the study area as a single large catchment (e.g. defined by an overall imperviousness of 10%) can substantially reduce model setup effort, this simplification introduces inherent structural assumptions that may affect simulated hydrological responses. In particular, the averaging of parameters and omission of internal flow processes may alter runoff generation and routing behaviour independently of SuDS representation. This chapter therefore explicitly introduces and quantifies the hydrological implications of subcatchment aggregation, an issue not addressed in earlier chapters of this thesis. By isolating and characterising these effects, the study ensures that subsequent evaluations of SuDS aggregation strategies are not misled by discretisation-related factor, thereby strengthening the robustness and interpretability of the results.

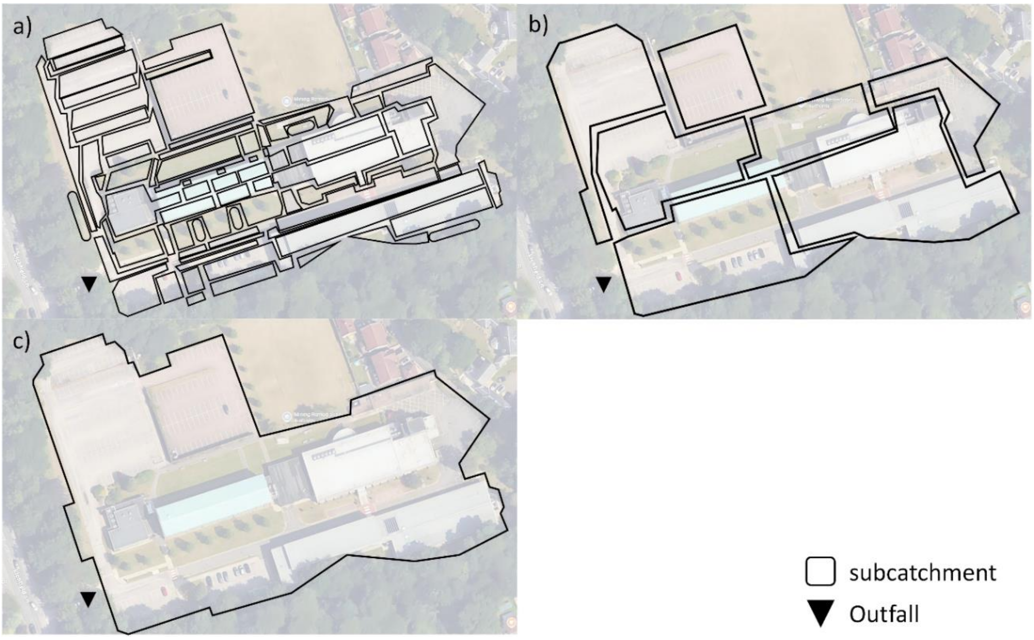

Figure 6.4. Subcatchment spatial discretisation levels in SWMM. (a) Fully Distributed catchment; (b) Semi-lumped catchment; (c) Lumped catchment.

6.2.4 Simulation Scenarios

To evaluate SuDS retrofit effects at the MRA site, this study implemented a factorial set of scenarios spanning three subcatchment spatial discretisation levels and four SuDS representation cases. SuDS parameterisations (Section 6.2.2) were applied consistently where relevant.

Subcatchment spatial discretisation (Section 6.2.3):

- *FD — Fully distributed* sub-catchments (highest spatial fidelity).
- *SLC — Semi-lumped* catchment (intermediate fidelity).
- *LC — Lumped* catchment (single unit).

SuDS representation (Section 5.2.2):

- *Base* — No SuDS (hydrological baseline).
- *Detailed* — Device-level SuDS explicitly represented (bioswale, permeable pavement, RDP as per SWMM LID types).
- *LumpN* — Aggregated SuDS represented as N equivalent units per discretisation (area-preserving). The classification of bioswales is further refined into two categories, depending on whether the exfiltration rate exceeds zero.
- *LumpOne* — All SuDS aggregated to one equivalent unit at the catchment scale (area-preserving).

Figure 6.5 provides a schematic illustration of the six SuDS modelling scenarios summarised in Table 6.4. In the *Detailed* representation (Figure 6.5 a, b, d), the three subcatchment spatial discretisation strategies do not affect the inflow to individual SuDS units, as each device is assigned a clearly defined contributing area based on available spatial information. In the two *LumpN* scenarios (Figure 6.5 c, e), partial aggregation of SuDS units is applied. In *SLC_LumpN*, SuDS devices within selected subcatchments are aggregated, the same as their contributing area. The *LC_LumpN* aggregates all subcatchments into a single catchment, and SuDS units are grouped by type, preserving separate representations for PP, unlined BIO, and lined BIO (including two RDPs). The *LumpOne* scenario (Figure 6.5f) represents the most aggregated configuration, in which all SuDS devices across the study area are combined into a single BIO unit.

It should be noted that Figure 6.5a corresponds directly to the *Detailed* strategy illustrated in Figure 5.2, while Figure 6.5f represents the *LumpOne* strategy. For *LumpN* strategy (Figure 6.5 c and e), SuDS contributing areas can be defined within individual subcatchments; consequently, each delineated subcatchment implements the *LumpN* aggregation strategy.

Table 6.4. Nine simulation scenarios

	Base	*Detailed*	*LumpN*	*LumpOne*
FD	*FD_Base*	*FD_Detailed*	—	—
SLC	*SLC_Base*	*SLC_Detailed*	*SLC_LumpN*	—
LC	*LC_Base*	*LC_Detailed*	*LC_LumpN*	*LC_LumpOne*

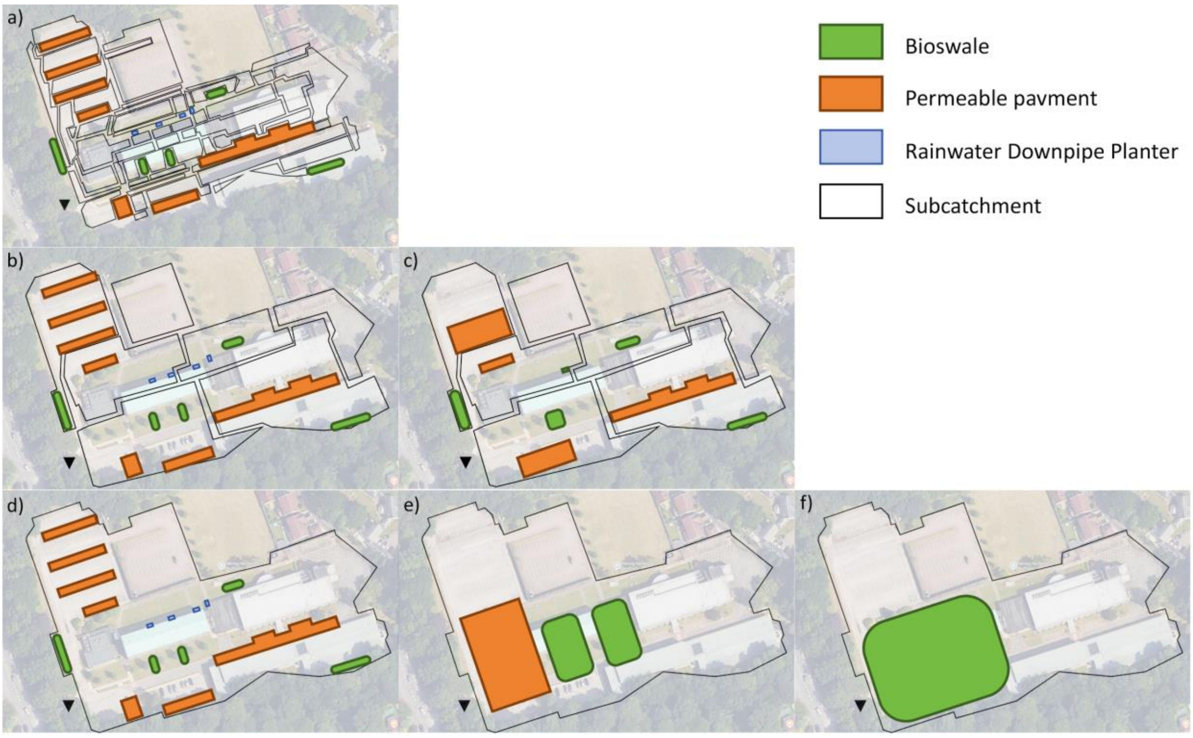

Figure 6.5. MRA simulation scenarios (with SuDS): a). FD_Detailed; b). SLC_Detailed; c). SLC_LumpN; d). LC_Detailed; e). LC_LumpN; f). LC_LumpOne.

6.2.5 Meteorological Data Inputs

SuDS hydrological modelling tools are required to quantify expected responses to both routine and extreme rainfall events. The comparative performance of the modelling scenarios was therefore evaluated against one design storm (30-year return period) (the same in Section 4.2.3); and a one-year continuous time-series rainfall in Sheffield (UK) during 2007 (the same in Section 4.2.3).

The design storm was simulated at 1-min intervals, with the initial soil moisture of all SuDS units set to zero (i.e. a best-case scenario with moisture content equal to PWP). The continuous simulations used the observed rainfall at 5-min intervals.

The monthly potential evapotranspiration (PET) rates were calculated using the Thornthwaite equations (Stovin et al., 2013b) (Chapter 4, Table 4.2). In the simulations, the ET function was only considered in the continuous rainfall series, and when there was no rainfall.

6.2.6 Model Evaluation Metrics

The effectiveness of SuDS aggregation methods was evaluated through a set of hydrological performance metrics, which quantify the deviation of aggregated model simulations from the baseline reference. In this study, the *FD_Base and FD_Detailed* served as the baseline scenarios. All other scenarios were assessed by comparing their simulation outputs to baseline scenario results.

The Nash-Sutcliffe model efficiency (NSE) index (Equation 4.1) was employed to objectively estimate how well the runoff profiles were predicted by the SuDS aggregation modelling compared with the specific baseline scenarios.

6.3 Results and Analysis

6.3.1 Catchment Simulation Performance

The total outflow performance of the study catchment across different rainfall simulations and various simulation scenarios is first examined. Table 6.5 presents the NSE values comparing the outflow profiles (whole time series) of the aggregated scenarios against the fully disaggregated baseline (*FD_Base* and *FD_Detailed*). Overall, the NSE analysis confirms high model accuracy across most simulations: almost all scenarios achieve NSE values above 0.95 when compared against the *FD* baselines, with the sole exception being the *LC_LumpOne* result during the annual continuous simulation. Figure 6.6 illustrates the runoff profiles during the 30yr design storm simulation. For annual rainfall series, Figure 6.7a presents the cumulative catchment outflow profiles; Figure 6.7b presents the cumulative catchment outflow bar chart; Figure 6.7c depicts the rainfall runoff profiles during a significant rainfall event (June 13^{th}–16^{th}) from the annual simulation.

Table 6.5. NSE value of simulation scenarios

	Design storm		2007 rainfall series	
	FD_Base	*FD_Detailed*	*FD_Base*	*FD_Detailed*
SLC_Base	0.998	——	0.994	——
LC_Base	0.991	——	0.979	——
SLC_Detailed	——	0.999	——	0.995
SLC_LumpN	——	0.998	——	0.992
LC_Detailed	——	0.984	——	0.979
LC_LumpN	——	0.984	——	0.953
LC_LumpOne	——	0.965	——	0.936

A primary observation across both simulation types is the significant reduction in cumulative outflow volumes for all scenarios incorporating SuDS compared to the No-SuDS Baseline (represented by the *FD_Base, SLC_Base*, and *LC_Base*). This clearly establishes the critical role of the implemented SuDS configuration in substantially reducing catchment runoff volume within the study area.

Analysis of the design storm profiles (Figure 6.6) reveals that while the overall outflow results of the baseline scenarios are comparable, a misalignment in the runoff peak timing exists. Specifically, the peak discharge in the *LC* occurs approximately one minute earlier than in the *SLC* model, while the *SLC* peak occurs about one minute earlier than in the *Detailed* model. This shift in the time to peak is also observed across the SuDS scenarios, indicating that it is fundamentally driven by the subcatchment spatial discretisation rather than the SuDS aggregation. This phenomenon is rooted in the sensitivity of the hydrological model (i.e., SWMM) to the effective flow length used in the runoff calculation and time of concentration.

At higher spatial discretisation levels, individual subcatchments are shorter and hydrologically simpler; however, runoff from upstream units is routed sequentially through downstream subcatchments, each exhibiting slightly different response times and peak magnitudes. The superposition of these asynchronous responses increases local lag effects and produces an attenuated and smooth composite hydrograph at the outlet. Lower spatial discretisation averages the hydraulic heterogeneity over a larger area, reducing internal routing complexity while effectively extending the dominant flow path. This leads to more synchronised runoff generation, resulting in sharp and early peaks in the aggregated hydrographs. Despite these shifts in timing, the peak magnitudes in the SuDS scenarios remain largely consistent across different spatial discretisation.

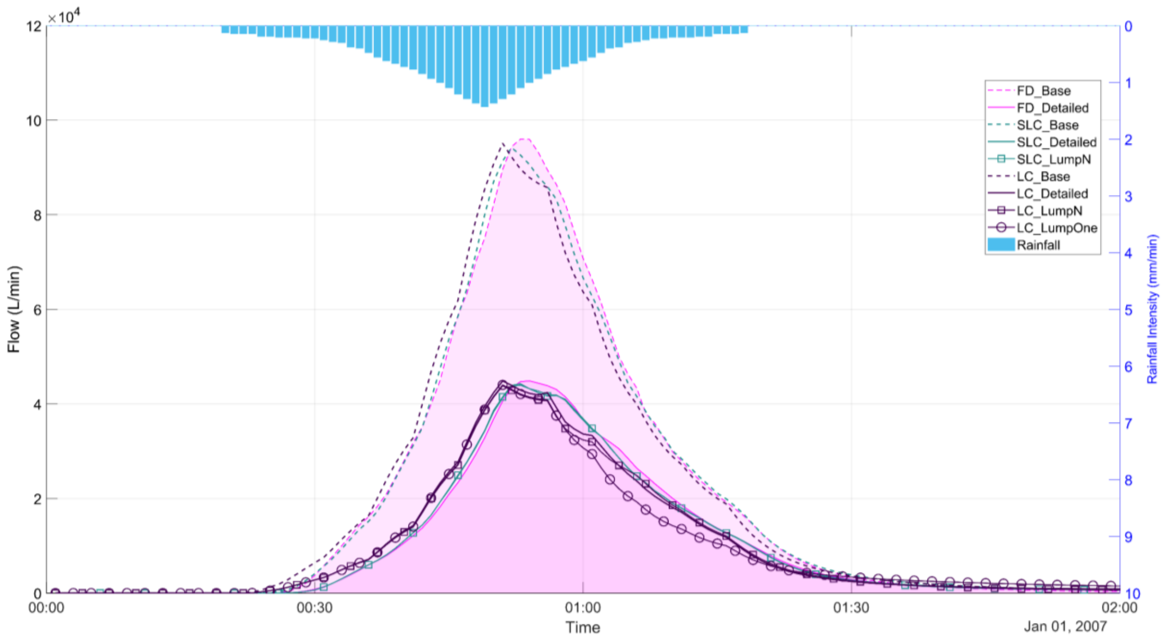

Figure 6.6. Design storm catchment rainfall-runoff profiles

The cumulative outflow in response to the annual rainfall series (Figure 6.7 a&b) provides a focused evaluation of the modelling strategies. When comparing the No-SuDS scenarios, *SLC_Base* and *LC_Base* both exhibit higher cumulative outflow volumes than the *FD_Base* scenario. This difference reveals an inherent subcatchment aggregation error: in the *FD_Base* detailed delineation, runoff from impervious areas is often explicitly routed across pervious subcatchments, facilitating direct infiltration before reaching the drainage network. In contrast, the *SLC* and *LC* lumped baselines assume runoff from both impervious and pervious areas is immediately discharged to the outlet node, effectively bypassing surface infiltration opportunities. Since the interaction of impervious and pervious area runoff cannot be explicitly defined by numerical percentages in the standard SWMM subcatchment setup, this aggregation simplification introduces a consistent overestimation of runoff in the *SLC* and *LC* baseline models. Considering the scenarios that include SuDS, and conceptually accounting for this subcatchment aggregation bias, the *Detailed* and *LumpN* strategies demonstrate comparable and relatively reasonable performance in terms of cumulative outflow when evaluated against the *FD_Detailed* baseline. This result supports the finding that type-based aggregation (*LumpN*) is a relatively reliable strategy. Conversely, the *LC_LumpOne* strategy substantially underestimates the total catchment outflow volume, aligning with observations that full aggregation (*LumpOne*) tends to overestimate losses (such as exfiltration), leading to an unrealistically low predicted discharge to the sewer network.

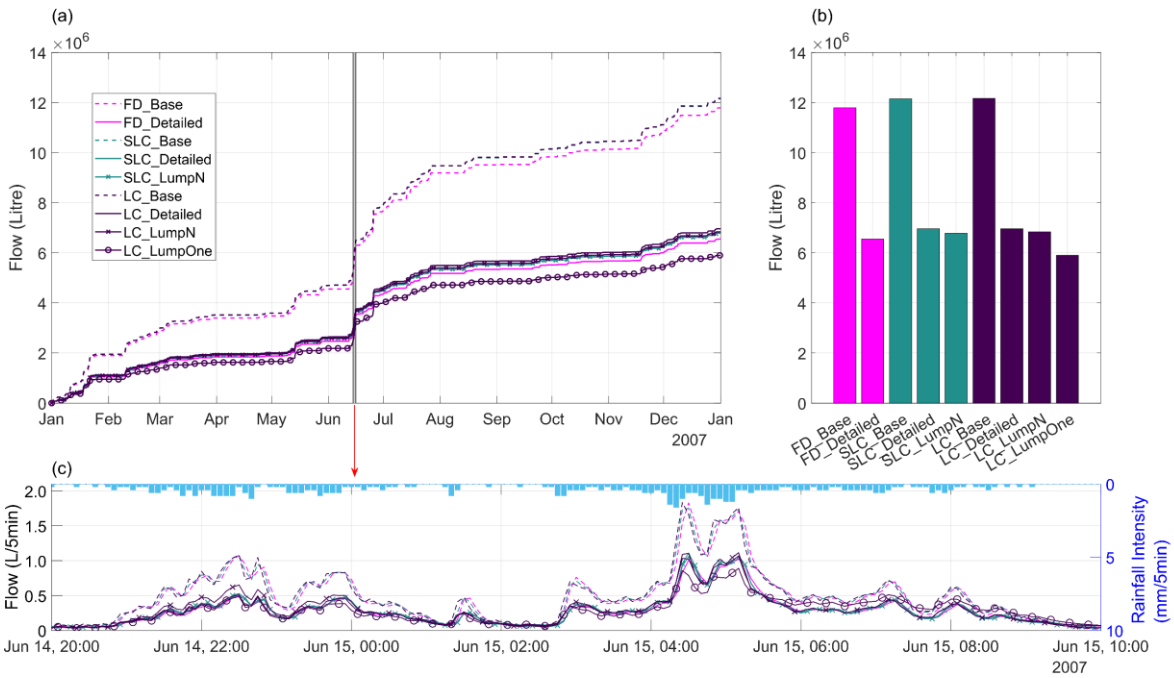

Figure 6.7. (a). 2007 rainfall series cumulative catchment runoff profiles; (b). Cumulative runoff bar chart; (c). Catchment rainfall-runoff profiles on June 13th event in 2007 rainfall series

The aggregated SuDS scenarios *LC_LumpOne* and *LC_LumpN* yield less accurate results compared to the others. *LC_LumpOne* demonstrates particular deficiencies (Figure 6.7c), often failing to accurately reproduce the magnitude of the *FD_Detailed* peaks during significant events, exhibiting both overestimation and underestimation. The *Detailed* method consistently provides the best performance. The *LumpOne* method is characterised by a significant underestimation of total outflow and poor peak flow simulation. The effect of subcatchment spatial discretisation is further highlighted by the comparison between *SLC_LumpN* and *LC_LumpN*, where *SLC_LumpN* yields a clearly superior outcome, suggesting that the subcatchment grouping interacts with the type-based aggregation to produce variable results.

To accurately evaluate the performance of the various SuDS modelling strategies, the internal water balance and flow pathways within the aggregated SuDS units were investigated. Figure 6.8 illustrates the cumulative profiles for SuDS inflow and various hydrological losses during the June 13th rainfall event of the annual simulation. Figure 6.9 provides a dynamic view of the SuDS underdrain outflow profiles during the same event. ET loss was excluded from the cumulative profiles as the volume was negligible and consistent across all SuDS scenarios.

Across all scenarios incorporating SuDS, the inflow volume to the SuDS facilities was consistent. Analysis of the cumulative underdrain outflow reveals that the three detail scenarios (*FD_Detailed, SLC_Detailed,* and *LC_Detailed*) are nearly overlapping, indicating dynamic hydrological consistency in the detailed representations. However, the aggregated strategies (*SLC_LumpN, LC_LumpN,* and *LC_LumpOne*) all underestimated the total cumulative underdrain flow volume.

Furthermore, a specific examination of the flow losses indicates that only the *LC_LumpOne* scenario significantly overestimates the cumulative exfiltration volume. The underdrain flow deficit observed in the three lumped scenarios (*SLC_LumpN, LC_LumpN,* and *LC_LumpOne*) is largely accounted for by an overestimation of overflow (Figure 6.8). This suggests that these three aggregation strategies fail to accurately reproduce the hydrological dynamics leading to overflow within the SuDS facilities.

The dynamic underdrain flow profiles (Figure 6.9) further highlight the performance discrepancies. All three lumped scenarios (*SLC_LumpN, LC_LumpN,* and *LC_LumpOne*) demonstrably underestimated the peak underdrain flow. This inability to accurately capture peak flow rates and the observed overestimation of overflow volumes confirm the limitations of the aggregated approaches, particularly their failure to robustly represent the detention and discharge relationship of the fully disaggregated baseline system during high-intensity rainfall.

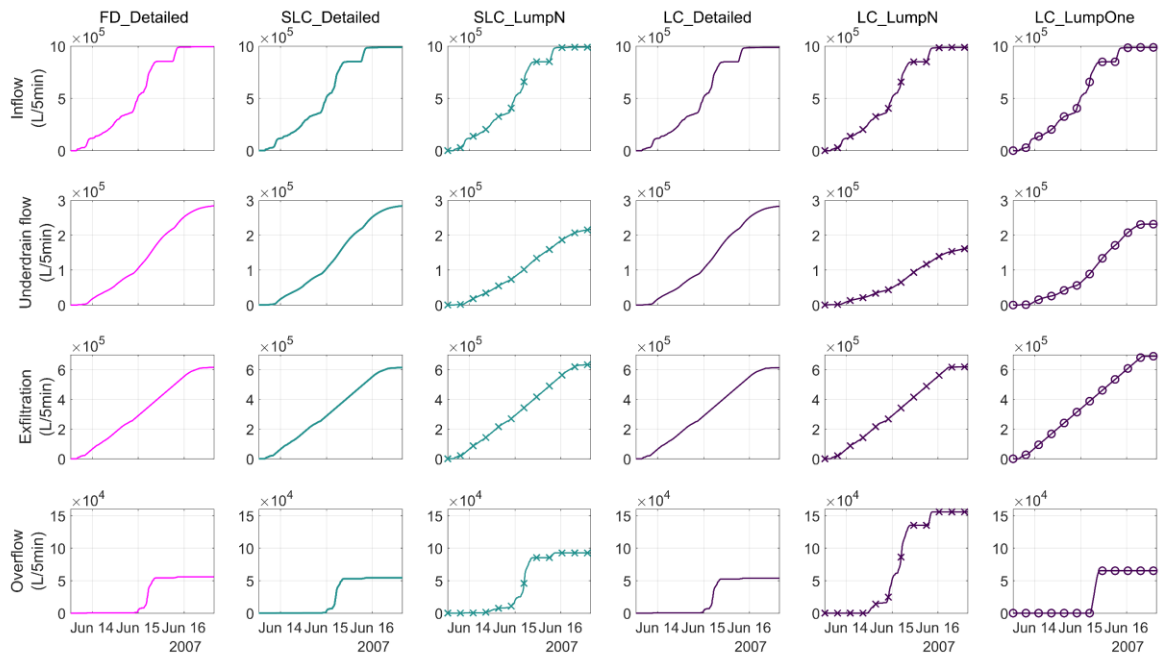

Figure 6.8. SuDS cumulative profiles on June 13th event in 2007 rainfall series. Inflow water volume; Underdrain flow water volume; Exfiltration volume; Overflow volume.

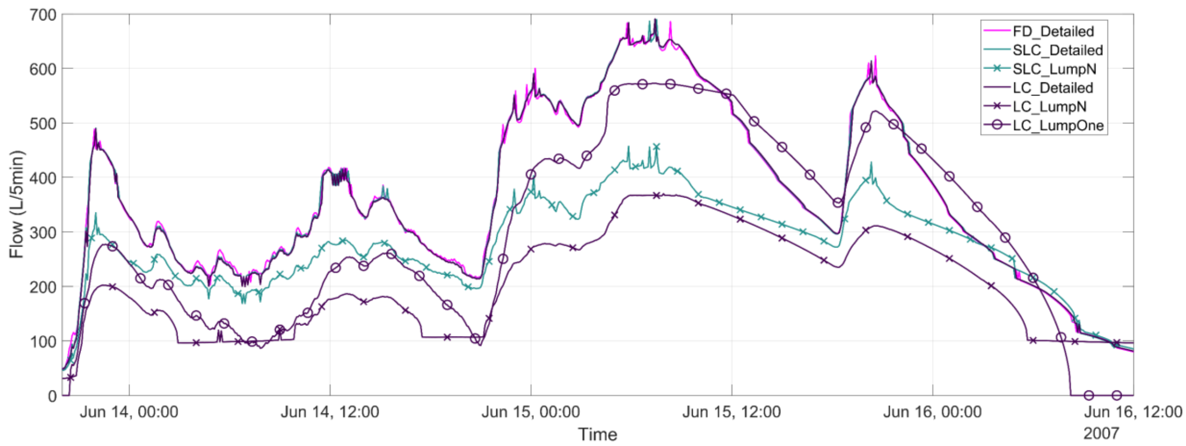

Figure 6.9. SuDS underdrain flow profiles on June 13th event in 2007 rainfall series.

6.3.2 Detailed SuDS Performance

The relationship between water level and orifice-controlled underdrain flow needs to be considered. In this study, the majority of SuDS facilities (with the exception of PP001, PP002 and PP009) employ orifice structures to regulate drainage outflow. Following aggregation, SuDS parameters were re-estimated to approximate the head-discharge relationship of the detailed configuration.

Figure 6.10 plots the relationship between hydraulic head and total underdrain flow for the sum of the 14 detailed individual SuDS units and the single aggregated *LumpOne* SuDS. Due to the maximum hydraulic head limits inherent in the design of the individual SuDS facilities, the resulting head-discharge curve exhibits mild inflection points as certain units reach their capacity limits. Before the maximum head of the *LumpOne* SuDS is reached (at 0.663 m), the aggregated *LumpOne* discharge shows a close correspondence to the total outflow response of the *Detailed* SuDSs. This close agreement suggests that, provided the aggregated parameters are estimated accurately (e.g., via the area-weighted mean method), the aggregated SuDS approach can maintain a reasonable degree of accuracy in simulating underdrain flow controlled by the orifice structure.

However, the idealised correspondence shown in Figure 6.10 is not fully reproduced in the dynamic simulations. This discrepancy arises because some SuDS units exhibit zero exfiltration capacity, while others lack a dedicated underdrain flow pipe, resulting in heterogeneous drainage pathways that cannot be fully captured through parameter aggregation alone. Figure 6.11 presents the hydraulic head profiles within the 14 individual SuDS units in the *FD_Detailed* scenario, along with the head profile within the aggregated SuDS unit of the *LC_LumpOne* scenario, during the June 13th rainfall event. It is observed that the head profile of the *LC_LumpOne* aggregated SuDS closely aligns with the profile of the permeable pavement unit. This alignment is directly attributed to the fact that the permeable pavement unit represents the largest single area among the individual SuDS facilities. Its physical characteristics exert a dominant influence on the aggregated parameters of the *LumpOne* system. In summary, the *LumpOne SuDS* (Figure 6.9 *FD_Detailed* vs *LC_LumpOne*) is unable to replicate the time-varying discharge dynamics of the detailed configuration.

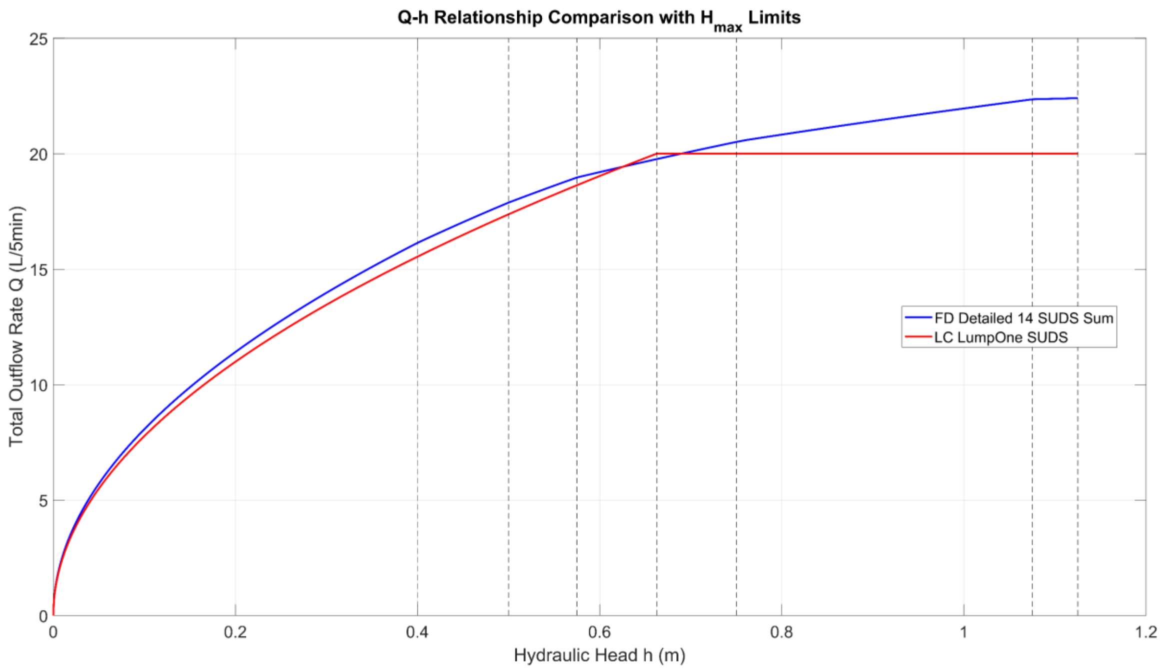

Figure 6.10. Q-h relationship comparison

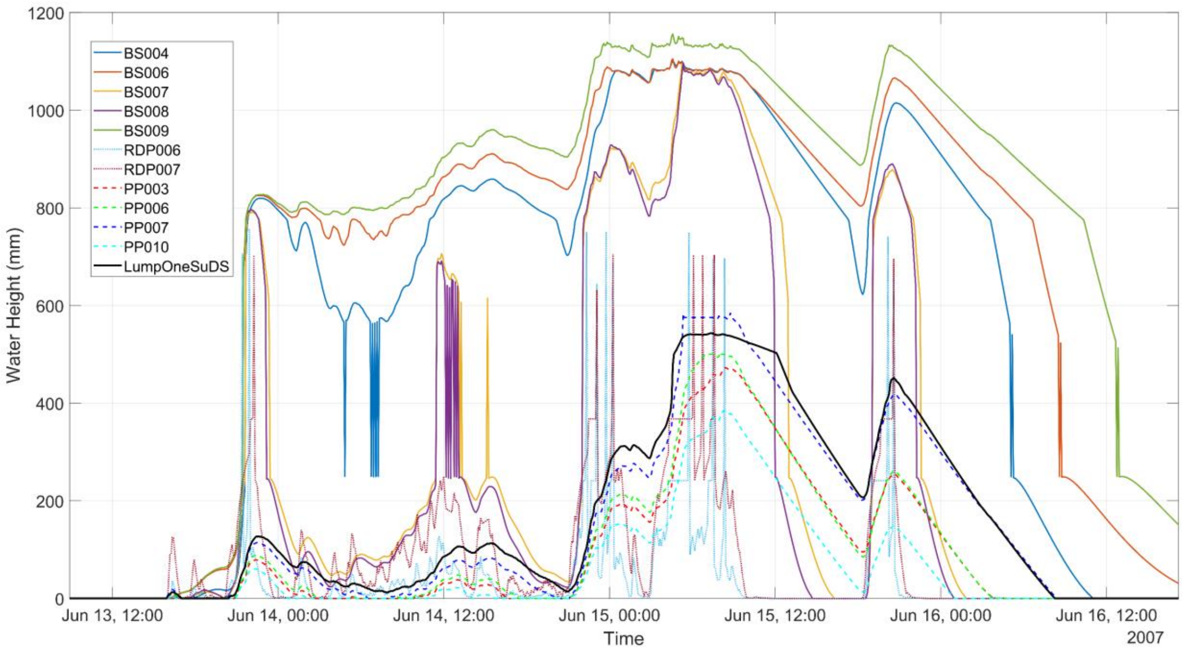

Figure 6.11. Water height within SuDS devices in FD_Detailed & LC_LumpOne on June 13th event in 2007 rainfall series.

6.4 Discussion and Conclusions

This case study evaluated the performance trade-offs associated with different subcatchment spatial discretisation and SuDS aggregation strategies within a street-scale catchment. The analysis focused on two critical aspects: overall catchment outflow response and the accuracy of simulated SuDS internal hydrological dynamics.

The evaluation confirmed that SuDS are critically effective in reducing total runoff volume regardless of the modelling strategy employed. From the perspective of overall catchment outflow, the predictive accuracy of the models remained high (NSE > 0.95 for most scenarios). Provided that the contributing area of each SuDS unit is correctly identified, and hence the inflow volume to SuDS is appropriately represented, aggregation-based modelling approaches are able to preserve a satisfactory level of accuracy in simulating overall catchment response under SuDS retrofitting conditions.

However, the analysis of internal SuDS hydrological dynamics revealed critical limitations. While the *Detailed* method provided accurate insights into internal water partitioning, the aggregated strategies failed to replicate this fidelity. The *LC_LumpOne* scenario, in particular, consistently underestimated the cumulative underdrain flow volume and exhibited inaccuracies in flow partitioning, specifically by overestimating exfiltration. The *LumpN* method significantly misrepresented overflow volumes. These failures suggest that the lumped parameter set compromises the non-linear hydraulic representation necessary for high-fidelity internal flow analysis.

In this case study, almost all SuDS devices include exfiltration, and where present the exfiltration rate is designed to be consistent across devices. Parameter variability among SuDS units is relatively small. Consequently, the simulated annual catchment outflow volume for the *LC_LumpOne* configuration differs from the *LC_Detailed* model by around 1000 m^3 ($\approx$8.3%). Although this difference appears small relative to the total outflow volume in other scenarios (Figure 6.7b), it still represents a noticeable absolute number.

The acceptability of this error is context dependent. An error of this magnitude may be acceptable for preliminary planning or comparative scenario testing, particularly as hydraulic model assessments often use tolerance bands rather than a single universal threshold. For example, the CIWEM UDG Code of Practice provides an illustrative qualitative scoring approach in which volume and peak-flow differences are assessed using green, amber and red tolerance bands (Chisholm, 2017). However, stricter design verification or regulatory applications may require lower tolerances, for example around 5–10%, and the direction of error is also important. Underestimation of runoff or overflow may be less acceptable than overestimation where it could lead to undersized infrastructure or underestimated downstream risk.

Subcatchment Spatial Discretisation

The influence of subcatchment spatial discretisation itself on the total outflow volume was minimal, although it affects the timing of the peak flow by altering the simulated time of concentration, as noted by Elliott et al. (2009). Comparison of the configurations shown in Figure 6.5 a, b, d indicates that variations in subcatchment spatial aggregation produced negligible differences in simulated SuDS performance at the scale considered in this study (approximately 17,500 m^2).

From a practical modelling perspective, these results suggest that once the contributing area to each SuDS unit is correctly defined, it is not necessary to delineate highly detailed subcatchment boundaries. Instead, the spatial discretisation of subcatchments can be simplified without significantly affecting the simulated catchment outflow volume.

Applicability and Computational Trade-offs

The study concluded that model selection must be guided by the study objective, balancing accuracy with computational efficiency:

1. For Preliminary Design and Catchment-Scale Runoff Studies: If the primary goal is to assess overall catchment runoff reduction and analyse the outlet hydrograph without requiring fine-scale detail, the aggregated strategies offer a highly efficient alternative. Through reasonable parameter estimation, these approaches maintain adequate predictive accuracy while providing substantial computational benefits.
2. For Detailed SuDS Design and Internal Dynamics: If the objective requires a detailed investigation into the specific internal water balance of the SuDS facilities (e.g., quantifying exfiltration or validating device sizing), the fully detailed (FD) model structure is indispensable. Aggregated methods should not be considered for applications requiring this level of hydrological fidelity.

The reduction in model complexity offers significant practical advantages for urban planners and modellers. The decrease in subcatchment spatial discretisation scale (FD - SLC - LC) had a decisive impact on computational overhead: In the continuous annual simulation, the file size was reduced from ~ 300 MB (FD) to ~ 17 MB (LC). Model runtime decreased dramatically, from 45 seconds (FD) to less than 1 second (LC). SuDS aggregation measures minimize the impact on runtime and significantly reduce the tedious work required for initial model setup and configuration. In conclusion, with appropriate parameter estimation, aggregated modelling strategies can ensure computational efficiency and reduce file storage needs while maintaining acceptable accuracy for preliminary design and catchment-level impact assessments.

7. Discussion

A central implication of this thesis is that SuDS modelling should be understood as a scale-dependent exercise, in which model structure must reflect the purpose of the assessment. At the device scale, accurate representation of internal processes is important because detention, percolation, underdrain flow, overflow and exfiltration directly determine whether a SuDS unit performs as designed. This is why the representation of hydraulic conductivity in Chapter 3 and device-scale simplification in Chapter 4 are critical. At the street scale, however, the modelling emphasis shifts towards aggregate outputs, such as total runoff volume, peak flow attenuation and combined downstream discharge. This does not mean that internal SuDS processes become unimportant, but their influence may be diluted or redistributed when combined with runoff from untreated areas and other catchment components. For example, in the MRA case, even SuDS treated approximately 49% of the catchment area, almost 80% of the catchment runoff came from untreated surfaces.

Detailed differences in individual SuDS water balance components may have a smaller effect on the total catchment outflow than they do at the device scale. This helps explain why Chapter 5 & 6 show that type-based aggregation can reproduce overall runoff dynamics effectively, provided that key functional distinctions between SuDS types are preserved. In contrast, full aggregation (*LumpOne*) remains problematic because it merges systems with different storage, drainage and exfiltration behaviour, thereby distorting the processes that continue to control catchment-scale performance.

The results in Chapter 5 & 6 show that subcatchment spatial aggregation can affect simulated hydrological responses independently of SuDS representation. Under the detailed subcatchments representation, local subcatchment properties and inter-subcatchment flow transfers are retained. When the catchment is represented as a single lumped unit, these heterogeneities and internal routing pathways are homogenised. As a result, local effects such as runoff transfer from impervious to adjacent pervious areas, leading to infiltration before reaching the drainage network, may be lost. This can introduce runoff bias even when the SuDS aggregation method itself is unchanged. Similar effects have been reported in previous studies of subcatchment aggregation. Stephenson (1989) and Elliott et al. (2009) found that increasing subcatchment spatial aggregation can reduce simulated runoff volume, while lower spatial resolution may also distort peak flow estimation by routing runoff directly to the outlet. Krebs et al. (2014) further showed that changes in runoff pathways in aggregated SWMM models can reduce model performance. They also noted that simplification may remain acceptable where parameter similarity is high. At the scale considered in this study, however, subcatchment aggregation does not alter the overall conclusions regarding the relative performance of the SuDS aggregation strategies.

The Monte Carlo simulations intentionally explored a broader configuration space than is typically expected in practice. The purpose was to test model aggregation performance across a wide range of SuDS combinations, including highly heterogeneous cases, in order to identify the limits of aggregation reliability and reveal the mechanisms through which simplified representations may fail. In contrast, real street-scale SuDS schemes are expected to be shaped by locational, engineering, and regulatory constraints that produce fewer variable configurations. Retrofit schemes may be standardised by shared hydrological objectives, design guidance and material specifications. Discharge control or runoff reduction targets constrain characteristics such as storage, outlet controls and loading ratios, while local guidance may constrain parameters such as substrate thickness, K_{sat}, and storage void ratio (Department for Environment, Food & Rural Affairs, 2025; Woods-Ballard et al., 2015). In the MRA case, this is evident in the uniform substrate K_{sat} (400 mm/hr) and porosity (0.35 m^3/m^3) shared across all bioswale units (Table 6.3). Native soil properties, which strongly influence exfiltration, will generally show spatial continuity at the subcatchment scale. Where variation does occur, it is often systematic rather than random. For example, lining decisions may depend on proximity to building foundations or buried infrastructure. In the MRA scheme, lined bioswales (BS006, BS009) are associated with locations close to buildings, whereas unlined units are found in more open settings. Taken together, these constraints suggest that real street-scale SuDS schemes may exhibit narrower parameter ranges compared with the Monte Carlo simulations. The MRA site, characterised by standardised materials, shared design objectives, and spatially correlated site conditions, reflects this tendency.

7.1 Metrics for Model Evaluation

Throughout this thesis, different performance metrics were used to quantify the accuracy of the modelling approaches examined in each chapter. In Chapter 3, R_t^2 (Equation 7.1, the same as Equation 3.7) was used to evaluate the device-scale SuDS substrate outflow profile, while in Chapters 4, 5 and 6, *NSE*, total runoff volume error, peak runoff error and overflow volume error were applied to compare simplified, aggregated and detailed model representations. The use of multiple metrics was intentional. No single metric can fully describe all aspects of hydrological model performance (Knoben et al., 2019). The evaluation therefore considered several dimensions of model behaviour, including the magnitude and timing of the hydrograph peak, the overall shape of the outflow profile, and the volumes discharged through evapotranspiration, infiltration, underdrain flow and overflow.

NSE (Equation 7.2, the same as Equation 4.1) is routinely employed in hydrological analyses, whereas R_t^2 (Young et al., 1980) has been more commonly applied in solute transport and residence-time modelling. Previous work within the research group has suggested that both metrics provide comparable levels of discrimination between alternative model outputs (Sonnenwald et al., 2013; Peng et al., 2020). Sonnenwald et al. (2013), for example, systematically compared several performance measures and concluded that *NSE,* R_t^2 were all suitable for model evaluation. This previous evidence supported the use of *NSE* and R_t^2 in this thesis to quantify the overall fit of temporal profiles.

$$R_t^2 = 1 - \frac{\sum_{i=1}^{T}\left(q_{obs}(i) - q_{sim}(i)\right)^2}{\sum_{i=1}^{T}\left(q_{obs}(i)\right)^2} \qquad \text{Equation 7.1}$$

$$NSE = 1 - \left[\frac{\sum_1^N (Q_{sim} - Q_{obs})^2}{\sum_1^N (Q_{obs} - Q_{Aobs})^2}\right] \qquad \text{Equation 7.2}$$

However, *NSE* also has recognised limitations. Because it is based on squared errors, it is sensitive to larger deviations, which often occur during high-flow periods. This can make *NSE* responsive to errors around hydrograph peaks. At the same time, this does not necessarily mean that *NSE* provides a reliable assessment of peak-flow accuracy. Gupta et al. (2009) showed that *NSE* combines correlation, bias and flow variability within a single aggregated score, and that optimisation based on *NSE* can favour simulations with underestimated variability. In hydrological terms, this means that a model may achieve a relatively good *NSE* while still producing a smoother hydrograph and underestimating peak flows. This limitation is particularly relevant for SuDS aggregation, where simplified representations may preserve the general hydrograph shape while altering peak attenuation, storage response or outflow variability.

Kling–Gupta Efficiency (*KGE* Equation 7.3) has therefore been proposed as a useful alternative or complementary metric to *NSE*. *KGE* evaluates model performance using three explicit components: the linear correlation between simulated and reference values, the variability ratio, and the bias ratio. These components respectively indicate whether the model reproduces the timing and shape of the hydrograph, the magnitude of flow variability, and the overall water balance. *KGE* is calculated as:

$$KGE = 1 - \sqrt{(r-1)^2 + \left(\frac{\sigma_{sim}}{\sigma_{obs}} - 1\right)^2 + \left(\frac{\mu_{sim}}{\mu_{obs}} - 1\right)^2} \qquad \text{Equation 7.3}$$

where r is the linear correlation between the observations and simulations; σ_{obs} is the standard deviation in observations, σ_{sim} the standard deviation in simulations, μ_{sim} the simulation means, and μ_{obs} the observation means (i.e. equivalent to Q_{Aobs} the mean observed runoff).

To examine whether the choice of metric influenced the interpretation of aggregation performance, Figure 7.1 compares *NSE,* R_t^2 and *KGE* values for the 13–16 June storm event, using the *Detailed* model as the baseline. The *NSE* values reproduce those presented in Figure 7.1 of the main thesis. This comparison was not used to redefine the main results, but to test whether the relative ranking of aggregation strategies was sensitive to the choice of evaluation metric.

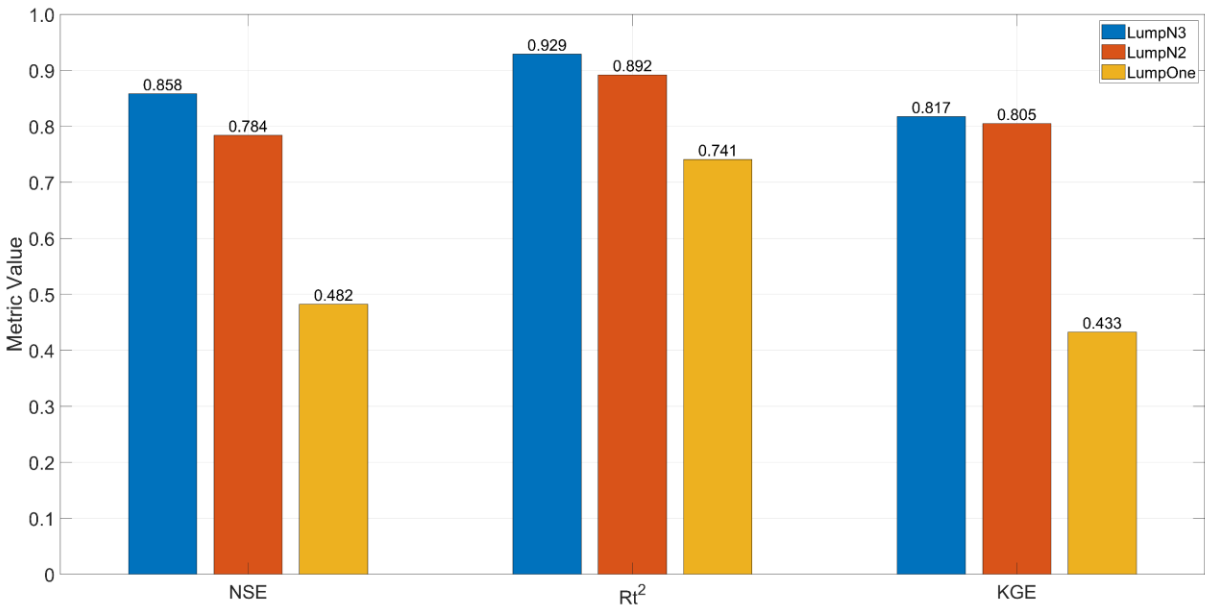

Figure 7.1 Comparison of aggregation model performance in 13-16 June event under different metrics. (No. 126 synthetic catchment in Monte Carlo simulation)

Figure 7.1 shows that *NSE*, which was used mostly throughout the thesis, provides greater discrimination between the three aggregation strategies than R_t^2. The comparison between *NSE* and *KGE* suggests that *KGE* gives slightly stronger separation between the best and worst performing strategies, but is less discriminating between the two *LumpN* configurations. Nevertheless, all three metrics produce the same overall ranking of aggregation approaches. In particular, *LumpOne* remains the least accurate strategy, supporting the recommendation that highly simplified single-unit aggregation should be avoided where hydrograph shape, peak response or overflow prediction are important.

Overall, this comparison does not provide strong evidence that *KGE* would have been a more appropriate primary metric than NSE for the purposes of this thesis. *NSE* remains useful as a widely recognised measure of overall hydrograph fit, especially when it is not used in isolation. However, the comparison reinforces the need to interpret *NSE* together with event-based hydrological indicators. For this reason, the thesis did not rely solely on temporal profile metrics. It also considered total outflow volume, overflow volume and peak flow rate, which are directly linked to the functional performance of SuDS systems.

It should also be noted that no fixed acceptability thresholds were applied to *NSE*, R_t^2, *KGE* or any other metric in this thesis. The metrics were used comparatively, to rank alternative modelling approaches against the *Detailed* model, rather than to classify simulations as simply acceptable or unacceptable. This avoids the problematic use of universal thresholds across different events, SuDS types and aggregation structures. Importantly, the rank order of the aggregation strategies was not affected by the choice of temporal profile metric, which increases confidence in the robustness of the main conclusions.

7.2 Practical Implications

The integrated findings of this thesis provide structured guidance for the practical representation of SuDS in real-world drainage modelling. To illustrate how these findings may inform engineering practice, consider a hypothetical scenario in which SuDS retrofitting is being evaluated to mitigate combined sewer overflows (CSOs) within a defined area (e.g. Mansfield). Based on the analyses presented in this thesis, a staged modelling approach can be adopted, with increasing levels of structural detail as project requirements evolve.

At the preliminary screening stage, highly simplified representations may be sufficient to provide a rapid estimate of potential SuDS benefits. Approaches such as the *Disconnect* and *TransferP* methods (Chapter 4) can be applied. These involve either removing the SuDS treated area from direct runoff contribution or converting the treated area to an equivalent pervious surface. Alternatively, the *LumpOne* aggregation strategy (Chapter 5), in which all SuDS within the study area are represented as a single composite unit, may be used. However, as demonstrated in Chapters 4 and 5, these approaches tend to overestimate SuDS performance because they simplify or omit internal storage dynamics, hydraulic controls and differences between SuDS types. They should therefore be used mainly for early-stage feasibility assessment, rather than detailed design or regulatory evaluation.

Where more robust evidence is required, type-based aggregation provides a more defensible modelling strategy. The *LumpN* approach developed and tested in this thesis allows multiple SuDS units to be grouped within each subcatchment according to their typology and functional behaviour. For example, in a large retrofit scheme containing thousands of SuDS units distributed across many street blocks, devices can be grouped into categories such as bioretention systems, permeable pavements and detention basins. Where relevant, these categories can be further subdivided according to key functional differences, such as the presence or absence of exfiltration. This preserves the main hydrological distinctions controlling runoff partitioning while avoiding the computational burden of modelling every individual SuDS unit.

For post-construction or as-built assessment, further refinement may be required. At this stage, SuDS units may need to be classified not only by nominal type, but also by hydraulic controls such as outlet configuration, storage geometry, percolation behaviour and exfiltration rate. However, the findings suggest that individual modelling of every unit is not always necessary. Units with comparable hydrological behaviour can still be grouped, provided that the aggregation preserves the processes most relevant to the modelling objective.

Overall, the practical implication of this thesis is that SuDS modelling should be guided by functional similarity rather than by model simplicity alone. Highly simplified methods may be useful for early screening, while *LumpN* offers a more reliable balance between computational efficiency and hydrological realism for street- and catchment-scale retrofit planning. Fully detailed representations remain most appropriate where device-level water balance, internal flow pathways or as-built performance are the primary concern.

7.3 Limitations

7.3.1 Lack of Validation at Different Scales

The first limitation of this research concerns the availability of validation data at different scales. At the device-scale, the modelling framework was informed and evaluated using empirical datasets, including monitored performance data from green roof media column tests. These datasets enabled direct comparison between simulated and observed hydrological responses, supporting the assessment of percolation representation.

At larger spatial scales, validation was more limited. Monitoring data do exist for the MRA site, and these datasets include observations collected during the implementation of the retrofit programme. However, processing and integrating these data for model validation was beyond the timeframe of the present research. As a result, the aggregation strategies developed in this study were evaluated primarily through systematic comparison with fully detailed model representations.

7.3.2 Insufficient SuDS Types

The second limitation relates to the range of SuDS types examined in this research. The thesis focuses primarily on green roofs and bioretention systems, reflecting both their widespread implementation and their distinct hydrological process structures. These two SuDS types formed the basis for the evaluation of simplified modelling approaches and aggregation strategies.

While this focus enabled a detailed and coherent investigation of model structure, simplification, and aggregation, it necessarily limits the generalisability of the findings to other SuDS types. In practice, large retrofit schemes, such as the Mansfield project examined in this thesis, may incorporate a wider range of SuDS components than those explicitly represented, further complicating direct validation at the subcatchment scale. Components such as infiltration trenches, swales, or tree pits exhibit different storage mechanisms, flow controls, and interactions with surrounding soils, which may influence the suitability of particular aggregation strategies. The inclusion of additional SuDS typologies could reveal alternative grouping criteria or aggregation approaches that further improve predictive performance under specific configurations.

8. Conclusions

The overall aim of this thesis was to develop, test and synthesise modelling frameworks for predicting the hydrological performance of SuDS across multiple spatial scales, from individual devices to street-scale implementation. Rather than proposing a new universal modelling tool, the thesis critically examined how different levels of process representation, simplification and aggregation influence predictive accuracy, robustness and practical applicability. The findings show that effective SuDS modelling depends on selecting a level of model detail appropriate to the spatial scale, modelling objective and hydrological processes of interest.

8.1 Representation of Unsaturated Percolation in Engineering Media

In response to Objective 1, Chapter 3 evaluated and improved the representation of unsaturated percolation in engineering SuDS media. The results show that the hydraulic conductivity function used within the SWMM LID framework strongly controls simulated detention behaviour. In particular, the representation of moisture-dependent drainage between field capacity and saturation affects the timing, shape and stability of the simulated underdrain response.

The proposed "*NewHCF*" formulation provided a more physically consistent representation of unsaturated percolation by explicitly constraining hydraulic conductivity between field capacity and saturation. This enabled gradual drainage and stable runoff responses to be reproduced across multiple storm events, while retaining a simple parameter structure compatible with SWMM LID. In contrast, the *Kslope* and *Campbell* formulations showed systematic limitations, including underestimated peak flows, delayed drainage and unrealistic "on–off" outflow behaviour. These limitations arise because these formulations are not constrained to operate only when $\theta > \theta_{FC}$, allowing inconsistency with the SWMM assumption that percolation ceases at field capacity.

This chapter therefore contributes a clearer conceptual understanding of how unsaturated percolation controls detention behaviour in engineered SuDS media. It also demonstrates that calibration alone cannot fully compensate for inappropriate process representation.

8.2 Accuracy of Device-scale SuDS Modelling Simplification

In response to Objective 2, Chapter 4 quantified the hydrological consequences of simplified device-scale SuDS modelling approaches. The results show that simplified models differ substantially in their ability to reproduce detailed SWMM LID simulations. Highly simplified approaches, such as subcatchment disconnection or transfer to pervious areas, tended to overestimate SuDS performance because they omitted key storage, drainage and overflow processes.

More structured simplified approaches performed better under certain conditions, particularly where system behaviour was dominated by downstream outlet control. However, the results also show that simplified models are not reliable substitutes for detailed representations when internal drainage dynamics, overflow behaviour or device-level water balance are important. This establishes an important boundary for simplification: simplified approaches may be useful for preliminary assessment, but they should be applied cautiously when detailed design or performance verification is required.

The device-scale analysis therefore demonstrates that uncertainties introduced by model simplification cannot be assumed negligible before models are scaled up or aggregated. Accurate representation of key internal processes remains essential when the modelling objective concerns the performance of individual SuDS units.

8.3 Street-scale Aggregation under Parameter Heterogeneity

In response to Objective 3, Chapter 5 evaluated SuDS aggregation strategies at the street scale using Monte Carlo simulations of synthetic catchments. This allowed the performance of different aggregation methods to be tested across a wide range of heterogeneous SuDS configurations, including variation in device type, size and physical parameters.

The results show that aggregation performance depends strongly on whether important hydrological distinctions between SuDS types are preserved. The type-based *LumpN* strategy consistently reproduced overall catchment runoff dynamics with high accuracy, with NSE values typically exceeding 0.9 across many configurations. In contrast, full aggregation into a single composite unit, represented by *LumpOne*, produced substantial errors in heterogeneous systems. In mixed green roof and bioretention configurations, *LumpOne* caused severe underestimation of total runoff in some cases and misrepresented overflow and exfiltration volumes.

These findings demonstrate that aggregation should not be based only on reducing model complexity. Instead, SuDS units should be grouped according to comparable structural configuration and hydrological function. This provides a practical rule for aggregation: simplification is most defensible when it preserves the processes controlling the outputs of interest.

8.4 Real-World Application of Street-scale Aggregation

In response to Objective 4, Chapter 6 applied the aggregation framework to a real-world street-scale case study. The case study confirmed that aggregated SuDS representations can reproduce overall catchment outflow responses with high accuracy, with NSE values exceeding 0.95 in most scenarios. This supports the use of type-based aggregation for strategic planning, scenario testing and preliminary design at the street scale.

At the same time, the case study also confirmed the limitations of aggregation. While aggregated models performed well for total catchment outflow, they did not reproduce internal SuDS water balance components, including underdrain flow, overflow and exfiltration, with the same level of reliability. Fully detailed representations therefore remain necessary where the objective is to evaluate device-level behaviour or as-built SuDS performance.

The case study also demonstrated the practical value of aggregation. Simplified and aggregated models substantially reduced model file size and simulation runtime, while maintaining acceptable accuracy for overall catchment outflow. This confirms that aggregation can provide an efficient modelling strategy when the purpose is large-scale assessment rather than detailed device-level diagnosis.

8.5 Synthesis

Taken together, the thesis demonstrates that SuDS modelling should be understood as a scale-dependent and purpose-dependent exercise. Detailed representations are essential when the aim is to evaluate internal device processes, such as percolation, underdrain flow, overflow or exfiltration. However, at the street or catchment scale, aggregated representations can be appropriate when the main objective is to estimate total runoff, peak attenuation or combined downstream discharge.

The main contribution of this thesis is therefore not a single universal modelling framework, but a structured basis for deciding when and how SuDS models can be simplified or aggregated. The findings show that model simplification is acceptable only when the hydrological functions relevant to the modelling objective are preserved. Type-based aggregation, as represented by the *LumpN* approach, offers a practical balance between computational efficiency and hydrological reliability. Full aggregation of all SuDS units into a single composite representation should be avoided in heterogeneous systems, as it can distort key water balance components and lead to misleading predictions.

Overall, this thesis provides both conceptual and practical guidance for multi-scale SuDS modelling. It clarifies how unsaturated percolation should be represented at the device scale, quantifies the limits of device-scale simplification, evaluates aggregation strategies under heterogeneous street-scale conditions, and demonstrates their practical application in a real-world case study. In doing so, it supports more transparent and evidence-based selection of SuDS modelling strategies for engineering design, planning and performance assessment.

8.6 Future Work

While this thesis advances the methodological basis for SuDS modelling, several avenues for future research remain.

8.6.1 Extending Aggregation Frameworks through Multi-type SuDS Integration and Monitoring Data

Future work should prioritise the extension of the proposed aggregation frameworks through the integration of multi-type SuDS systems supported by field-based monitoring data. While the present thesis systematically compared aggregation strategies using controlled numerical experiments and Monte Carlo simulations, empirical validation at the subcatchment or street scale remains limited.

A particularly suitable testbed for this extension is the MRA area, where a large number of SuDS interventions have been implemented and monitoring datasets are available for several components of the drainage system. Future work could involve the processing and integration of these existing datasets, including flow and water-level observations from selected SuDS installations and network nodes, to enable direct comparison between observed hydrological responses and those predicted by different aggregation strategies, such as *LumpN* and *LumpOne* approaches.

In addition, the modelling framework could be extended to incorporate further SuDS interventions across Mansfield beyond the MRA area, enabling evaluation of aggregation performance under varying spatial configurations, device densities, and connectivity patterns. Such validation would allow assessment of how well aggregation strategies reproduce observed runoff volumes, peak flows, and discharge timing within a complex retrofit scheme.

8.6.2 Typological Classification of SuDS within Aggregation Strategy

A second priority for future research concerns the development of a structured framework for typological classification within the *LumpN* aggregation strategy. While this thesis demonstrates that aggregation based on SuDS type and key hydraulic controls, such as exfiltration, can significantly improve predictive performance, further refinement of classification criteria remains necessary to enhance model transferability and robustness.

Beyond distinguishing between nominal SuDS types and the presence or absence of exfiltration and/or orifices, future work should explore classification schemes grounded in the conceptual layer structure of SuDS systems. At the surface layer, differentiation could consider the presence and density of vegetation, surface roughness characteristics, and their influence on runoff routing and flow attenuation. At the substrate layer, classification could account for variations in engineered media properties, including porosity, hydraulic conductivity, and percolation response, which directly influence detention behaviour. At the drainage layer, distinctions could be made based on outlet configuration, such as the presence of underdrains, orifice controls, and their corresponding discharge coefficients or control thresholds.

By integrating these layer-specific attributes into a hierarchical classification framework, it would be possible to establish clearer rules for defining the value of ***N*** within the *LumpN* strategy. Such a framework would allow practitioners to group SuDS units according to dominant hydraulic behaviour rather than nominal type alone, thereby improving aggregation fidelity without requiring full device-level modelling. Importantly, this approach would provide a transparent basis for balancing model complexity against predictive accuracy, enabling practitioners to make informed decisions regarding the appropriate level of typological differentiation in different project contexts.

8.6.3 Extending Scale-aware SuDS Modelling Strategies to Larger Catchments

The third important direction for future work is the extension of scale-aware SuDS aggregation strategies to larger catchments. In this thesis, aggregation methods such as *LumpN* were evaluated within a defined subcatchment or street-scale context, where SuDS numbers and spatial extents were intentionally constrained. However, in practical planning and strategic drainage assessments, SuDS are increasingly implemented across much larger urban catchments, raising questions about the transferability of aggregation strategies across scales.

Future research should therefore investigate how aggregation performance varies systematically with catchment size, SuDS density, depth in the engineered media properties and spatial configuration. This could be achieved by designing a series of modelling experiments in which the same aggregation strategies are applied to progressively larger catchments, while controlling for rainfall inputs and network structure. Key research questions would include identifying threshold catchment areas beyond which individual SuDS representation becomes impractical, and determining how many SuDS units or how large the area of SuDS can be aggregated before loss of hydrological fidelity becomes unacceptable.

In addition, future work should explore whether different aggregation strategies are more appropriate at different spatial scales. For example, smaller subcatchments with limited SuDS numbers may benefit from *LumpN*-type representations that preserve internal heterogeneity, whereas larger catchments could require hierarchical aggregation approaches, in which the catchment is first divided into intermediate zones or sub-areas, each with its own aggregated SuDS representation. These zone-level aggregates could then be linked within the wider drainage network to enable rapid simulation of catchment-scale runoff mitigation.

8.6.4 Applicability of Simplification Strategies in Two-dimensional Modelling Contexts

The fourth area for future work concerns the applicability of SuDS aggregation and simplification strategies within two-dimensional (2D) hydrodynamic modelling contexts. The present thesis focuses exclusively on one-dimensional (1D) modelling frameworks, where SuDS impacts are evaluated primarily through runoff hydrographs, peak flow attenuation, and cumulative discharge metrics. In practice, however, many engineering and planning applications require spatially explicit flood information, such as inundation extent, depth, and velocity, which are typically obtained using coupled 1D–2D or fully 2D models.

Future research should therefore explore how the outputs of aggregated 1D SuDS models can be effectively integrated into 2D flood modelling workflows. A key step in this process is clarifying the interface between 1D and 2D models, including how aggregated SuDS representations modify boundary conditions, source terms, or inflow hydrographs supplied to the 2D domain. For example, aggregated SuDS models could be used to generate modified inflow hydrographs at critical nodes, which are then passed to the 2D surface model to simulate flood propagation and inundation patterns.

Further work should also assess whether aggregation-induced simplifications introduce biases when translated into spatial flood metrics. This could be examined by comparing 2D flood maps generated using fully detailed SuDS representations with those produced using aggregated SuDS inputs under identical rainfall scenarios. Differences in flood extent, depth distribution, and timing could then be quantified to evaluate the suitability of aggregation strategies for flood risk assessment purposes.

8.7 Key Findings

Chapter 3: The representation of unsaturated percolation has a strong influence on simulated SuDS detention behaviour. The *NewHCF* formulation improves the representation of moisture-dependent drainage in engineered media by constraining hydraulic conductivity between field capacity and saturation, leading to more stable and physically consistent outflow responses within the SWMM LID framework.

Chapter 4: Simplified device-scale SuDS modelling approaches can introduce substantial errors when key internal processes, such as storage, percolation, overflow and outlet control, are omitted. While some simplified approaches may be useful for preliminary assessment, detailed representations remain necessary when internal drainage dynamics and device-level water balance are important.

Chapter 5: Street-scale SuDS aggregation is feasible when key hydrological distinctions between SuDS types are preserved. The *LumpN* approach provides a reliable balance between computational efficiency and predictive accuracy, whereas *LumpOne* can generate substantial errors in heterogeneous systems by merging SuDS units with different storage, drainage and exfiltration behaviours.

Chapter 6: The real-world case study confirms that aggregated SuDS models can reproduce overall catchment outflow responses with high accuracy and substantially reduce model size and runtime. However, aggregated models are less reliable for representing internal SuDS water balance components, reinforcing the need for detailed models where device-level performance assessment is required.

Overall finding: SuDS modelling should be scale- and purpose-dependent. The appropriate level of model detail depends on whether the modelling objective is device-level design, preliminary screening, street-scale planning, runoff volume assessment or catchment-scale hydraulic evaluation.

References

Autodesk, 2025a. Autodesk InfoWorks ICM 2026. URL https://www.autodesk.co.uk/products/infoworks-icm/overview (accessed 7.5.25).

Autodesk, 2025b. Help | Welcome to InfoDrainage | Autodesk. URL https://help.autodesk.com/view/INFDS/ENU/?guid=GUID-FC6BDDC8-8AD0-4165-8DD0-02AE22974F99 (accessed 1.13.26).

Ball, J.E., Rankin, K., 2010. The hydrological performance of a permeable pavement. *Urban Water Journal* 7, 79–90. https://doi.org/10.1080/15730620902969773

Barnhart, B., Pettus, P., Halama, J., McKane, R., Mayer, P., Djang, K., Brookes, A., Moskal, L.M., 2021. Modeling the hydrologic effects of watershed-scale green roof implementation in the Pacific Northwest, United States. *Journal of Environmental Management* 277, 111418. https://doi.org/10.1016/j.jenvman.2020.111418

Batalini De Macedo, M., Gomes Júnior, M.N., Jochelavicius, V., De Oliveira, T.R.P., Mendiondo, E.M., 2022. Modular Design of Bioretention Systems for Sustainable Stormwater Management under Drivers of Urbanization and Climate Change. *Sustainability* 14, 6799. https://doi.org/10.3390/su14116799

Benedict, M.A., McMahon, E.T., 2012. Green infrastructure: linking landscapes and communities. Island press.

Berretta, C., Aiello, A., Jensen, H.S., Tillotson, M.R., Boxall, A., Stovin, V., 2018. Influence of design and media amendments on the performance of stormwater biofilters. Proceedings of the Institution of Civil Engineers - *Water Management* 171, 87–98. https://doi.org/10.1680/jwama.16.00121

Boucher, A., Howe, H., 2025. Nature-Based Solution in Practice: Modelling the Impact of SuDS in Mansfield. Presented at the CIWEM UDG Conference.

Campbell, G.S., 1974. A Simple Method for Determining Unsaturated Conductivity from Moisture Retention Data. *Soil Science* 117, 311–314. https://doi.org/10.1097/00010694-197406000-00001

Chapman, C., Horner, R.R., 2010. Performance Assessment of a Street-Drainage Bioretention System. *Water Environment Research* 82, 109–119. https://doi.org/10.2175/106143009X426112

Collins, K.A., Hunt, W.F., Hathaway, J.M., 2008. Hydrologic Comparison of Four Types of Permeable Pavement and Standard Asphalt in Eastern North Carolina. *Journal of Hydrologic Engineering* 13, 1146–1157. https://doi.org/10.1061/(ASCE)1084-0699(2008)13:12(1146)

Davis, A.P., 2008. Field Performance of Bioretention: Hydrology Impacts. *Journal of Hydrologic Engineering* 13, 90–95. https://doi.org/10.1061/(ASCE)1084-0699(2008)13:2(90)

Davis, A.P., Hunt, W.F., Traver, R.G., 2022. Green Stormwater Infrastructure Fundamentals and Design. John Wiley & Sons.

de Sá Silva, A.C.R., Bimbato, A.M., Balestieri, J.A.P., Vilanova, M.R.N., 2022. Exploring environmental, economic and social aspects of rainwater harvesting systems: A review. *Sustainable Cities and Society* 76, 103475. https://doi.org/10.1016/j.scs.2021.103475

Dell, T., Razzaghmanesh, M., Sharvelle, S., Arabi, M., 2021. Development and Application of a SWMM-Based Simulation Model for Municipal Scale Hydrologic Assessments. *Water* 13, 1644. https://doi.org/10.3390/w13121644

Department for Environment, Food & Rural Affairs, 2025. National standards for sustainable drainage systems (SuDS). GOV.UK. URL https://www.gov.uk/government/publications/national-standards-for-sustainable-drainage-systems/national-standards-for-sustainable-drainage-systems-suds (accessed 7.22.25).

Department for Environment Food & Rural Affairs, 2023. The review for implementation of Schedule 3 to The Flood and Water Management Act 2010.

Devia, G.K., Ganasri, B.P., Dwarakish, G.S., 2015. A Review on Hydrological Models. *Aquatic Procedia, INTERNATIONAL CONFERENCE ON WATER RESOURCES, COASTAL AND OCEAN ENGINEERING (ICWRCOE'15)* 4, 1001–1007. https://doi.org/10.1016/j.aqpro.2015.02.126

De-Ville, S., Green, D., Edmondson, J., Stirling, R., Dawson, R., Stovin, V., 2021. Evaluating the Potential Hydrological Performance of a Bioretention Media with 100% Recycled Waste Components. *Water* 13, 2014. https://doi.org/10.3390/w13152014

De-Ville, S., Ren, S., Stovin, V., 2025a. Bioretention column detention test data for percolation model evaluation. *Urban Water Journal* 22, 693–705. https://doi.org/https://doi.org/10.1080/1573062X.2025.2495874

De-Ville, S., Ren, S., Stovin, V., 2025b. A New Hydraulic Conductivity Function for LID Percolation Modelling in SWMM. Presented at the Urban Drainage Modelling Conference.

De-Ville, S., Stovin, V., 2022. Using LID Physical Properties to Predict Unsaturated Flows with SWMM, in: 12th Urban Drainage Modelling Conference. Presented at the 12th Urban Drainage Modelling Conference, Costa Mesa, CA, USA.

De-Ville, S., Wilson, F., Stovin, V., 2024. Briefing: How long-term monitoring of SuDS will inform next-generation guidance and modelling tools. Proceedings of the Institution of Civil Engineers - Civil Engineering 177, 144–146. https://doi.org/10.1680/jcien.24.00101

DHI, 2024. MIKE Powered by DHI | Water Modelling Software. DHI. URL https://www.dhigroup.com/technologies/mikepoweredbydhi (accessed 7.2.25).

Dietz, M.E., 2007. Low Impact Development Practices: A Review of Current Research and Recommendations for Future Directions. *Water Air Soil Pollution* 186, 351–363. https://doi.org/10.1007/s11270-007-9484-z

Dietz, M.E., Clausen, J.C., 2005. A Field Evaluation of Rain Garden Flow and Pollutant Treatment. *Water Air Soil Pollution* 167, 123–138. https://doi.org/10.1007/s11270-005-8266-8

Digman, C., Ashley, R., Balmforth, David, Stovin, V., Balmforth, Dominic, Glerum, J., 2012. Retrofitting to manage surface water. CIRIA: London, UK.

Duarte Lopes, M., Barbosa Lima da Silva, G., 2021. An efficient simulation-optimization approach based on genetic algorithms and hydrologic modeling to assist in identifying optimal low impact development designs. *Landscape and Urban Planning* 216, 104251. https://doi.org/10.1016/j.landurbplan.2021.104251

Durner, W., 1994. Hydraulic conductivity estimation for soils with heterogeneous pore structure. *Water Resources Research* 30, 211–223. https://doi.org/10.1029/93WR02676

Elliott, A.H., Trowsdale, S.A., Wadhwa, S., 2009. Effect of Aggregation of On-Site Storm-Water Control Devices in an Urban Catchment Model. *Journal of Hydrologic Engineering* 14, 975–983. https://doi.org/10.1061/(ASCE)HE.1943-5584.0000064

Elshorbagy, A., Corzo, G., Srinivasulu, S., Solomatine, D.P., 2010. Experimental investigation of the predictive capabilities of data driven modeling techniques in hydrology - Part 1: Concepts and methodology. *Hydrology and Earth System Sciences* 14, 1931–1941. https://doi.org/10.5194/hess-14-1931-2010

Environmental Services City of Portland, 2019. Downspout Disconnection Program (No. ENB-4.21).

Ercolani, G., Chiaradia, E.A., Gandolfi, C., Castelli, F., Masseroni, D., 2018. Evaluating performances of green roofs for stormwater runoff mitigation in a high flood risk urban catchment. *Journal of Hydrology* 566, 830–845. https://doi.org/10.1016/j.jhydrol.2018.09.050

eWater Ltd, 2005. eWater MUSIC. eWater MUSIC - eWater. URL https://ewater.org.au/ewater-solutions/tools/music/ (accessed 10.28.24).

Fassman, E.A., Blackbourn, S., 2010. Urban Runoff Mitigation by a Permeable Pavement System over Impermeable Soils. *Journal of Hydrologic Engineering* 15, 475–485. https://doi.org/10.1061/(ASCE)HE.1943-5584.0000238

FLL, 2018. Guidelines for the planning, construction and maintenance of green roofing: Green roofing guideline. Forschungsgesellschaft Landschaftsentwickung Landschaftsbau.

Fortier, C., Mailhot, A., 2015. Climate Change Impact on Combined Sewer Overflows. *Journal of Water Resources Planning and Management* 141, 04014073. https://doi.org/10.1061/(ASCE)WR.1943-5452.0000468

Freeflush Ltd, 2026. Prestige 225 Litre Attenuation SuDS Planter. Freeflush Water Management Ltd. URL https://www.freeflush.co.uk/products/prestige-235-litre-attenuation-suds-planter (accessed 1.27.26).

Ghodsi, S.H., Zhu, Z., Gheith, H., Rabideau, A.J., Torres, M.N., Meindl, K., 2021. Modeling the Effectiveness of Rain Barrels, Cisterns, and Downspout Disconnections for Reducing Combined Sewer Overflows in a City-Scale Watershed. *Water Resources Management* 35, 2895–2908. https://doi.org/10.1007/s11269-021-02875-7

Gomes, M., Pires, A., Ferreira Carneiro, P.R., 2012. Sustainable Drainage Systems: An Integrated Approach, Combining Hydraulic Engineering Design, Urban Land Control and River Revitalisation Aspects, in: Javaid, M.S. (Ed.), Drainage Systems. InTech. https://doi.org/10.5772/33896

Google Map, 2025. Mining Remediation Authority, 200 Lichfield Ln, Mansfield NG18 4RG, United Kingdom.

GreenBlue Urban Ltd, 2026. SuDSPod - GreenBlue Urban. URL https://greenblue.com/gb/sudspod/ (accessed 1.27.26).

Gupta, H. V., Kling, H., Yilmaz, K. K., & Martinez, G. F. (2009). Decomposition of the mean squared error and NSE performance criteria: Implications for improving hydrological modelling. Journal of hydrology, 377(1-2), 80-91.

Haghighatafshar, S., la Cour Jansen, J., Aspegren, H., Jönsson, K., 2018. Conceptualization and Schematization of Mesoscale Sustainable Drainage Systems: A Full-Scale Study. *Water* 10, 1041. https://doi.org/10.3390/w10081041

Haghighatafshar, S., Yamanee-Nolin, M., Klinting, A., Roldin, M., Gustafsson, L.-G., Aspegren, H., Jönsson, K., 2019a. Hydroeconomic optimization of mesoscale blue-green stormwater systems at the city level. *Journal of Hydrology* 578, 124125. https://doi.org/10.1016/j.jhydrol.2019.124125

Haghighatafshar, S., Yamanee-Nolin, M., Larson, M., 2019b. A physically based model for mesoscale SuDS – an alternative to large-scale urban drainage simulations. *Journal of Environmental Management* 240, 527–536. https://doi.org/10.1016/j.jenvman.2019.03.037

Hamann, F., Blecken, G.-T., Ashley, R.M., Viklander, M., 2020. Valuing the multiple benefits of blue-green infrastructure for a Swedish case study: contrasting the economic assessment tools B£ ST and TEEB. *Journal of Sustainable Water in the Built Environment* 6, 05020003.

Hekl, J.A., Dymond, R.L., 2016. Runoff Impacts and LID Techniques for Mansionization-Based Stormwater Effects in Fairfax County, Virginia. *Journal of Sustainable Water in the Built Environment* 2, 05016001. https://doi.org/10.1061/JSWBAY.0000815

Hibbs, B.J., Sharp, J.M., JR, 2012. Hydrogeological Impacts of Urbanization. *Environmental & Engineering Geoscience* 18, 3–24. https://doi.org/10.2113/gseegeosci.18.1.3

Hörnschemeyer, B., Henrichs, M., Uhl, M., 2021. SWMM-UrbanEVA: A Model for the Evapotranspiration of Urban Vegetation. *Water* 13, 243. https://doi.org/10.3390/w13020243

Hrachowitz, M., Clark, M.P., 2017. HESS Opinions: The complementary merits of competing modelling philosophies in hydrology. *Hydrology and Earth System Sciences* 21, 3953–3973. https://doi.org/10.5194/hess-21-3953-2017

Huang S, Kumar R, Flörke M, et al. Evaluation of an ensemble of regional hydrological models in 12 large-scale river basins worldwide[J]. Climatic Change, 2017, 141(3): 381-397.

Israelsen, O., West, F., 1922. Bulletin No. 183 - Water-Holding Capacity of Irrigated Soils. UAES Bulletins.

Jajarmizad, M., Harun, S., Salarpour, M., 2012. A Review on Theoretical Consideration and Types of Models in Hydrology. *Journal of Environmental Science and Technology* 5, 249–261. https://doi.org/10.3923/jest.2012.249.261

Johnson, D., & Geisendorf, S. (2019). Are neighborhood-level SUDS worth it? An assessment of the economic value of sustainable urban drainage system scenarios using cost-benefit analyses. Ecological Economics, 158, 194-205.

Joshi, P., Leitão, J.P., Maurer, M., Bach, P.M., 2021. Not all SuDS are created equal: Impact of different approaches on combined sewer overflows. Water Research 191, 116780. https://doi.org/10.1016/j.watres.2020.116780

Knoben, W. J., Freer, J. E., & Woods, R. A. (2019). Inherent benchmark or not? Comparing Nash–Sutcliffe and Kling–Gupta efficiency scores. Hydrology and Earth System Sciences, 23(10), 4323-4331.

Krebs, G., Kokkonen, T., Valtanen, M., Setälä, H., Koivusalo, H., 2014. Spatial resolution considerations for urban hydrological modelling. Journal of Hydrology 512, 482–497. https://doi.org/10.1016/j.jhydrol.2014.03.013

Kuruppu, U., Rahman, A., Rahman, M.A., 2019. Permeable pavement as a stormwater best management practice: a review and discussion. *Environmental Earth Sciences* 78, 327. https://doi.org/10.1007/s12665-019-8312-2

Lashford, C., Charlesworth, S., Warwick, F., Blackett, M., 2020. Modelling the Role of SuDS Management Trains in Minimising Flood Risk, Using MicroDrainage. *Water* 12, 2559. https://doi.org/10.3390/w12092559

Le Floch, N., Pons, V., Hassan Abdalla, E.M., Alfredsen, K., 2022. Catchment scale effects of low impact development implementation scenarios at different urbanization densities. *Journal of Hydrology* 612, 128178. https://doi.org/10.1016/j.jhydrol.2022.128178

Lee, J.G., Selvakumar, A., Alvi, K., Riverson, J., Zhen, J.X., Shoemaker, L., Lai, F., 2012. A watershed-scale design optimization model for stormwater best management practices. *Environmental Modelling & Software* 37, 6–18. https://doi.org/10.1016/j.envsoft.2012.04.011

Lisenbee, W.A., Hathaway, J.M., Burns, M.J., Fletcher, T.D., 2021. Modeling bioretention stormwater systems: Current models and future research needs. *Environmental Modelling & Software* 144, 105146. https://doi.org/10.1016/j.envsoft.2021.105146

Liu, J., Sample, D., Bell, C., Guan, Y., 2014. Review and Research Needs of Bioretention Used for the Treatment of Urban Stormwater. *Water* 6, 1069–1099. https://doi.org/10.3390/w6041069

Liu, R., Fassman-Beck, E., 2018. Pore Structure and Unsaturated Hydraulic Conductivity of Engineered Media for Living Roofs and Bioretention Based on Water Retention Data. *Journal of Hydrologic Engineering* 23, 04017065. https://doi.org/10.1061/(ASCE)HE.1943-5584.0001621

Liu, R., Fassman-Beck, E., 2017. Hydrologic response of engineered media in living roofs and bioretention to large rainfalls: experiments and modeling. *Hydrological Processes* 31, 556–572. https://doi.org/10.1002/hyp.11044

Liu, W., Engel, B.A., Feng, Q., 2021. Modelling the hydrological responses of green roofs under different substrate designs and rainfall characteristics using a simple water balance model. *Journal of Hydrology* 602, 126786. https://doi.org/10.1016/j.jhydrol.2021.126786

Locatelli, L., Mark, O., Mikkelsen, P.S., Arnbjerg-Nielsen, K., Bergen Jensen, M., Binning, P.J., 2014. Modelling of green roof hydrological performance for urban drainage applications. *Journal of Hydrology*. https://doi.org/10.1016/j.jhydrol.2014.10.030

Lucke, T., Beecham, S., 2011. Field investigation of clogging in a permeable pavement system. *Building Research & Information* 39, 603–615. https://doi.org/10.1080/09613218.2011.602182

Madrazo-Uribeetxebarria, E., Garmendia Antín, M., Almandoz Berrondo, J., Andrés-Doménech, I., 2021. Sensitivity analysis of permeable pavement hydrological modelling in the Storm Water Management Model. *Journal of Hydrology* 600, 126525. https://doi.org/10.1016/j.jhydrol.2021.126525

Melbourne Water, 2022. Raingardens | Melbourne Water. URL https://www.melbournewater.com.au/water-and-environment/saving-water/raingardens (accessed 8.4.25).

Meristem Design Ltd, 2026. SuDS Planters | Sustainable Drainage Systems | Meristem. URL https://www.meristemdesign.co.uk/product/suds-planters/ (accessed 1.27.26).

Metcalfe, P., Beven, K., Hankin, B., Lamb, R., 2018. Simplified representation of runoff attenuation features within analysis of the hydrological performance of a natural flood management scheme. *Hydrology and Earth System Sciences* 22, 2589–2605. https://doi.org/10.5194/hess-2017-398

Mooney, C.Z., 1997. Monte carlo simulation. Sage.

Muhandes, S., Dobson, B., Mijic, A., 2022. The Value of Aggregated City Scale Models to Rapidly Assess SuDS in Combined Sewer Systems. Frontiers in Water 3.

Nash, J.E., Sutcliffe, J.V., 1970. River flow forecasting through conceptual models part I — A discussion of principles. *Journal of Hydrology* 10, 282–290. https://doi.org/10.1016/0022-1694(70)90255-6

National Cooperative Soil Survey, 2006. Official Series Description - SHEFFIELD Series. URL https://soilseries.sc.egov.usda.gov/OSD_Docs/S/SHEFFIELD.html (accessed 11.9.23).

Nazarpour, S., Gnecco, I., Palla, A., 2023. Evaluating the Effectiveness of Bioretention Cells for Urban Stormwater Management: A Systematic Review. *Water* 15, 913. https://doi.org/10.3390/w15050913

NERC, A., 1999. Flood Estimation Handbook CD-ROM, Version 1.0. Centre for Ecology and Hydrology, Wallingford.

Nissen K.A., Borst M., Fassman-Beck E., Sousa R., 2026. Bioretention Flow-Through Planter Performance and Design Considerations. *Journal of Sustainable Water in the Built Environment* 12, 04025018. https://doi.org/10.1061/JSWBAY.SWENG-582

Ossa-Moreno, J., Smith, K. M., & Mijic, A. (2017). Economic analysis of wider benefits to facilitate SuDS uptake in London, UK. Sustainable Cities and Society, 28, 411-419.

Peng, X., Ampatzoglou, A., Bhowmik, T. (Eds.), 2019. Reuse in the Big Data Era: 18th International Conference on Software and Systems Reuse, ICSR 2019, Cincinnati, OH, USA, June 26–28, 2019, Proceedings, Lecture Notes in Computer Science. Springer International Publishing, Cham. https://doi.org/10.1007/978-3-030-22888-0

Peng, Z., Smith, C., Stovin, V., 2020. The importance of unsaturated hydraulic conductivity measurements for green roof detention modelling. *Journal of Hydrology* 590, 125273. https://doi.org/10.1016/j.jhydrol.2020.125273

Peng, Z., Stovin, V., 2017. Independent Validation of the SWMM Green Roof Module. *Journal of Hydrologic Engineering* 22, 04017037. https://doi.org/10.1061/(ASCE)HE.1943-5584.0001558

Perry, W.B., Ahmadian, R., Munday, M., Jones, O., Ormerod, S.J., Durance, I., 2024. Addressing the challenges of combined sewer overflows. *Environmental Pollution* 343, 123225. https://doi.org/10.1016/j.envpol.2023.123225

Raimondi, A., Quinn, R., Abhijith, G.R., Becciu, G., Ostfeld, A., 2023. Rainwater Harvesting and Treatment: State of the Art and Perspectives. Water 15, 1518. https://doi.org/10.3390/w15081518

Razzaghmanesh, M., Beecham, S., 2018. A Review of Permeable Pavement Clogging Investigations and Recommended Maintenance Regimes. *Water* 10, 337. https://doi.org/10.3390/w10030337

Rodriguez-Hernandez, J., Andrés-Valeri, V.C., Ascorbe-Salcedo, A., Castro-Fresno, D., 2016. Laboratory study on the stormwater retention and runoff attenuation capacity of four permeable pavements. *Journal of Environmental Engineering (United States)* 142. https://doi.org/10.1061/(ASCE)EE.1943-7870.0001033

Roldin, M., Mark, O., Kuczera, G., Mikkelsen, P.S., Binning, P.J., 2012. Representing soakaways in a physically distributed urban drainage model – Upscaling individual allotments to an aggregated scale. *Journal of Hydrology* 414–415, 530–538. https://doi.org/10.1016/j.jhydrol.2011.11.030

Rossman, L.A., 2016a. Storm Water Management Model Reference Manual Volume I - Hydrology (Revised). US Environmental Protection Agency. Cincinnati, OH 45268, National Risk Management Laboratory, Office of Research and Development.

Rossman, L.A., 2016b. Storm Water Management Model Reference Manual Volume II – Hydraulics. US Environmental Protection Agency, Cincinnati, OH 45268, National Risk Management Laboratory, Office of Research and Development.

Rossman, L.A., 2016c. Storm Water Management Model Reference Manual Volume III – Water Quality. US Environmental Protection Agency. Cincinnati, OH 45268, National Risk Management Laboratory, Office of Research and Development.

Rowell, D.L., 2014. Soil Science: Methods & Applications. Routledge.

Saxton, K.E., Rawls, W.J., 2006. Soil Water Characteristic Estimates by Texture and Organic Matter for Hydrologic Solutions. *Soil Science Society of America Journal* 70, 1569–1578. https://doi.org/10.2136/sssaj2005.0117

Schueler, T.R., 1987. Controlling urban runoff: A practical manual for planning and designing urban BMPs. Metropolitan Washington Council of Governments Washington, DC

Severn Trent Water, 2025. Sustainable Drainage Systems | Overview | Building and Developing | Severn Trent Water. URL https://www.stwater.co.uk/building-and-developing/overview/sustainable-drainage-systems/ (accessed 11.18.25).

Severn Trent Water, 2016. Mansfield sustainable flood resilience | Green recovery | Wonderful on Tap | Severn Trent Water. URL https://www.stwater.co.uk/wonderful-on-tap/green-recovery/mansfield-sustainable-flood-resilience/ (accessed 7.28.25).

Šimůnek, J., Van Genuchten, M.T., Šejna, M., 2006. The HYDRUS software package for simulating two- and three-dimensional movement of water, heat, and multiple solutes in variably-saturated media. Technical manual, version 1, 241.

Šimůnek, J., van Genuchten, M.Th., Šejna, M., 2016. Recent Developments and Applications of the HYDRUS Computer Software Packages. *Vadose Zone Journal* 15, vzj2016.04.0033. https://doi.org/10.2136/vzj2016.04.0033

Solomatine, D.P., Ostfeld, A., 2008. Data-driven modelling: some past experiences and new approaches. *Journal of Hydroinformatics* 10, 3–22. https://doi.org/10.2166/hydro.2008.015

Sonnenwald, F., Stovin, V., Guymer, I., 2014. Configuring Maximum Entropy Deconvolution for the Identification of Residence Time Distributions in Solute Transport Applications. *Journal of Hydrologic Engineering* 19, 1413–1421. https://doi.org/10.1061/(ASCE)HE.1943-5584.0000929

Stephenson, D., 1989. Selection of Stormwater Model Parameters. J. Environ. Eng. 115, 210–220. https://doi.org/10.1061/(ASCE)0733-9372(1989)115:1(210)

Stovin, V., 2024. Mappin Green Roof Test Bed Rainfall and Runoff Data 2007. https://doi.org/10.15131/SHEF.DATA.27918345.V1

Stovin, V., Moore, S.L., Wall, M., Ashley, R.M., 2013a. The potential to retrofit sustainable drainage systems to address combined sewer overflow discharges in the Thames Tideway catchment. *Water and Environment Journal* 27, 216–228. https://doi.org/10.1111/j.1747-6593.2012.00353.x

Stovin, V., Poë, S., Berretta, C., 2013b. A modelling study of long term green roof retention performance. *Journal of Environmental Management* 131, 206–215. https://doi.org/10.1016/j.jenvman.2013.09.026

Stovin, V., Poë, S., De-Ville, S., Berretta, C., 2015. The influence of substrate and vegetation configuration on green roof hydrological performance. *Ecological Engineering* 85, 159–172. https://doi.org/https://doi.org/10.1016/j.ecoleng.2015.09.076

Stovin, V., Vesuviano, G., De-Ville, S., 2017. Defining green roof detention performance. *Urban Water Journal* 14, 574–588. https://doi.org/10.1080/1573062X.2015.1049279

Stovin, V., Vesuviano, G., Kasmin, H., 2012. The hydrological performance of a green roof test bed under UK climatic conditions. *Journal of Hydrology* 414–415, 148–161. https://doi.org/10.1016/j.jhydrol.2011.10.022

Sudsplanter Ltd, 2025. Products | SuDSPlanter®. URL https://www.sudsplanter.com/products/ (accessed 1.27.26).

Sun, N., Hall, M., Hong, B., Zhang, L., 2014. Impact of SWMM Catchment Discretization: Case Study in Syracuse, New York. *Journal of Hydrologic Engineering* 19, 223–234. https://doi.org/10.1061/(ASCE)HE.1943-5584.0000777

Tansar, H., Duan, H.-F., Mark, O., 2022. Catchment-Scale and Local-Scale Based Evaluation of LID Effectiveness on Urban Drainage System Performance. *Water Resources Management* 36, 507–526. https://doi.org/10.1007/s11269-021-03036-6

Titterington, J., Squibbs, G., Digman, C., Allitt, R., Osborne, M., Eccleston, P., & Wisdish, A. (2017). Code of practice for the hydraulic modelling of urban drainage systems 2017. The Chartered Institution of Water and Environmental Management (CIWEM), Version, 1.

UK Centre for Ecology & Hydrology, 2024. UK Centre for Ecology & Hydrology, Flood Estimation Handbook Web Service. URL https://fehweb.ceh.ac.uk/Map (accessed 12.16.24).

Van Genuchten, M.Th., 1980. A Closed-form Equation for Predicting the Hydraulic Conductivity of Unsaturated Soils. *Soil Science Society of America Journal* 44, 892–898. https://doi.org/10.2136/sssaj1980.03615995004400050002x

Versini, P.-A., Ramier, D., Berthier, E., de Gouvello, B., 2015. Assessment of the hydrological impacts of green roof: From building scale to basin scale. *Journal of Hydrology* 524, 562–575. https://doi.org/10.1016/j.jhydrol.2015.03.020

Winston, R.J., Dorsey, J.D., Hunt, W.F., 2016. Quantifying volume reduction and peak flow mitigation for three bioretention cells in clay soils in northeast Ohio. *Science of The Total Environment* 553, 83–95. https://doi.org/https://doi.org/10.1016/j.scitotenv.2016.02.081

Wong, T.H., 2006. An overview of water sensitive urban design practices in Australia. *Water Practice and Technology* 1.

Woods-Ballard, B., Wilson, S., Udale-Clarke, H., Illman, S., Scott, T., Ashley, R., Kellagher, R., 2015. The SuDS Manual. CIRIA, London, UK.

Xia, J., Zhang, Y., Xiong, L., He, S., Wang, L., Yu, Z., 2017. Opportunities and challenges of the Sponge City construction related to urban water issues in China. *Science China Earth Sciences* 60, 652–658. https://doi.org/10.1007/s11430-016-0111-8

Yan, J., Zhang, Shouhong, Zhang, J., Zhang, Sunxun, Zhang, C., Yang, H., Wang, R., Wei, L., 2022. Stormwater retention performance of green roofs with various configurations in different climatic zones. *Journal of Environmental Management* 319, 115447. https://doi.org/10.1016/j.jenvman.2022.115447

Yio, M.H.N., Stovin, V., Werdin, J., Vesuviano, G., 2013. Experimental analysis of green roof substrate detention characteristics. *Water Science and Technology* 68, 1477–1486. https://doi.org/10.2166/wst.2013.381

Young, P., Jakeman, A., McMurtrie, R., 1980. An instrumental variable method for model order identification. *Automatica* 16, 281–294. https://doi.org/10.1016/0005-1098(80)90037-0

Zevenbergen, C., Cashman, A., Evelpidou, N., Pasche, E., Garvin, S., Ashley, R., 2010. *Urban Flood Management.* CRC Press.

Zhang, Z., Hu, W., Wang, W., Zhou, J., Liu, D., Qi, X., Zhao, X., 2022. The hydrological effect and uncertainty assessment by runoff indicators based on SWMM for various LID facilities. *Journal of Hydrology* 613, 128418. https://doi.org/10.1016/j.jhydrol.2022.128418

Appendix

A1. SWMM Models Setup

A1.1 "LID" Model

Figure A1 shows the green roof (GR) and bioretention (BIO) *LID* model setup in SWMM. Table A1 presents key subcatchment parameters for both GR and BIO. The subcatchment is 10 m × 10 m, with a slope of about 5 degrees (8.8%). The subcatchment is 100% impervious, with all runoff draining to the LID control. The Manning's N value and storage depths for the impervious and pervious areas were selected based on (Rossman, 2016a). A junction and an outfall were added to make a closed network.

Table A2 shows the parameter settings of the LID Controls in the model. The green roof size is equal to the whole subcatchment, and bioretention size is equal to 20 percent of the subcatchment. The initial saturation was set depending on different simulation scenarios.

Table A3 presents the physical parameters for the GR and BIO scenarios using the LID module. Two saturated hydraulic conductivity (K_{sat} = 200 or 600 mm/hr) values were set to represent different BIO substrate characteristics. In BIO3, which incorporates a 10 mm orifice control, the drain coefficient is 1.25, as explained below. In contrast, for the BIO scenarios without orifice control, the drain coefficient was set to a large value (1000) to ensure the drainage layer does not limit the outflow rate. BIO4 represents a scenario with exfiltration rate of 7.2 mm/hr, whereas this value was set to zero for the other three BIO models, indicating no exfiltration.

BIO3 (A_{LID}= 20 m^2) drain coefficient estimation process:

$$q_{orifice\_unit} = C \cdot h_{mm}^{n} \quad \text{Equation A1}$$

$$Q_{orifice} = C_d \cdot A_{orifice} \cdot \sqrt{2 \cdot g \cdot h_m} \quad \text{Equation A2}$$

$$q_{orifice\_unit} = \frac{Q_{orifice}}{A_{LID}} = \frac{C_d \cdot A_{orifice} \cdot \sqrt{2 \cdot g \cdot h_m}}{A_{LID}} \quad \text{Equation A3}$$

$$C \cdot h_{mm}^{n} = \left(\frac{C_d \cdot A_{orifice} \cdot \sqrt{2 \cdot g \cdot (h_m/1000)}}{A_{LID}} \right) \times (3.6 \times 10^6) \quad \text{Equation A4}$$

$$C = \left(\frac{C_d \cdot A_{orifice} \cdot \sqrt{2 \cdot g \cdot}}{A_{LID}} \right) \times \frac{1}{\sqrt{1000}} \times (3.6 \times 10^6) \approx 1.25 \quad \text{Equation A5}$$

Where $q_{orifice\_unit}$ is the outflow per unit LID area (mm/hr); C is the drain coefficient; h_{mm} is the depth of water surface above the bottom in the reservoir (here offset is set to 0) (mm); n is the flow exponent, here set to 0.5; $Q_{orifice}$ is the orifice flow rate (m^3/s); C_d is the discharge coefficient, here set to 0.65; $A_{orifice}$ is the orifice area (m^2); g is acceleration due to gravity, 9.81 m/s^2; and h_m is head (water depth) above the center of the orifice (m).

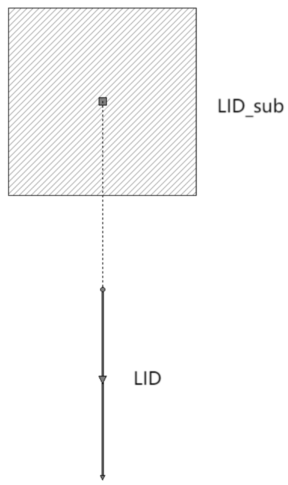

Figure A1. LID model in SWMM

Table A1. Key subcatchment parameters in LID model

Property	Unit	Value
Area	ha	0.01
Width	m	10
% Slope	%	8.8
% Imperv	%	100
N-Imperv		0.013
N-Perv		0.15
Dstore-Imperv	mm	0
Dstore-Perv	mm	5
%Zero-Imperv	%	25
Subarea Routing		OUTLET
Percent Routed		100
LID Controls		1

Table A2. LID Usage Editor parameters

Property	Unit	**GR**	**BIO 1, 2, 3 & 4**
Area of Each Unit	m^2	100	20
Number of Units		1	1
Surface Width per Unit	m	10	10
% Initially Saturated	%	0-100, depending on scenario	
% of Impervious Area Treated	%	100	100
% of Pervious Area Treated	%	100	100

Table A3. SuDS parameters for SWMM LID model

Layer	variable	unit	**GR**	**BIO1**	**BIO2**	**BIO3**	**BIO4**
Surface	Berm Height	mm	0	100	100	100	100
	Vegetation Volume Fraction	v/v	0	0	0	0	0
	Surface Roughness (n)		0.15	0	0	0	0
	Surface Slope	%	2.60	0	0	0	0
Substrate	Thickness	mm	100	700	700	700	700
	Porosity	v/v	0.5	0.44	0.44	0.44	0.44
	Field Capacity	v/v	0.3	0.15	0.15	0.15	0.15
	Wilting Point	v/v	0.1	0.12	0.12	0.12	0.12
	Conductivity	mm/hr	1000	200	**600**	200	200
	Conductivity Slope		40	40	40	40	40
	Suction Head	mm	50	50	50	50	50
Drainage /Storage	Thickness	mm	50	300	300	300	300
	Void Fraction (GR: Voids/Total) (BIO: Voids/Solids)	-	0.5	0.8	0.8	0.8	0.8
	Roughness (n)		0.03	—	—	—	—
	Seepage Rate	mm/hr	—	0	0	0	**7.2**
	Clogging Factor	-	—	0	0	0	0
Drain	Flow Coefficient	mm/hr		1000	1000	**1.25**	1000
	Flow Exponent	-		0.5	0.5	0.5	0.5
	Offset	mm		0	0	0	0
	Open Level	mm		—	—	—	—
	Closed level	mm		—	—	—	—

A1.2 "Disconnect" Model

Figure A2 shows the GR & BIO *Disconnect* model in SWMM. The SuDS is designed to treat the entire catchment, thus the entire subcatchment is eliminated.

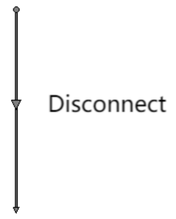

Figure A2. Disconnect model in SWMM

A1.3 "TransferP" Model

Figure A3 shows the GR & BIO *TransferP* model in SWMM. Table A4 presents the key subcatchment parameters of the model. In this model, the entire subcatchment is treated by a GR or BIO, i.e. all the area transfers to pervious area, so that "% Imperv" is changed to 0. Surface runoff can infiltrate into the soil zone of the pervious area. The infiltration rate is set equal to 7.2 mm/hr, which corresponds to the natural soil characteristic in Sheffield, UK. To ensure that all the surface runoff in the subcatchment flows into the SuDS device, the "Subarea Routing" is changed to PERVIOUS.

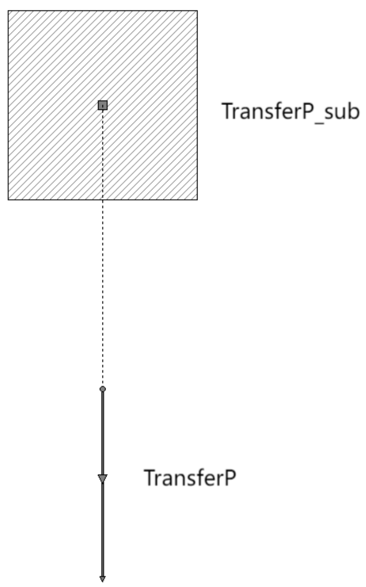

Figure A3. TransferP model in SWMM

Table A4. Subcatchment key parameters in TransferP model

Property	Value	Unit
Area	0.01	ha
Width	10	m
% Slope	8.8	%
% Imperv	0	%
N-Imperv	0.013	
N-Perv	0.15	
Dstore-Imperv	0	mm
Dstore-Perv	5	mm
%Zero-Imperv	25	%
Subarea Routing	PERVIOUS	
Percent Routed	100	
LID Controls	0	

A1.4 "Daily Loss" Model

Figure A4 shows the *Daily Loss* model as implemented in SWMM. Table A5 presents the key subcatchment parameters. It should be noted that in the *Daily Loss* model, the subcatchment is set as entirely impervious (% Imperv = 100). It has a very small Manning's coefficient (0.001) and there is no depression storage (Dstore-Imperv = 0 mm). In this model, the subcatchment is only utilized to receive rainwater and generate runoff.

Table A6 shows other key hydraulic unit parameters for the GR & BIO *Daily Loss* models. Many of the parameter values reported here were either set to zero (not relevant) or set sufficiently large to ensure that they would not constrain the flow or lead to model instabilities. Only the parameter values that directly control the retention and detention mechanisms associated with the SuDS devices are explained in detail below.

Initial losses (retention) associated with the SuDS device are modelled via the "Dailyloss_recharge", "Dailyloss_pipe" and "release" units. The maximum possible initial loss associated with the two SuDS types were determined from the substrate parameters presented in Table A3, i.e. $Substrate\ thick * (field\ capacity - wilting\ point)$. This value is 20 mm and 21 mm for GR and BIO respectively. Rainfall runoff will initially enter the "Dailyloss_recharge" storage unit. The "Dailyloss_pipe" Inlet Offset is set to the initial losses depth, such that runoff will fill the "Dailyloss_recharge" unit up to that depth, with any excess flow passing to the detention storage units via the "Dailyloss_pipe". As noted in the main paper, the initial losses depth was reduced below these maximum levels for certain scenarios.

In GR, the storage unit area is equal to the green roof's physical area (100 m^2). In BIO, the storage unit area is equal to the bioretention cell's physical area (20 m^2). The water in the storage unit is discharged to the sewer when it exceeds the pipe inlet (0.021 m).

The recharge tank is designed to fully discharge during one simulation timestep every 24 hours to simulate the replenishment of initial losses. Here, the emptying mechanism is determined by the "release" orifice through Modulated Controls in SWMM. Custom rules in the *Daily Loss* model open the orifice at midnight, drain the storage unit to empty in one time step, and close it again. However, SWMM's discretisation method does not guarantee complete emptying of the recharge tank within that time step, potentially leaving a negligible amount of residual water. This minor discrepancy is considered insignificant and has minimal influence on water balance. Additionally, if further runoff from rainfall enters the recharge tank during the emptying period, it adds to the water volume being emptied, leading to an overestimation of water loss during that time step.

Detention processes are represented through the combination of the "Dailyloss_storage", "Dailyloss_outcontrol" and "Dailyloss_overflow" units. The key parameters here are the Max Depth in the "Dailyloss_storage" and the "Dailyloss_outcontrol" Orifice Height.

The "Dailyloss_storage" storage unit represents the combined BIO detention depth (0.436 m) made up of the substrate's large pores (between field capacity and saturation/porosity) and the storage layer void depth.

$$Storage\ Volume = Substrate\ thick * (porosity - field\ capacity) + Storage\ thick * \frac{void}{void+1} + Berm\ Height \qquad \text{Equation A6}$$

The orifice control is used to represent detention due to either percolation through the growing media or a physical orifice installed at the downstream end of the SuDS device. The maximum outflow rate here depends on the saturated hydraulic conductivity (K_{Sat}) of the SuDS substrate and the maximum underdrain flow.

$$Outflow_{max} = \begin{cases} K_{Sat}, & K_{Sat} < Orifice \\ Underdrain\ (Orifice), & K_{Sat} \geq Orifice \end{cases} \qquad \text{Equation A7}$$

The "Dailyloss_outcontrol" orifice (d = 0.010 m) represents the BIO3 10 mm orifice.

In BIO cells without orifice control, the "Dailyloss_outcontrol" orifice represents the percolation rate. For BIO1, d = 0.027 m corresponds to $K_{Sat} = 200\ \text{mm/hr}$ and for BIO2, d = 0.047 m corresponds to $K_{Sat} = 600\ \text{mm/hr}$.

Orifice control diameter estimation process:

$$Q_{orifice} = K_{sat} \times A_{LID} = 200(or\ 600)mm/hr \times \frac{1m}{1000mm} \times \frac{1hr}{3600s} \times 20m^2 \qquad \text{Equation A8}$$

$$A_{orifice} = \frac{Q_{orifice}}{C_d \cdot \sqrt{2 \cdot g \cdot h_m}}\ (m^2) \qquad \text{Equation A9}$$

$$D = \sqrt{\frac{4 \cdot A_{orifice}}{\pi}} \approx 0.027(or\ 0.047)(m) \qquad \text{Equation A10}$$

Where h_m maximum depth equal to 0.436 m.

The exfiltration rate of 7.2 mm/hr associated with BIO4 is represented using "Seepage Loss" in "Dailyloss_storage".

The "Dailyloss_overflow" orifice allows the water in the "Dailyloss_storage" storage unit to be exceeded and drain to the sewer.

Detention processes are considered negligible for the GR, so the key parameter values are all zero for this device.

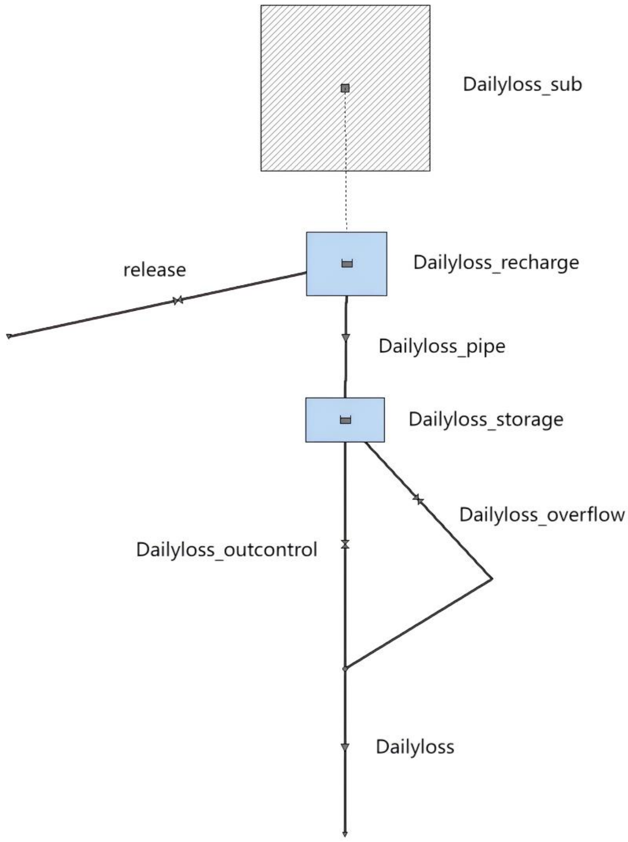

Figure A4. Daily Loss model in SWMM

Table A5. Subcatchment key parameters in Daily Loss model

Property	Unit	Value
Area	ha	0.01
Width	m	10
% Slope	%	8.8
% Imperv	%	100
N-Imperv		0.001
N-Perv		0.15
Dstore-Imperv	mm	0
Dstore-Perv	mm	5
%Zero-Imperv	%	100
Subarea Routing		OUTLET
Percent Routed		100
LID Controls		0

Table A6. Other key hydraulic units parameters in Daily Loss model

				GR	**BIO1**	**BIO2**	**BIO3**	**BIO4**
Name	Hydraulic unit	Property	Unit	Value	Value	Value	Value	Value
Dailyloss_recharge	Storage unit	Max Depth	m	0.05	0.05	0.05	0.05	0.05
		Initial Depth	m	0	0	0	0	0
		Evap Factor	-	0	0	0	0	0
		Seepage Loss	mm/hr	0	0	0	0	0
		Storage Shape	m^2	100	20	20	20	20
Dailyloss_pipe	Pipe	Max Depth	m	10	10	10	10	10
		Length	m	1	1	1	1	1
		Roughness	m	0.001	0.001	0.001	0.001	0.001
		Inlet Offset	m	0.020	0.021	0.021	0.021	0.021
		Outlet Offset	m	0	0	0	0	0
release	Orifice	Type		Bottom	Bottom	Bottom	Bottom	Bottom
		Shape		Circular	Circular	Circular	Circular	Circular
		Height	m	1.6	0.6	0.6	0.6	0.6
		Width	m	0	0	0	0	0
		Inlet Offset	m	0	0	0	0	0
		Discharge Coeff.	-	1	1	1	1	1
Dailyloss_storage	Storage unit	Max Depth	m	0	0.436	0.436	0.436	0.436
		Initial Depth	m	0	0	0	0	0
		Evap Factor	-	0	0	0	0	0
		Seepage Loss	mm/hr	0	0	0	0	**7.2**
		Storage Shape	m^2	0	20	20	20	20
Dailyloss_outcontrol	Orifice	Type		Bottom	Bottom	Bottom	Bottom	Bottom
		Shape		Circular	Circular	Circular	Circular	Circular
		Height	m	0	**0.027**	**0.047**	**0.010**	0.027
		Width	m	0	0	0	0	0
		Inlet Offset	m	0	0	0	0	0
		Discharge Coeff.	-	0	0.65	0.65	0.65	0.65
Dailyloss_overflow	Orifice	Type		Side	Side	Side	Side	Side
		Shape		Circular	Circular	Circular	Circular	Circular
		Height	m	0	1	1	1	1
		Width	m	0	0	0	0	0
		Inlet Offset	m	0	0.436	0.436	0.436	0.436
		Discharge Coeff.	-	0	0.65	0.65	0.65	0.65

A1.5 "Cont. Loss" Model

Figure A5 shows the GR & BIO *Cont. Loss* model as implemented in SWMM. Table A7 presents the key subcatchment parameters.

In GR, the entire subcatchment is converted into a structure with 20 mm ($Substrate\ thick * (field\ capacity - wilting\ point)$) depression storage to represent the maximum GR initial losses. This modification enables the initial losses to be dynamically updated through the ET losses, offering a more realistic depiction of the SuDS substrate's retention recovery.

In BIO, the depression storage depth was set to 21 mm ($Substrate\ thick * (field\ capacity - wilting\ point)$), this represents the volume of retention in BIO substrate.

The depth of depression storage was varied to reproduce different initial moisture content scenarios for design storm simulations.

The detention model set-up is identical to the *Daily Loss* model.

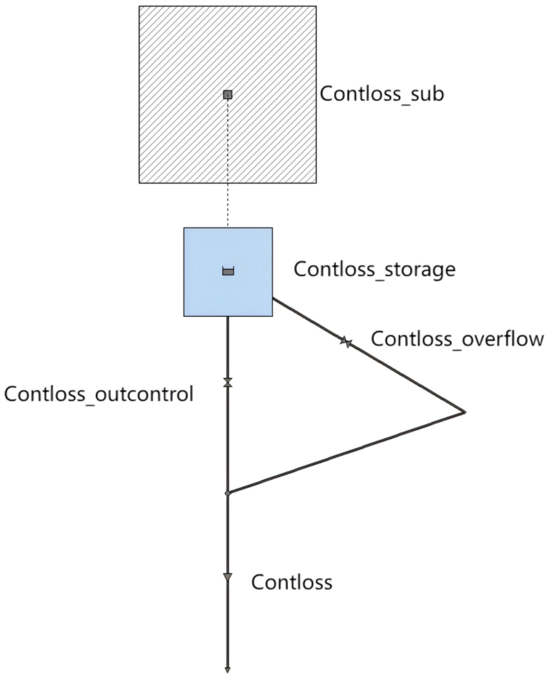

Figure A5. Cont. Loss model in SWMM

Table A7. Subcatchment key parameters in Cont. Loss model

		GR	**BIO1, 2, 3 & 4**
Property	Unit		
Area	ha	0.01	0.01
Width	m	10	10
% Slope	%	8.8	8.8
% Imperv	%	100	100
N-Imperv		0.013	0.013
N-Perv		0.15	0.15
Dstore-Imperv	mm	**20**	**21**
Dstore-Perv	mm	5	5
%Zero-Imperv	%	0	80
Subarea Routing		OUTLET	OUTLET
Percent Routed		100	100
LID Controls		0	0

A2. Initial Moisture Content for the Design Storm Simulations

Three different initial moisture content values were specified for the design storm-based comparisons. These were permanent wilting point (PWP), field capacity (FC) and the Median value determined from the simulation of the 2007 annual time series. PWP represents the maximum possible retention storage, equivalent to 20 mm in GR and 21 mm in BIO. FC represents the condition when the SuDS device has drained down following a storm, but additional losses due to ET have not started to take effect. The Median value represents the most likely condition in the context of UK rainfall time series, as explained later. The input values relevant to the *LID, Daily Loss* and *Cont Loss* models are presented in Table A8.

Table A8. Parameter values applied to represent alternative initial moisture contents

	GR PWP	BIO PWP	GR FC	BIO FC	GR Median	BIO Median
Moisture content (m^3/m^3)	0.1	0.12	0.3	0.5	0.18	0.23
LID - % initial saturated	0	0	50	9.375	20	34.375
Daily Loss – Inlet Offset (m)	0.020	0.021	0.000	0.000	0.012	0.000
Cont. Loss – Dstore-Imperv (m)	0.020	0.021	0.000	0.000	0.012	0.000*

* Additionally, “Contloss_storage” initial depth is 56 mm.

The Median values were derived as follows. Figure A6 presents the cumulative probability distribution of initial moisture content at the start of rainfall events in the SWMM LID GR, BIO1 & BIO2 simulations in response to the 2007 annual time series rainfall input. Individual events were defined as being separated by a minimum ADWP of 24 hr, resulting in 71 individual rainfall events. The main paper provides a detailed description and discussion of the continuous simulation based model comparisons.

The Median initial moisture condition values were found to be 0.18 m^3/m^3 (GR) and 0.23 m^3/m^3 (mean of BIO1 & BIO2). For GR, the initial moisture content in all events lay somewhere between FC and PWP. In BIO, the substrate K_{sat} is typically lower than that of green roofs, resulting in longer drainage times under practical conditions. BIO inflows also exceed GR inputs due to the loading ratio; in this case by a factor of 5. BIO flows were observed to continue from the underdrains for many hours, and frequently, for several days at very low flow rates. Consequently, the initial moisture content in BIO devices was frequently above FC, and the Median value (0.23 m^3/m^3) significantly exceeds FC (0.15 m^3/m^3).

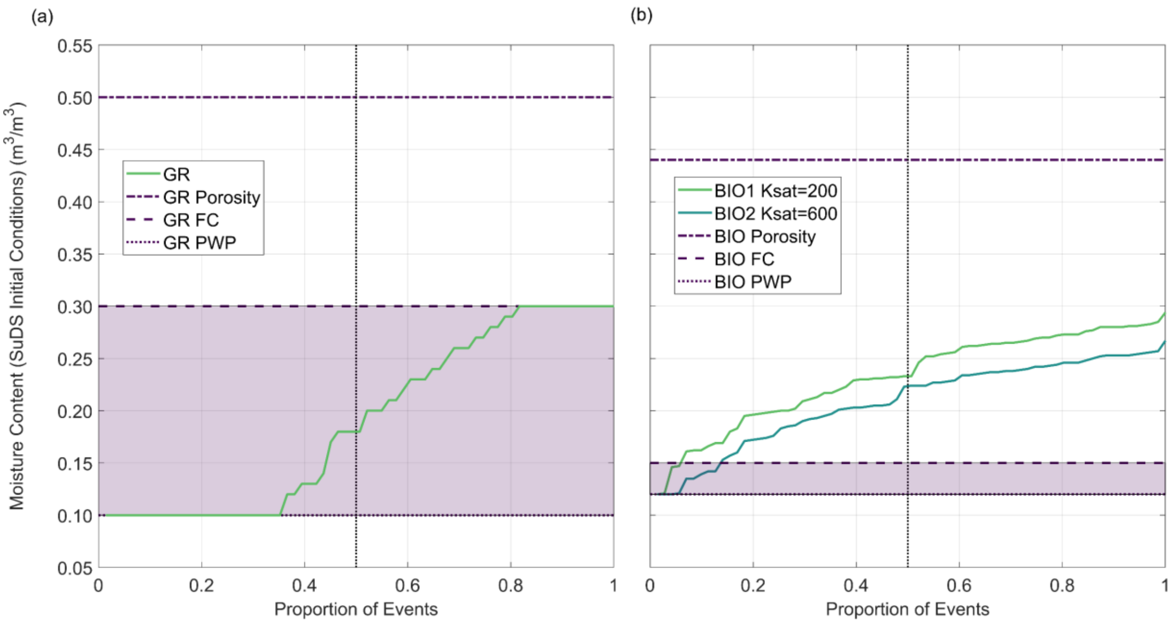

Figure A6. Initial substrate moisture PDFs for (a) GR and (b) BIO1 & BIO2 for all event. Shaded areas represent retention moisture ranges for SuDS substrates.

In the BIO simulation, the median value (0.23 m^3/m^3) is above FC, so that there is an initial depth in the detention store element of the models.

A2.1 Settings for the continuous rainfall series

In continuous simulations, initial conditions are less critical; however, certain settings still require consideration.

In the *Daily Loss* model, the “Inlet Offset” (Table A6) of “Dailyloss_pipe” is 0.00208 m, representing 2.08 mm available recharge depth (mean daily PET value over 12 months). In other models, parameters remain consistent with those set for the PWP initial moisture content conditions.

A3. Additional Results

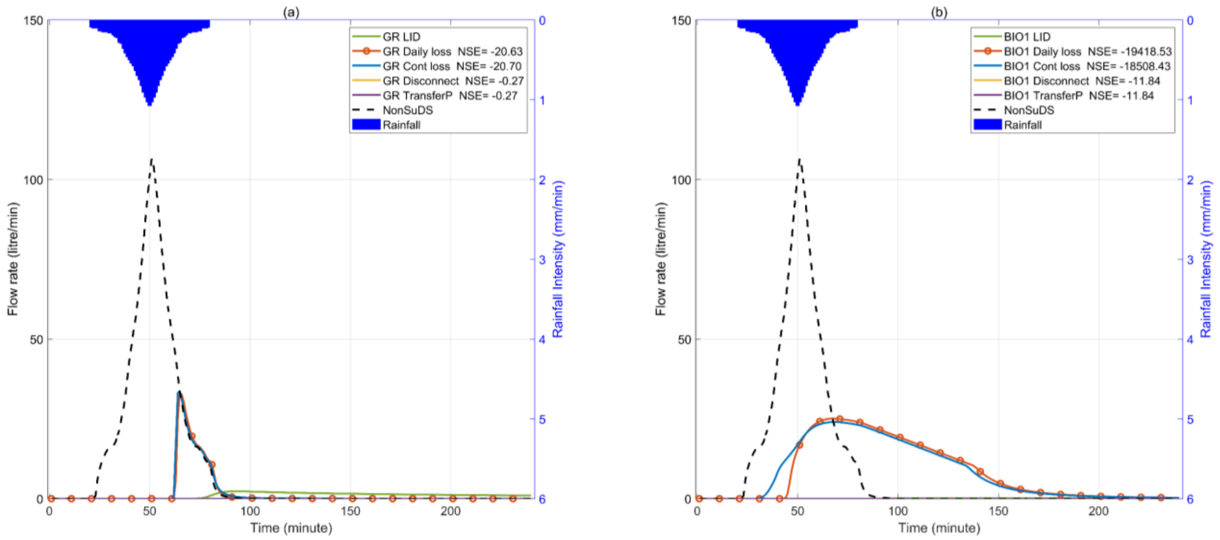

Figure A7. (a) GR and (b) BIO1 runoff profiles using different modelling methods in response to the 1 in 10 year design storm

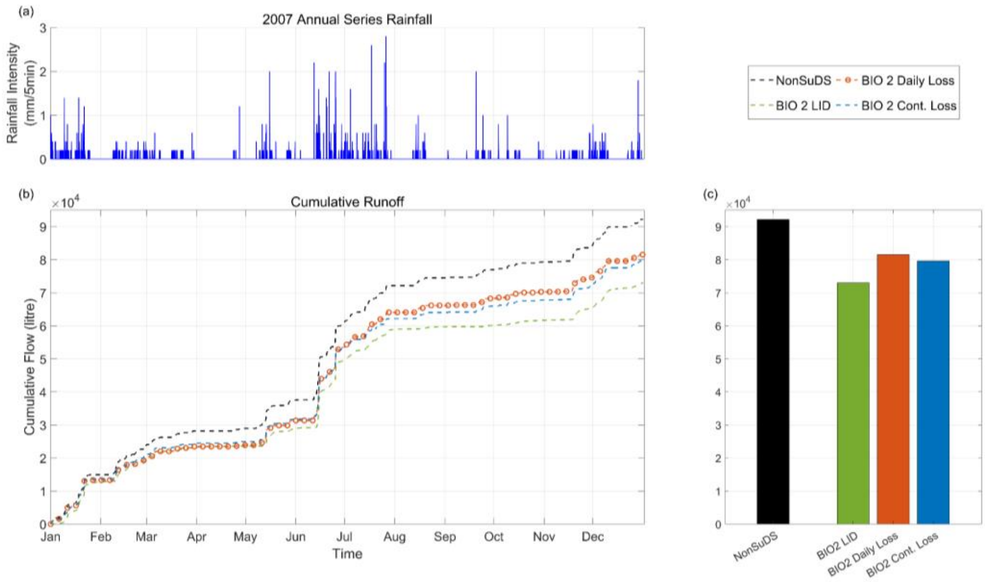

Figure A8. Modelled runoff in response to an annual rainfall recorded in Sheffield in 2007 at a 5-minute timestep. Bottom Left: Cumulative flow volumes for SuDS device-scale modelling methods in annual rainfall for BIO 2 (K_{sat} = 600 mm/hr). Bottom Right: Comparison of total volumes for several SuDS device-scale modelling methods.

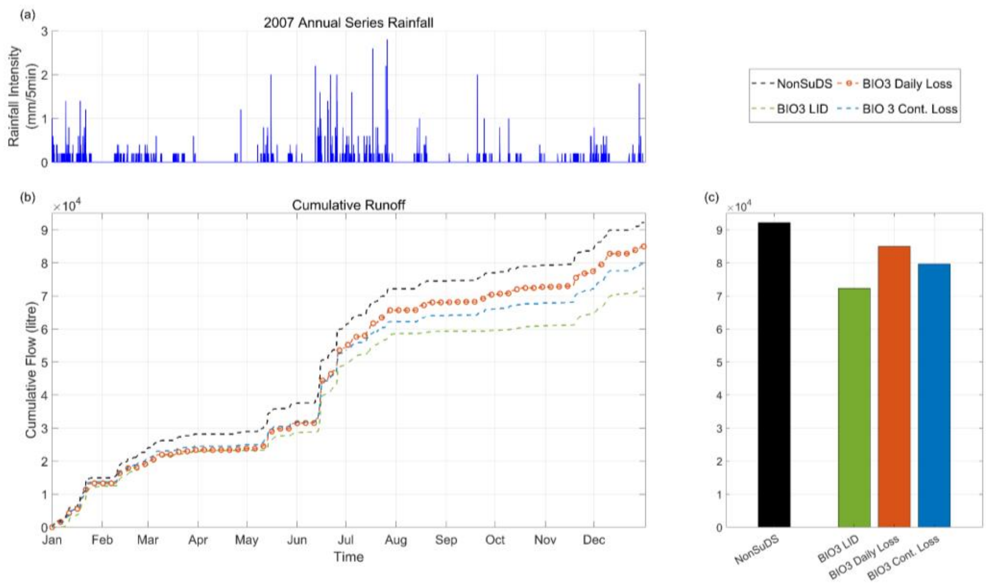

Figure A9. Modelled runoff in response to an annual rainfall recorded in Sheffield in 2007 at a 5-minute timestep. Bottom Left: Cumulative flow volumes for SuDS device-scale modelling methods in annual rainfall for BIO 3 (d = 10 mm orifice). Bottom Right: Comparison of total volumes for several SuDS device-scale modelling methods.

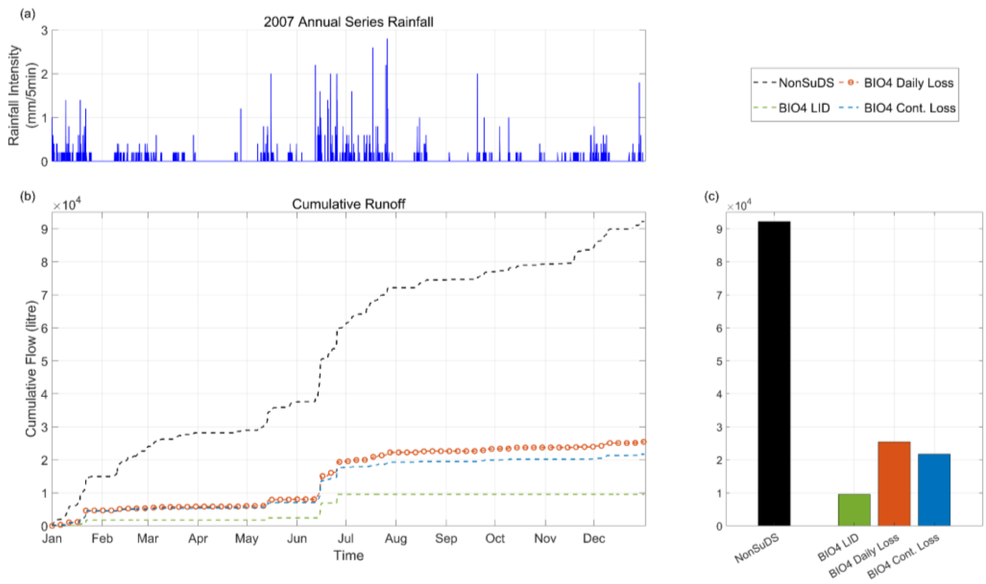

Figure A10. Modelled runoff in response to an annual rainfall recorded in Sheffield in 2007 at a 5-minute timestep. Bottom Left: Cumulative flow volumes for SuDS device-scale modelling methods in annual rainfall for BIO 4 (Exfiltration rate = 7.2 mm/hr). Bottom Right: Comparison of total volumes for several SuDS device-scale modelling methods.